

GTH. 36478

Karakterisering van potentiële immuno-evasie  
mechanismen van het feline infectieuze peritonitis virus

Characterization of putative immune evasion mechanisms  
of feline infectious peritonitis virus

Hannah L. Dewerchin

Promotor: Prof. dr. H. Nauwynck

Medepromotoren: Prof. dr. B. Verhasselt, Prof. dr. ir. H. Favoreel

Proefschrift ingediend tot het behalen van de graad van

Doctor in de Diergeneeskundige Wetenschappen

Laboratorium voor Virologie

Vakgroep Virologie, Parasitologie en Immunologie

Faculteit Diergeneeskunde

Universiteit Gent

Academiejaar 2007-2008



ISBN 978-90-5864-146-5

Cover:

Picasso's Cats Meeting Miro's Cat on a Dark and Starry Night

Original painting by Eve Riser-Roberts

Copyright 1996, All Rights Reserved

Used with permission from the artist

Philosophy begins in wonder. And, at the end, when philosophic  
thought has done its best, the wonder remains.

Alfred North Whitehead



# Contents

<b>List of symbols and acronyms</b>	<b>v</b>
<b>1 Introduction</b>	<b>1</b>
1.1 Feline coronaviruses . . . . .	1
1.1.1 Classification . . . . .	1
1.1.2 Relation between FIPV and FECV . . . . .	2
1.1.3 The virus . . . . .	4
1.1.4 Replication cycle . . . . .	8
1.1.5 Pathogenesis . . . . .	12
1.1.6 Treatment and prevention . . . . .	14
1.2 Immune evasion by coronaviruses . . . . .	16
1.2.1 Evasion of interferon mediated immune responses . . . . .	16
1.2.2 Evasion of antibody-dependent lysis . . . . .	17
1.2.3 Evasion of major histocompatibility complex I dependent cell lysis . . . . .	18
1.2.4 Evasion of apoptosis . . . . .	20
1.3 Aims of the study . . . . .	21
<b>2 Replication of feline coronaviruses in peripheral blood monocytes</b>	<b>35</b>
2.1 Introduction . . . . .	36
2.2 Materials and Methods . . . . .	37
2.3 Results . . . . .	40

2.3.1	Growth curves of feline coronaviruses in CrFK cells . . . . .	40
2.3.2	Expression kinetics of cytoplasmic and surface-expressed viral antigens in FCoV-infected CrFK cells . . . . .	40
2.3.3	Growth curves of feline coronaviruses in monocytes . . . . .	42
2.3.4	Expression kinetics of cytoplasmic and surface-expressed viral antigens in FCoV-infected monocytes . . . . .	42
2.3.5	Infection kinetics in a larger population of cats . . . . .	46
2.4	Discussion . . . . .	47
<b>3</b>	<b>FIPV-infected monocytes internalize viral membrane-bound proteins upon antibody addition</b>	<b>57</b>
3.1	Introduction . . . . .	58
3.2	Materials and Methods . . . . .	59
3.3	Results . . . . .	62
3.3.1	Redistribution of membrane-bound viral proteins induced by polyclonal FCoV specific antibodies . . . . .	62
3.3.2	The viral membrane-bound proteins are not spontaneously internalized . . . . .	62
3.3.3	Redistribution of membrane-bound viral proteins induced by monoclonal anti-S and/or anti-M antibodies . . . . .	64
3.3.4	Antibody-mediated internalization is specific for monocytes . . . . .	65
3.4	Discussion . . . . .	66
<b>4</b>	<b>Going off the beaten track: a new internalization pathway revealed by FIPV</b>	<b>73</b>
4.1	Introduction . . . . .	74
4.2	Materials and Methods . . . . .	76
4.3	Results . . . . .	80
4.3.1	Internalization of viral plasma membrane-bound proteins does not occur via phagocytosis or macropinocytosis . . . . .	80

4.3.2	Internalization of viral plasma membrane-bound proteins is not mediated by clathrin . . . . .	80
4.3.3	Internalization of viral plasma membrane-bound proteins is not mediated by caveolae . . . . .	82
4.3.4	Internalization of viral plasma membrane-bound proteins does not occur via a known clathrin- and caveolae-independent pathway . . . . .	83
4.3.5	Co-localization of viral antigen-antibody complexes and endosomal compartments . . . . .	85
4.4	Discussion . . . . .	86
<b>5</b>	<b>Microtubules, actin and myosins cooperate during internalization and trafficking of antigen-antibody complexes in FIPV infected monocytes</b>	<b>93</b>
5.1	Introduction . . . . .	94
5.2	Material and Methods . . . . .	96
5.3	Results . . . . .	99
5.3.1	The role of microtubules in transportation of viral antigen-antibody complexes into the cell . . . . .	99
5.3.2	Co-localization of viral antigen-antibody complexes and microtubules . . . . .	100
5.3.3	The role of actin in internalization of viral antigen-antibody complexes . . . . .	100
5.3.4	Co-localization of viral antigen-antibody complexes and actin . . . . .	102
5.3.5	Co-localization of viral antigen-antibody complexes and myosins . . . . .	104
5.4	Discussion . . . . .	105
<b>6</b>	<b>Regulation of a clathrin- and caveolae- independent internalization pathway in FIPV-infected monocytes</b>	<b>119</b>
6.1	Introduction . . . . .	120
6.2	Material and Methods . . . . .	122
6.3	Results . . . . .	125

6.3.1	Internalization of viral antigens is energy-dependent and regulated by a serine/threonine kinase . . . . .	125
6.3.2	Internalization of viral antigens is regulated by myosin light chain kinase . . . . .	127
6.3.3	Internalization of viral antigens is regulated by MAPKs 128	
6.3.4	Co-localization of viral antigen-antibody complexes with p-ERK, p-p38 and p-JNK . . . . .	130
6.3.5	Mode of regulation by MAPKs . . . . .	132
6.4	Discussion . . . . .	134
<b>7</b>	<b>General Discussion</b>	<b>141</b>
	<b>Summary</b>	<b>161</b>
	<b>Samenvatting</b>	<b>167</b>
	<b>Curriculum Vitae</b>	<b>175</b>
	<b>Dankwoord</b>	<b>181</b>



## List of Symbols and Acronyms

2',5'OAS	2',5' oligoadenylate synthetase
Ψ	bulky hydrophobic amino acid
Ab	antibody
ADEI	antibody dependent enhancement of infectivity
Ag	antigen
AP-2	adaptor protein-2
BCV	bovine coronavirus
CaMK	Ca/calmodulin dependent kinase
CCoV	canine coronavirus
ChTB	Cholera toxin B
CoV	coronavirus
CrFK cells	Crandell feline kidney cells
CTL	cytotoxic T-lymphocyte
Dab-2	Disabled-2
DABCO	1,4-diazabicyclo(2, 2, 2)octane
DN	dominant negative
EEA1	early endosome antigen 1
EGFP	enhanced green fluorescent protein
EH-domain	Eps15 homology domain
E protein	small envelope protein
ER	endoplasmic reticulum
ERGIC	ER-to-Golgi intermediate compartment
ERK	extracellular signal regulated kinase
FCoV	feline coronavirus
fewf cells	felis catus whole fetus cells
FECV	feline enteric coronavirus
FeLV	feline leukemia virus
FIPV	feline infectious peritonitis virus
FITC	fluorescein isothiocyanate
FIV	feline immuno deficiency virus

## LIST OF SYMBOLS AND ACRONYMS

---

H	histidine
HCoV	human coronavirus
hpi	hours post inoculation
hps	hours post seeding
HSP	heat shock protein
I	isoleucine
IBV	avian infectious bronchitis virus
IFN	interferon
IRF	interferon response factor
JNK	c-Jun N-terminal kinase
K	lysine
kDa	kilo Dalton
L	leucine
MAPK	mitogen activated protein kinase
MAPKAPK	MAPK associated protein kinase
MHC	major histocompatibility complex
MHV	mouse hepatitis virus
MLCK	myosin light chain kinase
moi	multiplicity of infection
M protein	membrane protein
mRNA	messenger RNA
MTOC	microtubule organizing center
myo1, myo2, ...	myosin 1, myosin2, ...
N protein	nucleocapsid protein
ORF	open reading frame
PAK	p21-activated kinase
PBS	phosphate buffered saline
PCR	polymerase chain reaction
p-ERK, p-JNK,...	phosphorylated-ERK, phosphorylated-JNK,...
PI-3K	phosphatidylinositol-3 kinase
PKA, PKC, PKG	protein kinase A, C, G
PKR	protein kinase R
Pol	polymerase
PrV	pseudorabies virus
rER	rough endoplasmic reticulum
RTC	replication-transcription complex
SAPK	stress activated protein kinase
SARSV	severe acute respiratory syndrome virus
SD	standard deviation
SH domain	Src homology domain
SPF	specific pathogen free

S protein	spike protein
TCID <sub>50</sub>	tissue culture infectious dose with a 50% endpoint
TGEV	transmissible gastroenteritis virus
TRS	transcription regulation sequence
WASP	Wiscott Aldrich syndrome protein
WT	wild type
X	any amino acid
Y	tyrosine



# 1

## Introduction

### 1.1 Feline coronaviruses

Two closely related coronaviruses (CoVs) are described in cats: feline infectious peritonitis virus, or FIPV, and feline enteric coronavirus, or FECV. Feline coronaviruses (FCoVs) can infect all members of the *Felidae* family and are found world-wide. The first report on a possible FIP case dates back to 1912. A cat was found with a swollen abdomen, dyspnea, fever and lesions in the eyes. However, it took until the late sixties to establish that the disease was mediated by a virus, more specifically, a coronavirus (Ward et al., 1968; Zook et al., 1968; Ward, 1970). In 1972, another manifestation form of FIP was described, characterized by granulomas and absence of exudate, which was, until then, thought to be typical for a FIPV infection (Montali and Strandberg, 1972). This form was named “dry FIP” while, from then on, the first reported form was referred to as “wet FIP”. The second feline coronavirus, FECV, remained undiscovered until 1981 mainly due to the fact that an FECV infection mostly dwells sub-clinically (Pedersen et al., 1981).

#### 1.1.1 Classification

In 1968, the *Coronaviridae* were acknowledged as a separate virus family, based on the morphology and intracellular budding site of the virions. Coronaviruses were identified as large (60-220 nm), spherical or pleomorphic viruses with a helical nucleocapsid and an envelope from which large peplomers protrude (Wege et al., 1982; Holmes, 1985). The families of the *Coronaviridae*, *Arteriviridae* and *Roniviridae*, are grouped in the order of the *Nidovirales*: viruses with a positive, single stranded RNA genome that is made up of a nested\* set of mRNAs with a common 3' end.

---

\*Nido in Latin means “nest”.

The *Coronaviridae* family consists of the genera Coronaviruses and Toroviruses. Coronaviruses are further divided into 3 groups. Historically, this division was based on serological properties, and it was confirmed by phylogenetic analysis of the viral proteins (Gonzalez et al., 2003).<sup>†</sup> The best known member of the CoVs is undoubtedly severe acute respiratory syndrome virus (SARSV). However, coronaviruses can infect a whole range of vertebrates as is illustrated in Table 1.1. Since the outbreak of SARS in 2003 many new CoVs have been identified, including some human CoVs. The FCoV belongs to group 1.

### 1.1.2 Relation between FIPV and FECV

It was already mentioned that FIPV and FECV are closely related. They are genetically almost identical. In fact, they are not two different species but merely virulence variants, 2 biotypes of the same species: FCoV. It is now commonly accepted that FIPV arises from FECV by mutation. Several observations led to this conclusion:

- A general phylogenetic comparison showed that FIPV and FECV strains from one geographical area were more closely related than FIPV (or FECV) strains from two different areas (Vennema et al., 1995). Further, FIPV and FECV strains isolated from the same cattery were up to 99,5% identical (Vennema et al., 1998).
- There were also reports of FIP cases in FECV positive closed households (Vennema et al., 1995).
- Two FIPV strains were isolated from cats that were experimentally infected with FECV (Poland et al., 1996). The two FIPV strains were genetically almost identical to each other and to the original FECV strain.

Identifying the mutation(s) responsible for conversion from FECV to FIPV proved not be easy. There seems to be a correlation between appearance of FIPV and mutations in the 3c and 7b gene but no consensus has been found (Vennema et al., 1998). There is also a report of a deletion in the 7a gene, associated with occurrence of FIP (Kennedy et al., 2001).

Based on serological properties, FIPV and FECV strains are divided into serotype I or serotype II strains. Antibodies mounted against one serotype can neutralize FIPV or FECV strains belonging to that serotype but not strains from the

---

<sup>†</sup>Based on comparative sequence analysis, it has been suggested that the genera coronavirus and torovirus should be redefined as two sub-families within the *Coronaviridae* or even as two families in the order of the *Nidovirales*, while the groups within the coronaviruses should be considered as 3 genera (Gonzalez et al., 2003). No consensus has yet been reached.

Group	Virus	Acronym	Host
1	Human coronavirus 229E	HCoV 229E	Man
	Human coronavirus NL63	HCoV NL63	Man
	Transmissible gastroenteritis virus	TGEV	Pig
	Porcine Epidemic diarrhea virus	PEDV	Pig
	Canine coronavirus	CCoV	Dog
	Feline coronavirus	FCoV	Cat
	Ferret enteric coronavirus	FrECV*	Ferret
	Bat coronavirus	BatCoV	Bat
2a	Human coronavirus OC43	HCoV OC43	Man
	Human coronavirus HKU1	HCoV HKU1	Man
	Mouse hepatitis virus	MHV	Mouse
	Bovine coronavirus	BCoV	Cattle
	Hemagglutinating encephalomyelitis virus	HEV	Pig
	Rat coronavirus	RCoV	Rat
	Equine coronavirus	ECoV	Horse
	Turkey coronavirus	TCoV	Turkey
2b	Severe acute respiratory syndrome virus	SARSV	Man
3	Avian infectious bronchitis virus	IBV	Chicken
	Pheasant coronavirus	PCoV	Pheasant
	Goose coronavirus	GCoV	Goose
	Duck coronavirus	DCoV	Duck
	Pigeon coronavirus	PiCoV	Pigeon

Table 1.1: The coronaviruses and their hosts. \* The acronym for ferret enteric coronavirus was presented in literature as FECV. Here, it was changed to FrECV to allow discrimination with the feline enteric coronavirus (FECV), which was characterized first.

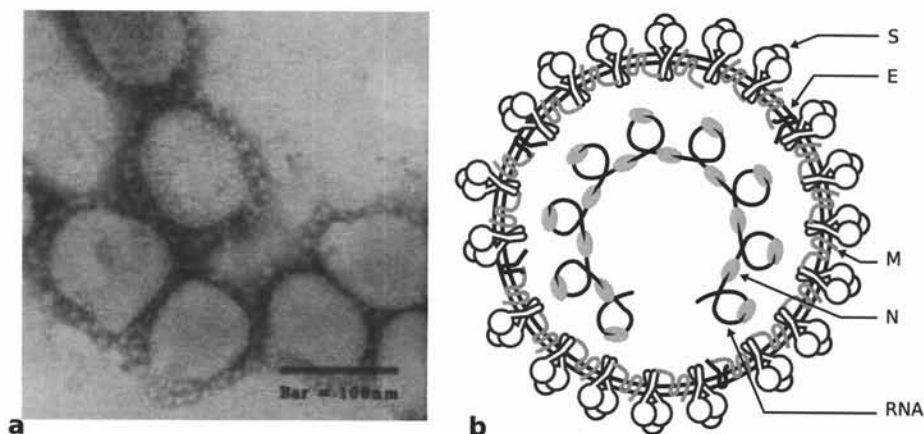


Figure 1.1: Coronavirus particles. a) virions visualized by electron microscopy. b) Schematic representation of a feline coronavirus with the genome and the structural spike (S), membrane (M), small envelope (E) and nucleocapsid (N) proteins.

other serotype (Pedersen et al., 1983). More differences between the serotypes came to light with the establishment of continuous feline cell lines, which enabled easier isolation of new virus strains (O'Reilly et al., 1979; Black, 1980; Evermann et al., 1981). It was found that serotype I prevailed in the field (in Japan, the USA, Great Britain and Austria) with 70 to 95% of the isolates belonging to this serotype (Pedersen et al., 1983; Hohdatsu et al., 1992; Addie et al., 2003; Benetka et al., 2004). Serotype I replication in continuous cell lines was also more limited than serotype II replication. Additionally, serotype II strains were found to be closely related to canine coronavirus (CCoV) and were later proved to be recombinants of type I strains and CCoV (Pedersen et al., 1983; Herrewegh et al., 1998; Vennema et al., 1995).

### 1.1.3 The virus

In the intestines of cats infected with FIPV, coronavirus particles were found with a diameter of 94 nm and petal shaped projections of 15 nm (Hoshino and Scott, 1980). These projections are spike proteins which give the virion the typical appearance of a coronavirus on electron microscopy images as is illustrated in Figure 1.1a. Coronavirus particles are spherical with a helical nucleocapsid surrounded by a phospholipid bilayer in which the structural viral proteins are embedded: the spike, membrane and small envelope protein. An illustration is given in Figure 1.1b.



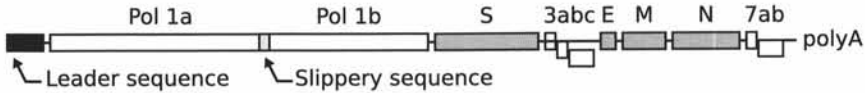


Figure 1.2: Genome organization of feline coronaviruses. The gray boxes represent the genes encoding structural proteins.

**The genome** The first coronavirus to be fully sequenced was the avian infectious bronchitis virus (IBV) (Bournsell et al., 1987). The genome length was 30 kilobases, making it the longest RNA virus in vertebrates. The genome is organized as a 3' nested set<sup>‡</sup> of mRNAs which is capped at the 5' end and polyadenylated at the 3' end. A representation of the genome is given in Figure 1.2. Due to the nested set organization of the genome, the mRNAs are structurally polycistronic.<sup>§</sup> However, most are functionally monocistronic since only the first open reading frame (ORF) will be translated. The order of the major proteins is identical for all coronaviruses. The first and largest ORF occupies two thirds of the genome and encodes the polymerase polyprotein (Pol1a and Pol1b). It is followed by the ORFs for the spike (S), the small envelope (E), the membrane (M) and the nucleocapsid (N) protein. There are some additional ORFs that are positioned at different locations in the several coronaviruses: the accessory or group-specific genes. For the feline coronaviruses these are ORF 3a, b and c and ORF 7a and b. The numbers indicate their relative location in the genome.

**The polymerase polyprotein** The polymerase gene comprises two ORFs connected by a slippery sequence: Pol1a and Pol1b. Thus two proteins are translated from ORF1, an ORF1a-encoded protein and an ORF1a+ORF1b-encoded protein. Both proteins are synthesized as precursor proteins and autocatalytically processed by viral proteases to generate the 16 functional subunits of the replication/transcription machinery among which the RNA-dependent RNA polymerase and the helicase. ORF1 also encodes the viral proteases needed for the proteolytic processing. The replicase products assemble into replication-transcription complexes (RTCs) which are embedded in cellular membranes to generate double-membrane vesicles. These are the sites of viral RNA synthesis (Pedersen et al., 1999; Gosert et al., 2002).

<sup>‡</sup>In a nested set organization, all subgenomic RNAs have the same 3'-termini, but because of discontinuous transcription each mRNA has a unique coding sequence and is transcribed into a unique viral protein. This allows to encode more proteins in the same genome sequence.

<sup>§</sup>Polycistronic mRNA contains more than 1 ORF while monocistronic mRNA contains only 1 ORF. Most eukaryotic mRNAs are monocistronic.

**The spike or S protein** The S, or peplomer protein, is synthesized in the rough endoplasmic reticulum (rER) as a precursor protein of 150 kiloDalton (kDa). Oligosaccharides are added cotranslationally attributing to the molecular weight (Rottier et al., 1981). S proteins form oligomers, probably trimers which results in a final molecular weight of 180-205 kDa (Delmas and Laude, 1990; Vennema et al., 1990b). S proteins are type I membrane-bound proteins, with the majority of the protein lying outside the viral membrane and a short cytoplasmic tail or endodomain. The incorporation of the S protein into virions is mediated by the membrane proximal part of this cytoplasmic tail (Godeke et al., 2000; Bosch et al., 2005).

Although the S protein is not required for the formation of new virus particles, it is essential for the infection cycle of the virus since it mediates binding of the virus to its receptor and defines the tropism of the virus (Kuo et al., 2000; Haijema et al., 2004). The S protein can also mediate cell-cell fusion and induce neutralizing antibodies (de Groot et al., 1989).

**The small envelope or E protein** The E protein is a small protein of 10 kDa that is retained in the pre-Golgi membranes. It is found in the virion in low numbers. The protein spans the lipid bilayer twice and is almost entirely embedded in the membrane with only a short endodomain at the N terminus (Maeda et al., 2001). The E protein is a viroporin that exhibits ion channel activity of which the role is not yet elucidated (Wilson et al., 2004). Severely impaired virus particles can be formed without the E protein during mouse hepatitis virus (MHV) and severe acute respiratory syndrome virus (SARSV) infection but not during transmissible gastroenteritis virus (TGEV) infection (Ortego et al., 2002; Kuo and Masters, 2003; DeDiego et al., 2007). Nevertheless, the E protein is essential for proper formation of new virus particles with normal morphology and infectivity (Kuo and Masters, 2003). Not only is it required for the coronavirus envelope formation, it also captures the other membrane proteins at the budding site, the ER-to-Golgi intermediate compartment (ERGIC), by interacting with the membrane protein (Godet et al., 1992; Yu et al., 1994; Lim and Liu, 2001).

**The membrane or M protein** The M protein is the major envelope component and has a molecular mass of 25-30 kDa. Only 10% of the protein protrudes outside the viral membrane. It has a large transmembrane domain spanning the viral membrane 3 times and a c-terminal endodomain (Armstrong et al., 1984; Rottier et al., 1986). When expressed by itself, the M protein is retained in the Golgi, and in infected cells, the M protein is found together with the S protein in heteromultimeric protein complexes in the Golgi (Rottier

and Rose, 1987; Opstelten et al., 1995). It is this interaction between the M and S protein that prevents the S protein from being transported to the plasma membrane and ensures its encapsulation into new virions. There are also some indications that the M protein might be required for infection at the level of receptor binding since antibodies against the M protein could block infection of macrophages (Kida et al., 2000).

**The nucleocapsid or N protein** The N protein has a molecular weight of 43-50 kDa and is phosphorylated on the serine residues (Stohlman and Lai, 1979). By binding to a packaging signal, N proteins encapsulate the genome to form the helical ribonucleocapsid (Parker and Masters, 1990). This ribonucleocapsid is then incorporated into newly formed virions through interactions between the N and M proteins (Narayanan et al., 2000).

The N proteins are also thought to play a role in translation and transcription since they interact with leader sequences on the genome. It was suggested that the N protein is part of the transcription complex (Baric et al., 1988; Stohlman et al., 1988) in which it might act as a strong translation initiation signal (Tahara et al., 1998). It has recently been confirmed that the N protein is an RNA chaperon and that it partially localizes to the RTC (Sawicki et al., 2007; Zuniga et al., 2007). The N protein is found in the nucleoli as well, were it would delay the cell cycle in the interphase to ensure maximal translation of viral mRNAs (Chen et al., 2002). In addition, the N protein plays an important role in circumventing the innate immune response since it is an interferon antagonist (Kopecky-Bromberg et al., 2007; Ye et al., 2007).

**The accessory or group-specific proteins** The mRNAs 3 and 7 encode the 5 accessory, most likely non-structural, proteins. The function of these proteins is still unknown. They are not required for infection since a mutated virus in which ORF 3 and 7 is deleted can still replicate in vitro with identical infection kinetics as the wild type strain (Haijema et al., 2004). However, the mutated virus could no longer cause FIP in inoculated cats. Hence, the accessory proteins are essential for development of FIP (Haijema et al., 2004).

mRNA 3 is 5.2 kb long and consists of 3 ORFs. The function of the encoded proteins and whether they are expressed during infection is still unknown (Horsburgh et al., 1992). The putative protein from ORF 3c might play a role in virulence since mutations in 3c have been linked to development of FIPV strains from FECV strains (Vennema et al., 1998).

mRNA 7 is 1.6 kb long and contains 2 ORFs. ORF7a would encode a hydrophobic protein of 11 kDa with a hitherto unknown function. ORF7b en-

codes a secretory, hydrophilic protein of 22 kDa. Its precise function remains to be elucidated, but it has been suggested that it serves as an immune modulator, a “virokine” (Rottier, 1999). The 7b protein is not essential for replication and ORF7b is easily lost in *in vitro* passages of the virus. However, it is likely to provide a selective advantage *in vivo*, since all wild type strains harbor an intact ORF7b (Herrewegh et al., 1995b).

### 1.1.4 Replication cycle

An overview of the replication cycle is given in Figure 1.3.

**Virus entry** It has long been a matter of debate whether coronaviruses enter their host cell through fusion at the plasma membrane or whether they enter via endocytosis and fuse with the endosomal membranes. As with many viruses, the mode of entry turned out to be dependent on the virus strain and on the host cell (Kooi et al., 1991; Nash and Buchmeier, 1997). The entry of feline coronaviruses was not studied until recently. It was shown in our lab that FIPV strains from serotype I and II enter monocytes, their *in vivo* target cells, by endocytosis (Figure 1.3 step 2) (Van Hamme et al., 2007). Internalization occurs through a clathrin- and caveolae-independent pathway which is dependent on dynamin (Van Hamme et al., 2008). Uptake of virus particles by the host cell is triggered by binding of the S protein to the receptor (Figure 1.3 step 1). Aminopeptidase N acts as a receptor for several coronaviruses, including FIPV (Tresnan et al., 1996). However, aminopeptidase N is only a receptor for the entry into feline cell lines of serotype II strains but not of serotype I strains (Hohdatsu et al., 1998). The receptor for serotype I strains remains to be identified and it needs to be verified if the same receptor is used for entry into feline monocytes.

**Genome replication** Mouse hepatitis virus (MHV) was used as a model for the research on coronaviral replication and transcription. Not much research has been done using feline coronaviruses. However, one can assume these steps in the replication cycle occur in the same way for all coronaviruses.

After entry of a virus particle, the viral and the endosomal membranes will fuse, resulting in release of the nucleocapsid (Figure 1.3 step 3). Since it is positive stranded, the genome can be translated immediately upon release into the cytoplasm (Figure 1.3 step 4). The 16 replicase-transcriptase proteins are synthesized which will assemble into the RTCs together with other viral proteins (such as the N protein) and possibly cellular proteins (Figure 1.3

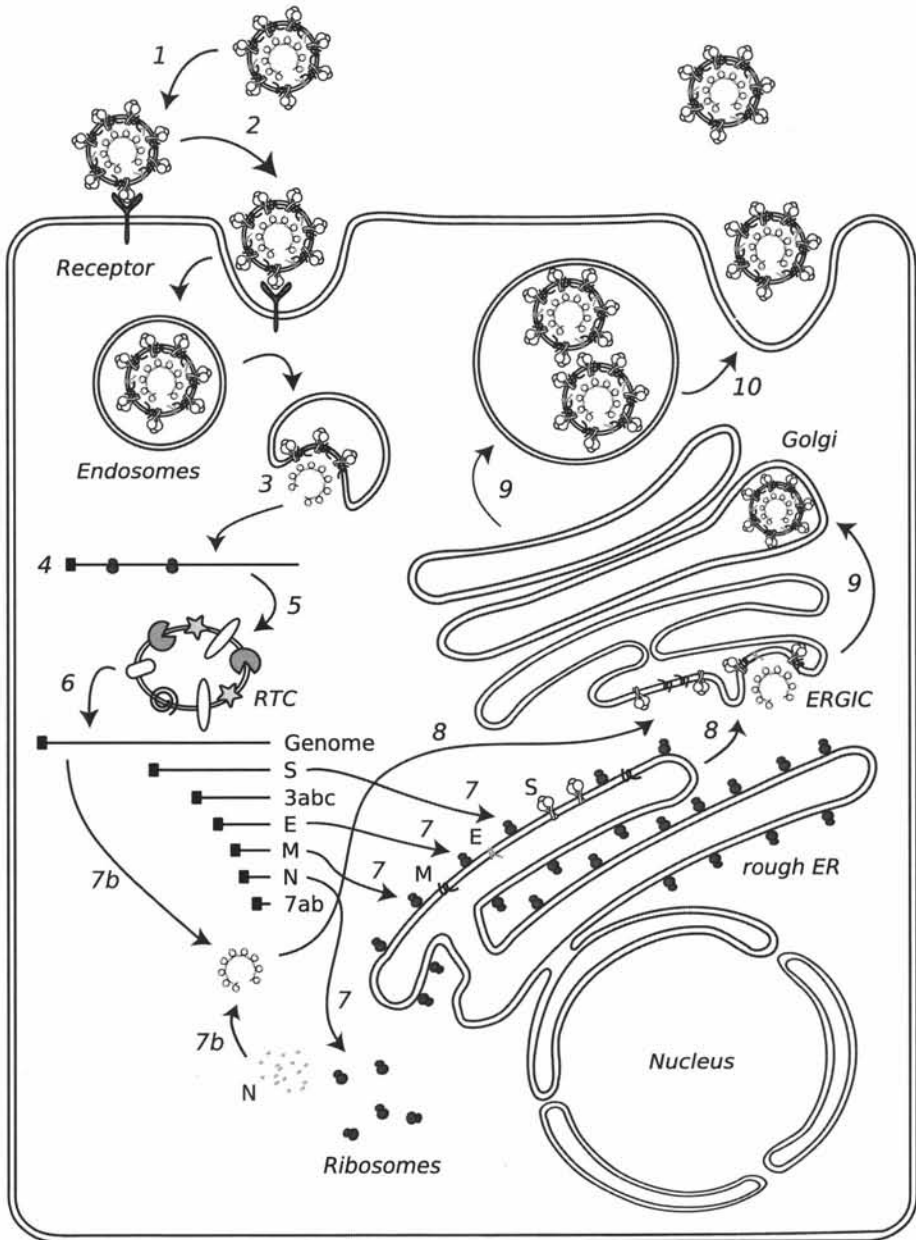


Figure 1.3: Cell cycle of feline coronaviruses. 1) Binding to the receptor. 2) Entry by endocytosis. 3) Release of the genome. 4) translation of the replicase-transcriptase proteins. 5) Formation of the replication-transcription complex (RTC). 6) synthesis of new genomes and mRNAs. 7) Translation of mRNAs to proteins. 7b) Association of nucleocapsid proteins and the genome to form the ribonucleocapsid 8) Accumulation of the viral proteins in the ER-to-Golgi intermediate compartment (ERGIC) and budding of new virions. 9) Transport through the secretory pathway. 10) Release of progeny virus.

step 5) (Pedersen et al., 1999; Gosert et al., 2002). The RNA dependent RNA polymerase will transcribe the genome to its complementary negative stranded RNA, which will serve as a template for the synthesis of new genomes (Figure 1.3 step 6).

During the replication of coronaviruses, mutations are frequently build into the genome and also recombinations of larger RNA segments can occur. These mutations could lead to altered virulence or tissue tropism (Vennema et al., 1998; Kuo et al., 2000; Kennedy et al., 2001; Rottier et al., 2005).

**Genome transcription** In an infected cell, the mRNAs are produced in different amounts (Figure 1.3 step 6). The number of copies rises if the gene is located closer to the 3' end of the genome. The leader sequence, positioned at the 5' end of the genome can be found on all subgenomic mRNAs. This implies that during transcription, non-adjacent sequences need to be fused. The junction of the leader sequence and the body element of each mRNA can be identified as a short motif (10 nucleotides): the transcription regulation sequence (TRS). TRS can be found in the genome at the 3' end of the leader sequence and in front of each ORF. Several models have been developed to explain the discontinuous synthesis of mRNAs. Figure 1.4 gives an overview of the current model for CoVs transcription as is presented in Sawicki et al. (2007). First an RTC is formed and minus-strand synthesis is initiated. Elongation continues until the first TRS is encountered. Then the RTCs will either disregard the TRS motif and continue the elongation or will stop synthesis of the minus strand and relocate to the 5' end of the genome in order to complete its synthesis. This completed subgenomic minus-strand RNA will then serve as a template for the actual mRNA synthesis. It is still unknown how this relocation to the 5' end of the genome is achieved.

**Translation** Coronaviral mRNAs have the same structure as eukaryotic mRNAs; they possess a CAP structure, a leader sequence, an UAG start codon and a stop codon. Therefore they are easily recognized by the ribosomes of the host cell which will start translation (Figure 1.3 step 7). In eukaryotic cells, translation is regulated by ribosomal scanning. This method is also used for the viral mRNAs, except for the polymerase gene. In order to translate both the 1a and ab ORFs, a ribosomal -1 frame shift needs to be made on the slippery sequence AAUUUC (Brierley et al., 1987; Bredenbeek et al., 1990). One third of the ribosomes makes this frame shift.

The N protein is synthesized in the cytoplasm. The membrane-bound proteins, S, M and E, are synthesized on the rER and co-translationally embedded in its membranes.

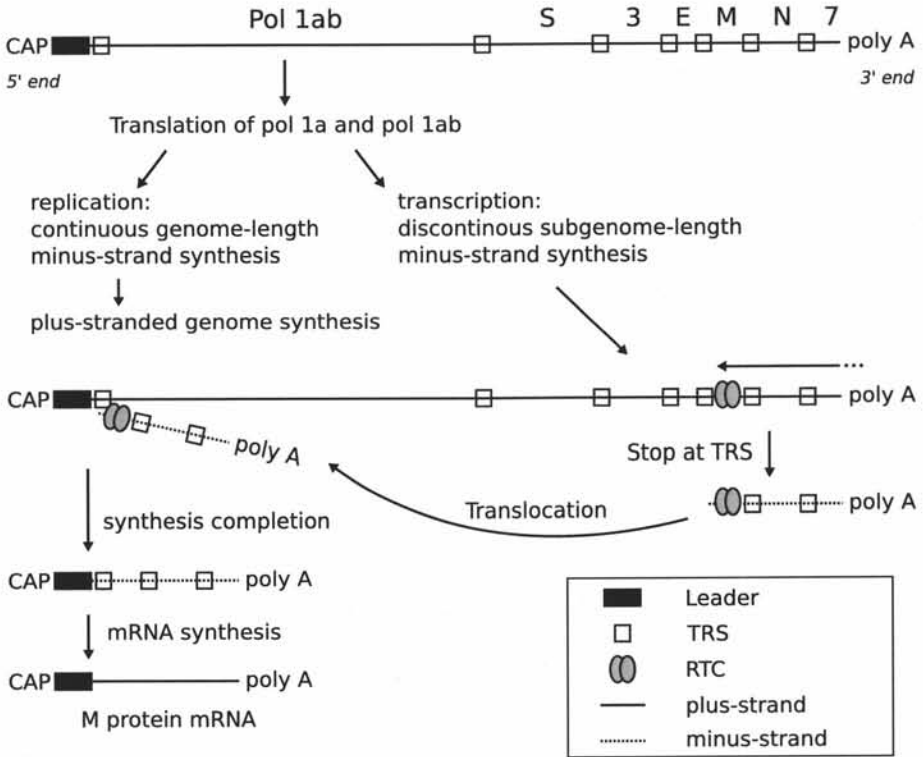


Figure 1.4: Model for coronavirus replication and transcription. TRS=transcription regulation sequence; RTC=replication-transcription complex

**Budding of progeny virus** After translation, the N proteins will bind to the newly replicated genomic RNA strain to form the helical ribonucleocapsid (Figure 1.3 step 7b). The E, M and S proteins and the ribonucleocapsid will accumulate in the ERGIC, the site of budding (Figure 1.3 step 8) (Opstelten et al., 1995). Although the exact mechanism for budding is not fully elucidated, it is clear that the M and the E proteins play crucial roles in deformation of the membranes and retention of all needed proteins to form new virions. After budding in the ERGIC, the virions will leave the infected cell via exocytosis, undergoing various modifications on their way (Figure 1.3 step 9 and 10).

### 1.1.5 Pathogenesis

**Pathogenesis of FECV** Infection with FECV occurs orally or by inhalation after direct or indirect contact with a virus shedder. Indirect contact can take place via shared cat's boxes, eating and drinking from the same bowls and via animal care takers. After uptake, FECV will replicate in the enterocytes of the small intestines and colon. This will lead to enteritis and diarrhea in cases of severe infection, especially in kittens (McKeirnan et al., 1981; Pedersen et al., 1981). In contrast to what was initially believed, FECV infection leads to a systemic disease since virus can also be detected in mesenteric lymph nodes, spleen, bone marrow, tonsils, thymus and in the blood (in both plasma and monocytes) (Pedersen et al., 1984; Herrewegh et al., 1995a; Gunn-Moore et al., 1998; Meli et al., 2004). Lymphatic hyperplasia and a transient increase in T cells has been reported (Paltrinieri et al., 2003; Meli et al., 2004). Seroconversion occurs at 3 to 4 weeks after infection (Meli et al., 2004).

FECV can cause chronic enteric infections during which a cat will shed virus at any time. This shedding will start 2 days after infection (in experimental infections) (Meli et al., 2004). However, most cats undergo cycles of infection and shedding, followed by recovery and reinfection (Herrewegh et al., 1997; Foley et al., 1997). So the mounted immune response can clear the virus from a cat but cannot protect against new infections. Cats can be reinfected by the same or a different strain. This reinfection does not appear to increase the chance of conversion to FIPV (Addie et al., 2003).

**Pathogenesis of FIPV** After experimental inoculation of seronegative cats, FIPV replicates in pharyngeal, respiratory and intestinal epithelial cells (Weiss and Scott, 1981b). Then, at 6 days post challenge, a monocyte-associated viremia occurs which brings the virus to other target-organs (Weiss and Scott, 1981a,b). First, virus is found in the tracheobronchial lymph nodes, and in



vascular lesions of the lungs and trachea. Then in the liver and spleen, followed by the kidneys and omentum. Ultimately, FIPV can also be detected in other lymph nodes, thymus, bone marrow, eyes and brain. The last stages are accompanied with systemic lesions: perivascular granulomas in all affected organs, fibrinous serositis and lymphoid necrosis (Weiss and Scott, 1981b). Lymphatic tissues in FIP cats show lymphocyte depletion and in the blood a severe decrease in all subsets of lymphocytes is detected (Kipar et al., 2001; Paltrinieri et al., 2003). Interestingly, a viral soluble factor is shown to cause apoptosis of activated T-cells, leading to T-cell depletion (Haagmans et al., 1996).

Development of the hallmark lesions in FIP cats: vasculitis and granulomas, was first attributed to a type III hypersensitivity reaction (Pedersen and Boyle, 1980; Jacobse-Geels et al., 1980, 1982). Circulating immune complexes sediment in small vessels leading to complement activation. This triggers vasodilatation and the release of chemotactic mediators which attract monocytes and granulocytes. In turn, these cells release inflammatory cytokines and lysosomal enzymes and thereby enhance the inflammatory reaction. However, it was recently shown that the FIP vasculitis is mediated by activated and infected circulating monocytes (Kipar et al., 2005). The monocytes show strong expression of CD18, which mediates the binding of monocytes to endothelial cells. Expression of the cytokines tumor necrosis factor $\alpha$  and interleukin1 $\beta$ , further increases the adhesion of monocytes to endothelial cells. Monocyte attachment and emigration to (peri)vascular granulomas is accompanied with destruction of the vascular basal lamina due to the secretion of matrix metalloproteinase B by the activated monocytes. Hence the vasculitis and possible leakage of plasma into the body cavities. The endothelial cells also appear to contribute to the development of vasculitis since a strong up-regulation of MHCII expression and generalized activation of the cells is observed.

In cats with “wet” FIP, the inflammatory reactions will lead to release of exudate in one or more body cavities. Exudate is a viscous fluid that contains a high concentration of proteins, especially albumin. The amount of fluid varies from a few milliliter to over 1 liter. Exudate is often found in the peritoneal cavity giving the cat a strongly swollen abdomen, the typical appearance of a FIP cat. In cats with “dry” FIP, no exudate is formed and the granulomas tend to be larger, sometimes more than 1 centimeter in diameter. Cats with wet FIP deteriorate quickly and die within weeks or a few months. Dry FIP progresses more slowly and ill cats can live for several months after initial infection.

A FIP infection does not progress gradually but rather in bouts of disease. It was shown that FIP develops in waves of enhanced viral replication coinciding with fever, weight loss and depletion of CD4 and CD8 T cells (de Groot-

Mijnes et al., 2005). Between waves, disease progression halts, fever subsides, body weight stabilizes and lymphocyte counts increase. How many bouts of disease a cat could suffer before it succumbs or (occasionally) recovers cannot be linked to the onset of the humoral immune response or antibody titer nor to the course of the initial wave of disease. However, it could be shown that the final stages of FIP development are always accompanied with rising amounts of viral RNA, indicating that progression of fatal disease is a direct consequence of loss of immune control (de Groot-Mijnes et al., 2005).

It is not the humoral immune response but the cell mediated immunity that plays a key role in a possible (albeit unlikely) recovery from FIP. In fact, antibodies play a peculiar role in the pathogenesis of FIP. Most cats infected with FIPV have very high antibody titers. However, these antibodies seem not to offer any protection since most cats succumb to the disease. It has been described in numerous vaccination studies that FIP develops much faster in seropositive cats than in seronegative cats. Enhanced disease progression was observed in experimentally inoculated cats that had actively acquired antibodies after vaccination and also in cats that were administered antibodies passively (Pedersen and Boyle, 1980; Weiss and Scott, 1981a,b; Pedersen and Black, 1983; Vennema et al., 1990a; McArdle et al., 1992). The current hypothesis to explain this phenomenon is antibody-dependent enhancement of infectivity (ADEI). In ADEI, antibodies facilitate the infection of monocytes/macrophages by binding to the virus and subsequently enabling uptake of the virus via the Fc-receptor on the cells. The existence of ADEI could be proved *in vitro* and was mediated by epitopes on the S and M protein (Stoddart and Scott, 1989; Hohdatsu et al., 1991; Corapi et al., 1992; Olsen et al., 1992). However, ADEI only occurs at sub-neutralizing antibody concentrations. To complicate matters even further, the antibody concentration in FIP cats is so high that it would lead to virus neutralization and not ADEI. Additionally, no indications of the occurrence of enhanced disease progression in naturally infected cats have been reported. On the contrary, the risk of development of FIP in seropositive cats seems to decrease over time, which suggests some sort of increased immunity of seropositive cats and not an increased susceptibility (Addie et al., 1995).

It is clear that many unsolved questions remain regarding the interactions of FIPV with the host immune system, both humoral and cell mediated.

### 1.1.6 Treatment and prevention

**Treatment of FIPV** Currently, there is no efficient treatment for FIPV. Sometimes corticosteroids, interferons and antivirals are administered to ill cats but

this can only increase the live expectancy of the affected cat and will not result in recovery (Watari et al., 1998; Ishida et al., 2004; Ritz et al., 2007). When clinical symptoms arise, a FIP infection will lead to death in 95% of the cases. Recently, some new compounds were found that can inhibit FIPV replication *in vitro*: pyridine N-oxide derivatives, derivatives of glycopeptide antibiotics and several plant lectins (Balzarini et al., 2006b,a; Keyaerts et al., 2007). However, these compounds still need to be tested *in vivo*. Many compounds with antiviral activity against SARSV have been discovered or developed over the last years (Haagmans and Osterhaus, 2006). Testing these antivirals might lead to the discovery of new drugs that are active against FIPV as well.

**Prevention of FIPV** Much more research has been done on the prevention of FIP through vaccination. There is one commercial vaccine on the market: Primucell FIP (from Pfizer Animal Health) based on an attenuated FIPV strain. The vaccine is administered intranasally, induces a strong mucosal IgA response and stimulates cellular immunity (Gerber et al., 1990). The vaccine provided protection in seronegative kittens of at least 16 weeks of age in 50 to 75% of the cases (Gerber, 1995; Postorino Reeves, 1995). So the efficacy of the vaccine is not 100% and vaccination should be repeated often (every 6 to 9 months) in animals living in elevated risk environments. Moreover, vaccination campaigns in seropositive catteries are probably futile since all kittens will be infected before they can be vaccinated. Promising results were reported with a new vaccine consisting of an attenuated FIPV strains in which the 3abc or the 7ab accessory proteins had been deleted (Haijema et al., 2004). Immunization with these strains led to protection after a lethal homologous challenge. However, these vaccine candidates are not yet commercially available.

There is another (more labor intensive) way to prevent FIP. By eradicating FECV from a cattery, FIPV can no longer emerge since it arises from FECV by mutation. In the ideal situation, a cattery should be kept coronavirus free by removing the shedders, keeping the seropositive cats in quarantine until they have cleared the virus, testing all animals that enter the cattery before they are placed with the other cats and preventing fecal-oral virus transmission by maintaining high hygiene standards (frequent disinfection of cages, floors, eating and drinking bowls, cat's boxes...).

## 1.2 Immune evasion by coronaviruses

### 1.2.1 Evasion of interferon mediated immune responses

The innate immune response is part of the first line of defense against viruses. Type I interferons (IFN), IFN- $\alpha$  and IFN- $\beta$ , are key components of the innate immune system that is activated after initial virus-host cell interactions. Infection of cells causes activation of several cellular transcription factors, such as interferon regulatory factor-3 (IRF-3) and NF- $\kappa$ B, leading to the expression of IFN genes. The produced IFN in turn triggers JAK/STAT-mediated signal transduction pathways that stimulate expression of more than 100 gene products with an IFN-stimulated response element in their promotor. Activation of these genes will result in an antiviral state. Among those gene products are protein kinase R (PKR) and 2',5' oligoadenylate synthetase (2',5' OAS). PKR synthesis is induced by IFN and dimerized and activated by double-stranded RNA (dsRNA), a byproduct of viral replication. This will ultimately lead to inhibition of protein synthesis and thus progeny virus production will be halted (so step in 7 Figure 1.3 will be blocked). dsRNA will also activate 2',5' OAS which will in turn activate RNase L. This will lead to the degradation of mRNA and consequently to the inhibition of viral replication (block before step 7 in Figure 1.3).

It was recently reported that the N protein of MHV is a type I IFN antagonist (Ye et al., 2007). In MHV infected cells, the PKR and 2',5' OAS pathways are not activated, resulting in a lack of RNA degradation and protein translation shutoff. The N protein was shown to inhibit 2',5' OAS/RNase L activity. It could be that the double membrane vesicles (in which the RNA molecules replicate) help to prevent detection by the host cell and activation of PKR and 2',5' OAS by shielding the dsRNA.

Also in SARS patients, low levels of IFN are detected. In SARSV infected cells, IFN- $\beta$  responses were indeed found to be effectively blocked (Spiegel et al., 2005; Kopecky-Bromberg et al., 2007; Versteeg et al., 2007). Several proteins are involved: the N protein and two SARSV specific accessory proteins encoded from ORF 3b and ORF 6 (Kopecky-Bromberg et al., 2007). The N protein inhibits the synthesis of IFN while ORF 3b and ORF 6 proteins block IFN production and IFN signaling. All three proteins inhibit the activation of IRF-3. NF- $\kappa$ B is inhibited by the N protein. ORF 3b and 6 proteins interfere with expression from promoters containing an IFN-stimulated response element and ORF 6 protein blocks STAT1 translocation to the nucleus.

Until now, there are no reports on IFN antagonists encoded by other coronaviruses, but it is likely that the N protein will perform the same function in all

coronaviruses.

IFN- $\gamma$  plays an important role in the adaptive immune responses. It inhibits viral replication and is an important inducer of major histocompatibility complex I molecules and macrophage activation. Interestingly, there are several reports that IFN- $\gamma$  is down-regulated in coronavirus infected cats that develop FIP, while it is up-regulated in healthy coronavirus infected cats (Gunn-Moore et al., 1998; Kiss et al., 2004; Gelain et al., 2006). In a remarkable experiment, IFN- $\gamma$  knock-out mice were infected with MHV, resulting a fatal peritonitis (Kyuwa et al., 1998). This form of disease manifestation is very atypical for MHV but strongly resembles FIP. This is another indication that IFNs (and control of IFN expression) play a crucial role in the development of FIP.

### 1.2.2 Evasion of antibody-dependent lysis

In antibody-dependent lysis, antibodies will bind to viral antigens either on virions or on infected cells, if these express viral proteins in their plasma membrane. The Fc domain of these bound antibodies can be recognized by complement (=antibody-dependent complement mediated lysis) or by phagocytic or natural killer cells (=antibody-dependent cell mediated lysis). Activation of the (classical) complement cascade will eventually lead to formation of membrane attack complexes which will perforate the membrane of the virion or the infected cell, resulting in their destruction. Natural killer cells or phagocytes can recognize bound antibodies with Fc receptors that are expressed on their surfaces. Recognition by natural killer cells will force the infected cell to undergo apoptosis while the phagocyte will internalize and degrade the infected cell (or the virion).

**Antibody dependent enhancement of infectivity (ADEI)** ADEI is a mechanism that is used by cell free FIPV to evade antibody-dependent lysis. Antibodies bind to the virus particles which are consequently taken up by monocytes/macrophages via their Fc-receptor. Normally this should lead to destruction of the virus, but FIPV somehow manages to escape from the phagosomes or lysosomes and is able to infect the monocyte/macrophage. So, antibodies may help to spread FIPV in stead of mediating its destruction. ADEI is a mechanism that has been reported for *in vitro* infection only.

**Fc receptor activity** Another mechanism to circumvent antibody-dependent lysis of either infected cells or virus particles, is to avoid recognition of the Fc ends of bound antibodies by either complement, phagocytes or natural killer

cells. The S proteins of MHV, BCV, TGEV and IBV but not HCoV-OC43 possess Fc receptor activity, which enables binding of the Fc end of antibodies (Oleszak et al., 1993, 1995). This could inhibit the binding of virus-specific antibodies to the antigenic domains on the S protein by sterical hindrance. It could also lead to “antibody bipolar bridging” in which virus-specific antibodies are captured by S proteins with both their Fab and Fc end, rendering them unrecognizable for immune components.

**Retention of viral proteins** A third mechanism to avoid antibody-dependent lysis of infected cells, is ensuring that there are no viral antigens for antibodies to bind on. This can be obtained by efficient intracellular retention of the viral proteins. Since all CoVs bud in the ERGIC, the viral proteins must be retained there. The retention of the structural proteins is mediated by the E protein (determines location) via M protein (captures the S protein). TGEV S protein is retained by a YXXI signal (Schwegmann-Wessels et al., 2004). This motif is present in the cytoplasmic tails of all group 1 CoVs. However, in the group 2 CoVs, only the HCoV strain OC43 has an YXX $\Psi$  motif in its tail. Such a retention signal was not found in the SARSV (a group 2b CoV) S protein either, and the S protein is indeed transported to the cell surface in SARSV infected cells. For SARSV an alternative mechanism was proposed in which the SARSV specific accessory protein U274, also called 3a, binds to the surface expressed S proteins and mediates their internalization (Tan, 2005). The S protein of IBV, the group 3 CoV, is also intracellularly retained, but by a dilysine motif (Lontok et al., 2004). Additionally, the ER retrieval signals KKXX and KXHXX (to retrieve proteins from post ER compartments back to the ER) are found in the S proteins of group 3 and group 1 CoVs (and SARSV) respectively (Lontok et al., 2004; McBride et al., 2007). Thus S proteins that might be on their way to the plasma membrane can still be stopped and recruited back to the ERGIC.

### 1.2.3 Evasion of major histocompatibility complex I dependent cell lysis

Most cells are able to express major histocompatibility complex I (MHCI) molecules on their plasma membrane. In the ER, MHCI molecules are loaded with oligopeptides from cellular, in normal situations, or viral origin, in case of an infected cell. The loaded MHCI molecules are then transported to the plasma membrane for presentation to the cytotoxic T-lymphocytes (CTL) and natural killer cells. Circulating CTLs check the presented peptides on the MHCI molecules and recognition of a peptide of foreign origin will lead to

destruction or curing of the presenting cell.<sup>¶</sup> A lack of MHC I presentation, which can be virus induced, will activate natural killer cells resulting in destruction of the cell.

**Down-regulation of MHC I expression** One way to circumvent MHC I dependent cell lysis often used by viruses, is down-regulating the MHC I expression. Not much research has been done on MHC I expression during CoV infection and most reports (circumstantially) point into the direction of a strong MHC I-dependent response. For instance, IBV-infected cells are effectively eliminated by cytotoxic T-cells, indicating that IBV infection does not severely down-regulate MHC I expression (Seo and Collisson, 1997). However, there are some diversifying reports. The hepatotropic strains of MHV are potent inducers of MHC I expression while the neurotropic strain (JHMV) did not stimulate MHC I expression (Gilmore et al., 1994). It was also found that during MHV persistence (strains A59 and JHMV) MHC I expression was not up-regulated although viral proteins were detectable in the cell (Correale et al., 1995). In *in vivo* infection of the central nervous system with MHV, MHC I expression was enhanced in the acute phase, but expression decreased during the chronic phase of disease (Redwine et al., 2001). It was recently reported that MHC I (and MHC II) expression levels were down-regulated in patients with late stage, severe SARS (Cameron et al., 2007). These are indications that late in infection or during chronic infection, some coronaviruses are able to down-regulate MHC I expression.

**Loading of MHC I** An alternative approach is preventing that oligopeptides of viral origin are loaded onto the MHC I molecules. So far, it has not been investigated if CoVs use this immune evasion mechanism.

**Elimination of effector cells** Another straightforward approach is to eliminate the CTLs or natural killer cells themselves. During FIPV infection, T-cells are strongly depleted (Kipar et al., 2001; Paltrinieri et al., 2003). It was found that a (yet unidentified) viral soluble factor can induce apoptosis in T-cells (Haagmans et al., 1996). Similar observations have been made for MHV type 3. This MHV strain causes fulminate hepatitis and induces impairment of natural killer cells by infection and subsequent apoptosis of these cells (Lehoux et al., 2004). A SARSV infection leads to lymphopenia in all subsets of lymphocytes but in patients with severe clinical illness or in patients who died,

---

<sup>¶</sup>CTLs can directly lyse a targeted cell by release of perforin and granzyme proteins, they can induce apoptosis by activating the Fas signaling pathway or they can “heal” an infected cell by production of antiviral cytokines (Andersen et al., 2006).

a more profound T-cell depletion was observed (He et al., 2005). It not yet elucidated what causes this depletion, but it is unlikely that it is caused by infection of the T-cells since lymphocytes do not express angiotensin-converting enzyme-2, the SARSV receptor.

#### 1.2.4 Evasion of apoptosis

Apoptosis or programmed cell death can be induced by virus replication directly or indirectly upon recognition of the infected cell by CTLs or natural killer cells. Inhibition of apoptosis can be useful for a virus to increase the time available for progeny virus production and to establish a state of persistent infection.

Stimulation of both apoptotic and antiapoptotic molecules during CoV infection has been described (Enjuanes et al., 2006). The outcome of this balance of the up-regulated molecules, is probably tissue and virus strain specific. For example, in epithelial cells of the enteric tract, SARSV induces antiapoptotic responses while it induces apoptosis in T cells, hepatocytes and several cell lines.

**Persistent infection** Coronaviruses from all groups are able to cause persistent infection. Although the HCoV normally cause common colds, there are reports that the group 1 HCoV 229E, possesses neurotropic properties and can cause persistent infection in the central nervous system of infected humans. HCoV 229E can indeed persistently infect oligodendrocytic and neuroglioma cell lines (Arbour et al., 1999). Persistence during FECV (also belonging to group 1) infection has been reported many times (Herrewegh et al., 1995a, 1997; Rottier, 1999; Addie and Jarret, 2001; Addie et al., 2003; de Groot-Mijnes et al., 2005). Virus can be isolated from cats that have remained in quarantine for up to 7 months (Rottier, 1999). It was found that virus persists in the lower intestinal tract where low level replication continues. Some genetic variation occurs during persistent infection. It was found that infected cats from a closed household all carry their own FECV quasispecies, while it is likely that all quasispecies originate from a single founder infection (Herrewegh et al., 1997).

Infection of mice with MHV, a group 2a CoV, can lead to a persistent infection of the central nervous system. These mice often harbor a variety of spike deletion variants, which was considered a mechanism of escaping the immune system. However, these deletions are not required for establishment of a persistent infection (Rowe et al., 1997). SARSV (group 2b) can persistently infect



Vero cells by up-regulating the antiapoptotic proteins Bcl-2 and Bcl-xL (Mizutani et al., 2006).

Persistent infection of chickens by IBV, the most important group 3 CoV, has also been reported (Naqi et al., 2003). IBV could be isolated from chickens long after shedding and clinical signs had subsided. The isolated IBV genomes had remained stable.

It remains to be elucidated how these persistent infections are established and maintained, but it is obvious that these CoV need to prevent apoptosis during their prolonged stay in their hosts. Hence, they must possess antiapoptotic properties.

### 1.3 Aims of the study

FECV is endemic in cat populations. Most infections pass by unnoticed but occasionally FECV mutates to its highly virulent counterpart: FIPV. Infection with FIPV causes chronic, mostly fatal peritonitis/vasculitis. For many years now, researchers and pharmaceutical companies have been trying to develop an efficient vaccine against FIPV. Most vaccination attempts did not provide protection. On the contrary, vaccination often led to an enhanced disease manifestation upon challenge. There is one commercial vaccine available but it is only effective under specific conditions, which are difficult to achieve in most catteries. These vaccination studies were mostly based on trial and error because the interaction of FIPV with the host immune system is poorly understood. The first part of this doctoral research consisted in examining the virus-host cell interactions of FIPV (and FECV). For the first time, this was done in the *in vivo* target and carrier cell of FIPV, the feline blood monocyte. These results are presented in Chapter 2.

It is clear however, that FIPV has developed at least one immune evasion strategy since the virus can continue replicating and spreading in the presence of a very strong humoral immune response. Based on *in vitro* studies, a mechanism was proposed that can explain how FIPV is able to spread in the presence of antibodies. Opsonization of the virus particles facilitates infection by allowing uptake via the Fc receptor instead of the virus receptor. Hence, antibodies actually may help the virus instead of counteracting it. This could explain why disease manifestation is more fulminate in seropositive than in seronegative animals upon experimental inoculation. This mechanism is known as “antibody dependent enhancement of infectivity” or ADEI. There is still some debate whether or not ADEI is important during a natural infection, since enhanced disease in seropositive cats in the field has never been reported.

Almost 20 years have passed since the initial *in vitro* studies describing ADEI were performed. In all those years, an important question has remained unanswered (and even unasked). How can an infected monocyte survive in the presence of these high antibody titers? In a FIP cat, lesions are found all over the body, so spreading must occur and infected monocytes have indeed been found to circulate in the blood stream. One would expect that the infected monocytes are eliminated by antibody-dependent complement-mediated cell lysis or antibody-dependent cell-mediated cell lysis. The pathogenesis of FIP strongly suggests that there is another immune evasion mechanism at play here.

Ergo, the second part of the present thesis consisted of finding (Chapter 3) and characterizing (Chapter 4, 5 and 6) this immune evasion mechanism.

## References

- Addie, D. and Jarret, O. (2001). Use of a reverse-transcriptase polymerase chain reaction for monitoring the shedding of feline coronavirus by healthy cats. *Vet Rec*, 148:649–653.
- Addie, D., Schaap, I., Nicolson, L., and Jarret, O. (2003). Persistence and transmission of natural type I feline coronavirus infection. *J Gen Virol*, 84:2735–2744.
- Addie, D., Toth, S., Murray, G., and Jarret, O. (1995). Risk of feline infectious peritonitis in cats naturally infected with feline coronavirus. *Am J Vet Res*, 56:429–434.
- Andersen, M., Schrama, D., Thor Straten, P., and Becker, J. (2006). Cytotoxic T cells. *J Invest Dermatol*, 126:32–41.
- Arbour, N., Ekande, S., Cote, G., Lachance, C., Chagnon, F., Tardieu, M., Cashman, N., and Talbot, P. (1999). Persistent infection of human oligodendrocytic and neuroglial cell lines by human coronavirus 299E. *J Virol*, 73:3326–3337.
- Armstrong, J., Niemann, H., Smekens, S., Rottier, P., and Warren, G. (1984). Sequence and topology of a model intracellular membrane protein, E1 glycoprotein, from a coronavirus. *Nature*, 308:5181–5185.
- Balzarini, J., Keyaerts, E., Vijgen, L., Egberink, H., De Clercq, E., Van Ranst, M., Printsevskaya, S., Olsufyeva, E., Solovieva, S., and Preobrazhenskaya, M. (2006a). Inhibition of feline (FIPV) and human (SARS) coronavirus by semisynthetic derivatives of glycopeptide antibiotics. *Antiviral Res*, 72:20–33.

- Balzarini, J., Keyaerts, E., Vijgen, L., Vandermeer, F., Stevens, M., De Clercq, E., Egberink, H., and Van Ranst, M. (2006b). Pyridine n-oxide derivatives are inhibitory to the human SARS and feline infectious peritonitis coronavirus in cell culture. *J Antimicrob Chemother*, 57:472–481.
- Baric, R., Nelson, G., Fleming, J., Deans, R., Keck, J., Casteel, N., and Stohlman, S. (1988). Interactions between coronavirus nucleocapsid protein and viral RNAs: implications for viral transcription. *J Virol*, 62:4280–4287.
- Benetka, V., Kubber-Heiss, A., Kolodziejek, J., Nowotny, N., Hofmann-Parisot, M., and Mostl, K. (2004). Prevalence of feline coronavirus types I and II in cats with histopathologically verified feline infectious peritonitis. *Vet Microbiol*, 99:31–42.
- Black, J. (1980). Recovery and in vitro cultivation of a coronavirus from laboratory induced cases of feline infectious peritonitis (FIP). *Vet Med Small Anim Clin*, 34:811–814.
- Bosch, B., de Haan, C., Smits, S., and Rottier, P. (2005). Spike protein assembly into the coronavirus: Exploring the limits of its sequence requirements. *Virology*, 334:306–318.
- Boursnell, M., Brown, T., Fould, I., Green, P., Tomley, F., and Binns, M. (1987). Completion of the sequence of the genome of the coronavirus avian infectious bronchitis virus. *J Gen Virol*, 68:57–77.
- Bredenbeek, P., Pachuk, C., Noten, A., Charite, J., Luytjes, W., Weiss, S., and W.J.M., S. (1990). The primary structure and expression of the 2nd open reading frame of the polymerase gene of the coronavirus MHV-A59 - A highly conserved polymerase is expressed by an efficient ribosomal frame shifting mechanism. *Nucleic Acids Res*, 18:1825–1832.
- Brierley, I., Boursnell, M., Binns, M., Bilimoria, B., Blok, V., Brown, T., and Inglis, S. (1987). An efficient ribosomal frame shifting signal in the polymerase-encoding region of the coronavirus IBV. *EMBO J*, 6:3779–3785.
- Cameron, M., Bermejo-Martin, J., Danesh, A., Muller, M., and Kelvin, D. (2007). Human immunopathogenesis of severe acute respiratory syndrome (SARS). *Virus Res*, in press.
- Chen, H., Wurm, T., Britton, P., Brooks, G., and Hiscox, J. (2002). Interaction of the coronavirus nucleoprotein with nucleolar antigens and the host cell. *J Virol*, 76:5233–5250.

- Corapi, W., Olsen, C., and Scott, F. (1992). Monoclonal antibody analysis of neutralization and antibody-dependent enhancement of feline infectious peritonitis virus. *J Virol*, 11:6695–6705.
- Correale, J., Li, S., Weiner, L., and Gilmore, W. (1995). Effect of persistent mouse hepatitis virus infection on MHC class I expression in murine astrocytes. *J Neurosci Res*, 40:10–21.
- de Groot, R., van Leen, R., Dalderup, M., Vennema, H., Horzinek, M., and Spaan, W. (1989). Stably expressed FIPV peplomer protein induces cell fusion and elicits neutralizing antibodies in mice. *Virology*, 171:493–502.
- de Groot-Mijnes, J., van Dun, J., van der Most, R., and de Groot, R. (2005). Natural history of a recurrent feline coronavirus infection and the role of cellular immunity in survival and disease. *J Virol*, 79:1036–1044.
- DeDiego, M., Alvarez, E., Almazan, F., Rejas, M., Lamirande, E., Roberts, A., Shieh, W., Zaki, S., Subbarao, K., and Enjuanes, L. (2007). A severe acute respiratory syndrome coronavirus that lacks the E gene is attenuated in vitro and in vivo. *J Virol*, 81:1701–1713.
- Delmas, B. and Laude, H. (1990). Assembly of coronavirus spike protein into trimers and its role in epitope expression. *J Virol*, 42:5367–5375.
- Enjuanes, L., Almazan, F., Sola, I., and Zuniga, S. (2006). Biochemical aspects of coronavirus replication and virus-host interaction. *Annu Rev Microbiol*, 60:211–230.
- Evermann, J., Baumgartner, L., Ott, R., Davis, E., and McKeirnan, A. (1981). Characterization of a feline infectious peritonitis virus isolate. *Vet Path*, 18:256–259.
- Foley, J., Poland, A., Carlson, J., and Pedersen, N. (1997). Patterns of feline coronavirus infection and fecal shedding from cats in multiple-cat environments. *J Am Vet Med Assoc*, 210:1307–1312.
- Gelain, M., Meli, M., and Paltrinieri, S. (2006). Whole blood cytokine profiles in cats infected by feline coronavirus and healthy non-FCoV infected specific pathogen-free cats. *J Fel Med Surg*, 8:389–399.
- Gerber, J. (1995). Overview of the development of a modified live temperature sensitive FIP virus vaccine. *Feline Pract*, 23:62–71.
- Gerber, J., Ingersoll, J., Gast, A., Christianson, K., Selzer, N., Landon, R., Pfeiffer, N., Sharpee, R., and Beckenhauer, W. (1990). Protection against feline infectious peritonitis by intranasal inoculation of a temperature-sensitive FIPV vaccine. *Vaccine*, 8:536–541.

- Gilmore, W., Correale, J., and Weiner, L. (1994). Coronavirus induction of class I major histocompatibility complex expression in murine astrocytes is virus strain specific. *J Exp Med*, 180:1013–1023.
- Godeke, G.-J., de Haan, C., Rossen, J., Vennema, H., and Rottier, P. (2000). Assembly of spikes into coronavirus particles is mediated by the carboxy-terminal domain of the spike protein. *J Virol*, 74:1566–1571.
- Godet, M., L'Haridon, R., Vautherot, J., and Laude, H. (1992). TGEV coronavirus ORF4 encodes a membrane protein that is incorporated into virions. *Virology*, 188:666–675.
- Gonzalez, J., Gomez-Puertas, P., Cavanagh, D., Gorbalenya, A., and Enjuanes, L. (2003). A comparative sequence analysis to revise the current taxonomy of the family Coronaviridae. *Arch Virol*, 148:2207–2235.
- Gosert, R., Kanjanahaluethai, A., Egger, D., Bienz, K., and Baker, S. (2002). RNA replication of mouse hepatitis virus takes place at double-membrane vesicles. *J Virol*, 76:3697–3708.
- Gunn-Moore, D., Gruffydd-Jones, T., and Harbour, D. (1998). Detection of feline coronaviruses by culture and reverse transcriptase-polymerase chain reaction of blood samples from healthy cats and cats with clinical feline infectious peritonitis. *Vet Microbiol*, 62:193–205.
- Haagmans, B., Egberink, H., and Horzinek, M. (1996). Apoptosis and t-cell depletion during feline infectious peritonitis. *J Virol*, 70:8977–8983.
- Haagmans, B. and Osterhaus, A. (2006). Coronaviruses and their therapy. *Antiviral Res*, 71:397–403.
- Haijema, B., Volders, H., and Rottier, P. (2004). Live, attenuated coronavirus vaccines through the directed deletion of group-specific genes provide protection against feline infectious peritonitis. *J Virol*, 78:3863–3871.
- He, Z., Zhao, C., Dong, Q., Zhuang, H., Song, S., Peng, G., and Dwyer, D. (2005). Effects of severe acute respiratory syndrome (SARS) coronavirus infection on peripheral blood lymphocytes and their subsets. *J Inf Dis*, 9:323–330.
- Herrewegh, A., de Groot, R., Cepica, A., Egberink, H., Horzinek, M., and Rottier, P. (1995a). Detection of feline coronavirus RNA in feces, tissues, and body fluids of naturally infected cats by reverse transcriptase PCR. *Clin Microbiol*, 33:684–689.

- Herrewegh, A., Mahler, M., Hedrich, H., Haagmans, B., Egberink, H., Horzinek, M., Rottier, P., and de Groot, R. (1997). Persistence and evolution of feline coronavirus in a closed cat-breeding colony. *Virology*, 234:349–363.
- Herrewegh, A., Smeenk, I., Horzinek, M., Rottier, P., and de Groot, R. (1998). Feline coronavirus type II strain 79-1683 and 79-1146 originate from a double recombination between feline coronavirus type I and canine coronavirus. *J Virol*, 72:4508–4514.
- Herrewegh, A., Vennema, H., Horzinek, M., Rottier, P., and de Groot, R. (1995b). The molecular genetics of feline coronaviruses: comparative sequence analysis of the ORF7a/7b transcription unit of different biotypes. *Virology*, 212:622–631.
- Hohdatsu, T., Izumiya, Y., and Yokoyama, Y. (1998). Differences in virus receptor for type I and type II feline infectious peritonitis virus. *Arch Virol*, 143:839–850.
- Hohdatsu, T., Nakamura, M., Ishizuka, Y., Yamada, H., and Koyama, H. (1991). A study on the mechanism of antibody-dependent enhancement of feline infectious peritonitis virus infection in feline macrophages by monoclonal antibodies. *Arch Virol*, 120:207–217.
- Hohdatsu, T., Okada, S., Ishizuka, Y., Yamada, H., and Koyoma, H. (1992). The prevalence of types I and II feline coronavirus infections in cats. *J Vet Med Sci*, 54:557–562.
- Holmes, K. (1985). *Coronavirus replication*. Raven Press, New York.
- Horsburgh, B., Brierley, I., and Brown, T. (1992). Analysis of a 9.6 kb sequence from the 3' end of canine coronavirus genomic RNA. *J Gen Virol*, 73:2849–2862.
- Hoshino, Y. and Scott, F. (1980). Immunofluorescent and electron microscopic studies of feline small intestinal organ cultures infected with feline infectious peritonitis virus. *Am J Vet Res*, 41:672–681.
- Ishida, T., Shibana, A., Tanaka, S., Uchida, K., and Mochizuki, M. (2004). Use of recombinant feline interferon and glucocorticoid in the treatment of feline infectious peritonitis. *J Feline Med Surg*, 6:107–109.
- Jacobse-Geels, H., Daha, M., and Horzinek, M. (1980). Isolation and characterization of feline C3 and evidence for the immune complex pathogenesis of feline infectious peritonitis virus. *J Immunol*, 125:1606–1610.

- Jacobse-Geels, H., Daha, M., and Horzinek, M. (1982). Antibody, immune complexes and complement activity fluctuations in experimental feline infectious peritonitis. *Am J Vet Res*, 43:666–670.
- Kennedy, M., Boedeker, N., Gibbs, P., and Kania, S. (2001). Deletions in the 7a ORF of feline coronavirus associated with an epidemic of feline infectious peritonitis. *Vet microbiol*, 81:227–234.
- Keyaerts, E., Vijgen, L., Pannecouque, C., Van Damme, E., Peumans, W., Egberink, H., Balzarini, J., and Van Ranst, M. (2007). Plant lectins are potent inhibitors of coronaviruses by interfering with two targets in the viral replication cycle. *Antiviral Res*, 75:179–187.
- Kida, K., Hohdatsu, T., Kashimoto-Tokunaga, J., and Koyama, H. (2000). Neutralization of feline infectious peritonitis virus: preparation of monoclonal antibody that shows cell tropism in neutralizing activity after viral absorption into cells. *Arch Virol*, 145:1–12.
- Kipar, A., Kohler, K., Leukert, W., and Reinacher, M. (2001). A comparison of lymphatic tissues from cats with spontaneous feline infectious peritonitis (FIP), cats with FIP virus infection but no FIP, and cats with no infection. *J Comp Path*, 125:182–191.
- Kipar, A., May, H., Menger, S., Weber, M., Leukert, W., and Reinacher, M. (2005). Morphologic features and development of granulomatous vasculitis in feline infectious peritonitis. *Vet Pathol*, 42:321–330.
- Kiss, I., Poland, A., and Pedersen, N. (2004). Disease outcome and cytokine responses in cats immunized with an avirulent feline infectious peritonitis virus (FIPV)-UCD1 and challenge-exposed with virulent FIPV-UCD8. *J Fel Med Sur*, 6:89–97.
- Kooi, C., Cervin, M., and Anderson, R. (1991). Differentiation of acid-pH-dependent and -nondependent entry pathways for mouse hepatitis virus. *Virology*, 180:108–119.
- Kopecky-Bromberg, S., Martinez-Sobrido, L., Frieman, M., Baric, R., and Palese, P. (2007). Severe acute respiratory syndrome coronavirus open reading frame (ORF) 3b, ORF 6 and nucleocapsid proteins function as interferon antagonists. *J Virol*, 81:548–557.
- Kuo, L., Godeke, G.-J., Raamsman, M., Masters, P., and Rottier, P. (2000). Retargeting of coronavirus by substitution of the spike glycoprotein ectodomain: crossing the host cell species barrier. *J Virol*, 74:1393–1406.

- Kuo, L. and Masters, P. (2003). The small envelope protein E is not essential for murine coronavirus replication. *J Virol*, 77:4597–4608.
- Kyuwa, S., Tagawa, Y.-I., Shibata, S., Doi, K., Machii, K., and Iwakura, Y. (1998). Murine coronavirus-induced subacute fatal peritonitis in C57BL/6 mice deficient in gamma interferon. *J Virol*, 72:9286–9290.
- Lehoux, M., Jaques, A., Lusignan, S., and Lamontagne, L. (2004). Murine viral hepatitis involves NK cell depletion associated with virus-induced apoptosis. *Clin Exp Immunol*, 137:41–51.
- Lim, K. and Liu, D. (2001). The missing link in coronavirus assembly. *J Biol Chem*, 276:17515–17523.
- Lontok, E., Corse, E., and Machamer, C. (2004). Intracellular targeting signals contribute to localization of coronavirus spike proteins near the virus assembly site. *J Virol*, 78:5913–5922.
- Maeda, J., Repass, J., Maeda, A., and Makino, S. (2001). Membrane topology of coronavirus E protein. *Virology*, 281:163–169.
- McArdle, F., Bennet, M., Gaskell, R., Tennant, B., Kelly, D., and Gaskell, C. (1992). Induction and enhancement of feline infectious peritonitis by canine coronavirus. *Am J Vet Res*, 53:1500–1506.
- McBride, C., Li, J., and Machamer, C. (2007). The cytoplasmic tail of the severe acute respiratory syndrome coronavirus spike protein contains a novel endoplasmic reticulum retrieval signal that binds COPI and promotes interaction with membrane protein. *J Virol*, 81:2418–2428.
- McKeirnan, A., Evermann, J., Hargis, A., and Ott, R. (1981). Isolation of feline coronaviruses from 2 cats with diverse disease manifestations. *Feline Practice*, 11(3):16–20.
- Meli, M., Kipar, A., Muller, C., Jenal, K., Gonczi, E., Borel, N., Gunn-Moore, D., Chalmers, S., Lin, F., Reinacher, M., and Lutz, H. (2004). High viral loads despite absence of clinical and pathological findings in cats experimentally infected with feline coronavirus (FCoV) type I and in naturally FCoV-infected cats. *J Feline Med Surg*, 6:69–81.
- Mizutani, T., Fukushi, S., Ishii, K., Sasaki, Y., Kenri, T., Saijo, M., Kanaji, Y., Shirota, K., Kurane, I., and Morikawa, S. (2006). Mechanisms of establishment of persistent SARS-CoV-infected cells. *Biochem Biophys Res Commun*, 347:261–265.



- Montali, R. and Strandberg, J. (1972). Extraperitoneal lesions in FIP. *Vet Path*, 9:109–121.
- Naqi, S., Gay, K., Patalla, P., Mondal, S., and Liu, R. (2003). Establishment of persistent avian infectious bronchitis virus infection in antibody-free and antibody-positive chickens. *Avian Dis*, 47:594–601.
- Narayanan, K., Maeda, A., Maeda, J., and Makino, S. (2000). Characterization of the coronavirus m protein and nucleocapsid interaction in infected cells. *J Virol*, 74:8127–8134.
- Nash, T. and Buchmeier, M. (1997). Entry of mouse hepatitis virus into cells by endosomal and nonendosomal pathways. *Virology*, 233:1–8.
- Oleszak, E., Kuzmak, J., Hogue, B., Parr, R., Collisson, E., Rodkey, L., and Leibowitz, J. (1995). Molecular mimicry between Fc receptor and S peplomer protein of mouse hepatitis virus, bovine coronavirus, and transmissible gastroenteritis virus. *Hybridoma*, 14:1–8.
- Oleszak, E., Perlman, S., Parr, R., Collisson, E., and Leibowitz, J. (1993). Molecular mimicry between S peplomer proteins of coronaviruses MHV, BCV, TGEV and IBV and Fc receptor. *Adv Exp Med Biol*, 342:183–188.
- Olsen, C., Corapi, W., Ngichabe, C., Baines, J., and Scott, F. (1992). Monoclonal antibodies to the spike protein of feline infectious peritonitis virus mediate antibody-dependent enhancement of infection of feline macrophages. *J Virol*, 66:956–965.
- Opstelten, D.-J., Raamsman, M., Wolfs, K., Horzinek, M., and Rottier, P. (1995). Envelope glycoprotein interactions in coronavirus assembly. *J Cell Biol*, 131:339–349.
- O'Reilly, K. J., Fishman, L., and Hitchcock, L. (1979). Feline infectious peritonitis: isolation of a coronavirus. *Vet Rec*, 104:348–348.
- Ortego, J., Escors, D., Laude, H., and Enjuanes, L. (2002). Generation of a replication-competent, propagation-deficient virus vector based on the transmissible gastroenteritis coronavirus genome. *J Virol*, 76:11518–11529.
- Paltrinieri, S., Ponti, W., Comazzi, S., Giordano, A., and Poli, G. (2003). Shifts in circulating lymphocyte subsets in cats with feline infectious peritonitis (FIP): pathogenic role and diagnostic relevance. *Vet Immunol Immunopathol*, 96:141–148.
- Parker, M. and Masters, P. (1990). Sequence comparison of the N genes of five strains of the coronavirus mouse hepatitis virus suggests a three domain structure for the nucleocapsid protein. *Virology*, 179:463–468.

- Pedersen, K., van der Meer, Y., Roos, N., and E.J., S. (1999). Open reading frame 1a-encoded subunits of the arterivirus replicase induce endoplasmic reticulum-derived double-membrane vesicles which carry the virus replication complex. *J Virol*, 73:2016–2026.
- Pedersen, N. and Black, J. (1983). Attempted immunization of cats against feline infectious peritonitis using either avirulent virus or sublethal amounts of virulent virus. *Am J Vet Res*, 44:229–234.
- Pedersen, N., Black, J., Boyle, J., Evermann, J., McKeirnan, A., and Ott, R. (1983). Pathogenic differences between various feline coronavirus isolates. In *Molecular Biology and Pathogenesis of Coronaviruses*. London, Plenum Press.
- Pedersen, N. and Boyle, J. (1980). Immunologic phenomena in the effusive form of feline infectious peritonitis. *Am J Vet Res*, 41:868–876.
- Pedersen, N., Boyle, J., Floyd, K., Fudge, A., and Barker, J. (1981). An enteric coronavirus infection of cats and its relationship to feline infectious peritonitis. *Am J Vet Res*, 42:368–376.
- Pedersen, N., Evermann, J., McKeirnan, A., and Ott, R. (1984). Pathogenicity studies of feline coronavirus isolates 79-1146 and 79-1683. *Am J Vet Res*, 45:2580–2585.
- Poland, A., Vennema, H., Foley, J., and Pedersen, N. (1996). Two related strains of feline infectious peritonitis virus isolated from immunocompromised cats infected with a feline enteric coronavirus. *J clin microbiol*, 34:3180–3184.
- Postorino Reeves, N. (1995). Vaccination against naturally occurring FIP in a large cat shelter. *Feline Pract*, 23:80–82.
- Redwine, J., Buchmeier, M., and Evans, C. (2001). In vivo expression of major histocompatibility complex molecules on oligodendrocytes and neurons during viral infection. *Am J Pathol*, 159:1219–1224.
- Ritz, S., Egberink, H., and Hartmann, K. (2007). Effect of feline interferon-omega on the survival time and quality of life of cats with feline infectious peritonitis. *J Vet Intern Med*, 21:1193–1197.
- Rottier, P. (1999). The molecular dynamics of feline coronaviruses. *Vet Microbiol*, 69:117–125.
- Rottier, P., Horzinek, M., and van der Zeijst, B. (1981). Viral protein synthesis in mouse hepatitis virus strain A-59 infected cells: effect of tunicamycin. *J Virol*, 40:350–357.

- Rottier, P., Nakamura, K., Schellen, P., Volders, H., and Haijema, B. (2005). Acquisition of macrophage tropism during pathogenesis of feline infectious peritonitis is determined by mutations in the feline coronavirus spike protein. *J Virol*, 79:14122–14130.
- Rottier, P. and Rose, J. (1987). Coronavirus E1 glycoprotein expressed from cloned cDNA localizes in the golgi region. *J Virol*, 61:2042–2045.
- Rottier, P., Welling, G., Welling-Wester, S., Niesters, H., Lenstra, J., and van der Zeijst, B. (1986). Predicted membrane topology of the coronavirus protein E1. *Biochem*, 25:1335–1339.
- Rowe, C., Baker, S., Nathan, M., and Fleming, J. (1997). Evolution of mouse hepatitis virus: detection and characterization of spike deletion variants during persistent infection. *J Virol*, 71:2959–2969.
- Sawicki, S., Sawicki, D., and Siddell, S. (2007). A contemporary view of coronavirus transcription. *J Virol*, 81:20–29.
- Schwegmann-Wessels, C., Al-Falah, M., Escors, D., Wang, Z., Zimmer, G., Deng, H., Enjuanes, L., Naim, H., and Herrler, G. (2004). A novel sorting signal for intracellular localization is present in the s protein of a porcine coronavirus but absent from severe acute respiratory syndrome-associated coronavirus. *J Biol Chem*, 279:43661–43666.
- Seo, S. and Collisson, E. (1997). Specific cytotoxic T lymphocytes are involved in in vivo clearance of infectious bronchitis virus. *J Virol*, 71:5173–5177.
- Spiegel, M., Pichlmair, A., Martinez-Sobrido, L., Cros, J., Garcia-Sastre, A., Haller, O., and Weber, F. (2005). Inhibition of beta interferon induction by severe acute respiratory syndrome coronavirus suggests a two-step model for activation of interferon regulatory factor 3. *J Virol*, 79:2079–2086.
- Stoddart, M. and Scott, F. (1989). Intrinsic resistance of feline infectious peritoneal macrophages to coronavirus infection correlates with in vivo virulence. *J Virol*, 63:436–440.
- Stohlman, S., Baric, R., Nelson, G., Soe, L., Welter, L., and Deans, R. (1988). Specific interaction between coronavirus leader RNA and nucleocapsid protein. *J Virol*, 62:4288–4295.
- Stohlman, S. and Lai, M. (1979). Phosphoproteins of murine hepatitis viruses. *J Virol*, 32:672–675.

- Tahara, S., Dietlin, T., Nelson, G., Stohlman, S., and Manno, D. (1998). Mouse hepatitis virus nucleocapsid protein as a translational effector of viral mRNAs. *Adv Exp Med Biol*, 440:313–318.
- Tan, Y.-J. (2005). The severe acute respiratory syndrome (SARS)-coronavirus 3a protein may function as a modulator of the trafficking properties of the spike protein. *Virology*, 2:5.
- Tresnan, D., Levis, R., and Holmes, K. (1996). Feline aminopeptidase N serves as a receptor for feline, canine, porcine and human coronaviruses in serogroup I. *J Virol*, 70:8669–8674.
- Van Hamme, E., Dewerchin, H., Cornelissen, E., and Nauwynck, H. (2007). Attachment and internalization of feline infectious peritonitis virus in feline blood monocytes and Crandell feline kidney cells. *J Gen Virol*, 88:2527–2532.
- Van Hamme, E., Dewerchin, H., Cornelissen, E., Verhasselt, B., and Nauwynck, H. (2008). Clathrin- and caveolae-independent entry of feline infectious peritonitis virus in monocytes depends on dynamin. *J Gen Virol*, In press.
- Vennema, H., de Groot, R., Harbour, D., Dalderup, M., Gruffydd-Jones, T., Horzinek, M., and Spaan, W. (1990a). Early death after feline infectious peritonitis challenge due to recombinant vaccinia virus immunization. *J Virol*, 64:1407–1409.
- Vennema, H., Poland, A., Floyd Hawkins, K., and Pedersen, N. (1995). A comparison of the genomes of FECVs and FIPVs: what they tell us about the relationships between feline coronaviruses and their evolution. *Feline Pract*, 23:40–44.
- Vennema, H., Poland, A., Foley, J., and Pedersen, N. (1998). Feline infectious peritonitis viruses arise by mutation from endemic feline enteric coronaviruses. *Virology*, 243:150–157.
- Vennema, H., Rottier, P., Heijnen, L., Godeke, G., Horzinek, M., and Spaan, W. (1990b). Biosynthesis and function of the coronavirus spike protein. *Adv Exp Med Biol*, 276:9–19.
- Versteeg, G., Bredenbeek, P., van den Worm, S., and Spaan, W. (2007). Group 2 coronaviruses prevent immediate early interferon induction by protection of viral rna from host cell recognition. *Virology*, 361:18–26.
- Ward, J. (1970). Morphogenesis of a virus in cats with experimental feline infectious peritonitis. *Virology*, 41:191–194.

- Ward, J., Munn, R., Gribble, D., and Dungworth, D. (1968). An observation of FIP. *Vet Res*, 83:416–417.
- Watari, T., Kaneshima, T., Tsujimoto, H., Ono, K., and Hasegawa, A. (1998). Effect of thromboxane synthetase inhibitor on feline infectious peritonitis in cats. *J Vet Med Sci*, 60:657–659.
- Wege, H., Sidell, S., and Ter Meulen, V. (1982). The biology and pathogenesis of coronaviridae. *Curr Topics Microbiol Immunol*, 99:165–200.
- Weiss, R. and Scott, F. (1981a). Pathogenesis of feline infectious peritonitis: nature and development of viraemia. *Am J Vet Res*, 42:382–390.
- Weiss, R. and Scott, F. (1981b). Pathogenesis of feline infectious peritonitis: pathologic changes and immunofluorescence. *Am J Vet Res*, 42:2036–2048.
- Wilson, L., McKinlay, C., Gage, P., and Ewart, G. (2004). SARS coronavirus E protein forms cation-selective ion channels. *Virology*, 330:322–331.
- Ye, Y., Hauns, K., Langland, J., Jacobs, B., and Hogue, B. (2007). Mouse hepatitis coronavirus A59 nucleocapsid protein is a type I interferon antagonist. *J Virol*, 81:2554–2563.
- Yu, X., Bi, W., Weiss, S., and Leibowitz, J. (1994). Mouse hepatitis virus gene 5b protein is a new virion envelope protein. *Virology*, 202:1018–1023.
- Zook, B., King, N., Robinson, R., and McCombs, H. (1968). Ultrastructural evidence for the viral etiology of feline infectious peritonitis. *Pathol Vet*, 5:91.
- Zuniga, S., Sola, I., Moreno, J., Sabella, P., Plana-Duran, J., and Enjuanes, L. (2007). Coronavirus nucleocapsid protein is an RNA chaperone. *Virology*, 357:215–227.



# 2

## Replication of feline coronaviruses in peripheral blood monocytes\*

### Summary

Feline infectious peritonitis virus (FIPV), causes the most lethal viral infection in cats: FIP. The related feline enteric coronavirus (FECV) causes mild enteritis. Why these feline coronaviruses manifest so differently *in vivo* is not known. In this study, infection kinetics (titers and antigen expression) of FIPV 79-1146, and FECV 79-1683, were determined in peripheral blood monocytes from 3 donor cats and compared to those in Crandell feline kidney (CrFK) cells. The infection kinetics in monocytes were host dependent. Monocytes from 1 cat were resistant to both FIPV- and FECV-infection. Monocytes from the other 2 cats could initially be infected by both FIPV and FECV but FIPV infection was sustained in monocytes of only one cat. FECV-infection was never sustained and viral production was up to 100 times lower than in FIPV-infected monocytes. In CrFK cells, FIPV and FECV infection kinetics did not differ. In monocytes of a larger cat population (n=19) the 3 infection patterns were also found. Considering all 22 investigated cats, 3/22 were not susceptible for FIPV and FECV. The rest could be infected with FECV and FIPV but 10/22 cats had monocytes that only sustained FIPV infection and 9/22 sustained neither FIPV nor FECV infection.

---

\*This Chapter was based on Dewerchin et al. (2005).

## 2.1 Introduction

Two coronaviruses are described in cats: feline infectious peritonitis virus (FIPV) and feline enteric coronavirus (FECV). These feline coronaviruses are spread world-wide and infect cats and other members of the Felidae family. An infection with FECV is usually sub-clinical, except in young kittens where it may cause mild to severe diarrhea (Pedersen et al., 1981). In contrast, FIPV infection causes a chronic and very often fatal pleuritis/peritonitis. It is the most important cause of death of infectious origin in cats. Two forms of FIP exist: the effusive or wet form with the typical effusions in body cavities and the less common non-effusive or dry form (Addie et al., 2003). Characteristic lesions of both forms are granulomas on the surface of target tissues. Despite the large biological differences, more than 98% of the genome is identical in FIPV and FECV isolates from the same environment (Vennema et al., 1995). Therefore, it has been proposed that FIPV arises from FECV by mutation but the exact mutation and the inducing factors have not yet been clarified (Poland et al., 1996; Vennema et al., 1998).

The main difference between FECV and FIPV is the invasive nature of FIPV. FECV replicates mainly locally, in enterocytes of the intestine, whereas FIPV also infects monocytes and spreads systemically (Weiss and Scott, 1981a,b). The reason for this pathogenic difference is not understood. After infiltration of infected monocytes in the perivascular tissue, the infected monocytes and surrounding cells release numerous chemotactic and vasoactive factors (Weiss et al., 1988; Goitsuka et al., 1990, 1991). This leads to vasodilatation and increased vascular permeability and attraction of new monocytes to the area, which can be infected in turn. The outcome of the inflammatory reaction is a characteristic vasculitis which causes the venules to leak large amounts of protein rich plasma into the body cavity. The release of progeny virus also leads to the formation of virus-antibody-complement complexes which are concentrated around the small venules in the target organs (Jacobse-Geels et al., 1980). These complexes further activate inflammation.

Although the difference between FIPV and FECV is very clear *in vivo*, it is not *in vitro*. The first *in vitro* characterization of FIPV strain 79-1146 and FECV strain 79-1683 was done by McKeirnan et al. (1987) in Crandell feline kidney (CrFK) cells. They found similar growth curves for FIPV and FECV. The replication of FIPV and FECV was also studied in peritoneal macrophages (Stoddart and Scott, 1989). It was reported that FECV infected fewer macrophages and reached lower production titers than FIPV. The *in vivo* relevance of these infection studies is most likely higher than those performed in a continuous cell line. But, until now, the FIPV and FECV replication cycles have



never been studied in the *in vivo* target/carrier cell of FIPV: the feline blood monocyte.

In the present study, we present the *in vitro* replication kinetics of FIPV and FECV in the target cell of FIPV, the blood monocyte. It was found that the replication kinetics were dependent on the origin of the cells. No differences between FIPV and FECV were found in CrFK cells.

## 2.2 Materials and Methods

**Viruses** A third passage of FIPV strain 79-1146 and FECV strain 79-1683 on CrFK cells was used (McKeirnan et al., 1981). FECV strain 79-1683 was obtained from the American Type Culture Collection (ATCC) and FIPV strain 79-1146 was kindly provided by Dr. Egberink (Utrecht University, the Netherlands).

**Antibodies** Polyclonal antibodies originating from cats infected with FIPV 79-1146 were kindly provided by Dr. Egberink (Utrecht University, the Netherlands). These antibodies were purified and biotinylated according to manufacturer's instructions (Amersham Bioscience, Buckinghamshire, UK). The monoclonal antibodies 7-4-1, F19-1, E22-2, recognizing respectively the S, M and N protein, were kindly provided by Dr. Hohdatsu (Kitasato University, Japan). A monocyte marker, DH59B, recognizing CD 172a was purchased from Veterinary Medical Research and Development (Pullman, Washington, USA).

**Cats** Three cats of a non-specific breed from a FCoV free closed household were used as blood donors for the extensive infection kinetics study. Seventeen stray cats brought to the clinic of small animals in the Faculty of Veterinary Medicine (Ghent University) and 2 SPF cats were used for a study on the distribution of the infection kinetics patterns. The sex and FeLV, FIV and FCoV status of the cats are listed in Table 2.1.

**Isolation of blood monocytes** Six ml blood was collected on heparin (Leo, Zaventem, Belgium) (15U/ml) from the vena jugularis and blood mononuclear cells were separated on Ficoll-Paque (Pharmacia Biotech AB, Uppsala, Sweden) following manufacturer's instructions. Mononuclear cells were resuspended in RPMI-1640 (Gibco BRL, Merelbeke, Belgium) medium containing 10% fetal bovine serum (FBS), 0.3 mg/ml glutamine, 100 U/ml peni-

Cat no.	Sex <sup>a</sup>	FeLV antigen <sup>b</sup>	FIV antibody <sup>b</sup>	FCoV titer <sup>c</sup>
Closed household				
1	M	-	-	<20
2	M	-	-	<20
3	M	-	-	<20
Population of stray cats				
1	F	-	-	<20
2	F	-	-	<20
3	F	+	-	<20
4	F	-	+	<20
5	F	-	+	<20
6	M	-	-	<20
7	M	+	-	<20
8	F	+	-	<20
9	F	+	-	<20
10	F	-	-	80
11	M	-	-	<20
12	M	-	-	<20
13	F	-	-	<20
14	F	-	-	<20
15	F	-	-	<20
16	M	-	-	<20
17	F	-	-	<20
SPF cats				
1	F	-	-	<20
2	F	-	-	<20

Table 2.1: Sex and feline leukemia virus (FeLV), feline immuno deficiency virus (FIV) and feline coronavirus (FCoV) status of the cats. <sup>a</sup>M: male, F: female. <sup>b</sup>Tested on plasma samples with SNAP FIV Antibody/FeLV Antigen Combo Test (IDEXX). <sup>c</sup>IPMA antibody titer.

cillin, 0.1 mg/ml streptomycin, 0.1 mg/ml kanamycin, 10 U/ml heparin, 1mM sodium pyruvate, and 1% non-essential amino-acids 100x (Gibco BRL). Afterward, cells were seeded in a 24-well dish with cell culture coating (Nunc A/S, Roskilde, Denmark) at a concentration of  $2 \times 10^6$  cells/ml and cultivated at 37°C with 5% CO<sub>2</sub>. Non-adherent cells were removed by washing the dishes two times with RPMI-1640 at 2 and 24 hours after seeding. The adherent cells consisted for  $86 \pm 7\%$  of monocytes (as assessed by fluorescent staining with the monocyte marker DH59B).

**Inoculation of CrFK cells and monocytes** CrFK cells and monocytes were inoculated with FIPV strain 79-1146 or FECV strain 79-1683 at a multiplicity of infection (m.o.i.) of 5. After 1 hour incubation at 37°C with 5% CO<sub>2</sub>, cells were washed 3 times with RPMI-1640 and further incubated in medium.

**Growth curves of FCoV** At different time points post inoculation, culture medium was harvested and centrifuged at 400xg for 10 minutes. The supernatant was used for determination of extracellular virus titers. The cells were removed from the well by scraping and added to the pellet for determination of intracellular virus titer. Virus was released from the cells by 2 freeze-thaw cycles. The samples were stored at -70°C until titration. Both intra- and extracellular virus titers were assessed by a 50% tissue culture infective dose (TCID<sub>50</sub>) assay using CrFK cells. The fifty percent end-point was calculated according to the method of Reed and Muench (1938). A virus inactivation curve was determined by keeping cell free virus in medium at 37°C with 5% CO<sub>2</sub>. Samples were taken at different time points and stored at -70°C until titration. Three independent assays were carried out and the inactivation curve was calculated by linear regression.

**Visualization of viral antigens in FCoV infected cells** At different time points post inoculation, cells seeded on glass coverslips, were fixed with 1% formaldehyde. Surface-expressed viral proteins were labeled with biotinylated anti-FIPV polyclonal cat antibodies and streptavidin-FITC (Molecular Probes, Eugene, Oregon, USA). After permeabilization with 0.1% Triton X-100 (Sigma-Aldrich GmbH, Steinheim, Germany), cytoplasmic viral proteins were stained with a mixture of monoclonal antibodies (7-4-1, F19-1 and E22-2) and with goat anti-mouse-Texas Red (Molecular Probes). Finally, the glass coverslips were mounted on microscope slides using glycerin-PBS solution (0.9:0.1, vol/vol) with 2.5% 1,4-diazabicyclo(2, 2, 2)octane (Janssen Chimica, Beerse, Belgium) and analyzed by fluorescence microscopy. For the stray cats

and SPF cats, only cytoplasmic viral proteins were stained with FITC labeled anti-FIPV antibodies (VMRD Inc, Pullman, Washington, USA).

**Confocal laser scanning microscopy** The samples were stained to visualize the cytoplasmic and the surface-expressed viral proteins as described above and examined with a Leica TCS SP2 laser scanning spectral confocal system (Leica Microsystems GmbH, Wetzlar, Germany) linked to a DM IRB inverted microscope (Leica Microsystems). Argon and Helium/Neon laser lights were used to excite FITC (488 nm line) and Texas-Red (543 nm line) fluorochromes. The images were obtained and processed with Leica confocal software.

**Statistical analysis** All experiments were repeated 2 or more times. The “area under the curve” was calculated for each experiment. Triplicate assays were compared using a Mann-Whitney U test. Statistical analysis were performed with SPSS 11.0 (SPSS Inc. Chicago, Illinois, USA).

## 2.3 Results

### 2.3.1 Growth curves of feline coronaviruses in CrFK cells

The growth curves of FIPV and FECV in CrFK cells are given in Figure 2.1. Production of progeny virus started between 3 and 6 hpi and increased strongly until 12 hpi. Between 12 and 24 hpi there was only a slight increase of virus titers to reach a maximum of  $6.8 \log_{10} \text{TCID}_{50}/10^6 \text{cells}$  at 24 hpi. There was no significant difference between the growth curves of FIPV and FECV.

### 2.3.2 Expression kinetics of cytoplasmic and surface-expressed viral antigens in FCoV-infected CrFK cells

Figure 2.2 shows that the first viral antigen positive cells appeared between 3 and 6 hours post inoculation. Between 12 and 24 hpi, there was a vast increase of infected cells. At 24 hpi, 86% of the cells showed cytoplasmic expression of viral proteins and 75% surface expression. There is no significant difference (area under the curve) between the FIPV curve and the FECV curve. The amount of infectious virus produced per cell can, theoretically, be calculated from the virus titers and the percentage of infected cells. For both FIPV- and FECV-infected CrFK cells, productivity was less than 10 infectious viruses per infected cell.

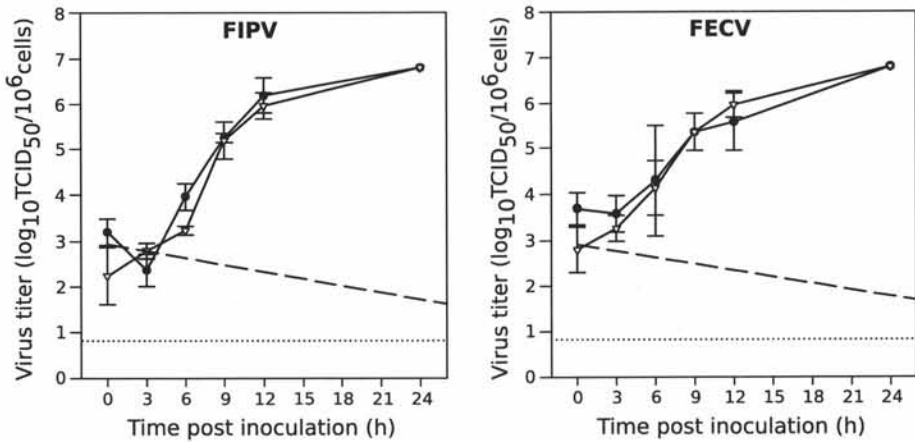


Figure 2.1: Kinetics of FIPV and FECV replication in CrFK cells. At designated time points post inoculation, the intracellular (●) and extracellular (▽) virus titers were determined. The dashed line represents the inactivation curve and the dotted line is the detection limit. The data represent means  $\pm$  SD of triplicate assays.

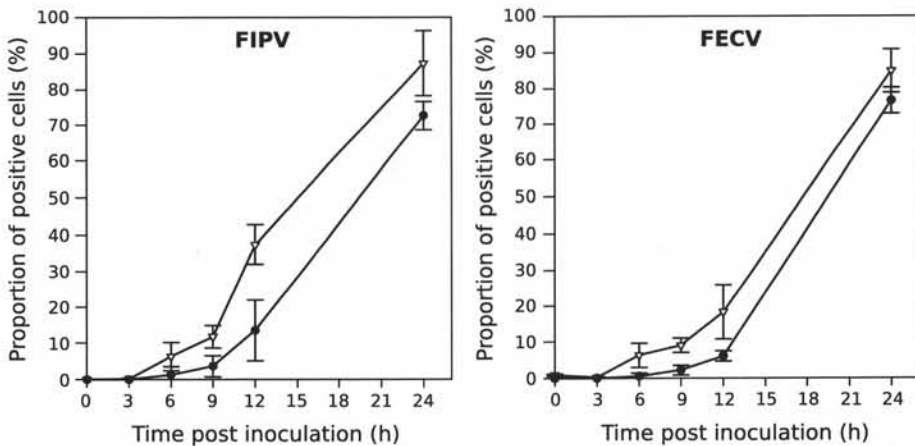


Figure 2.2: Kinetics of expression of viral antigens in FIPV and FECV infected CrFK cells. At designated time points post inoculation the cells were fixed and cytoplasmic (▽) and surface-expressed (●) viral proteins were visualized with an immunofluorescence staining. The data represent means  $\pm$  SD of triplicate assays.

### 2.3.3 Growth curves of feline coronaviruses in monocytes

The growth curves of FIPV and FECV in monocytes varied between three donor cats from a closed household. Figure 2.3a and 2.4a show that the production of FIPV started between 3 and 6 hours post inoculation for both cat 1 and 2. Between 12 and 24 hours post inoculation there was a slight increase in virus titer for cat 1 whereas the curve from cat 2 reached a plateau at 12 hours post inoculation. The virus release curves were similar (Figure 2.3c and 2.4c). The growth curves of cat 1 for FECV showed a low-level production (Figure 2.3b and d). The growth curves of cat 2 for FECV began with a slight titer increase, similar to the FIPV growth curve, but then the virus titer decreased with a slope comparable to the inactivation curve (Figure 2.4b and d). These findings suggest that monocytes could be infected by FECV but that the cells did not sustain a productive infection. Figure 2.5 shows that the growth curves for cat 3 followed the inactivation curve, suggesting that there was no progeny virus produced.

### 2.3.4 Expression kinetics of cytoplasmic and surface-expressed viral antigens in FCoV-infected monocytes

Figure 2.6 shows confocal images of cytoplasmic and surface-expressed viral antigens in monocytes infected with FIPV 79-1146. Surface expression was only detected in an average of 49% of the infected monocytes (24 hpi). No differences in the amount of infected cells with surface expression were seen between the cats or between FIPV and FECV infection. Depending on the cell, the amount of viral antigens expressed on the surface varied. The majority of the infected monocytes showed a small amount of surface-expressed viral proteins (Figure 2.6, lane 1). Some showed a larger amount of surface-expressed viral proteins (Figure 2.6, lane 2).

The antigen expression kinetics varied between the donor cats. Figure 2.3e and f show the FIPV and FECV cytoplasmic expression kinetics for cat 1. The percentage of FIPV infected cells with cytoplasmic expression increased till 24hpi. The infection of monocytes with FECV initiated in the same manner but at 12 hpi the curve started to decline. The cytoplasmic expression in monocytes of cat 2 is shown in Figure 2.4e and f. Infection with FIPV or FECV led to the same expression kinetics. After an increase till 6 or 12 hours post inoculation the percentage of cells with viral expression decreased rapidly. The number of FECV infected monocytes was lower than the FIPV-infected monocytes. The FIPV and FECV surface expression, for both cat 1 and 2, followed the same curve as the cytoplasmic expression but at a lower percentage (Figure 2.3g and h; Figure 2.4g and h). The results of cat 3 were quite different from cat 1 and

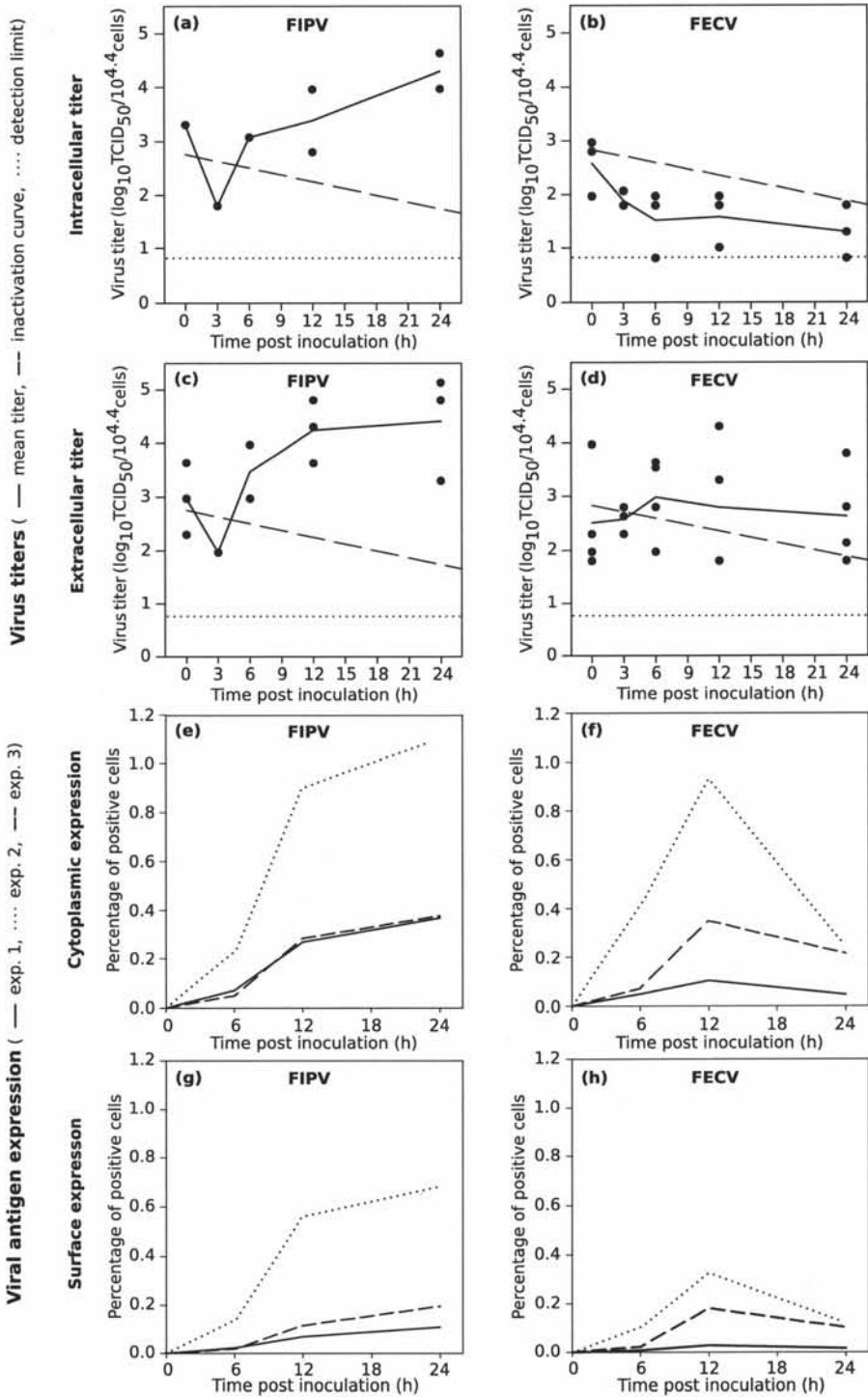


Figure 2.3: Kinetics of FIPV and FECV replication in blood monocytes from cat 1.

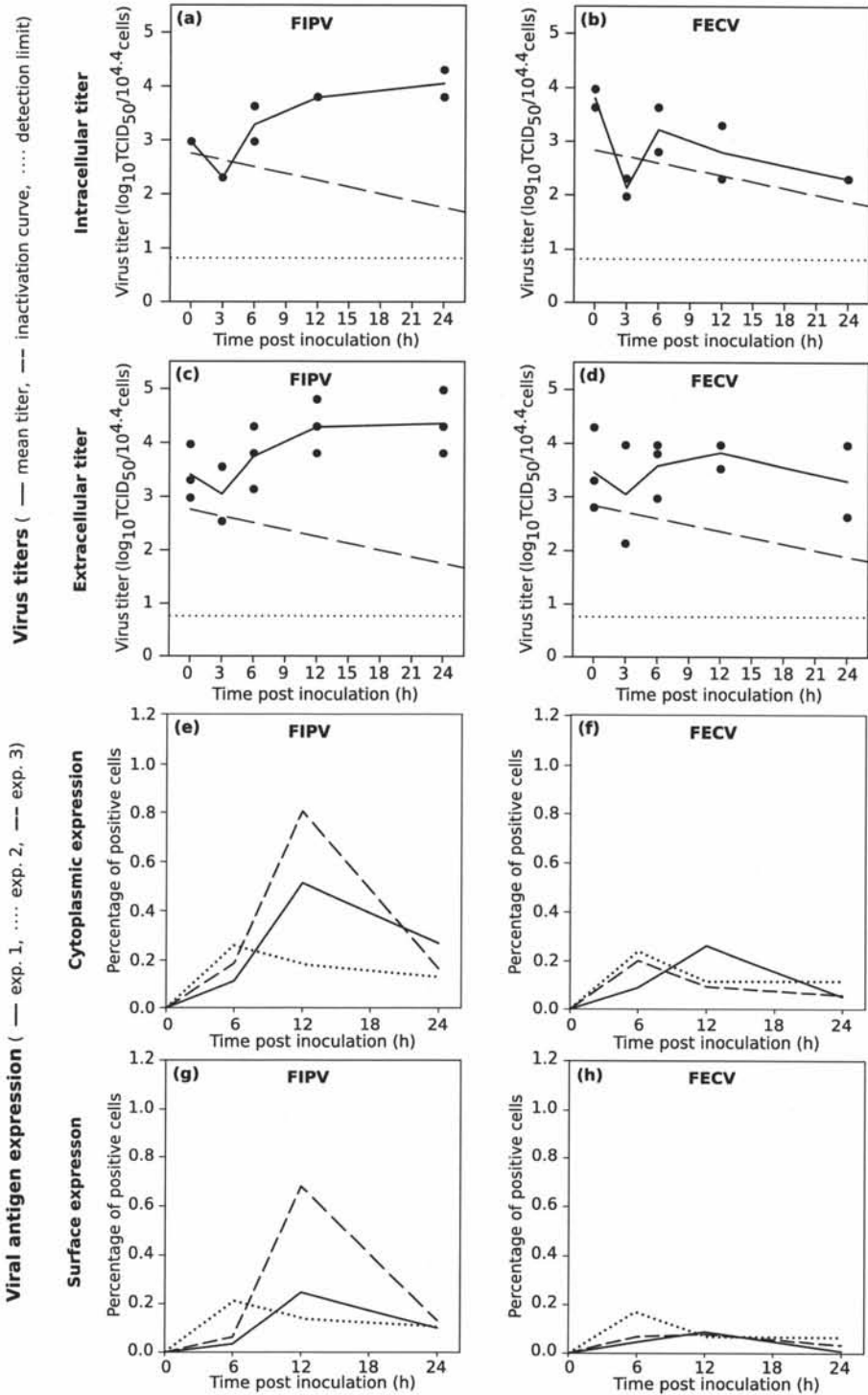


Figure 2.4: Kinetics of FIPV and FECV replication in blood monocytes from cat 2.



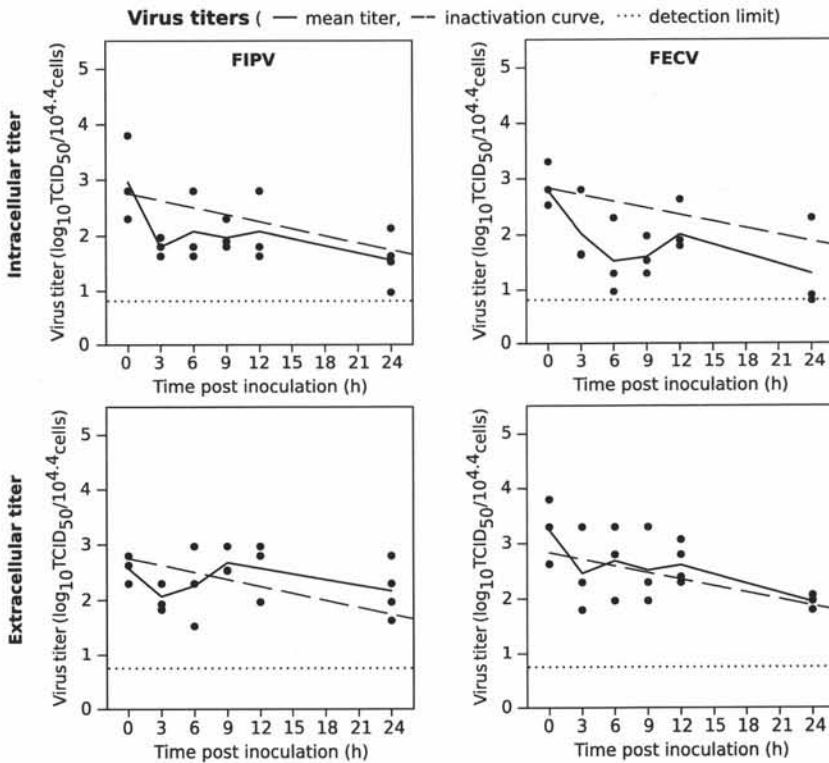


Figure 2.5: Kinetics of FIPV and FECV replication in blood monocytes from cat 3.

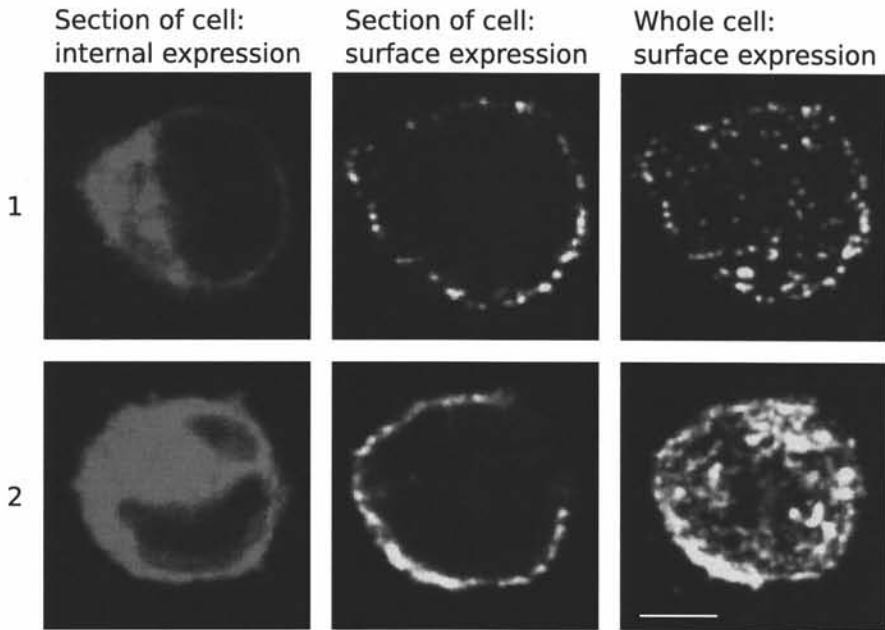


Figure 2.6: Cytoplasmic expression (left) and surface expression (right) of viral proteins in a monocyte infected with FIPV 79-1146, visualized by confocal microscopy. Bar= 5 $\mu$ m.

2. Here, viral antigen positive monocytes were not found.

Knowing the total production of infectious progeny virus and the number of infected cells, it can be calculated that FIPV-infected monocytes from both cat 1 and 2 have produced approximately 200 infectious viruses per infected cell at 12 hours post inoculation. FECV-infected monocytes from cat 1 produced 10 times less progeny virus at 12 hours post inoculation whereas the FECV-infected monocytes from cat 2 produced the same amount of progeny virus as the FIPV-infected monocytes.

### 2.3.5 Infection kinetics in a larger population of cats

In order to clarify the prevalence of the patterns of viral replication observed in this study in a bigger cat population, the antigen expression kinetics were studied in 17 stray cats and 2 SPF cats for both FIPV and FECV. The antigen expression was visualized at 0, 12 and 24 hours post inoculation. The results are presented in Figure 2.7. The 3 different expression kinetics that were found in monocytes from the closed household cats were also seen in monocytes from the stray cats and the SPF cats. Within this population of 19 cats, the monocytes isolated from 9 cats showed a continuous increase in viral antigen positive

cells during a 24 hour time span after inoculation with FIPV. When these monocytes were inoculated with FECV, the number of viral antigen positive cells increased until 12 hours post inoculation and then diminished. In monocytes from 8 cats, the percentages of both FIPV- and FECV-infected cells increased until 12 hpi and then decreased. The monocytes from 2 cats were resistant to infection.

## 2.4 Discussion

In this study, *in vitro* infection kinetics of FIPV (strain 79-1146) and FECV (strain 79-1683) were established in peripheral blood monocytes from 22 cats (3 cats of a closed household, 17 stray cats and 2 SPF cats). It is the first time that infection studies were performed in peripheral blood monocytes, the host/carrier cell of FIPV. Three distinct patterns were found in the infection studies.

Monocytes from 3 cats were not infected by either strain (first pattern). The reason for the insusceptibility of these cells is not yet clear. Virus particles were detected in the cells shortly after inoculation of the cells but no production of viral antigens was observed using polyclonal antibodies (data not shown). Thus, it seems that new viral proteins were not formed. This suggests that the block of infection is located after entry of the virus but before (or at) the translation step. *In vivo*, resistance to FIPV infection has been observed in experimental inoculations. After inoculation with a lethal dose of FIPV, a varying part of the cats (depending on experiment 8-50%) showed no clinical signs and some of them remained seronegative (Weiss and Cox, 1989). This was also seen in control groups of vaccination trials (no vaccination, only FIPV challenged) (McArdle et al., 1995; Scott et al., 1995). Resistance to FCoV infection has also been suggested to occur in natural infections in the field (Addie and Jarret, 2001). A small percentage of cats in FCoV endemic households had no shedding, remained seronegative or had a low antibody titer over a time period of 5 years. It would be most interesting to investigate the correlation between *in vitro* and *in vivo* resistance to FCoV. This might give perspectives for selection of cats insusceptible for FIP.

Monocytes from 10 cats showed an increase of FIPV antigen positive cells till 24 hpi whereas the amount of FECV antigen positive cells dropped after 12 hpi. This shows that the FIPV infection was sustained whereas the FECV infection was not sustained (second pattern). Monocytes from 9 cats did not sustain both FIPV and FECV infection since the number of viral antigen positive cells dropped after 6 or 12 hpi (third pattern). The drop in antigen positive

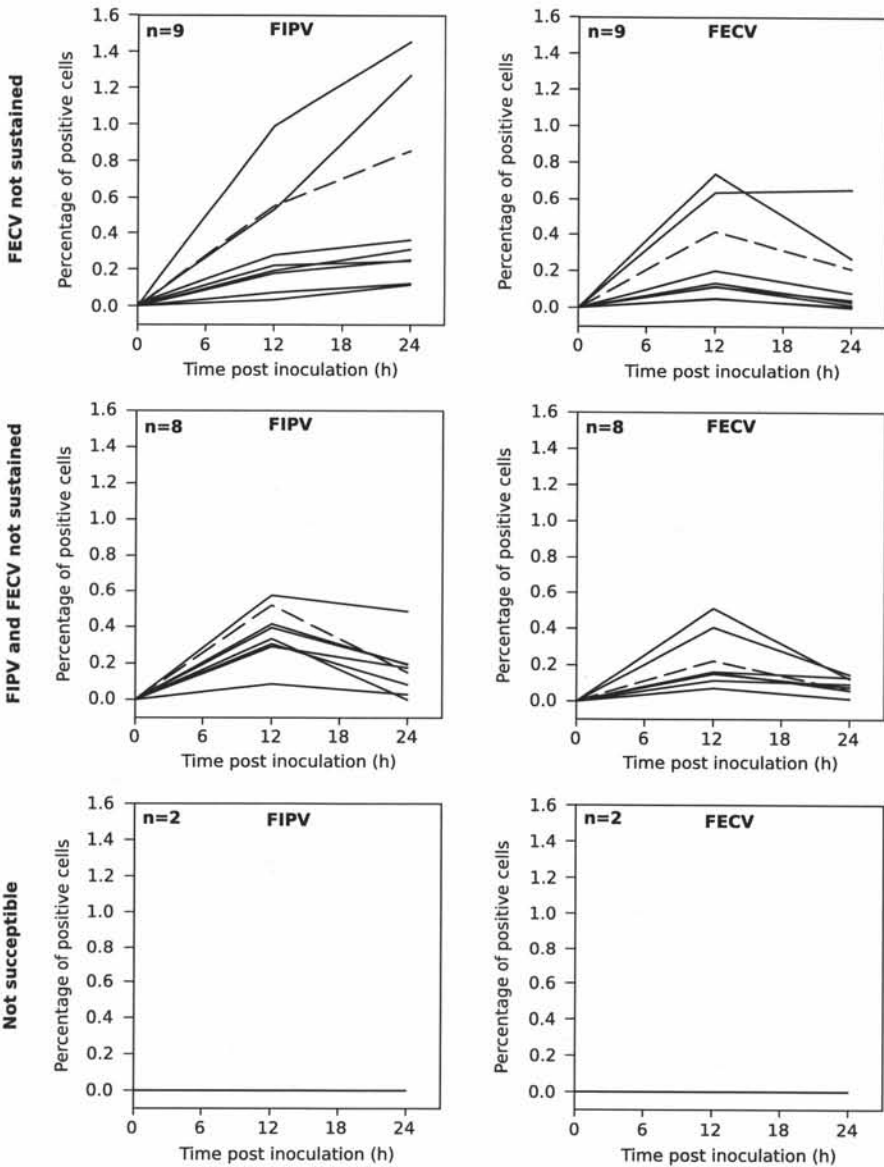


Figure 2.7: Kinetics of FIPV and FECV replication in blood monocytes from 17 stray cats (solid line) and 2 SPF cats (dashed line). Each curve represents the FIPV or FECV infection kinetics from 1 cat.

cells after 6 or 12 hours post inoculation may be explained by the fact that the infected cells died due to infection and were washed away during the staining. However, the same kinetics were found with staining in suspension, a technique which prevents cell loss (data not shown). Another explanation is that monocytes stopped producing viral proteins and assembling new virions. The extracellular virus titers showed indeed that (almost) no new progeny virus was produced between 12 and 24 hours post inoculation. Some graphs show differences in virus titers between 2 experiments (with the same virus and with monocytes from the same donor cat) of up to 2 log<sub>10</sub> units. These differences are intrinsic to working with primary cells and are reported in viral infection studies with porcine and equine monocytes as well (Nauwynck and Pensaert, 1994; van der Meulen et al., 2000).

Although FECV initially infects monocytes, the infection is never sustained. This implicates that FECV might reach the blood circulation *in vivo*. In several studies, healthy cats from FCoV endemic households were investigated (Gunn-Moore et al., 1998; Herrewegh et al., 1995a, 1997; Meli et al., 2004; Simons et al., 2005). In such households, where the FCoV was most likely FECV, a part of these healthy cats were viraemic for FCoV. FCoV was detected both in plasma and in monocytes. Therefore, it may be hypothesized that when FECV reaches the blood circulation, the lack of sustainability and long-term production of progeny virus (the total virus production was up to 100 times lower in FECV-infected monocytes) may be the reason for the lack of disease progress. This might form the basis for the difference with FIPV since FIPV infection is sustained and reaches higher titers. However, the non-sustained FECV infection, might also be attributed to the virus strain that was used. Although FECV 79-1683 is a reference strain, it may act differently from other FECV strains due to its deletion in the 7b ORF (Vennema et al., 1992). It has been described that loss of the 7ab ORFs results in loss in virulence (Haijema et al., 2004). It could be that this loss in virulence is translated in loss of the ability to replicate efficiently in monocytes. Thus, whether the hampered replication of strain 79-1683 in monocytes is a universal property of FECV strains or only of 7b deleted/mutated strains, remains to be determined.

The different FIPV infection kinetics depending on the cat from which the monocytes were isolated suggests that cellular factors, influenced by genetic background and/or differentiation/activation status, are very important in determining the outcome of a FIPV infection. In an infection kinetics study where another cell type, feline peritoneal macrophages, was used, different results in the antigen expression kinetics were obtained (Stoddart and Scott, 1989). The number of FECV infected peritoneal macrophages was lower than the number of FIPV infected peritoneal macrophages throughout the infection kinetics. Since the viral antigen kinetics was only performed till 14 hours post inocu-

lation, a possible drop in antigen expression, like reported here, could not be evaluated. In contrast, our results suggest that FIPV and FECV can initially infect the same amount of cells but at 24 hours post inoculation, differences in sustainability of the infection are prominent. Since the same viruses were used as in our study, the different results are most probably due to cellular factors and/or a different differentiation status of the cells. Differences in susceptibility depending on the differentiation and/or activation status of the monocytes/macrophages has been reported for different viruses such as porcine reproductive and respiratory syndrome virus, caprine arthritis-encephalitis virus, suid herpes virus 1, herpes simplex virus, human immunodeficiency virus type 1 and Maedi-Visna virus (Nauwynck and Pensaert, 1994; Duan et al., 1998; Zink et al., 2002). The differences in activation status might explain the discrepancy between our results and those of Stoddart and Scott (1989).

What this variation in susceptibility and sustainability means for the pathogenesis of FECV and FIPV *in vivo*, remains to be elucidated. In an inoculation study using FIPV 79-1146, different patterns of disease progression were detected, based upon survival time: progressors (rapid, intermediate and delayed) and survivors (prolonged and long-term) (de Groot-Mijnes et al., 2005). With natural *in vivo* FCoV infection, different clinical outcomes (besides resistance to FCoV) have been described: persistent carrier, transiently infection and development of FIP (Addie et al., 2003). It is not clear what the viral and host factors are that determine the different clinical outcomes. Since in the inoculation study the same strain (FIPV-79-1146) was used and considering the fact that in the field cats are often infected with the same strain of FCoV, it is likely that genomic variation between cats contributes to a different clinical outcome. A genetic background was also suggested during a field study with pure-bred cats, in which it was shown that susceptibility to FIP is indeed inheritable [7]. A possible explanation for the different disease progression is the possibility of the cats to develop an efficient T-cell response (de Groot-Mijnes et al., 2005). However, it could also be that the susceptibility of the monocytes to FIPV plays a role, considering the results presented here. It would be interesting to investigate if cats that show a different outcome to an experimental or natural infection also show different infection kinetics *in vitro*. This might be important since a correlation between *in vitro* and *in vivo* infection kinetics would allow easy screening and selection.

In this study, it was shown that viral proteins can be expressed on the surface of FCoV infected cells. However, only a part of the infected cells showed surface-expressed viral antigens. On 24 hpi, 87% of the infected CrFK cells and 49% of the infected monocytes showed surface-expressed viral antigens. S and M proteins, but no N proteins were found on the cell surface of both CrFK cells and monocytes using specific monoclonal antibodies (data not shown). This

indicates that the observed surface expression does not represent virus particles. Possible explanations for the observed differences in amount of surface-expressed viral antigens could be the retention of a part of the viral proteins or spontaneous internalization of the surface-expressed viral antigens. Retention of viral proteins has been described for porcine coronavirus (Schwegmann-Wessels et al., 2004). Spontaneous internalization of viral proteins has been described for suid herpes virus 1 (Van Minnebruggen et al., 2004).

The presence of viral antigens on the cell surface can be of importance for the recognition and elimination of infected cells by the immune system. Binding of virus-specific antibodies to viral proteins present on the surface, makes infected cells recognizable for the classical complement pathway, phagocytes and natural killer cells, which will lead to lysis of the infected cell (Harper, 1994). Interestingly, not all FIPV- and FECV-infected monocytes/macrophages showed surface expression. Absence of viral proteins on the cell surface has been described for other viruses, such as human cytomegalovirus and equine herpesvirus 1 as a strategy to avoid recognition by the antibody-dependent immune responses (Fish et al., 1996; van der Meulen et al., 2003). Why only half of the infected cells showed surface expression and whether the cells without surface expression are indeed less susceptible towards antibody-dependent complement mediated lysis, remains to be elucidated.

In FIP research, the CrFK cell line is often used to perform *in vitro* experiments. The results of this study reveal that the CrFK cell line is not the best suitable *in vitro* model for the study of FIPV and FECV replication at a cellular level. Firstly, the course of infection of FIPV and FECV is similar in CrFK cells, whereas in monocytes there is a clear difference (as there is *in vivo*). Secondly, a high percentage of infected cells can be reached in CrFK cells (up to 90% of the inoculated cells) with each cell producing and releasing a relatively small amount of infectious virus (< 10 viruses/cell). In monocytes on the other hand, less than 1 % of the cells can be infected, but a single FIPV-infected monocyte releases up to 200 new infectious viruses. Thirdly, CrFK cells showed surface expression in almost all infected cells, in contrast to monocytes, which showed surface expression in only half of the infected cells.

In conclusion, it can be stated that FCoV infection kinetics *in vitro* are strongly dependent on cellular factors. Monocytes from some cats cannot be infected. If monocytes are susceptible to FCoV infection, then both FIPV and FECV can infect them. However, FECV infections are never sustained and production of viral antigens and progeny virus ceases at 24 hours post inoculation. Sustainability of a FIPV infection depends on the origin of the host cells. FIPV production in susceptible monocytes was always 10 to 100 times higher than

FECV production. What this variation in susceptibility and sustainability implicates for the development and pathogenesis of FIP and/or FECV *in vivo*, remains to be elucidated.

## Acknowledgments

We are grateful to Dr. Hohdatsu and Dr. Egberink for supplying antibodies. We thank Chantal Vanmaercke for excellent technical assistance, Myriam Hesta and Kris Gommeren for their help with handling the cats, H. Favoreel, S. Van Gucht and P. Delputte for critical reading of this manuscript. We also thank the small animal clinic of the Faculty of Veterinary Medicine for their cooperation. H. L. Dewerchin was supported by the Institute for the Promotion of Innovation through Science and Technology in Flanders (IWT-Vlaanderen) and E. Cornelissen was supported by a grant of the Ghent University.

## References

- Addie, D. and Jarret, O. (2001). Use of a reverse-transcriptase polymerase chain reaction for monitoring the shedding of feline coronavirus by healthy cats. *Vet Rec*, 148:649–653.
- Addie, D., Schaap, I., Nicolson, L., and Jarret, O. (2003). Persistence and transmission of natural type I feline coronavirus infection. *J Gen Virol*, 84:2735–2744.
- de Groot-Mijnes, J., van Dun, J., van der Most, R., and de Groot, R. (2005). Natural history of a recurrent feline coronavirus infection and the role of cellular immunity in survival and disease. *J Virol*, 79:1036–1044.
- Duan, X., Nauwynck, H., Favoreel, H., and Pensaert, M. (1998). Porcine reproductive and respiratory syndrome virus infection of alveolar macrophages can be blocked by monoclonal antibodies against cell surface antigens. *Adv Exp Med Biol*, 440:81–88.
- Fish, K., Britt, W., and Nelson, J. (1996). A novel mechanism for persistence of human cytomegalovirus in macrophages. *J Virol*, 70:1855–1862.
- Goitsuka, R., Furusawa, S., Mizoguchi, M., and Hasegawa, A. (1991). Detection of interleukin 1 in ascites from cats with feline infectious peritonitis. *J Vet Med Sci*, 53:487–489.



- Goitsuka, R., Ohashi, T., Ono, K., Yasukawa, K., Koishibara, Y., Fukui, H., Oshugi, Y., and Hasegawa, A. (1990). IL-6 activity in feline infectious peritonitis. *J Immunol*, 144:2599–2603.
- Gunn-Moore, D., Gruffydd-Jones, T., and Harbour, D. (1998). Detection of feline coronaviruses by culture and reverse transcriptase-polymerase chain reaction of blood samples from healthy cats and cats with clinical feline infectious peritonitis. *Vet Microbiol*, 62:193–205.
- Haijema, B., Volders, H., and Rottier, P. (2004). Live, attenuated coronavirus vaccines through the directed deletion of group-specific genes provide protection against feline infectious peritonitis. *J Virol*, 78:3863–3871.
- Harper, D. (1994). Viral interactions with the immune system. In *Molecular Virology*, pages 51–73. BIOS Scientific Publishers Ltd, Oxford, 1st edition.
- Herrewegh, A., de Groot, R., Cepica, A., Egberink, H., Horzinek, M., and Rottier, P. (1995a). Detection of feline coronavirus RNA in feces, tissues, and body fluids of naturally infected cats by reverse transcriptase PCR. *Clin Microbiol*, 33:684–689.
- Herrewegh, A., Mahler, M., Hedrich, H., Haagmans, B., Egberink, H., Horzinek, M., Rottier, P., and de Groot, R. (1997). Persistence and evolution of feline coronavirus in a closed cat-breeding colony. *Virology*, 234:349–363.
- Jacobse-Geels, H., Daha, M., and Horzinek, M. (1980). Isolation and characterization of feline C3 and evidence for the immune complex pathogenesis of feline infectious peritonitis virus. *J Immunol*, 125:1606–1610.
- McArdle, F., Tennant, B., Bennett, M., Kelly, D., Gaskell, C., and Gaskell, R. (1995). Independent evaluation of a modified live FIPV vaccine under experimental conditions (University of Liverpool experience). *Feline Pract*, 23 (3):67–71.
- McKeirnan, A., Evermann, J., Davis, E., and Ott, R. (1987). Comparative properties of feline coronaviruses in vitro. *Can J Vet Res*, 51:212–216.
- McKeirnan, A., Evermann, J., Hargis, A., and Ott, R. (1981). Isolation of feline coronaviruses from 2 cats with diverse disease manifestations. *Feline Practice*, 11(3):16–20.
- Meli, M., Kipar, A., Muller, C., Jenal, K., Gonczi, E., Borel, N., Gunn-Moore, D., Chalmers, S., Lin, F., Reinacher, M., and Lutz, H. (2004). High viral

- loads despite absence of clinical and pathological findings in cats experimentally infected with feline coronavirus (FCoV) type I and in naturally FCoV-infected cats. *J Feline Med Surg*, 6:69–81.
- Nauwynck, H. and Pensaert, M. (1994). Virus production and viral antigen expression in porcine blood monocytes inoculated with pseudorabies virus. *Arch Virol*, 137:69–79.
- Pedersen, N., Boyle, J., Floyd, K., Fudge, A., and Barker, J. (1981). An enteric coronavirus infection of cats and its relationship to feline infectious peritonitis. *Am J Vet Res*, 42:368–376.
- Poland, A., Vennema, H., Foley, J., and Pedersen, N. (1996). Two related strains of feline infectious peritonitis virus isolated from immunocompromised cats infected with a feline enteric coronavirus. *J clin microbiol*, 34:3180–3184.
- Reed, L. and Muench, H. (1938). A simple method of estimating fifty percent endpoints. *Am J Hyg*, 27:493–497.
- Schwegmann-Wessels, C., Al-Falah, M., Escors, D., Wang, Z., Zimmer, G., Deng, H., Enjuanes, L., Naim, H., and Herrler, G. (2004). A novel sorting signal for intracellular localization is present in the s protein of a porcine coronavirus but absent from severe acute respiratory syndrome-associated coronavirus. *J Biol Chem*, 279:43661–43666.
- Scott, F., Wayne, V., and Olsen, C. (1995). Independent evaluation of a modified live FIPV vaccine under experimental conditions (Cornell experience). *Feline Pract*, 23 (3):74–76.
- Simons, F., Vennema, H., Rofina, J., Pol, J., Horzinek, M., Rottier, P., and Egberink, H. (2005). A mRNA PCR for the diagnosis of feline infectious peritonitis. *J Virol Methods*, 124:111–116.
- Stoddart, M. and Scott, F. (1989). Intrinsic resistance of feline infectious peritoneal macrophages to coronavirus infection correlates with in vivo virulence. *J Virol*, 63:436–440.
- van der Meulen, K., Nauwynck, H., Buddaert, W., and Pensaert, M. (2000). Replication of equine herpesvirus type 1 in freshly isolated equine peripheral blood mononuclear cells and changes in susceptibility following mitogen stimulation. *J Gen Virol*, 81:21–25.
- van der Meulen, K., Nauwynck, H., and Pensaert, M. (2003). Absence of viral antigens on the surface of equine herpesvirus-1-infected peripheral blood

- mononuclear cells: a strategy to avoid complement-mediated lysis. *J Gen Virol*, 84:93–97.
- Van Minnebruggen, G., Favoreel, H., and Nauwynck, H. (2004). Internalization of pseudorabies virus glycoprotein B is mediated by an interaction between the YQRL motif in its cytoplasmic domain and the clathrin-associated AP-2 adaptor complex. *J Virol*, 78:8852–8859.
- Vennema, H., Poland, A., Floyd Hawkins, K., and Pedersen, N. (1995). A comparison of the genomes of FECVs and FIPVs: what they tell us about the relationships between feline coronaviruses and their evolution. *Feline Pract*, 23:40–44.
- Vennema, H., Poland, A., Foley, J., and Pedersen, N. (1998). Feline infectious peritonitis viruses arise by mutation from endemic feline enteric coronaviruses. *Virology*, 243:150–157.
- Vennema, H., Rossen, J., Wesseling, J., Horzinek, M., and Rottier, P. (1992). Genomic organization and expression of the 3' end of the canine and feline enteric coronaviruses. *Virology*, 191:134–140.
- Weiss, R. and Cox, N. (1989). Evaluation of immunity to feline infectious peritonitis in cats with cutaneous viral-induced delayed hypersensitivity. *Vet Immunol Immunopathol*, 21:293–309.
- Weiss, R. and Scott, F. (1981a). Pathogenesis of feline infectious peritonitis: nature and development of viraemia. *Am J Vet Res*, 42:382–390.
- Weiss, R. and Scott, F. (1981b). Pathogenesis of feline infectious peritonitis: pathologic changes and immunofluorescence. *Am J Vet Res*, 42:2036–2048.
- Weiss, R., Vaugh, D., and Cox, N. (1988). Increased plasma levels of leukotriene B4 and prostaglandin E2 in cats experimentally inoculated with feline infectious peritonitis virus. *Vet Res Commun*, 12:313–323.
- Zink, W., Ryan, L., and Gendelman, H. (2002). Macrophage-virus interactions. In Burke, B. and Lewis, C., editors, *The macrophage*, pages 138–209. Oxford University Press, New York, 2nd edition.



# 3

## FIPV-infected monocytes internalize viral membrane-bound proteins upon antibody addition\*

### Summary

Feline infectious peritonitis virus (FIPV) may cause a highly lethal infection in cats, in spite of a usually very strong humoral immune response. Antibodies seem to be unable to identify infected cells and/or mark them for antibody-dependent cell lysis. In this study, the effect of feline coronavirus (FCoV)-specific antibodies on FIPV-infected monocytes was investigated. FCoV-infected cells were incubated with specific antibodies during different time periods. Upon antibody addition, the surface expressed viral proteins were internalized through a highly efficient and fast process resulting in FCoV-infected cells without visually detectable viral proteins on their plasma membrane. The internalization was also induced by monoclonal antibodies against the S and the M protein, though to a somewhat lesser extent, suggesting that both proteins play a role in the internalization process. The internalization did not occur spontaneously, as it was not observed in cells that were incubated with medium or with non-specific antibodies. Further, the internalization process could not be reproduced in feline cell lines indicating its cell type specificity. The results show that the process requires antigen specific antibodies and a special cellular machinery. This study can put the immune evasive nature of a FIPV infection in a new light.

---

\*This Chapter is based on Dewerchin et al. (2006).

### 3.1 Introduction

Feline infectious peritonitis virus (FIPV) and feline enteric coronavirus (FECV) are two coronaviruses described in cats. These feline coronaviruses are spread world-wide and infect all members of the Felidae family. Very little is known about the interactions of FIPV with the host immune system. Cats with clinical FIP often have very high titres of FIPV-specific antibodies; however, these antibodies are not able to block infection. This suggests that, for unknown reasons, antibodies and antibody-driven immune effectors are not able to efficiently clear the body from virus and/or virus-infected cells. There are indications that the immune system does even play an adverse role in the development of FIP. It has been reported in experimental infections that cats, which have obtained FIPV-specific antibodies actively or passively, develop FIP faster and more severely than naive cats (Pedersen and Boyle, 1980). This accelerated FIP has been the reason for the failure of most vaccination attempts (Woods and Pedersen, 1979; Pedersen and Black, 1983; Barlough et al., 1984, 1985; Vennema et al., 1990a; McArdle et al., 1992). A mechanism was proposed that could explain this accelerated development of FIP in the presence of antibodies: Antibody-Dependent Enhancement of Infectivity (ADEI) (Hohdatsu et al., 1991; Corapi et al., 1992; Olsen et al., 1992). ADEI suggests that antibodies might help the spread of the virus in an infected cat by facilitating the virus uptake through the formation of virus-antibody complexes which are taken up by uninfected monocytes/macrophages via the Fc-receptor. ADEI may explain why a larger number of cells can be infected in the presence of antibodies but it cannot explain why these infected cells are not eliminated by the immune system. It is believed that the only effective defense against FIP is cell-mediated immunity (Pedersen, 1987).

The role of antibodies in the pathogenesis of naturally occurring FIP, and more specifically how antibodies interact with infected cells is unknown. In the present study, we investigated the effect of FCoV-specific antibodies on FIPV-infected monocytes to clarify why antibodies seem to be unable to identify infected cells and/or mark them for antibody-dependent cell lysis. We report that membrane bound viral proteins are internalized upon addition of FCoV specific antibodies through a highly efficient and fast process resulting in FIPV-infected cells without visually detectable viral proteins on their plasma membrane.

## 3.2 Materials and Methods

**Viruses and antibodies** A third passage of FIPV strain 79-1146 and FECV strain 79-1683 on Crandell feline kidney (CrFK) cells was used (McKeirnan et al., 1981). FIPV strain 79-1146 was obtained from the American Type Culture Collection (ATCC) and FECV strain 79-1683 was kindly provided by Dr. Egberink (Utrecht University, the Netherlands). Also the polyclonal anti-FCoV antibodies were kindly provided by Dr Egberink. The antibodies were purified and biotinylated according to manufacturers instructions (Pierce, Rockford, Illinois, USA). FITC-labeled polyclonal anti-FIPV antibodies were purchased from Veterinary Medical Research and Development (VMRD, Pullman, Washington, USA). The monoclonal antibodies 7-4-1 (isotype IgG2b), F19-1 (isotype IgG1) and E22-2 (isotype IgG1) recognizing respectively the S, M and N protein, were kindly provided by Dr. Hohdatsu (Kitasato University, Japan). As non-specific isotype-matched monoclonal antibodies, 41D3 (isotype IgG1) recognizing porcine sialoadhesin and Mil2 (isotype IgG2b) recognizing porcine CD14 were used (Duan et al., 1998; Thacker et al., 2001; Vanderheijden et al., 2003). The polyclonal non-specific, FCoV negative antibodies were obtained from SPF cats that were vaccinated with Nobivac Tri-cat (Intervet, Boxmeer, The Netherlands). Blood was taken from the cat one week after the booster vaccination and antibodies were purified. The monocyte marker DH59B, recognizing CD172a, was purchased from VMRD.

**Isolation and inoculation of blood monocytes** Feline Coronavirus (FCoV), Feline Leukemia Virus (FeLV) and Feline Immunodeficiency Virus (FIV) negative cats were used as blood donors. Blood was collected from the *vena jugularis* on heparin (15U/ml) (Leo, Zaventem, Belgium) and blood mononuclear cells were separated on Ficoll-Paque (Pharmacia Biotech AB, Uppsala, Sweden). Mononuclear cells were resuspended in RPMI-1640 (Gibco BRL, Merelbeke, Belgium) medium containing 10% fetal bovine serum (FBS), 0.3 mg/ml glutamine, 100 U/ml penicillin, 0.1 mg/ml streptomycin, 0.1 mg/ml kanamycin, 10 U/ml heparin, 1mM sodium pyruvate, and 1% non-essential amino-acids 100x (Gibco BRL). Afterwards, cells were seeded on glass coverslips inserted in a 24-well dish (Nunc A/S, Roskilde, Denmark) at a concentration of  $2 \times 10^6$  cells/ml and cultivated at 37°C with 5% CO<sub>2</sub>. Non-adherent cells were removed by washing the dishes two times with RPMI-1640 at 2 and 24 hours after seeding. The adherent cells consisted for  $86 \pm 7\%$  of monocytes (as assessed by fluorescent staining with the monocyte marker DH59B). At 36 hours post seeding, monocytes were inoculated with FIPV or FECV at a multiplicity of infection (m.o.i.) of 5.

**Internalization assay with polyclonal antibodies** Twelve hours after inoculation, monocytes seeded on glass coverslips were incubated with biotinylated anti-FCoV polyclonal antibodies at 37°C. At different times (0, 1, 3, 10, 30 or 60 minutes) post antibody addition, cells were fixed with 1% formaldehyde, permeabilized with 0.1% Triton X-100 (Sigma-Aldrich, Saint Luis, Missouri, USA) and incubated with streptavidin-FITC (Molecular Probes, Eugene, Oregon, USA) for 1 hour at 37°C. Next, infected cells were incubated with a mixture of FIPV-specific monoclonal antibodies against the S, M and N protein for 1 hour at 37°C and visualized with goat anti-mouse-Texas Red (Molecular Probes) (1 hour at 37°C). The glass coverslips were mounted on microscope slides using glycerin-DABCO (Janssen Chimica) and analyzed by confocal microscopy.

As a control, inoculated monocytes seeded on glass coverslips were incubated with non-specific polyclonal antibodies for different time periods (0, 10, 30 or 60 minutes). After fixation of the cells with 1% formaldehyde, surface expression of viral proteins was visualized by a subsequent incubation with a mixture of anti-S and anti-M monoclonal antibodies and goat anti-mouse-Texas Red (Molecular Probes), each time for 1 hour at 37°C. Next, the cells were permeabilized with 0.1% Triton X-100 (Sigma-Aldrich) and incubated with goat anti-cat-FITC (Sigma-Aldrich) for 1 hour at 37°C to visualize possible internalization caused by the non-specific polyclonal antibodies. Finally, the glass coverslips were mounted on microscope slides using glycerin-DABCO (Janssen Chimica) and analyzed by confocal microscopy.

For the internalization assays on cell lines, CrFK cells or felis catus whole fetus (fcwf) cells were seeded on glass coverslips and incubated with biotinylated anti-FCoV polyclonal antibodies at 37°C. At 30 minutes post antibody addition, cells were fixed with 1% formaldehyde, permeabilized with 0.1% Triton X-100 (Sigma-Aldrich) and incubated with streptavidin-Texas Red (Molecular Probes) for 1 hour at 37°C. Then, cytoplasmic expression of antigens was visualized with anti-FIPV-FITC. The glass coverslips were mounted on microscope slides using glycerin-DABCO (Janssen Chimica) and analyzed by confocal microscopy.

**Internalization assay with monoclonal antibodies** Twelve hours after inoculation, monocytes seeded on glass coverslips were incubated at 37°C with anti-S (7-4-1, sub-isotype IgG2b) antibodies, anti-M (F19-1, sub-isotype IgG1) antibodies or a combination of both. At different times (0, 10, 30 or 60 minutes) post antibody addition, cells were fixed with 1% formaldehyde, permeabilized with 0.1% Triton X-100 (Sigma-Aldrich) and incubated with goat anti-mouse-Texas Red (Molecular Probes) for 1 hour at 37°C. Next, infected



cells were visualized with FITC labeled anti-FIPV antibodies. The glass coverslips were mounted on microscope slides using glycerin-DABCO (Janssen Chimica) and analyzed by confocal microscopy.

As a control, inoculated monocytes seeded on glass coverslips were incubated with a mixture of non-specific, isotype matched monoclonal antibodies for different time periods (0, 10, 30 or 60 minutes). The antibodies 41D3 against porcine sialoadhesin, isotype IgG1, and Mil2 against porcine CD14, isotype IgG2b, were used in order to include isotype specific interactions. After fixation of the cells with 1% formaldehyde, surface expression of viral proteins was visualized by incubation with biotinylated anti-FCoV polyclonal antibodies and then streptavidin Texas Red (Molecular Probes), each time for 1 hour at 37°C. Next, the cells were permeabilized with 0.1% Triton X-100 (Sigma-Aldrich) and incubated with goat anti-mouse-FITC (Sigma-Aldrich) for 1 hour at 37°C to visualize possible internalization caused by the non-specific monoclonal antibodies. Finally, the glass coverslips were mounted on microscope slides using glycerin-DABCO (Janssen Chimica) and analyzed by confocal microscopy.

**Spontaneous internalization assay** At 12 hours after inoculation, monocytes seeded on glass coverslips were placed on ice, washed twice with ice-cold phosphate buffered saline (PBS) solution and incubated with 2mM of biotinylation reagent EZ-Link sulfo-NHS-LC-Biotin (Pierce). After 30 minutes, the biotin was removed and replaced by cold medium supplemented with 10mM glycine for 10 minutes. Then, the monocytes were washed twice with cold supplemented medium and twice with cold medium without FBS or heparin. Cells were shifted to 37°C and incubated with biotinylated anti-FIPV polyclonal antibodies, non-specific antibodies or RPMI for 30 minutes. The control cells were fixed before the temperature shift. To visualize internalized biotinylated proteins, cells were fixed with 1% formaldehyde, permeabilized with 0.1% Triton X-100 (Sigma-Aldrich) and incubated with streptavidin-Texas Red (Molecular Probes) for 1 hour at 37°C. Afterwards, cells were washed and incubated with FITC-labeled polyclonal anti-FIPV to enable identification of infected cells. The glass coverslips were mounted on microscope slides using glycerin-DABCO (Janssen Chimica) and analyzed by confocal microscopy.

**Confocal laser scanning microscopy** The samples were stained as described above and examined with a Leica TCS SP2 laser scanning spectral confocal system (Leica Microsystems GmbH, Wetzlar, Germany) linked to a DM IRB inverted microscope (Leica Microsystems). Argon and Helium/Neon laser lights were used to excite FITC (488 nm line) and Texas-Red (543 nm line)

fluorochromes. The images were obtained and processed with Leica confocal software.

### 3.3 Results

#### 3.3.1 Redistribution of membrane-bound viral proteins induced by polyclonal FCoV specific antibodies

The role of antibodies in the pathogenesis of naturally occurring FIP, and more specifically how antibodies interact with infected cells, is unknown. Therefore, the effect of FCoV specific antibodies on FIPV- or FECV-infected monocytes was investigated in this study. Figure 3.1 illustrates that after FCoV-specific antibody addition, the surface expressed viral proteins moved from the plasma membrane into the cytoplasm. In contrast, after addition of non-specific antibodies, the surface expressed viral proteins remained in the plasma membrane. Figure 3.2 shows that internalization of the viral glycoproteins was initiated very shortly after antibody addition and is completed rapidly. In Figure 3.2, internalization was represented as the percentage of cells which are internalizing viral proteins and not as amount of internalized antibody-antigen complexes because the amount of viral proteins that is expressed in the plasma membrane varies strongly between cells (Dewerchin et al., 2005). The internalization occurred in both FIPV- and FECV-infected monocytes in the same manner. The curves indicate that  $89\pm 9\%$  and  $84\pm 4\%$  of respectively FIPV- and FECV-infected monocytes showed internalization of the plasma membrane-bound viral proteins after 3 minutes of incubation. At 30 minutes almost 100% of the infected monocytes internalized their membrane-bound proteins ( $98\pm 3\%$  and  $97\pm 4\%$  for FIPV and FECV infection respectively). Figure 3.2 also shows that internalization was not observed at any time point post addition of non-specific antibodies. These findings indicate that antibody-mediated internalization is a specific process that occurs through Fab interactions with its antigens and is not mediated by the Fc activity of the S protein.

#### 3.3.2 The viral membrane-bound proteins are not spontaneously internalized

To determine whether addition of anti-FCoV antibodies is necessary for internalization to occur, all surface expressed proteins were labeled by biotinylation and then an internalization assay was performed. In this assay, it was tested if internalization occurred spontaneously (by shifting the cells to  $37^{\circ}\text{C}$  without adding antibodies), if internalization could be induced by non-specific cat

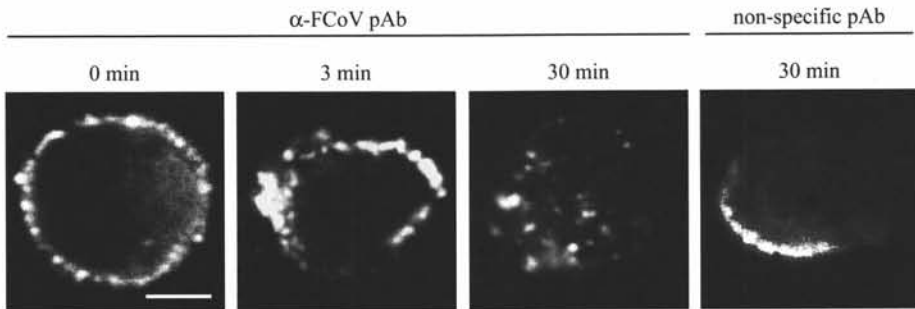


Figure 3.1: Antibody-induced redistribution of surface expressed viral proteins in FCoV infected monocytes. The images show the middle section of a cell at different time points post addition of  $\alpha$ -FCoV polyclonal antibodies or after addition of non-specific polyclonal antibodies. Bar: 5 $\mu$ m.

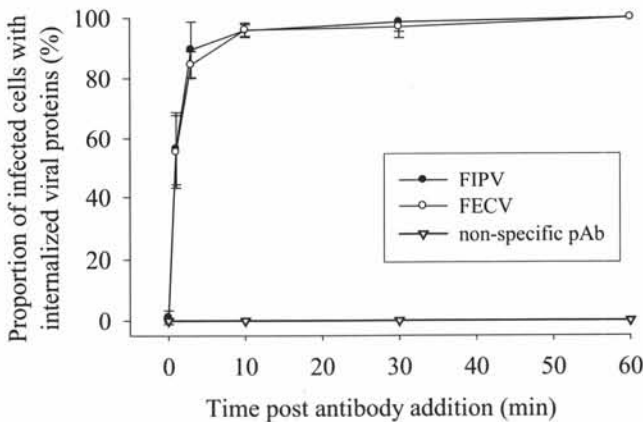


Figure 3.2: Antibody-induced internalization of surface expressed viral proteins in FIPV or FECV infected monocytes after addition of  $\alpha$ -FCoV or non-specific polyclonal antibodies. Data represents means  $\pm$  standard deviation of triplicate assays.

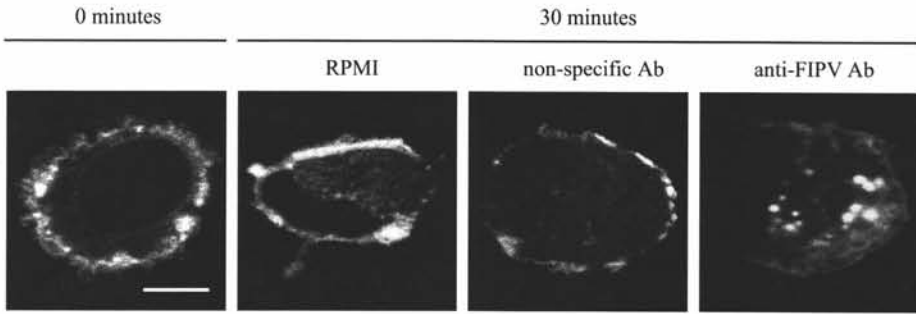


Figure 3.3: Surface expressed proteins were biotinylated and their distribution was visualized at 0 or at 30 minutes of incubation with RPMI,  $\alpha$ -FCoV or non-specific polyclonal antibodies at 37°C. All images are a single section through the middle of the cell. Bar: 5 $\mu$ m.

antibodies or if internalization could only be induced by specific antibodies. Figure 3.3 shows that a temperature shift on itself did not lead to internalization nor did incubation with non-specific antibodies. Only the monocytes that were incubated with anti-FCoV antibodies showed internalized proteins. These results indicate that spontaneous internalization did not occur.

### 3.3.3 Redistribution of membrane-bound viral proteins induced by monoclonal anti-S and/or anti-M antibodies

To further investigate which membrane-bound viral proteins are of importance for the internalization process, the distribution of the proteins was studied in presence of monoclonal antibodies directed against the S or the M protein. The confocal images in Figure 3.4 illustrate that both the anti-S and the anti-M antibodies were able to induce internalization. Figure 3.5 shows that 82 $\pm$ 9% and 66 $\pm$ 4% of the infected cells showed internalization at 10 min after addition of anti-S or anti-M antibodies respectively. This percentage further increased and after 1 hour of incubation with anti-S or anti-M antibodies, respectively 85 $\pm$ 4% and 81 $\pm$ 4% of the cells showed internalization. The results demonstrate that the internalization induced by monoclonal antibodies occurred less efficiently than the internalization induced by polyclonal anti-FIPV antibodies. However, incubation with both anti-S and anti-M antibodies led to internalization in 100% of the infected monocytes. Thus, with a combination of anti-S and anti-M antibodies, the same efficiency was reached as with polyclonal antibodies. These findings suggest that the S and the M protein operate together to mediate the internalization process. Since the monoclonal antibodies against S and M protein are of mouse origin, non-specific mouse monoclonals of the same isotype were tested as a control. Figure 3.5 shows that addition of non-specific antibodies did not lead to internalization, confirming that the

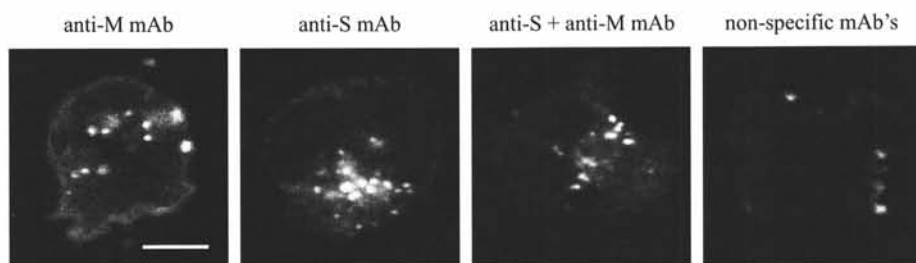


Figure 3.4: Redistribution of surface expressed viral proteins can be mediated by monoclonal anti-S (IgG2b) or anti-M (IgG1) antibodies but not by a combination of the non-specific, isotype-matched monoclonal antibodies 41D3 (IgG1) and Mil2 (IgG2b). The images show a section through the middle of the cells at 30 minutes post antibody addition. Bar: 5 $\mu$ m.

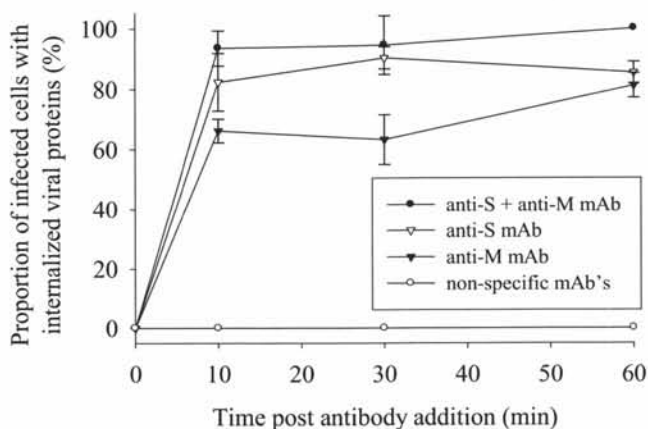


Figure 3.5: Internalization of surface expressed viral proteins upon addition of monoclonal anti-S (IgG2b), anti-M (IgG1), a mixture of anti-S and M or a combination of non-specific isotype-matched monoclonal antibodies 1D3 (IgG1) and Mil2 (IgG2b). Data represents means  $\pm$  standard deviation of triplicate assays.

internalization process requires FCoV specific antibodies and is not mediated by Fc interaction nor isotype specific interactions.

### 3.3.4 Antibody-mediated internalization is specific for monocytes

The commonly used feline cell lines “Crandell feline kidney” (CrFK) and the macrophage-like “felis catus whole fetus” (fcwf) were infected with FIPV and tested for their ability to internalize surface expressed viral proteins. Figure 3.6 shows that after addition of antibodies, the antigens were somewhat more clustered than in non-treated cells but in none of these cell lines internalization was observed. These findings suggest that the cellular machinery that is

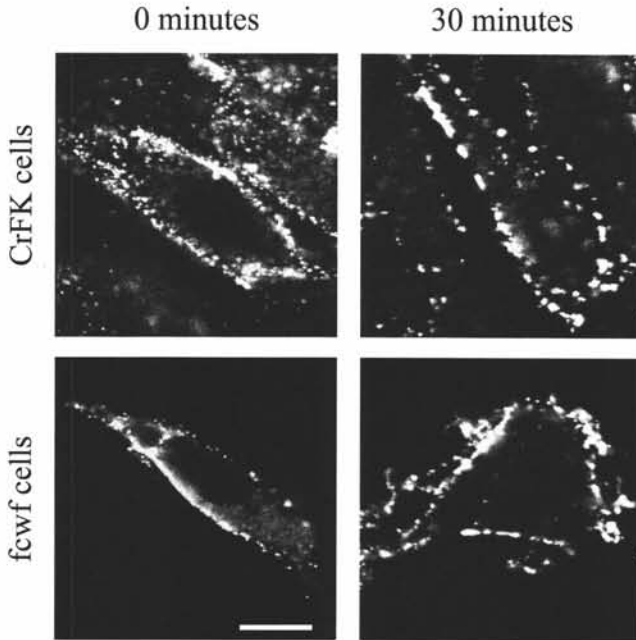


Figure 3.6: Continuous cell lines do not internalize surface expressed viral proteins upon antibody addition. Cells of CrFK or fcwf cell line were incubated with biotinylated polyclonal anti-FCoV antibodies for 30 minutes and antigen-antibody complexes were visualized with streptavidin Texas-Red. The images show a section through the middle of the cells. Bar: 5 $\mu$ m.

required for the internalization, is not, or not completely, present in cell lines.

### 3.4 Discussion

Very little is known about the interactions of FIPV with the host immune system. Judging by the devastating development of a FIP infection in cats, the immune system cannot counter this virus during its destructive replication and invasion. There are indications that the immune system does even play an adverse role in the development of FIP. It has been reported in experimental infections that cats, which have obtained FIPV-specific antibodies actively or passively, develop FIP faster and more severely than naive cats (Pedersen and Boyle, 1980). This accelerated FIP has been the reason for the failure of most vaccination attempts (Woods and Pedersen, 1979; Pedersen and Black, 1983; Barlough et al., 1984, 1985; Vennema et al., 1990a; McArdle et al., 1992). A mechanism was proposed that could explain this accelerated development of FIP in the presence of antibodies: Antibody-Dependent Enhancement of Infectivity (ADEI) (Hohdatsu et al., 1991; Corapi et al., 1992; Olsen et al., 1992).

ADEI suggests that antibodies might help the spread of the virus in an infected cat by facilitating the virus uptake through the formation of virus-antibody complexes which are taken up by uninfected monocytes/macrophages via the Fc-receptor. ADEI may explain why a larger number of cells can be infected in the presence of antibodies than in the absence of antibodies. However, ADEI has never been reported under field conditions (Addie et al., 1995). Moreover, ADEI has only been reported in *in vitro* experiments with low concentrations of antibodies. Concentrations as high as the ones found in most FIP cats are neutralizing *in vitro*.

In this paper, a new mechanism is presented which might aid in explaining the adverse effect of the presence of antibodies. In our study, we observed that FCoV-specific antibodies trigger a putative immune evasion mechanism in FCoV-infected monocytes. Upon FCoV-specific antibody addition, FIPV and FECV infected monocytes rapidly internalized all visually detectable viral plasma membrane-bound proteins. This internalization process was initiated immediately after antibody addition and was completed very rapidly and efficiently. At 10 minutes post antibody addition,  $96 \pm 2\%$  of both FIPV- and FECV-infected monocytes with membrane expression showed internalization. At 30 minutes post antibody addition, 100% of the cells showed internalization. Considering that an immune-evasive nature (*in vivo*) is only attributed to FIPV, it was remarkable to find that FIPV and FECV show almost exactly the same internalization kinetics. These identical internalization kinetics implicate that the difference between FIP and FECV pathogenesis cannot be explained by the ability to internalize the viral proteins.

This internalization could only be induced by specific anti-FCoV antibodies and does not occur spontaneously. The fact that non-specific feline antibodies were not able to induce internalization indicates that specific Fab-antigen interactions are needed. Thus internalization is not mediated by the Fc-binding capacity that has been described for the S protein of several coronaviruses (Oleszak et al., 1993). To confirm that the membrane-bound structures were single proteins and not virus particles, infected cells were fixed and membrane expression was visualized. Then, the cells (and virus membrane) were permeabilized and nucleocapsid proteins stained. No co-localization was found between the nucleocapsid and membrane-bound proteins which shows that the structures were single proteins (data not shown).

In cells where all antigen-antibody complexes were internalized with one monoclonal against S or M protein, no residual expression could be found in the plasma membrane using a polyclonal antibody (data not shown). In cells where not all complexes were internalized with one monoclonal against the S or M protein, the complexes that were in the plasma membrane could also be stained

for the other protein (data not shown). These results indicate that S and M proteins reside in the plasma membrane as complexes. Interactions between the S and M proteins have already been described in mouse hepatitis virus infection during which the M and S protein form heteromultimeric complexes (Opstelten et al., 1995). Taken together, these findings suggest that S and M proteins operate together to mediate the internalization process. Internalization could not be induced using anti-N antibodies (data not shown).

In this study, a mechanism is presented which might aid in explaining why the humoral immune system is not effective against a FIP infection: internalization of viral plasma membrane-bound proteins induced by antibodies. This immune evasion mechanism has been described for the first time by Favoreel et al. (1999). They found that viral plasma membrane-bound proteins in pseudorabies virus (PrV) infected pig monocytes are internalized upon antibody addition. This internalization process is clathrin mediated and dependent on an YXX $\Psi$  motif (Y stands for tyrosine, X for any amino acid and  $\Psi$  for a bulky hydrophobic amino acid) in the cytoplasmic tail of the gB protein (Van de Walle et al., 2001; Favoreel et al., 2002). The viral plasma membrane-bound proteins in FIPV infected cells (S and M), contain putative internalization motifs in their cytoplasmic tails. The S protein contains a dileucine motif and a YXX $\Psi$  motif and the M protein contains 2 of each. The presence of these putative internalization motifs is another indication that both viral proteins are of importance in antibody-mediated internalization. The role of these motifs will be investigated in the future.

The internalization pathway presented here, seems to be very specific for monocytes. Some feline cell lines (CrFK and fcwf cells) were infected with FIPV and tested for their ability to perform antibody-induced internalization of membrane bound viral proteins. The cell lines expressed viral proteins on their cell surface but were not able to internalize these proteins upon antibody addition. These findings might indicate a role for specific cellular machinery or for special processing of the proteins that can only be found in cells of the monocyte/macrophage lineage. It also means that a more thorough study of this internalization pathway using dominant negative mutant cells will be hampered by the lack of adequate cell lines.

In previous work, we reported that only half of FIPV-infected monocytes express viral proteins on their plasma membrane Dewerchin et al. (2005). Here, we report that cells that do express viral proteins, internalize these proteins upon antibody-addition. With these findings, the following hypothetical model may aid in explaining the FIP pathogenesis. In a FIPV infected cat, part of the FIPV-infected monocytes may remain immune-masked because no viral antigens are expressed at the plasma membrane and part of the cells may ex-



press viral proteins in the plasma membrane. When antibodies bind to these membrane-bound proteins to mark the infected cells for cell lysis, internalization may be triggered. The plasma membrane is cleared from viral proteins and the infected cell remains invisible for the humoral immune system. In this way, the cell may be able to continue the production of progeny virus without being eliminated or it may enter a quiescent infection state, as is seen in PrV infected monocytes that were cultured in the presence of specific antibodies (Favoreel et al., 2003). This quiescent infection state would be an excellent cover for a carrier cell and might explain the sometimes long incubation period of a FIP infection. Further research on the *in vivo* relevance of antibody-dependent internalization is necessary. For PrV infected pig monocytes, it has been shown that cells with internalized viral glycoproteins are indeed protected against antibody-dependent complement mediated cell lysis (Van de Walle et al., 2003). Whether this is also true for a FIPV-infected monocyte, will be investigated in the near future.

In conclusion, it can be stated that surface expressed viral proteins in FIPV- and FECV-infected monocytes are internalized upon FCoV specific antibody addition in a very efficient manner. This internalization does not occur spontaneously nor can it be induced by non-specific antibodies. These findings might lead to new insights in strategies for immune evasion developed by feline coronaviruses.

## Acknowledgments

We are grateful to Dr. Hohdatsu and Dr Egberink for supplying antibodies. H. L. Dewerchin and E. Cornelissen were supported by the Institute for the Promotion of Innovation through Science and Technology in Flanders (IWT-Vlaanderen). We thank H. Favoreel for critical reading of this manuscript.

## References

- Addie, D., Toth, S., Murray, G., and Jarret, O. (1995). Risk of feline infectious peritonitis in cats naturally infected with feline coronavirus. *Am J Vet Res*, 56:429–434.
- Barlough, J., Johnson-Lussenburg, C., Stoddart, C., Jacobson, R., and Scott, F. (1985). Experimental inoculation of cats with human coronavirus 229E and subsequent challenge with feline infectious peritonitis virus. *Can J Comp Med*, 49:303–307.

- Barlough, J., Stoddart, C., Sorresso, G., Jacobson, R., and Scott, F. (1984). Experimental inoculation of cats with canine coronavirus and subsequent challenge with feline infectious peritonitis virus. *Lab Anim Sci*, 34:592–597.
- Corapi, W., Olsen, C., and Scott, F. (1992). Monoclonal antibody analysis of neutralization and antibody-dependent enhancement of feline infectious peritonitis virus. *J Virol*, 11:6695–6705.
- Dewerchin, H., Cornelissen, E., and Nauwynck, H. (2005). Replication of feline coronaviruses in peripheral blood monocytes. *Arch Virol*, 150(12):2483–2500.
- Duan, X., Nauwynck, H., Favoreel, H., and Pensaert, M. (1998). Porcine reproductive and respiratory syndrome virus infection of alveolar macrophages can be blocked by monoclonal antibodies against cell surface antigens. *Adv Exp Med Biol*, 440:81–88.
- Favoreel, H., Nauwynck, H., Halewyck, H., Van Oostveldt, P., Mettenleiter, T., and Pensaert, M. (1999). Antibody-induced endocytosis of viral glycoproteins and major histocompatibility complex class I on pseudorabies virus-infected monocytes. *J Gen Virol*, 80(5):1283–1291.
- Favoreel, H., Van de Walle, G., Nauwynck, H., Mettenleiter, T., and Pensaert, M. (2003). Pseudorabies virus (PRV)-specific antibodies suppress intracellular viral protein levels in PRV-infected monocytes. *J Gen Virol*, 84(11):2969–2973.
- Favoreel, H., Van Minnebruggen, G., Nauwynck, H., Enquist, L., and Pensaert, M. (2002). A tyrosine-based motif in the cytoplasmic tail of pseudorabies virus glycoprotein B is important for both antibody-induced internalization of viral glycoproteins and efficient cell-to-cell spread. *J Virol*, 76(13):6845–6851.
- Hohdatsu, T., Nakamura, M., Ishizuka, Y., Yamada, H., and Koyama, H. (1991). A study on the mechanism of antibody-dependent enhancement of feline infectious peritonitis virus infection in feline macrophages by monoclonal antibodies. *Arch Virol*, 120:207–217.
- McArdle, F., Bennet, M., Gaskell, R., Tennant, B., Kelly, D., and Gaskell, C. (1992). Induction and enhancement of feline infectious peritonitis by canine coronavirus. *Am J Vet Res*, 53:1500–1506.
- McKeirnan, A., Evermann, J., Hargis, A., and Ott, R. (1981). Isolation of feline coronaviruses from 2 cats with diverse disease manifestations. *Feline Practice*, 11(3):16–20.

- Oleszak, E., Perlman, S., Parr, R., Collisson, E., and Leibowitz, J. (1993). Molecular mimicry between S peplomer proteins of coronaviruses MHV, BCV, TGEV and IBV and Fc receptor. *Adv Exp Med Biol*, 342:183–188.
- Olsen, C., Corapi, W., Ngichabe, C., Baines, J., and Scott, F. (1992). Monoclonal antibodies to the spike protein of feline infectious peritonitis virus mediate antibody-dependent enhancement of infection of feline macrophages. *J Virol*, 66:956–965.
- Opstelten, D.-J., Raamsman, M., Wolfs, K., Horzinek, M., and Rottier, P. (1995). Envelope glycoprotein interactions in coronavirus assembly. *J Cell Biol*, 131:339–349.
- Pedersen, N. (1987). Virologic and immunologic aspects of feline infectious peritonitis virus infection. *Adv Exp Biol Med*, 218:529–550.
- Pedersen, N. and Black, J. (1983). Attempted immunization of cats against feline infectious peritonitis using either avirulent virus or sublethal amounts of virulent virus. *Am J Vet Res*, 44:229–234.
- Pedersen, N. and Boyle, J. (1980). Immunologic phenomena in the effusive form of feline infectious peritonitis. *Am J Vet Res*, 41:868–876.
- Thacker, E., Summerfield, A., McCullough, K., Ezquerra, A., Dominguez, J., Alonso, F., Lunney, J., Sinkora, J., and Haverson, K. (2001). Summary of workshop findings for porcine myelomonocytic markers. *Vet Immunol Immunopathol*, 80:93–109.
- Van de Walle, G., Favoreel, H., Nauwynck, H., and Pensaert, M. (2003). Antibody-induced internalization of viral glycoproteins and gE-gI Fc receptor activity protect pseudorabies virus-infected monocytes from efficient complement-mediated lysis. *J Gen Virol*, 84(4):939–947.
- Van de Walle, G., Favoreel, H., Nauwynck, H., Van Oostveldt, P., and Pensaert, M. (2001). Involvement of cellular cytoskeleton components in antibody-induced internalization of viral glycoproteins in pseudorabies virus-infected monocytes. *Virology*, 288:129–138.
- Vanderheijden, N., Delputte, P., Favoreel, H. W., Vandekerckhove, J., Van Damme, J., van Woensel, P., and Nauwynck, H. (2003). Involvement of sialoadhesin in entry of porcine reproductive and respiratory syndrome virus into alveolar macrophages. *J Virol*, 77:8207–8215.
- Vennema, H., de Groot, R., Harbour, D., Dalderup, M., Gruffydd-Jones, T., Horzinek, M., and Spaan, W. (1990a). Early death after feline infectious

peritonitis challenge due to recombinant vaccinia virus immunization. *J Virol*, 64:1407–1409.

Woods, R. and Pedersen, N. (1979). Cross-protection studies between feline infectious peritonitis and porcine transmissible gastroenteritis viruses. *Vet Microbiol*, 4:11–16.

# 4

## Going off the beaten track: a new internalization pathway revealed by FIPV\*

### Summary

Infection with feline infectious peritonitis (FIPV), a feline coronavirus, leads frequently to death in spite of a strong humoral immune response. In previous work, we reported that infected monocytes, the *in vivo* target cells of FIPV, express viral proteins in their plasma membranes. These proteins are quickly internalized upon binding of antibodies. As the cell surface is cleared from viral proteins, internalization might offer protection against antibody-dependent cell lysis. Here, the internalization and subsequent trafficking of the antigen-antibody complexes were characterized using biochemical, cell biological and genetic approaches. Internalization occurred through a clathrin- and caveolae-independent pathway that did not require dynamin, rafts, actin nor rho-GTPases. These findings indicate that the viral antigen-antibody complexes were not internalized through any of the previously described pathways. After internalization, the viral antigen-antibody complexes passed through the early endosomes, where they resided only briefly, and accumulated in the late endosomes. Between 30 and 60 minutes post antibody addition, the complexes left the late endosomes but were not degraded in the lysosomes. This study reveals what is probably a new internalization pathway into primary monocytes, confirming once more the complexity of endocytic processes.

---

\*This Chapter was based on Dewerchin et al. (2008)-submitted

## 4.1 Introduction

Coronaviruses may cause disease in humans (e.g. the severe acute respiratory syndrome, SARS) and in animals. In cats, two coronaviruses are described: feline enteric coronavirus (FECV) and feline infectious peritonitis virus (FIPV). These coronaviruses are spread world-wide and infect not only domestic cats but all members of the Felidae family. An infection with FIPV causes a severe pleuritis/peritonitis which mostly leads to death. Ill cats usually have very high titers of FIPV-specific antibodies. However, these antibodies are not able to block infection even though infected target cells, blood monocytes, do express viral proteins in their plasma membrane allowing antibody-dependent complement mediated cell lysis (Dewerchin et al., 2005). Also cell mediated immunity is impaired as cytotoxic T-cell are depleted during infection. This depletion is thought to be caused by a soluble viral factor inducing apoptosis in T-cell (Haagmans et al., 1996). In previous work, we reported that membrane bound viral proteins are internalized upon antibody binding through a highly efficient and fast process resulting in loss of detectable viral proteins on the plasma membrane (Dewerchin et al., 2006). The internalization process could explain why antibodies seem to be unable to identify infected cells and/or mark them for antibody-dependent cell lysis in a cat infected with FIPV. The fact that no viral antigens can be found on FIPV infected monocytes isolated from naturally infected FIP cats and that expression returns after isolation and *in vitro* cultivation of the monocytes, is a first indication that this immune evasion strategy might indeed be used *in vivo* (Cornelissen et al., 2007). As mentioned, a FIPV infection is accompanied by a strong humoral immune response but an impaired cellular immune response. If this internalization process could be blocked, than it may give the humoral immune system a chance to eliminate the infected monocytes either by antibody-dependent complement-mediated or antibody-dependent cell-mediated lysis. In order to elucidate how internalization can be blocked, the pathway needs to be identified.

In the present study, we investigated through which endocytosis pathway the antibody bound viral proteins are internalized. Multiple pathways for ligand internalization are described in literature. There are four “classical” pathways: phagocytosis, macropinocytosis, clathrin-mediated and caveolae-mediated internalization. Phagocytosis is a process by which large pathogens, such as yeast or bacteria are internalized into phagosomes (Aderem and Underhill, 1999). Macropinocytosis is a mechanism for non-selective uptake of solute macromolecules that occurs upon cell stimulation (Swanson and Watts, 1995). During clathrin-mediated endocytosis, clathrin-coated invaginations form at the plasma membrane which are pinched off upon stimulation to form clathrin-coated vesicles (Brodsky et al., 2001). Caveolae are stationary flask-shaped in-

vaginations which are present at the plasma membrane of many cell types, including monocytes/macrophages (Pelkmans and Helenius, 2002; Razani et al., 2002). Their internalization is triggered by a complex signaling cascade. To our knowledge, four clathrin- and caveolae-independent internalization or “non-classical” pathways are described in literature. For the characterization of these pathways, their dependence on rafts, dynamin and Rho-GTPases has been tested. The first one is the internalization pathway of interleukin 2 in leukocytes which is dynamin, raft and Rho-GTPase dependent (Lamaze et al., 2001). This internalization pathway might also be used by a rotavirus for entering cells (Sanchez-San Martin et al., 2004). The second one is the internalization pathway of the Menkes disease ATPase (ATP7A which is a defective copper transporting ATPase) which is Rac1 (a Rho-GTPase) dependent but raft and dynamin independent (Cobbold et al., 2003). Possibly, this pathway is also used by a polyomavirus for entry into a cell, although a role for (a) GTPase(s) is not yet clarified (Gilbert and Benjamin, 2000; Gilbert et al., 2003). The third internalization pathway is that of GPI-anchored proteins, like the folate receptor, which is raft and Cdc42 (a Rho-GTPase) dependent but dynamin independent (Sabharanjak et al., 2002; Sabharanjak and Mayor, 2004). Recently, a new entry pathway of simian virus 40 has been described in cells devoid of caveolae (Damm et al., 2005). This pathway was characterized to be raft dependent but dynamin independent and may be the same pathway as the one used by GPI-anchored proteins. The fourth internalization pathway is used by intracellular adhesion molecule-1 (ICAM-1) and platelet-endothelial cell adhesion molecule-1 (PECAM-1) which are internalized after binding of anti-ICAM-1 or anti-PECAM-1 antibodies. This internalization pathway is dynamin, actin and Rho-kinase (and Src kinase) dependent but raft independent (Muro et al., 2003). A clathrin- and caveolae-independent pathway which was independent from rafts, was described for the entry of influenza virus into HeLa cells (Sieczkarski and Whittaker, 2002). However, no further characterization was done, so classification of this entry pathway is not yet possible.

This variety of internalization processes leads to several endocytic trafficking routes. After internalization, ligands are found in endosomes and will undergo sorting and further trafficking by mechanisms that are not completely understood. Some pathways will lead to specialized compartments, phagocytosis will bring ingested particles to the phagosome and later the phagolysosome, internalization through caveolae will lead via the caveosome to the ER. Internalization through clathrin coated pits can lead from the early endosomes to (i) the recycling endosomes and back to the plasma membrane, (ii) the late endosomes and then to the lysosome for degradation or (iii) delivery to the Golgi or the endoplasmic reticulum (ER) after passing either the recycling or the late endosomes. These trafficking routes have also been described for clathrin-

and caveolae-independent internalization pathways. Besides the different endocytic routes leading to different compartments, there is also some cross-talk between these compartments which allows exchange of ligands.

Here, using biochemical, cell biological and genetic approaches, we report that FIPV antigen internalization upon antibody binding occurs via a new pathway. Our results indicate that this pathway was independent from clathrin, caveolin, dynamin, rafts, actin and Rho-GTPases. After internalization through this pathway, the viral antigen-antibody complexes traveled via the early endosomes to the late endosomes.

## 4.2 Materials and Methods

**Viruses and antibodies** A third passage of FIPV strain 79-1146 (American Type Culture Collection (ATCC)) on CrFK cells was used (McKeirnan et al., 1981). Polyclonal anti-FCoV antibodies were kindly provided by P. Rotter (Utrecht University, The Netherlands). The antibodies were purified and biotinylated according to manufacturers instructions (Amersham Bioscience, Buckinghamshire, UK). FITC-labeled polyclonal anti-FIPV antibodies were purchased from Veterinary Medical Research and Development (VMRD, Pullman, Washington, USA). The monoclonal antibodies E22-2 recognizing the N protein, were kindly provided by T. Hohdatsu (Kitasato University, Japan). The monocyte marker DH59B, which recognizes CD172a, was purchased from VMRD. A rabbit polyclonal against Rab 7 and goat polyclonals against early endosomal antigen 1 (EEA 1) and Cathepsin D were purchased from Santa Cruz Biotechnology. Secondary antibodies and reagents: goat anti-mouse Texas Red, goat anti-mouse Alexa Fluor 350, streptavidin Texas Red, streptavidin FITC and anti-rabbit and anti-goat Alexa Fluor 594 Zenon reagent were purchased from Molecular Probes-Invitrogen.

**Isolation and inoculation of blood monocytes** Feline monocytes were isolated as described previously (Dewerchin et al., 2005). Cells were seeded on glass coverslips inserted in a 24-well dish (Nunc A/S, Roskilde, Denmark) in RPMI-1640 medium containing 10% fetal bovine serum (FBS), 0.3 mg/ml glutamine, 100 U/ml penicillin, 0.1 mg/ml streptomycin, 0.1 mg/ml kanamycin, 10 U/ml heparin, 1mM sodium pyruvate, and 1% non-essential amino-acids 100x (GIBCO-Invitrogen, Merelbeke, Belgium). Non-adherent cells were removed by washing the dishes two times with RPMI-1640 at 2 and 24 hours after seeding. The adherent cells consisted for  $86 \pm 7\%$  of monocytes (as assessed by fluorescent staining with the monocyte marker DH59B). At 56 hours



post seeding, monocytes were inoculated with FIPV at a multiplicity of infection (m.o.i.) of 5. Between 20 and 60 cells were analyzed per assay.

**Internalization inhibition assays** Twelve hours after inoculation, monocytes seeded on glass coverslips were pre-incubated for 30 minutes at 37°C with 5% CO<sub>2</sub> in the presence of one of the following agents dissolved in RPMI (all products were purchased from Sigma-Aldrich GmbH (Steinheim, Germany) unless stated otherwise): 500 μM amantadine, 0,1 μM wortmannin, 0.74 nM *Clostridium Difficile* Toxin B, 20 μM latrunculin B (ICN Biochemicals Inc., OH), 10 mM methyl-beta-cyclodextrin, 50 μg/ml nystatin or 40 μM dynamin inhibitory peptide (Tocris Cookson ltd., Bristol, UK). The working concentration of each reagent was based on literature values and was optimized qualitatively in internalization assays with control ligands (data not shown). Viability of the cells during the inhibition assay was tested for each inhibitor using ethidium bromide monoazide (Molecular Probes-Invitrogen) and was always over 99%.

After pre-treatment, the cells were incubated with polyclonal biotinylated anti-FIPV antibodies in presence of one of the given inhibitors for 30 minutes at 37°C. Then, cells were fixed with 1% formaldehyde, permeabilized with 0.1% Triton X-100 (Sigma-Aldrich GmbH) and incubated with streptavidin-Texas Red for 1 hour at 37°C. Next, infected cells were visualized with polyclonal anti-FIPV-FITC. The glass coverslips were mounted on microscope slides using glycerin-PBS solution (0.9:0.1, vol/vol) with 1,4-diazabicyclo (2, 2, 2)octane (2.5%) (DABCO) (Janssen Chimica, Beerse, Belgium) and analyzed with confocal microscopy. Percentages of cells with fully internalized complexes were calculated relative to the total amount of monocytes which showed antibody binding and thus had membrane expression before antibodies were added. Those monocytes constitute about 50% of the total amount of infected cells (Dewerchin et al., 2005). Because of the variability on the amount of cells with membrane expression, visualization of the complexes remaining at the plasma membrane was needed. Therefore, an acid washing step to remove the extracellular antibodies was not performed.

To test the effectiveness of the reagents, a suitable control was used in each experiment. Monocytes seeded on glass coverslips were pre-incubated for 30 minutes at 37°C with 5% CO<sub>2</sub> in the presence of one of the inhibitors. After treatment, the cells were incubated with biotinylated transferrin (Sigma-Aldrich GmbH) or fluorescent 1μm polystyrene microspheres, FluoSpheres (Molecular Probes-Invitrogen), in presence of the inhibitor. Then, cells were fixed with 1% formaldehyde and permeabilized with 0.1% Triton X-100. The biotinylated transferrin was visualized by incubating the cells with streptavidin-FITC

for 1 hour at 37°C and cells incubated with fluorescent beads were incubated with phalloidin-Texas Red (Molecular Probes-Invitrogen) for 1 hour at 37°C to visualize the actin in the lamellipodia. The glass coverslips were mounted on microscope slides using glycerin-DABCO and analyzed by confocal microscopy. For the controls, the monocytes were scored analogously as FIPV infected cells: ligands were considered “fully internalized” when they were only observed inside the cell. Fluorescent beads were considered internalized when they were found inside the cortical actin labeling.

**Transfer plasmid construction** The TRIPΔU3-CMV-WPRE vector ( this is the TRIPΔU3-CMV-GFP-WPRE in which GFP was deleted by BamHI-SalI digestion) was used as transfer vector, pMD.G as envelope plasmid and p8.91 as packaging plasmid as described before (Stove et al., 2005).

The enhanced green fluorescent protein (EGFP) tagged dominant negative (DN) human eps15 construct, named DIII, and the EGFP tagged control construct D3Δ2 were kindly provided by A. Benmerah (Benmerah et al., 1998). Both constructs were excised from pEGFP-C2 by BclI and Eco47III digestion and double-blunt cloned into TRIPΔU3-CMV-WPRE vector.

The EGFP tagged wild type (WT) en DN canine caveolin-1 constructs were a kind gift from A. Helenius (Kurzychalia et al., 1992; Pelkmans et al., 2001). The WT caveolin-1-GFP construct was amplified by PCR from the pEGFP-N1 vector and cloned into the TRIPΔU3-CMV-WPRE vector. The DN caveolin-1-GFP construct was excised from pEGFP-C1 by Eco 47III and BamHI digestion and double-blunt cloned into TRIPΔU3-CMV-WPRE vector.

The EGFP tagged WT and DN rat dynamin2(aa) were kindly provided by M. McNiven (Cao et al., 1998, 2000). Both constructs were excised from pEGFP-N1 by HindIII and XbaI digestion and double-blunt cloned into TRIPΔU3-CMV-WPRE vector.

Biological activity of all constructs was tested on a feline cell line (CrFK) before and after transfer to pTRIPΔU3-CMV-WPRE.

**Production of lentiviral supernatant** 293FT cells (Invitrogen) were seeded in a 25 cm<sup>2</sup> culture dish in Iscove’s modified Dulbecco’s medium (IMDM, Gibco-Invitrogen) supplemented with 100 U/ml penicillin, 0.1 mg/ml streptomycin and 10% heat inactivated fetal bovine serum (FBS). At 70% confluency, cells were co-transfected with 1.66 μg packaging plasmids, 3.33 μg envelope plasmids and 3.33 μg transfer plasmids using a Calcium Phosphate Transfection kit (Invitrogen). Viral supernatant was harvested 40 hours later.

**Viral gene transfer, superinfection and internalization assays** Feline monocytes were isolated as described previously (Dewerchin et al., 2005). After 3 hours, the cells were washed and medium was replaced with lentiviral supernatant. At 24 hps, cells were washed and fresh medium was added. At 56 hps, cells were inoculated with FIPV. Twelve hours later, internalization assays were performed by adding biotinylated anti-FIPV antibodies for 30 minutes. Then, cells were fixed with 1% formaldehyde, permeabilized with 0.1% Triton X-100 and incubated with streptavidin-Texas Red to visualize the antigen-antibody complexes. Next, infected cells were visualized with anti-N monoclonal antibodies and goat anti-mouse Alexa Fluor 350 (not shown in images). Transduction efficiencies varied between 10 and 50%.

For the controls, transduced cells were incubated with biotinylated transferrin or biotinylated cholera toxin B (Sigma-Aldrich GmbH). Then, cells were fixed, permeabilized and ligands were visualized with streptavidin-Texas Red.

**Co-localization studies with endosomal markers** Twelve hours after inoculation, monocytes were incubated with biotinylated anti-FIPV polyclonal antibodies. At different times post antibody addition, cells were fixed with 1% formaldehyde, permeabilized with 0.1% Triton X-100 and antigen-antibody complexes were visualized with streptavidin-FITC followed by a blocking step with 10% negative goat serum. To visualize early endosomes, goat polyclonal antibodies against EEA 1 were tagged with anti-goat Alexa Fluor 594 Zenon reagent. To visualize late endosomes and lysosomes, rabbit polyclonal antibodies against Rab 7 and Cathepsin D, respectively, were tagged with anti-rabbit Alexa Fluor 594 Zenon reagent. After 45 minutes of incubation with the tagged antibodies, cells were fixed to stabilize the Zenon reagent. Finally, infected cells were visualized with anti-N monoclonal antibodies and goat anti-mouse Alexa Fluor 350 (not shown in images).

**Confocal laser scanning microscopy** Samples were examined with a Leica TCS SP2 laser scanning spectral confocal system (Leica Microsystems GmbH, Wetzlar, Germany) linked to a DM IRB inverted microscope (Leica Microsystems). Argon and Helium/Neon laser lights were used to excite FITC (488 nm line) and Texas-Red or Alexa Fluor 594 (543 nm line) fluorochromes. The images were obtained with Leica confocal software and processed with the GIMP.

**Statistical analysis** Triplicate assays were compared using a Mann-Whitney U test with SPSS 11.0 (SPSS Inc., Chicago, WA). P values <0.05 were con-

sidered significantly different. For each assay, between 20 and 60 cells were counted.

## 4.3 Results

### 4.3.1 Internalization of viral plasma membrane-bound proteins does not occur via phagocytosis or macropinocytosis

Around half of FIPV infected monocytes display viral proteins on their plasma membrane (Dewerchin et al., 2005). As we showed previously, binding of specific antibodies to these proteins leads to rapid internalization of the antigen-antibody complexes (Dewerchin et al., 2006). In this paper we wanted to investigate through which endocytic route the antigen-antibody complexes were internalized.

First, phagocytosis and macropinocytosis were tested as possible internalization routes using the inhibitors wortmannin (which interacts with phosphatidylinositol 3-kinase (PI3-K) and thereby prevents the closing of lamellipodia) and latrunculin B, (which disrupts existing actin filaments and prevents assembly of new filaments thus inhibiting the formation of membrane protrusions necessary for both phagocytosis and macropinocytosis). Activity of the inhibitors was validated by determining their effect on the phagocytosis of fluorescent beads (1 $\mu$ m in diameter). Figure 4.1, panel a, shows cells after the internalization assay in the presence of the inhibitors. The internalization of the control beads was reduced to  $49\pm 11\%$  and  $18\pm 6\%$  of untreated controls for wortmannin and latrunculin B, respectively, while the antibody-induced internalization of viral proteins remained unaffected (Figure 4.1, panel b). These data suggest that viral proteins were not internalized via phagocytosis nor macropinocytosis and that internalization did not require dynamic actin.

### 4.3.2 Internalization of viral plasma membrane-bound proteins is not mediated by clathrin

To test the dependence on clathrin, amantadine was used which stabilizes clathrin-coated pits and inhibits their internalization (Phonphok and Rosenthal, 1991). The internalization of viral antigens in the presence of amantadine was not significantly different from internalization in untreated monocytes while internalization of the control ligand transferrin (a marker for clathrin-mediated endocytosis) was reduced to  $2\pm 1\%$  of the internalization in untreated control cells (Figure 4.1).

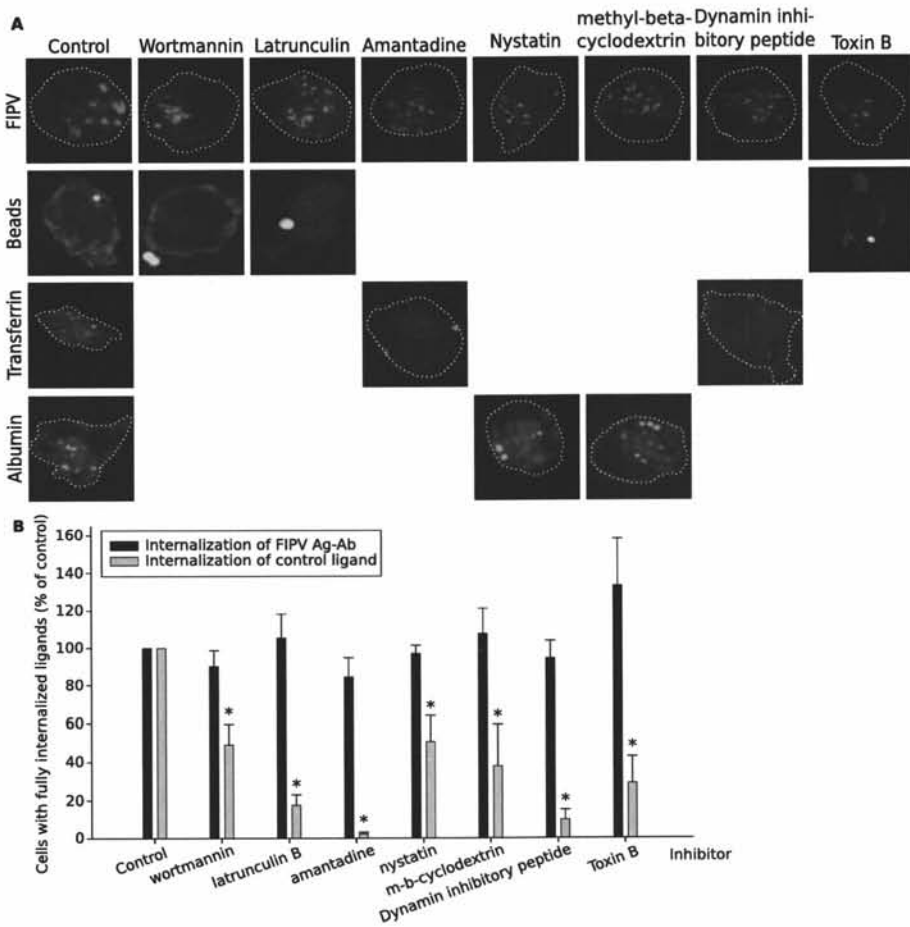


Figure 4.1: Antibody-induced internalization of surface expressed viral antigens in monocytes does not occur via a known internalization pathway. (a) Confocal images of feline monocytes after internalization assays in the presence of inhibitors. The images show a single optical section through the cell. The activity of each inhibitor was tested with an internalization assay using a suitable control. In row 2, cortical actin was stained (red) to visualize whether or not the lamellipodia were closed around the beads. (b) Quantification of the internalization. Results are given relatively to a control of untreated cells. The black bars represent the internalization of viral antigens. The gray bars represent the internalization of control ligands (beads, transferrin or albumin). Data are means and standard deviations of triplicate assays. The asterisk marks results that are significantly different from the untreated control ( $p < 0.05$ ).

Possible independence of clathrin-mediated internalization was confirmed using a dominant negative (DN) mutant of Eps15, a protein that is essential for docking of adaptor protein-2 (AP-2) to the plasma membrane during the assembly of the clathrin-coated pits (Benmerah et al., 1998, 1999). The DN construct of Eps15, named DIII, has a deletion at the Eps15 homology (EH) and coiled coil domains and a C-terminal enhanced green fluorescent protein (EGFP) tag. The construct D3 $\Delta$ 2, with an additional deletion of the AP-2 binding site, was used as a control. To enable expression of the DN protein in primary monocytes, the constructs were cloned into a lentiviral expression system. In monocytes transduced with the DN construct DIII, the uptake of the control ligand transferrin was reduced to  $40\pm 9\%$  while the internalization of viral proteins in DIII transduced, FIPV infected monocytes remained unaffected (Figure 4.2). The image in Figure 4.2 of transferrin uptake in a monocyte transduced with DN Eps15 show very little staining at the plasma membrane. This is because internalization assays are performed when the dominant negative proteins are already expressed for about 12 hours. By that time, the transferrin receptors that are locked at the plasma membrane are mostly saturated by the (unlabeled) transferrin that is present in the culture medium. In monocytes transduced with the control construct D3 $\Delta$ 2, internalization of both transferrin and viral proteins was not significantly different from the untransduced controls. Together, these results indicate that antibody-induced internalization of viral antigens in FIPV infected cells occurs independently of clathrin.

### **4.3.3 Internalization of viral plasma membrane-bound proteins is not mediated by caveolae**

Nystatin was used to obtain a first indication of a possible role for caveolae in the internalization process. Nystatin inhibits formation and maintenance of caveolae by binding to sterols which leads to depletion of cholesterol in the plasma membrane. There was no significant influence of nystatin on the internalization of viral antigens upon antibody addition while the internalization of control ligand albumin, a marker for caveolae-mediated endocytosis, was reduced to  $50\pm 14\%$  of the untreated control (Figure 4.1). The images in Figure 4.1 show how albumin accumulates in the preformed caveolae that are locked underneath to the plasma membrane when monocytes are treated with nystatin or methyl-beta-cyclodextrin.

The independence of the internalization process from caveolae was verified using a GFP-tagged DN mutant of caveolin-1 (Kurzychalia et al., 1992; Pelkmans et al., 2001). GFP-tagged wild type (WT) caveolin-1 was used as a control. Both constructs were cloned into the lentiviral expression system. In monocytes transduced with DN caveolin-1, there was no reduction in the in-

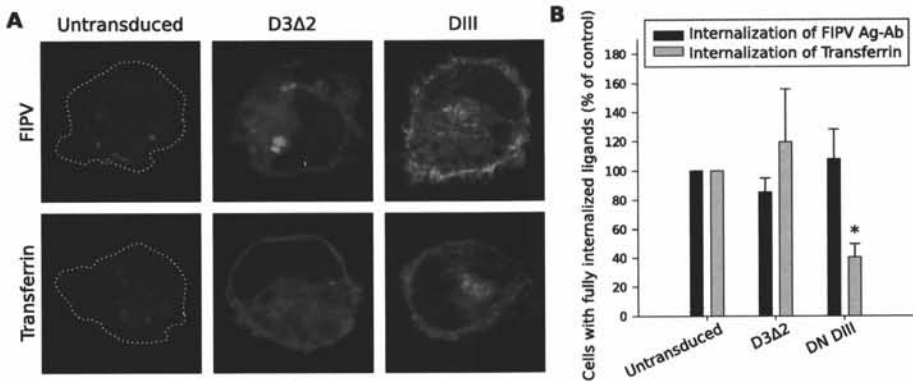


Figure 4.2: Esp15 is not required during the internalization of viral membrane bound proteins. Monocytes were transduced with DIII (DN Eps15) or the control construct D3Δ2. (A) Confocal images of feline monocytes after internalization assays. The images show a single optical section through the cell. The green signal represents the EGFP-tagged DIII or D3Δ2 proteins and the red signal is biotinylated transferrin or antigen-antibody complexes visualized with streptavidin-Texas Red. (B) Quantification of the internalization relatively to untransduced cells. The black bars represent the internalization of viral antigens, the gray bars the internalization of the control ligand transferrin. Data are means and standard deviations of triplicate assays. The asterisk marks results that are significantly different from the untransduced control ( $p < 0.05$ ).

ternalization of viral antigens whereas the uptake of the control ligand cholera toxin B was reduced to  $40 \pm 5\%$  compared to the untransduced monocytes (Figure 4.3). Transduction with WT caveolin did not have an effect on the internalization of viral proteins nor of cholera toxin B. Taken together, these results show that the internalization of viral surface expressed proteins is not mediated by caveolae.

#### 4.3.4 Internalization of viral plasma membrane-bound proteins does not occur via a known clathrin- and caveolae-independent pathway

Since the above results strongly suggest that internalization occurs through a clathrin- and caveolae-independent pathway, we wanted to compare the current pathway with independent pathways described in literature. In order to differentiate between the four clathrin- and caveolae-independent pathways, three inhibitors were used: methyl-beta-cyclodextrin, dynamin inhibitory peptide and *Clostridium Difficile* Toxin B. These inhibitors indicate dependence on rafts, dynamin and Rho-GTPases respectively. None of the inhibitors caused a significant difference in internalized antigens, although a slight increase was observed in monocytes treated with Toxin B. In contrast, the internalization

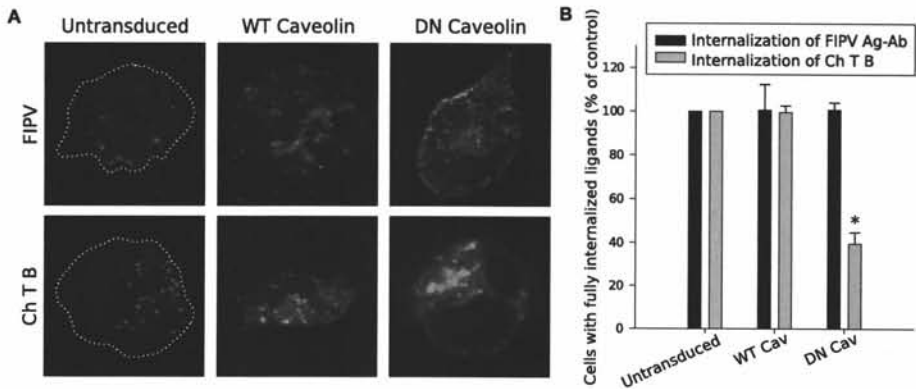


Figure 4.3: Caveolin-1 is not required during the internalization of viral membrane bound proteins. Monocytes were transduced with DN caveolin-1 or the control construct WT caveolin-1. (A) Confocal images of feline monocytes after internalization assays. The images show a single optical section through the cell. The green signal represents the EGFP-tagged WT or DN Caveolin-1 proteins and the red signal is biotinylated cholera toxin B or antigen-antibody complexes visualized with streptavidin-Texas Red. (B) Quantification of the internalization relatively to untransduced cells. The black bars represent the internalization of viral antigens, the gray bars the internalization of the control ligand cholera toxin B (Ch T B). Data are means and standard deviations of triplicate assays. The asterisk marks results that are significantly different from the untransduced control ( $p < 0.05$ ).

of the control ligands (albumin, transferrin or beads) was clearly inhibited to, respectively,  $38 \pm 21\%$ ,  $10 \pm 5\%$  and  $19 \pm 6\%$ , of the internalization in untreated control cells (Figure 4.1). Independence from rafts was also reinforced by the results with the inhibitor nystatin, which compromises the function of rafts by binding to cholesterol (Figure 4.1).

To confirm the independence of dynamin, the only structural protein that characterizes two of the clathrin- and caveolae-independent pathways, a GFP-tagged DN mutant from dynamin-2aa (K44A) was used (Cao et al., 1998). GFP-tagged WT dynamin-2aa was used as a control (Cao et al., 2000). The constructs were cloned into the lentiviral expression system to allow expression in primary monocytes. Transduction of monocytes with the DN dynamin-2aa construct led to a decrease in uptake of the control ligand transferrin to  $32 \pm 13\%$  of the untransduced control while transduction with the WT dynamin-2aa construct led to an increase to  $161 \pm 21\%$ . In contrast, internalization of the viral antigen-antibody complexes remained unaffected by either construct (Figure 4.4). These results indicate that dynamin, rafts and Rho-GTPases are not required for the internalization of viral antigens.

These findings also reinforce the independence from phagocytosis since dynamin 2 is required for phagocytosis in macrophages, presumably at the stage



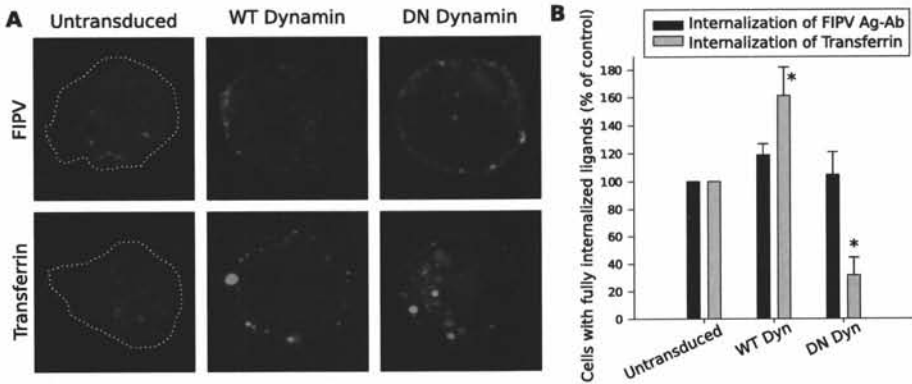


Figure 4.4: Dynamin-2aa is not required during the internalization of viral membrane bound proteins. Monocytes were transduced with DN dynamin-2aa or the control construct WT dynamin-2aa. (A) Confocal images of feline monocytes after internalization assays. The green signal represents the EGFP-tagged DN or WT dynamin-2aa proteins and the red signal is biotinylated transferrin or antigen-antibody complexes visualized with streptavidin-Texas Red. (B) Quantification of the internalization relatively to untransduced cells. The black bars represent the internalization of viral antigens, the gray bars the internalization of the control ligand transferrin. Data are means and standard deviations of triplicate assays. The asterisk marks results that are significantly different from the untransduced control ( $p < 0.05$ ).

of membrane extension (Gold et al., 1999). Furthermore, the inhibitors methyl-beta-cyclodextrin and dynamin inhibitory peptide and the DN dynamin construct confirmed the above results since they can block clathrin- and caveolae-mediated endocytosis (and two independent pathways) simultaneously.

#### 4.3.5 Co-localization of viral antigen-antibody complexes and endosomal compartments

After internalization, ligands are transported in endocytic compartments. To visualize this intracellular trafficking, co-localization stainings were performed with markers for early endosomes, late endosomes and lysosomes. First, passage through early endosomes was checked by staining early endosome antigen 1 (EEA1). The first row of images in Figure 4.5 shows that co-localization was only observed at 30 seconds and at 1 minute. In most monocytes, few internalized antigen-antibody complexes were found to co-localize with EEA1. This indicates that the antigen-antibody complexes resided in early endosomes only briefly before they were transported further into the cell. Co-localization stainings with Rab 7 (a late endosome marker) confirmed that the antigen-antibody complexes moved quickly to the late endosomes in which complexes were already observed as soon as 1 minute after internalization (Figure 4.5, row 2). The antigen-antibody complexes accumulated in the late endosomes

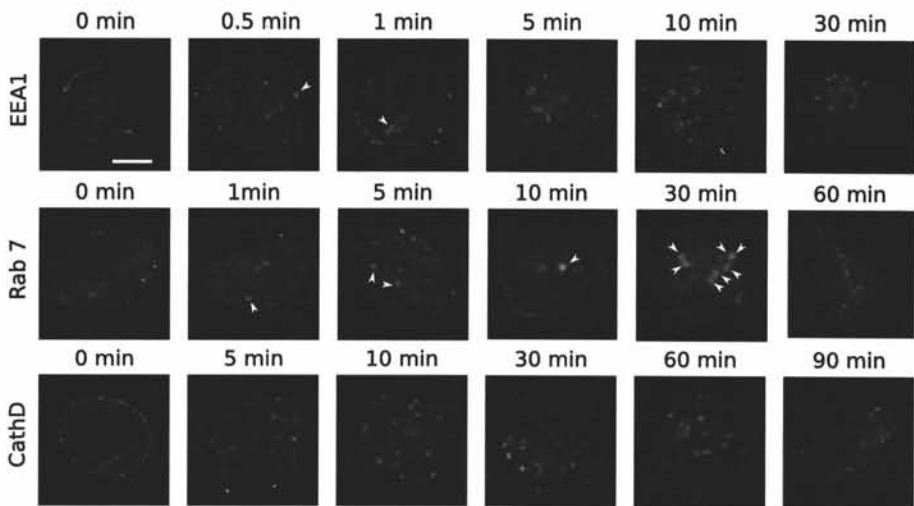


Figure 4.5: After passage through the early endosomes, viral antigens accumulate in the late endosomes but are not degraded in the lysosomes. Internalizing antigen-antibody complexes were visualized with streptavidin FITC (green signal). EEA1, Rab7 and Cathepsin D were used as markers for early endosomes, late endosomes and lysosomes respectively (red signal). Arrow heads indicate colocalization. The images show a single optical section through a monocyte. Scale bar:  $5\mu\text{m}$ .

until 30 minutes post antibody addition. By 60 minutes, all complexes had left the late endosomes. Stainings with the lysosome marker Cathepsin D showed no co-localization at any time point. Taken together, these stainings indicate that internalized antigens in FIPV infected monocytes quickly passed through the early endosomes ( $< 1$  minute) and then accumulated in the late endosomes, but did not continue along the degradative pathway.

## 4.4 Discussion

Internalization processes are being studied for decades. Over 100 years ago, phagocytosis was the first endocytic process to be described (Metchnikoff, 1905). Already in 1931, membrane ruffles were seen on macrophages, a phenomenon that was later named macropinocytosis (Lewis, 1931). In the 1950s, electron microscopists described cave-like invaginations at the plasma membrane which were called “caveolae intracellulare”. However, it took until 1992 before the major structural protein, caveolin, could be identified (Rothberg et al., 1992). In 1964 internalization through vesicles covered with a dense protein coat was first described (Roth and Porter, 1964). It took another 10 years to characterize the major coat protein: clathrin (Pearse, 1975). Since

then, knowledge about these four “classical” internalization pathways is being gathered at increasing speed. Around the turn of the century, the first clathrin- and caveolae-independent pathways were reported (Gilbert and Benjamin, 2000; Lamaze et al., 2001). To date, four independent pathways have been described, two of which involve dynamin for pinching off the vesicle from the plasma membrane. For the other two, no structural protein could be identified so far. They are distinguished from each other solely by the finding that they are mediated by different Rho-GTPases.

In this work, we sought to identify through which pathway the surface expressed viral proteins in FIPV infected monocytes were internalized after binding of antibodies. The used techniques were based on immunofluorescence and confocal microscopy. Considering the fact that the *in vitro* infection rate of monocytes varies between 0,1 and 1%, of which around 50% have membrane expression, experiments that require a lot of starting material (e.g. flowcytometry or western blots) could not be performed. In addition, we were restricted to monocytes to perform our experiments since internalization could not be induced in CrFK or fcwf cell lines (Dewerchin et al., 2006).

The surface expressed viral proteins in a FIPV infected monocyte are the Spike protein and the Membrane protein (Dewerchin et al., 2006). The experiments presented here, showed that internalization of these proteins was not clathrin-mediated, since it could not be blocked by 6 inhibitors (amantadine, latrunculin B, methyl-beta-cyclodextrin, dynamin inhibitory peptide, toxin B, sodium fluoride) and 2 DN constructs (eps15 and dynamin) known to inhibit clathrin-mediated internalization. Independence from caveolae was also confirmed with 6 inhibitors (nystatin, genistein, latrunculin B, methyl-beta-cyclodextrin, dynamin inhibitory peptide, toxin B, sodium vanadate) and 2 DN constructs (caveolin and dynamin). The experiments further indicated that the antigen-antibody complexes were not internalized via phagocytosis, macropinocytosis nor via any known clathrin- and caveolae-independent pathway.

After internalization, the viral antigen-antibody complexes were further transported into the cell. The main pinocytic trafficking routes are the recycling and the degradative pathway. In the recycling pathway, ligands pass through the early endosome, are transported over microtubules towards the perinuclear region and then accumulate in the recycling endosomes close to the microtubule organizing center (Mellman, 1996). Transit through the recycling pathway takes 5 to 10 minutes. In the degradative pathway, ligands also pass the early endosome but are then sorted to late endosome and transported towards the cell center where they are delivered to the lysosome by fusion (Mellman, 1996). In the internalization process studied here, internalized antigen-antibody complexes could be observed inside the cell for more than 1 hour,

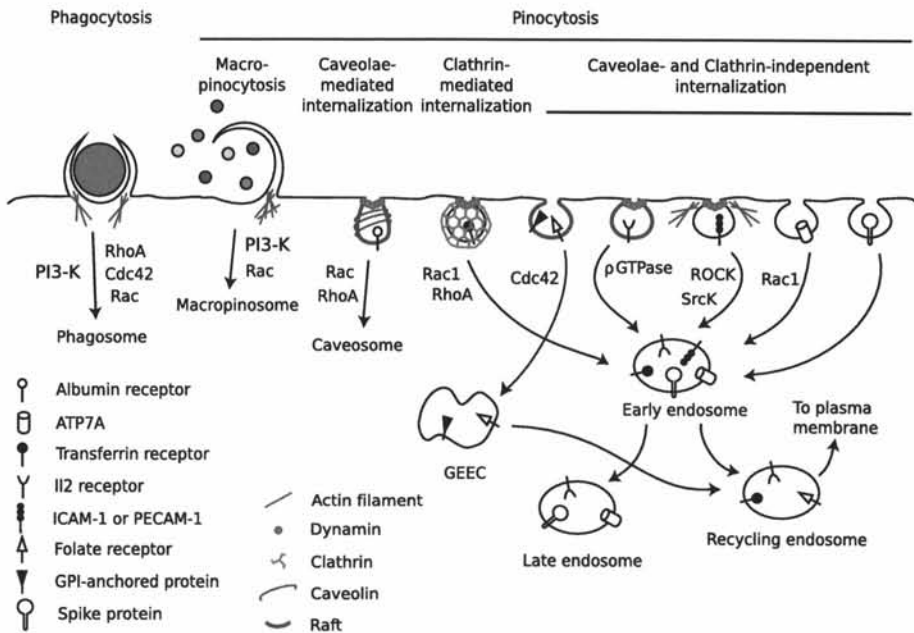


Figure 4.6: Overview of all internalization pathways with characterizing features and subsequent intracellular trafficking. GPI: Glycosyl-phosphatidylinositol, GEEC: GPI-anchored protein-enriched early endosomal compartment.

making the recycling pathway a highly unlikely route for trafficking. Therefore, co-localization stainings with markers for the degradative endocytic pathway were performed. The stainings revealed that the antigen-antibody complexes resided in the early endosomes only briefly. Then, antigen-antibody complexes accumulated in the late endosomes. The complexes left the late endosome between 30 and 60 minutes but were not observed in the lysosomes, indicating that they did not follow the degradative pathway. The fact that the antigen-antibody complexes could still be observed at 90 minutes post antibody addition, confirmed that the complexes were not degraded. It remains to be elucidated if these antigen-antibody complexes might be of importance during the infection cycle. An overview of all internalization pathways with addition of the pathway presented here, is given in Figure 4.6.

The finding that internalization of the viral antigen-antibody complexes occurs through an unusual pathway, actually increases the chance that blocking of internalization could be used as a treatment for FIP cats. We have previously shown that internalization could not be reproduced in the feline CrFK and fcwf cell lines (Dewerchin et al., 2006). This implies that specific cellular components are required that are not ubiquitously expressed, adding to the likelihood of finding a compound that will specifically block this internalization route

while leaving the more conventional pathways undisturbed.

In conclusion, surface expressed viral proteins in FIPV infected monocytes are internalized through a clathrin- and caveolae-independent internalization pathway which is independent of actin, rafts, dynamin and Rho-GTPases. Internalization of viral antigens through this pathway led to trafficking via the early endosomes to the late endosomes, but not to the lysosomes. Despite the growing number of independent internalization pathways, very little is known about the molecular mechanisms underlying these pathways. But, as the pathways are better characterized, it seems that they are very well regulated and cargo-specific. Undoubtedly, more internalization pathways await their discovery and characterization, which might lead to better understanding of the complex network of all internalization processes.

## Acknowledgments

We are very grateful to P. Rottier for supplying polyclonal anti-FCoV antibodies and to T. Hohdatsu for monoclonal anti-N protein antibodies; to A. Benmerah for the DIII and D3Δ2 constructs, to A. Helenius for the WT en DN caveolin-1 constructs, to M. McNiven for the WT en DN dynamin-2 constructs and to J. Vicca for supplying fluorescent beads. We thank E. Naessens for technical assistance and J. Vandekerckhove and C. Ampe for critical reading. H.L.D. and E.C. were supported by the Institute for the Promotion of Innovation through Science and Technology in Flanders (IWT-Vlaanderen). E.V.H. was supported by the Special Research Fund of Ghent University, grant 01D29005. K.S. is a PhD fellow and B.V. a senior clinical investigator supported by the Research Foundation Flanders (FWO), grant G.0061.05.

## References

- Aderem, A. and Underhill, D. (1999). Mechanisms of phagocytosis in macrophages. *Annu Rev Immunol*, 17:593–623.
- Benmerah, A., Bayrou, M., Cerf-Bensussan, N., and Dautry-Varsat, A. (1999). Inhibition of clathrin-coated pit assembly by an Eps15 mutant. *J cell Sci*, 112:1303–1311.
- Benmerah, A., Lamaze, C., Begue, B., Schmid, S., Dautry-Varsat, A., and Cerf-Bensussan, N. (1998). AP-2/Eps15 interaction is required for receptor-mediated endocytosis. *J Cell Biol*, 140:1055–1062.

- Brodsky, F., Chen, C.-Y., Knuehl, C., Towler, M., and Wakeham, D. (2001). Biological basket weaving: formation and function of clathrin-coated vesicles. *Annu Rev Cell Dev Biol*, 17:517–568.
- Cao, H., Garcia, F., and McNiven, M. (1998). Differential distribution of dynamin isoforms in mammalian cells. *Mol Biol Cell*, 9:2595–2609.
- Cao, H., Thompson, H., Krueger, E., and McNiven, M. (2000). Disruption of golgi structure and function in mammalian cells expressing a mutant dynamin. *J Cell Sci*, 113:1993–2002.
- Cobbold, C., Coventry, J., Ponnambalam, S., and Monaco, A. (2003). The menkes disease ATPase (ATP7A) is internalized via a Rac1-regulated, clathrin- and caveolae-independent pathway. *Hum Mol Genet*, 12(13):1523–1533.
- Cornelissen, E., Dewerchin, H., Van Hamme, E., and Nauwynck, H. (2007). Absence of surface expression of feline infectious peritonitis virus (FIPV) antigens on infected cells isolated from cats with FIP. *Vet Microbiol*, 121:131–137.
- Damm, E.-M., Pelkmans, L., Kartenbeck, J., Mezzacasa, A., Kurzchalia, T., and Helenius, A. (2005). Clathrin- and caveolin-1-independent endocytosis: entry of simian virus 40 into cells devoid of caveolae. *J Cell Biol*, 168:477–488.
- Dewerchin, H., Cornelissen, E., and Nauwynck, H. (2005). Replication of feline coronaviruses in peripheral blood monocytes. *Arch Virol*, 150(12):2483–2500.
- Dewerchin, H., Cornelissen, E., and Nauwynck, H. (2006). Feline infectious peritonitis virus-infected monocytes internalize viral membrane-bound proteins upon antibody addition. *J Gen Virol*, 87:1685–1690.
- Gilbert, J. and Benjamin, T. (2000). Early steps of polyomavirus entry into cells. *J Virol*, 74:8582–8588.
- Gilbert, J., Goldberg, I., and Benjamin, T. (2003). Cell penetration and trafficking of polyomavirus. *J Virol*, 77:2615–2622.
- Gold, E., Underhill, D., Morrissette, N., Guo, J., McNiven, M., and Aderem, A. (1999). Dynamin 2 is required for phagocytosis in macrophages. *J Exp Med*, 190:1849–1856.
- Haagmans, B., Egberink, H., and Horzinek, M. (1996). Apoptosis and t-cell depletion during feline infectious peritonitis. *J Virol*, 70:8977–8983.

- Kurzchalia, T., Dupree, P., Parton, R., Kellner, R., Virta, H., Lehnert, M., and Simons, K. (1992). VIP21, a 21kD membrane protein is an integral component of trans-golgi-derived transport vesicles. *J Cell Biol*, 118:1003–1014.
- Lamaze, C., Dujeancourt, A., Baba, T., Lo, C., Benmerah, A., and Dautry-Varsat, A. (2001). Interleukin 2 receptors and detergent-resistant membrane domains define a clathrin-independent endocytic pathway. *Mol Cell*, 7:661–671.
- Lewis, W. (1931). Pinocytosis. *Johns Hopkins Hosp Bull*, 49:17–27.
- McKeirnan, A., Evermann, J., Hargis, A., and Ott, R. (1981). Isolation of feline coronaviruses from 2 cats with diverse disease manifestations. *Feline Practice*, 11(3):16–20.
- Mellman, I. (1996). Endocytosis and molecular sorting. *Annu Rev Cell Dev Biol*, 12:575–625.
- Metchnikoff, E. (1905). *Immunity in infective diseases*. Cambridge Univ Press.
- Muro, S., Wiewrodt, R., Thomas, A., Koniaris, L., Albelda, S., Muzykantov, V., and Koval, M. (2003). A novel endocytic pathway induced by clustering endothelial ICAM-1 or PECAM-1. *J Cell Sci*, 116:1599–1609.
- Pearse, B. (1975). Coated vesicles from pig brain: purification and biochemical characterization. *J Mol Biol*, 97:93–98.
- Pelkmans, L. and Helenius, A. (2002). Endocytosis via caveolae. *Traffic*, 3:311–320.
- Pelkmans, L., Kartenbeck, J., and Helenius, A. (2001). Caveolar endocytosis of simian virus 40 reveals a new two-step vesicular-transport pathway to the ER. *Nature Cell Biol*, 3:473–483.
- Phonphok, Y. and Rosenthal, K. S. (1991). Stabilization of clathrin coated vesicles by amantadine, tromantadine and other hydrophobic amines. *FEBS Lett*, 281:188–190.
- Razani, B., Woodman, S., and Lisanti, M. (2002). Caveolae: from cell biology to animal physiology. *pharmacol rev*, 54:431–467.
- Roth, T. and Porter, K. (1964). Yolk protein uptake in the oocyte of the mosquito *Aedes aegypti*. *L J Cell Biol*, 20:313–332.

- Rothberg, K. G., Heuser, J. E., Donzell, W. C., Ying, Y. S., Glenney, J. R., and Anderson, R. G. (1992). Caveolin, a protein component of caveolae membrane coats. *Cell*, 68:673–682.
- Sabharanjak, S. and Mayor, S. (2004). Folate receptor endocytosis and trafficking. *Adv Drug Del Rev*, 56:1099–1109.
- Sabharanjak, S., Sharma, P., Parton, R., and Mayor, S. (2002). GPI-anchored proteins are delivered to recycling endosomes via a distinct Cdc42-regulated, clathrin-independent pinocytotic pathway. *Dev Cell*, 2:411–423.
- Sanchez-San Martin, C., Lopez, T., Arias, C., and Lopez, S. (2004). Characterization of rotavirus cell entry. *J Virol*, 78:2310–2318.
- Sieczkarski, S. and Whittaker, G. (2002). Influenza virus can enter and infect cells in the absence of clathrin-mediated endocytosis. *J Virol*, 76(20):10455–10464.
- Stove, V., Van de Walle, I., Naessens, E., Coene, E., Stove, C., Plum, J., and Verhasselt, B. (2005). Human immunodeficiency virus Nef induces rapid internalization of T-cell coreceptor CD8alpha-beta. *J Virol*, 79:11422–11433.
- Swanson, J. and Watts, C. (1995). Macropinocytosis. *Trends Cell Biol*, 5(11):424–428.



# 5

## Microtubules, actin and myosins cooperate during internalization and trafficking of antigen-antibody complexes in FIPV infected monocytes\*

### Summary

In previous work we reported that monocytes infected with feline infectious peritonitis virus, a coronavirus, express viral proteins in their plasma membranes. Upon binding of antibodies, these proteins are quickly internalized through a new clathrin- and caveolae-independent internalization pathway. In the present study, we investigated the importance of microtubules, actin and myosins during internalization and subsequent intracellular transport. The experiments showed that internalization and trafficking was dependent on microtubules but did not require actin polymerization. In fact, cortical actin formed a barrier that slowed down internalization. With co-localization stainings, it was found that myosin 2a, 2b, 5a, 7a, 9b and 10 were not involved in the internalization or subsequent trafficking of the antigen-antibody complexes. However, myosin 1 and 6 co-localized with the internalizing complexes during passage through the cortical actin and might thus be involved in the required actin reorganization. One minute after internalization started, vesicles had passed the cortical actin, co-localized with microtubules and association with myosin 6 was lost. The vesicles were further transported over the microtubules and accumulated at the microtubule organizing center after 10 to 30 minutes. During transport over microtubules, the vesicles were associated with myosin 1 and a small actin tail indicating that actin, myosin 1 and microtubules cooperated during intracellular trafficking.

---

\*Manuscript in preparation

## 5.1 Introduction

Two coronaviruses are described in cats: feline infectious peritonitis virus (FIPV) and feline enteric coronavirus (FECV). These coronaviruses can infect both cats and other members of the Felidae family. An infection with FECV is usually sub-clinical, except in young kittens where it may cause mild to severe diarrhea (Pedersen et al., 1981). In contrast, FIPV infection causes a chronic and very often fatal pleuritis/peritonitis. In fact, it is the most important cause of death of infectious origin in cats. Cats with clinical FIP often have very high titers of FIPV-specific antibodies. Yet, these antibodies are not able to block infection, which suggests that antibodies and antibody-driven immune effectors are not able to efficiently clear the body from virus and/or virus-infected cells.

In previous work, we presented an immune evasion strategy used by FIPV that could clarify why antibodies seem to be unable to identify infected cells and/or mark them for antibody-dependent cell lysis. We found that surface expressed viral proteins are internalized upon antibody addition through a highly efficient and fast process resulting in FIPV-infected cells without visually detectable viral proteins on their plasma membrane (Dewerchin et al., 2006). The fact that no viral antigens can be found on FIPV infected monocytes isolated from naturally infected FIP cats and that expression returns after isolation and *in vitro* cultivation of the monocytes, is a first indication that this immune evasion strategy occurs *in vivo* (Cornelissen et al., 2007). We then went on to elucidate through which internalization pathway these antigen-antibody complexes are internalized.

Ligands can be internalized into cells via several pathways. There are 4 “classical” pathways: phagocytosis, macropinocytosis, clathrin-mediated internalization and caveolae-mediated internalization (for extensive reviews readers are referred to (Swanson and Watts, 1995; Aderem and Underhill, 1999; Brodsky et al., 2001; Pelkmans and Helenius, 2002; Razani et al., 2002; Perrais and Merrifield, 2005; Benmerah and Lamaze, 2007)) and 5 less well defined “non-classical” pathways. These latter pathways are distinguished from one another by their dependence on rafts, dynamin and Rho-GTPases. Two pathways are dependent on dynamin. A first pathway is used by the interleukin 2 (IL2) receptor for up-take of IL2 in leukocytes and is dependent on rafts and (an) unidentified Rho-GTPase(s) (Lamaze et al., 2001). A second dynamin-dependent non-classical pathway is actin and Rho-kinase dependent but independent of rafts and is used by intracellular adhesion molecule-1 and platelet-endothelial cell adhesion molecule-1 (Muro et al., 2003). Of the 3 dynamin-independent pathways, 1 is dependent on rafts and Cdc42 (a Rho-GTPase) and is utilized

GPI-anchored proteins; like the folate receptor (Sabharanjak et al., 2002; Sabharanjak and Mayor, 2004). Another dynamin-independent pathway is used by Menkes disease ATPase (ATP7a), a defective copper transporting ATPase and is also independent from rafts but is regulated by Rac1 (a Rho-GTPase) (Cobbold et al., 2003). The third dynamin-independent internalization pathway was presented in our previous work and is the pathway through which viral surface expressed proteins in FIPV infected monocytes are internalized. This pathway, the fifth non-classical pathway, occurs independently from rafts, dynamin and rho-GTPases (Chapter 4).

Once internalized, these vesicles need active transportation to get through the dense, protein rich cytosol and around cytoskeleton components towards their final destination. Long-range transport to get from the cell periphery to the cell center runs over microtubules and is mediated by the motor proteins dynein and kinesin. Transport in the cell periphery and short-range transport inside the cell is mediated by actin and its associated motor proteins, myosins. Endosomes can be pushed forward by polymerizing actin filaments forming an “actin tail” or can be transported by myosins over actin filaments. Formation of actin tails has been described in a variety of internalization pathways. After phagocytosis, movement of phagosomes is mediated by actin tails in macrophages and *Dictyostelium* (Insall et al., 2001; Zhang et al., 2002; Southwick et al., 2003). Also macropinosomes are propelled by an actin tail towards the cell center (Merrifield et al., 2001; Orth et al., 2002). In clathrin-mediated internalization, actin has been implicated in several steps of the internalization process in both mammalian and yeast cells (Ayscough, 2005; Kaksonen et al., 2005; Yazar et al., 2005). However, actin requirements seem to be dependent on cell-type and experimental conditions (Fujimoto et al., 2000). Formation of an actin tail is seen in 80% of clathrin-coated pit internalization events but only during initial movement (Ayscough, 2005; Kaksonen et al., 2005; Perrais and Merrifield, 2005). Small actin tails polymerize on caveolae shortly after internalization induced by Simian Virus 40 (SV40) (Pelkmans et al., 2002). Actin comet tails have also been reported on endosomes and lysosomes in HeLa cells, cultured mast cells, NIH 3T3 cell, budding yeast and *Xenopus* eggs (Merrifield et al., 1999; Kaksonen et al., 2000; Taunton et al., 2000; Huckaba et al., 2004). Movement that is mediated by such an actin tail has no defined direction nor does it run over actin tracks. In contrast, transport mediated by myosin motors runs over actin filaments in a direction dictated by the myosin. Myosins from classes I, II, V, VI, VII, XI and X are known to play a role during one or more internalization pathways (Soldati and Schliwa, 2006). However, these myosins are mainly associated with the first steps of internalization being membrane remodeling and pinching off of the vesicles. So far, there are few reports on the role of myosins in trafficking of endosomes. In mouse hepatoma

cells, myosin 1 $\alpha$  (Myo1 $\alpha$ ) (an analogue of human Myo1b) contributes to the trafficking of lysosomes along microtubules (Cordonnier et al., 2001; Raposo et al., 1999). Myo6 transports recently uncoated vesicles through the cortical actin barrier after clathrin-mediated internalization in non-polarized epithelial cells (Aschenbrenner et al., 2003, 2004). Myo5 plays a role in outbound trafficking of secretory vesicles (Soldati and Schliwa, 2006).

The aim of this study was to clarify the role for microtubules, actin and myosins during and after internalization through this recently characterized pathway used by surface expressed antigens in FIPV infected monocytes. We have found that microtubules are required for both internalization and intracellular trafficking. Actin on the other hand, seemed to hamper passage of the internalized vesicles through the cortical actin network. Myo1 and Myo6 were recruited to the internalizing vesicles at the time the cortical actin needed to be crossed. Therefore, it is likely that Myo1 and 6 are involved in actin remodeling leading to free passage of the vesicles. During intracellular trafficking, small actin tails and Myo1 co-localized with the viral antigen-antibody complexes, indicating the Myo1, actin and microtubules might work together during intracellular trafficking.

## 5.2 Material and Methods

**Viruses and antibodies** A third passage of FIPV strain 79-1146 (American Type Culture Collection (ATCC)) on CrFK cells was used (McKeirnan et al., 1981). Polyclonal anti-FCoV antibodies were kindly provided by P. Rotter (Utrecht University, The Netherlands). The antibodies were purified and biotinylated according to manufacturers instructions (Amersham Bioscience, Buckinghamshire, UK). FITC-labeled polyclonal anti-FIPV antibodies were purchased from Veterinary Medical Research and Development (VMRD, Pullman, Washington, USA). The monoclonal antibody E22-2 recognizing the N protein, was kindly provided by T. Hohdatsu (Kitasato University, Japan). The monocyte marker DH59B, recognizing CD172a, was purchased from VMRD. Rabbit anti-tubuline polyclonal antibodies and monoclonal antibodies against non-muscle Myo1 were purchased from Abcam (Cambridge, UK), rabbit polyclonal antibodies against non-muscle Myo2a, 2b and 9b from Sigma-Aldrich (Steinheim, Germany) and rabbit polyclonal antibodies against Myo5a, 6, 7a and 10 from Santa Cruz Biotechnology (Santa Cruz, California, USA). Secondary antibodies and reagents: goat anti-mouse Texas Red, goat anti-mouse Alexa Fluor 350, streptavidin Texas Red, streptavidin FITC, anti-rabbit Alexa Fluor 594 Zenon reagent were purchased from Molecular Probes (Molecular Probes-Invitrogen, Eugene, Oregon, USA).

**Isolation and inoculation of blood monocytes** Feline monocytes were isolated as described previously (Dewerchin et al., 2005). Cells were seeded on glass coverslips inserted in a 24-well dish (Nunc A/S, Roskilde, Denmark) in RPMI-1640 medium containing 10% fetal bovine serum (FBS), 0.3 mg/ml glutamine, 100 U/ml penicillin, 0.1 mg/ml streptomycin, 0.1 mg/ml kanamycin, 10 U/ml heparin, 1mM sodium pyruvate, and 1% non-essential amino-acids 100x (GIBCO-Invitrogen, Merelbeke, Belgium). Non-adherent cells were removed by washing the dishes two times with RPMI-1640 at 2 and 24 hours after seeding. The adherent cells consisted for  $86 \pm 7\%$  of monocytes (as assessed by fluorescent staining with the monocyte marker DH59B). At 56 hours post seeding, monocytes were inoculated with FIPV at a multiplicity of infection (m.o.i.) of 5. Between 20 and 60 cells were analyzed per assay.

**Internalization inhibition assays** Twelve hours after inoculation, monocytes seeded on glass coverslips were pre-incubated for 30 minutes at 37°C with 5% CO<sub>2</sub> in the presence of one of the following agents dissolved in RPMI: 20 µM latrunculin B (ICN Biochemicals Inc., Ohio, USA), 50 µM Cytochalasin D (Sigma-Aldrich GmbH, Steinheim, Germany), 50 nM Jasplakinolide (Molecular Probes), 500 µM Colchicine (Sigma-Aldrich GmbH), 20 µM Nocodazole (Sigma-Aldrich GmbH), 5 µM Paclitaxel (Calbiochem, San Diego, California, USA). The working concentration of each reagent was based on literature values and was optimized qualitatively in internalization assays with control ligands (data not shown). Viability of the cells during the inhibition assay was tested for each inhibitor using ethidium bromide monoazide (Molecular Probes-Invitrogen) and was always over 99%.

After pre-treatment, the cells were incubated with polyclonal biotinylated anti-FIPV antibodies in presence of one of the given inhibitors for 30 minutes at 37°C. Then, cells were fixed with 1% formaldehyde, permeabilized with 0.1% Triton X-100 (Sigma-Aldrich GmbH) and incubated with streptavidin-Texas Red for 1 hour at 37°C. Next, infected cells were visualized with polyclonal anti-FIPV-FITC. The glass coverslips were mounted on microscope slides using glycerin-PBS solution (0.9:0.1, vol/vol) with 1,4-diazabicyclo(2, 2, 2) octane (2.5%) (DABCO) (Janssen Chimica, Beerse, Belgium) and analyzed with confocal microscopy. Percentages of cells with fully internalized complexes were calculated relative to the total amount of monocytes which showed antibody binding and thus had membrane expression before antibodies were added. Those monocytes constitute about 50% of the total amount of infected cells (Dewerchin et al., 2005). Because of the variability on the amount of cells with membrane expression, visualization of the complexes remaining at the plasma membrane was needed. Therefore, an acid washing step to remove the extracellular antibodies was not performed.

To test the effectiveness of all reagents, a suitable control was used in each experiment. Monocytes seeded on glass coverslips were pre-incubated for 30 minutes at 37°C with 5% CO<sub>2</sub> in the presence of one of the inhibitors. After treatment, the cells were incubated with biotinylated transferrin (Sigma-Aldrich GmbH) or fluorescent 1µm polystyrene microspheres, FluoSpheres (Molecular Probes-Invitrogen), in presence of the inhibitor. Then, all cells were fixed with 1% formaldehyde and permeabilized with 0.1% Triton X-100. The biotinylated transferrin was visualized by incubating the cells with streptavidin-FITC for 1 hour at 37°C and cells incubated with fluorescent beads were incubated with phalloidin-Texas Red (Molecular Probes-Invitrogen) for 1 hour at 37°C to visualize the lamellipodia. The glass coverslips were mounted on microscope slides using glycerin-DABCO and analyzed by confocal microscopy. For the controls, the monocytes were scored analogously as FIPV infected cells: ligands were considered “fully internalized” when they were only observed inside the cell. Fluorescent beads were considered internalized when they were found inside the cortical actin labeling.

**Co-localization studies with actin filaments, microtubules or myosins** At twelve hours after inoculation, monocytes were incubated with biotinylated anti-FIPV polyclonal antibodies. At different times post antibody addition, cells were fixed with 1% formaldehyde, permeabilized with 0.1% Triton X-100 and antigen- antibody complexes were visualized with streptavidin-FITC followed by a blocking step with 10% negative goat serum. Next, actin filaments, microtubules or myosins were stained. Cells were incubated with phalloidin Texas Red to visualize actin filaments. To stain the microtubules, polyclonal rabbit anti-tubuline antibodies were tagged with anti-rabbit Alexa Fluor 594 Zenon reagent. To visualize myo1, monoclonal anti-myo1 was used, followed by goat anti-mouse Texas Red. To visualize other myosins, rabbit anti-Myo2a, 2b, 5a, 6, 7a, 9b and 10 was tagged with anti-rabbit Alexa Fluor 594 Zenon reagent. After 45 minutes of incubation, cells were fixed to stabilize the Zenon reagent. Finally, infected cells were visualized with monoclonal anti-N and goat anti-mouse Alexa Fluor 350 (not shown in images).

For fluorescence intensity measurements, a stack of images was taken per couple of infected and non-infected cells (0.85 µm distance between optical sections), then an overlay was made, cells were delineated and total fluorescence intensity per cell was measured by the Leica confocal software package.

**Confocal laser scanning microscopy** The samples were stained as described above and examined with a Leica TCS SP2 laser scanning spectral confocal system (Leica Microsystems GmbH, Wetzlar, Germany) linked to a DM IRB

inverted microscope (Leica Microsystems). Argon and Helium/Neon laser lights were used to excite FITC (488 nm line) and Texas-Red (543 nm line) fluorochromes. The images were obtained with Leica confocal software and processed with the GIMP.

**Statistical analysis** Triplicate assays were compared using a Mann-Whitney U test with SPSS 11.0 (SPSS Inc., Chicago, WA). P values <0.05 were considered significantly different. For each assay, between 20 and 60 cells were counted.

## 5.3 Results

### 5.3.1 The role of microtubules in transportation of viral antigen-antibody complexes into the cell

The primary route for vesicles to move from the plasma membrane towards the cell center runs over the microtubules. The internalization studied here is a very fast and efficient process. Internalized antigen-antibody complexes can be found in the center of the cell as soon as 5 minutes after addition of antibodies. In this section we verified if internalized vesicles are transported over the microtubules to reach the cell center. First, internalization assays were performed in the presence of one of the following inhibitors: Colchicine, Nocodazole (which both disrupt microtubules) or Paclitaxel (which promotes the assembly and inhibits the disassembly of microtubules). The images in Figure 5.1 show that some internalization could still occur in the presence of either inhibitor since antigen-antibody complexes were observed inside the monocytes. However, most internalized vesicles remained close to the plasma membrane indicating that transportation to the center of the cell was inhibited. Quantification revealed a decrease in internalization when monocytes were treated with Colchicine or Nocodazole, to  $28\pm 15\%$  and  $18\pm 3\%$  of the untreated control respectively (Figure 5.1). Thus, not only transportation was inhibited but internalization itself as well. Treatment with Paclitaxel also led to a decrease in internalization, albeit less pronounced than with the other inhibitors ( $74\pm 15\%$  of the untreated control). Since Paclitaxel is a drug that stabilizes microtubules, these findings indicate that microtubules must not only be intact but they must also remain dynamic. Although the decrease was significantly different, it was minor compared to the strong reduction in internalization of the control ligand transferrin ( $8\pm 9\%$  of the untreated control). This indicates that the requirement for dynamic microtubules is not as stringent in the internalization

pathways studied here as it is in the clathrin-mediated internalization of transferrin.

### **5.3.2 Co-localization of viral antigen-antibody complexes and microtubules**

To confirm the role for microtubules in the transportation of internalized vesicles, microtubules were visualized during the internalization process. The confocal images in Figure 5.2 show that internalizing vesicles were associated with microtubules as soon as 1 minute after initiation of internalization, thus microtubule based transport started most likely right after passage through the cortical actin network. After 10 minutes, the first vesicles already reached the microtubule organizing center (MTOC). Association of the internalized vesicles with microtubules was maintained at all tested time points.

Taken together, these findings indicate that antigen-antibody complexes were transported over the microtubules towards the cell center and accumulated at the MTOC.

### **5.3.3 The role of actin in internalization of viral antigen-antibody complexes**

To investigate the role of actin during this independent pathway, internalization assays were performed in presence of the inhibitors Cytochalasin D (which inhibits formation of new filaments), Latrunculin B (which disrupts all actin filaments) and Jaspilakinolide (which stabilizes existing filaments and induces polymerization of new filaments). Figure 5.3 shows representative confocal images of monocytes at 30 minutes after addition of antibodies in the presence of one of the inhibitors. Cells treated with Cytochalasin D or Latrunculin B showed internalized viral antigen-antibody complexes in a pattern similar to that in the untreated control cells. Monocytes treated with Jaspilakinolide also internalized viral antigen-antibody complexes, however, the typical pattern of randomly distributed internalized complexes was not observed. And fewer internalized vesicles seemed to travel as far into the cell as in untreated monocytes or in monocytes treated with Cytochalasin D or Latrunculin B. In monocytes treated with Jaspilakinolide, one can expect to see a cortical actin network that might even be more extensive than in untreated cells because of the polymerization inducing capacity of the drug. Nevertheless, almost no filamentous actin can be seen in the image of the monocyte trying to internalize a fluorescent bead in Figure 5.3. The reason for this apparent discrepancy is that Jaspilakinolide impedes phalloidin-Texas Red from binding to actin filaments



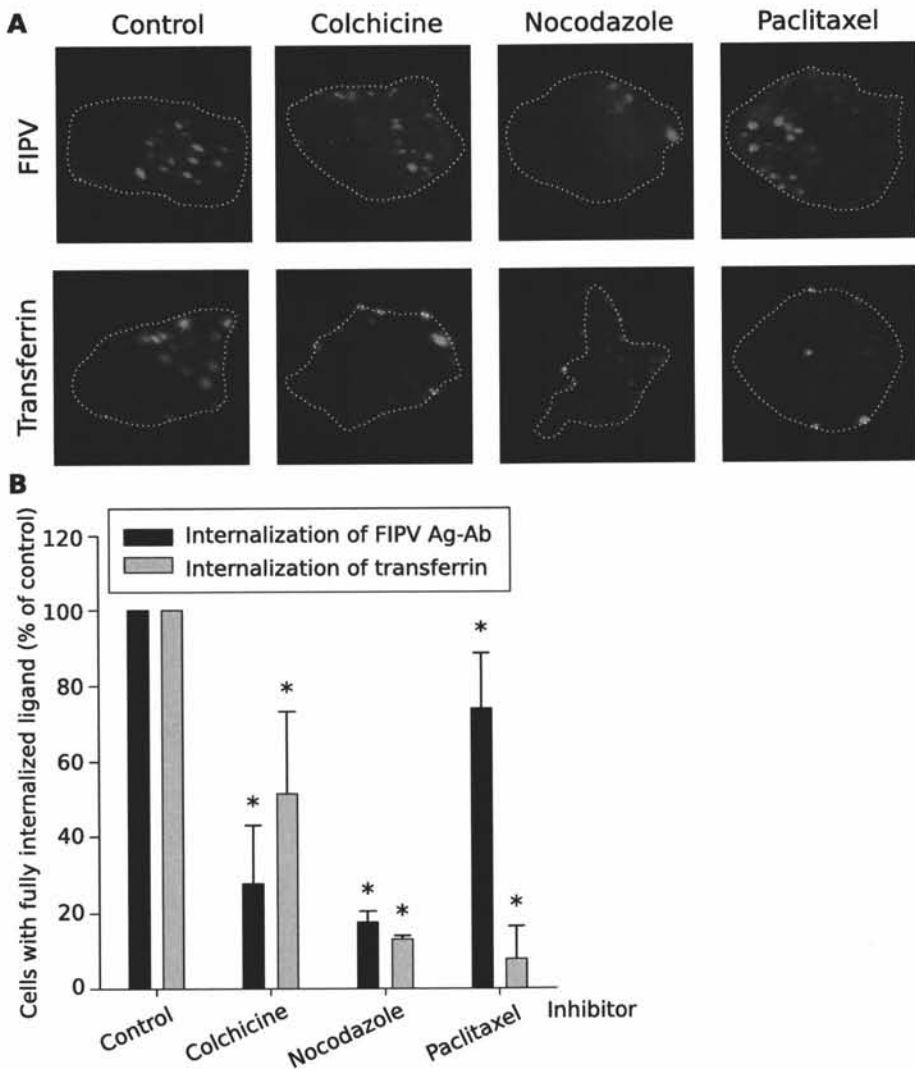


Figure 5.1: Role of microtubules during internalization of surface expressed viral antigens in FIPV infected monocytes. (A) Confocal images of monocytes after internalization in the presence of microtubule inhibitors. The activity of each inhibitor was tested with internalization assays of transferrin. The images show a single optical section through a monocyte. (B) Quantification of the internalization in the presence of microtubule inhibitors. Results are given relatively to a control of untreated cells. The black bars represent the internalization of viral antigens. The gray bars represent the internalization of the control ligands: transferrin. Data are means and standard deviations of triplicate assays. The asterisk marks results that are significantly different from the untreated control ( $p < 0.05$ ).

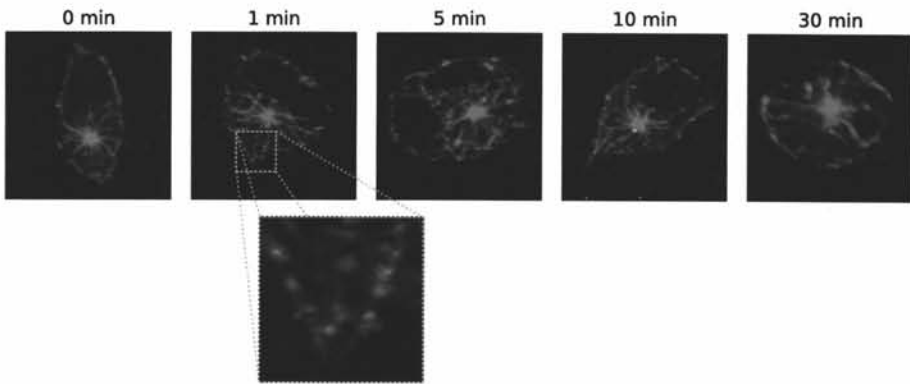


Figure 5.2: Visualization of the microtubules during antibody-induced internalization of surface expressed viral antigens in FIPV infected monocytes. The images show a single optical section through a monocyte.

resulting in a vaguely red cell even though a cortical actin network is present.

The quantification of the internalization in the presence of inhibitors confirmed that Cytochalasin D and Latrunculin B did not have a significant effect on the internalization process, while both inhibitors strongly reduced phagocytosis of fluorescent beads to respectively  $14 \pm 4\%$  and  $18 \pm 6\%$  of the untreated control (Figure 5.3). These results suggest that actin filaments are not required for the internalization process. Treatment of monocytes with Jasplakinolide gave a small but significant reduction in internalization ( $76 \pm 15\%$  of the untreated control), suggesting that a stabilized cortical actin network might hamper or slow down the internalization of antigen-antibody complexes. Since the internalization process could not be blocked by disruption of actin filaments and internalization itself was not stopped by stabilized filaments, it can be concluded that actin does not play an active role in the internalization process.

### 5.3.4 Co-localization of viral antigen-antibody complexes and actin

To further elucidate the role for actin during the internalization process, actin filaments were visualized with phalloidin-Texas Red at different times after initiation of the internalization. The confocal images in Figure 5.4 show that at 1 minute after addition of antibodies, antigen-antibody complexes moved into the cells and at the internalization sites a local absence of cortical actin could be observed. It could be that actin filaments were moved or broken down in order to make way for the internalizing complexes, which provides an explanation why Jasplakinolide reduced or slowed down the internalization.

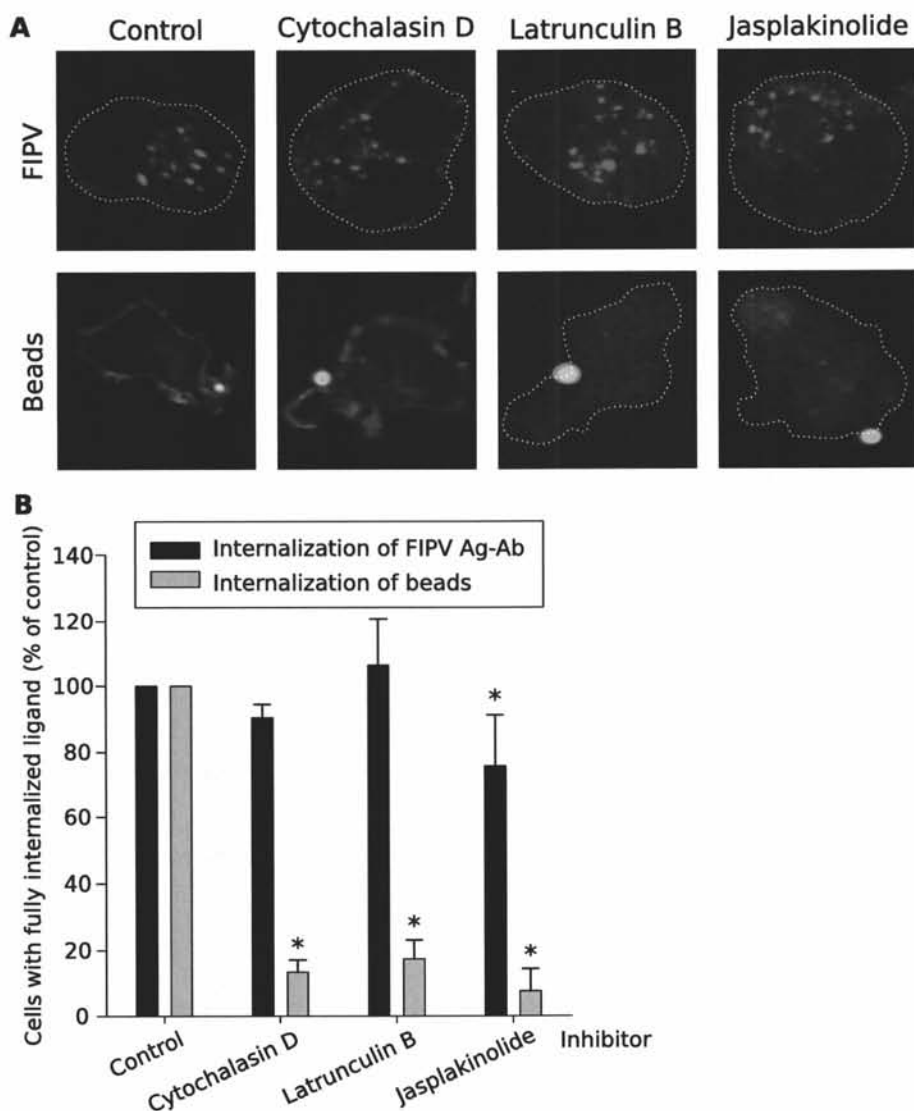


Figure 5.3: Role of actin in the internalization of surface expressed viral antigens in FIPV infected monocytes. (A) Confocal images of monocytes after internalization in the presence of actin inhibitors. The activity of each inhibitor was tested with internalization assays of fluorescent beads. In row 2, cortical actin was stained (red) to visualize whether or not the lamellipodia were closed around the beads. The images show a single optical section through a monocyte. (B) Quantification of the internalization of surface expressed viral antigens in the presence of actin inhibitors. Results are given relatively to a control of untreated cells. The black bars represent the internalization of viral antigens. The gray bars represent the internalization of the control ligands: beads. Data are means and standard deviations of triplicate assays. The asterisk marks results that are significantly different from the untreated control ( $p < 0.05$ ).

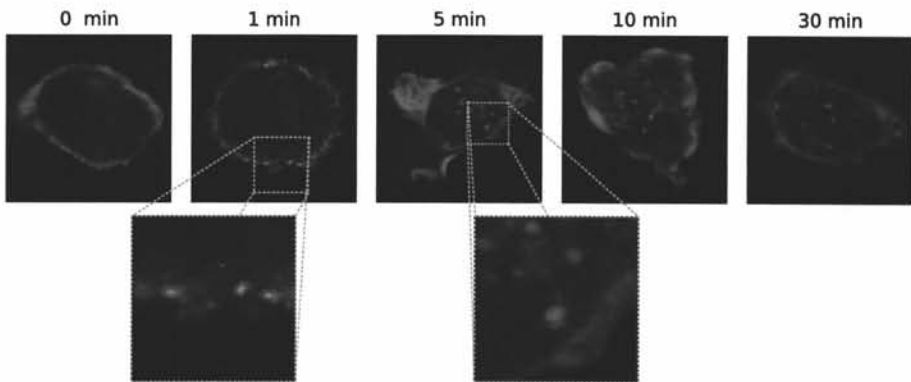


Figure 5.4: Visualization of actin dynamics during antibody-induced internalization of surface expressed viral antigens in FIPV infected monocytes. The images show a single optical section through a monocyte.

Another noteworthy observation was made at later stages of the internalization process. Figure 5.4 shows that vesicles that have past through the cortical actin network were still associated with actin in a way that resembles actin tails. This association of internalized vesicles with actin was still observed at 10 minutes after initiation of the internalization, but was lost at 30 minutes.

Taking these results together, actin might not be required for internalization, as indicated by Cytochalasin D and Latrunculin B. The actin stainings and the results with the actin stabilizing drug Jasplakinolide indicated that the cortical actin network forms a barrier that can slow down internalization and that must be overcome by moving or disintegrating actin filaments. However, actin may play an active role in further transportation into the cell since fully internalized complexes were associated with actin.

### 5.3.5 Co-localization of viral antigen-antibody complexes and myosins

Next, a possible role for myosins during internalization was investigated. Myo1, 2a, 2b, 5a, 6, 7a, 9b and 10 were selected based on their role during several internalization processes. Co-localization stainings revealed that all the tested myosins were expressed in monocytes (Figure 5.5 and 5.7). Myo1, 2b, 5a, 6, 7a, 9b and 10 were diffusely distributed in the cytoplasm. In a subset of monocytes, brighter “spots” could be observed which indicate local enrichment of myosin motors, probably at sites of myosin activity. An exception to the diffuse distribution was Myo2a, which was clearly localized at the plasma membrane. Interestingly, Myo1 expression was altered in infected monocytes.

Not only was Myo1 redistributed to the plasma membrane, fluorescence intensity measurements also revealed a 2.5-fold up-regulation in infected cells (Figure 5.6).

During the internalization experiments, no co-localization was found between Myo2a, 2b, 5a, 7a, 9b and 10 and the viral antigens at any time point (Figure 5.5). In contrast, viral antigens did co-localize with Myo1 and 6 (Figure 5.7). Already before the addition of antibodies, Myo1 was highly enriched at the plasma membrane, right underneath the viral proteins (see panel a-zoom of Fig. 5.7). Then, shortly after addition of the antibodies, Myo1 relocated between the internalized complex and the plasma membrane (see panel b-zoom of Fig. 5.7). As the antigen-antibody complexes moved further into the cell, they maintained their juxtaposed localization with Myo1. At 10 minutes after antibody addition, a loss of interaction was first observed (e.g. in the center of the cell depicted in panel e of Fig. 5.7). Further dissociation of Myo1 from the internalized complexes occurred as time passed and vesicles reached the center of the cell. Co-localization with Myo6 was also observed as quickly as 30 seconds after addition of the antibodies when antigen-antibody complexes were right under the plasma membrane (see panel h1-zoom of Fig. 5.7) but association was lost as soon as the viral antigen-antibody complexes moved further inside the cell (illustrated in panel h2 and h2-zoom of Fig. 5.7). The images in panel h1 and h2 are actually different sections through the same cell, which clearly illustrates how short-lived the Myo6 association with internalized complexes is. At later time points, cells with co-localization were still found, but never below the actin cortex (e.g. panel j-zoom of Fig. 5.7). We suggest that those co-localizations represent antigen-antibody complexes that just started to internalize at the moment of fixation.

These results indicate that Myo1 and 6 play a role during the antibody-induced internalization of viral antigens.

## 5.4 Discussion

When primary feline monocytes are infected with FIPV *in vitro*, a fraction of the expressed spike (S) protein and membrane (M) protein can be found in the plasma membrane (Dewerchin et al., 2005). In contrast, viral antigens were not detected in the plasma membrane of monocytes isolated from naturally infected cats (Cornelissen et al., 2007). When mimicking the *in vivo* situation by adding antibodies to the *in vitro* culture of FIPV infected monocytes, we found that the surface expressed antigens were quickly and efficiently internalized, leaving the plasma membrane cleared from visually detectable viral antigens

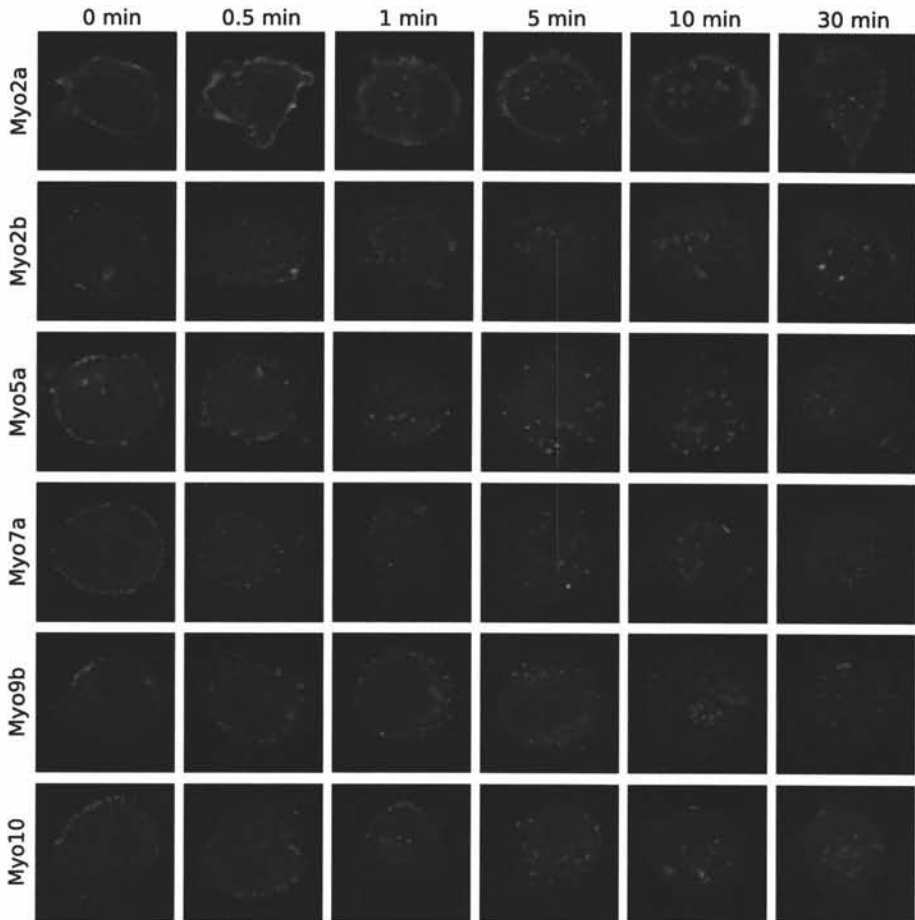


Figure 5.5: Myo2a, 2b, 5a, 7a, 9b and 10 are not recruited to the sites of internalization of viral antigens in FIPV infected monocytes. The internalization was stopped at different times post antibody addition, after which the internalization of the antibody-antigen complexes was visualized with FITC (green signal). Myosins were visualized with Alexa Fluor 594 (red signal). Images show a single optical section through the cell.

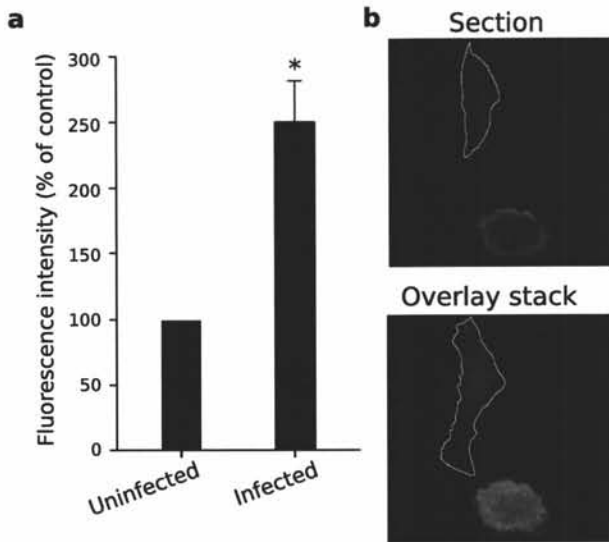


Figure 5.6: Myo1 is up-regulated and redistributed during infection. (a) Quantification of fluorescence intensity of Myo1 labeling in infected monocytes relatively to uninfected monocytes. Data represents mean and standard deviation of 6 assays. The asterisk marks significantly different results with respect to uninfected control ( $p < 0.05$ ). (b) Confocal images of a single section or an overlay of a stack of sections through an uninfected cell (delineated) and an infected cell. Myo1 was labeled with Texas Red (red signal).

(Dewerchin et al., 2006). The internalization of these antigen-antibody complexes occurred via a new clathrin- and caveolae-independent pathway which did not require dynamin, rafts nor rho-GTPases. Since the antigen-antibody complexes are internalized and transported towards the cell center so rapidly, we wanted to investigate how this intracellular transport was organized.

First, the importance of microtubules during the internalization pathway was studied. Disruption of the microtubule network with Colchicine or Nocodazole led to a strong decrease in internalization. Antigen-antibody complexes that could still internalize, remained close to the plasma membrane indicating that microtubules are essential for both the internalization process and intracellular trafficking. Co-localization stainings clearly showed that the internalized vesicles were indeed transported over the microtubules. Although microtubules are mainly thought of as tracks for long-range transport in the cell, it has been reported before that disruption of these filaments can lead to inhibition of internalization itself (Subtil and Dautry-Varsat, 1997).

Next, a role for actin was investigated. In phagocytosis and macropinocytosis, actin is crucial for membrane remodeling during the formation of the phagocytic cup or the lamellipodia respectively. In both pathways, actin also

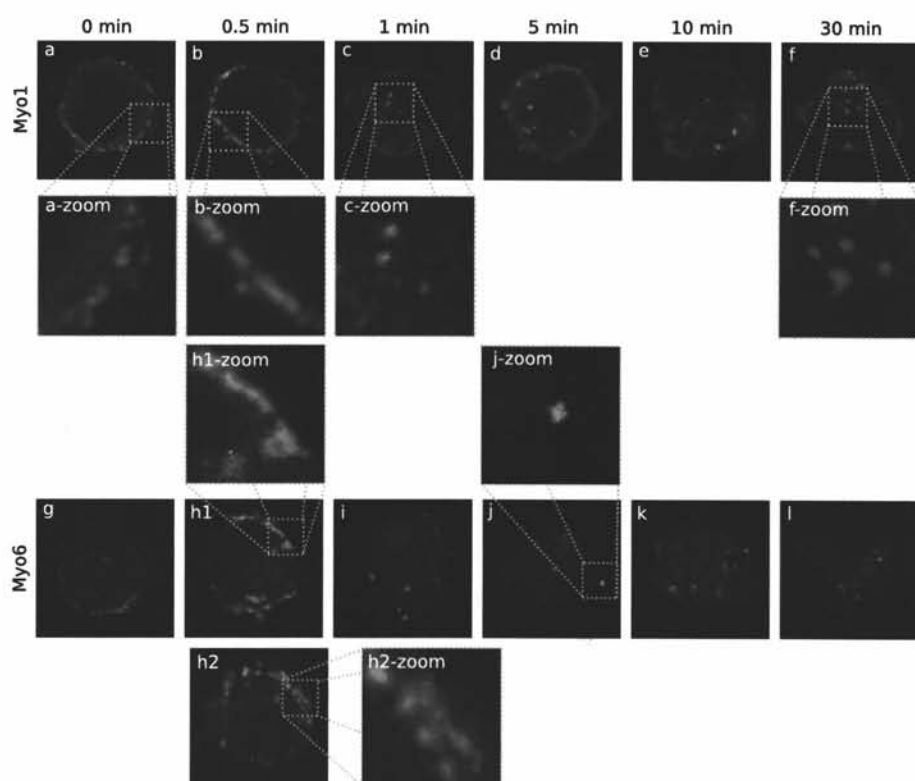


Figure 5.7: Myo1 and Myo6 co-localize during the internalization of viral antigens in FIPV infected monocytes. The internalization was stopped at different times post antibody addition, after which the internalization of the antibody-antigen complexes was visualized with FITC (green signal). Myosins were visualized with Texas Red (Myo1) or Alexa Fluor 594 (red signal). The images show a single optical section through the cell.



participates in trafficking since actin tails were reported to co-localize with recently internalized phagosomes or macropinosomes (Huckaba et al., 2004; Ayscough, 2005; Kaksonen et al., 2000). In micropinocytic internalization pathways, where the plasma membrane is invaginated and not protruded, the role for actin is not fully elucidated. Actin requirements might be cell type specific and it is not clear if actin is essential during membrane invagination but it is thought to play a role in pinching off of the vesicles from the plasma membrane (Lamaze et al., 1997; Fujimoto et al., 2000). In the clathrin- and caveolae-independent internalization pathway studied here, actin requirements were investigated with chemical inhibitors and co-localization stainings. We found that internalization could still occur when assembly of new filaments is inhibited by Cytochalasin D and even after complete destruction of the actin network by the inhibitor Latrunculin B. Treatment with the inhibitor Jasplakinolide, which stabilizes actin filaments, led to a small but significant reduction in internalization. This relatively small effect stands in strong contrast to the control internalization assay in which phagocytosis of fluorescent beads in the presence of Jasplakinolide was almost completely blocked. This large difference underscored that actin plays a different role in phagocytosis than in the internalization process studied here. While phagocytosis requires dynamic actin for the formation of pseudopods, the results with the inhibitors suggest that in the internalization pathway studied here, dynamic actin was not a prerequisite. Even more, the results with Jasplakinolide suggest that intact actin might hamper the initial movements of internalizing surface expressed viral proteins. This hypothesis is further corroborated by the co-localization stainings which clearly show that the cortical actin network forms a barrier that must be moved aside or locally degraded to allow the internalizing vesicle to pass through. Similar observation have been made during clathrin-mediated internalization in mammalian cells. It was reported that actin assembly is not required, that actin filaments are absent in the area around a forming clathrin-coated pit and that disruption of actin filaments leads to faster internalization of recently uncoated vesicles (Fujimoto et al., 2000; Aschenbrenner et al., 2004). Also during caveolae-mediated internalization, cortical actin would constrain vesicle formation from caveolae in the plasma membrane (Mundy et al., 2002).

The role for actin in further trafficking of the internalized vesicles towards the cell center is less clear. A staining with phalloidin Texas Red shows that internalizing vesicles co-localize with actin filaments organized like a small actin tail suggesting that intracellular movement of the vesicles could be driven by actin polymerization. Treatment of FIPV infected monocytes with Jasplakinolide allowed internalization but internalized vesicles seemed to remain close to the plasma membrane. This could mean that (i) a stabilized cortical actin impeded the vesicles to pass through or that (ii) the stabilized actin tails disabled

actin driven movement. However, the internalization pattern that is seen after Cytochalasin D or Latrunculin B treatment indicated that trafficking does not require actin filaments nor formation of new filaments since internalized vesicles could still be observed at the center of the cell. These results suggest that the actin tails are dispensable and thus they are not the (main) driving force for intracellular trafficking.

Then, we investigated if the forces needed for membrane remodeling during the internalization could be provided by myosins and if myosin-based transport over actin filaments also played a role during intracellular trafficking. The importance of myosin motors during internalization is best studied in phagocytosis where several myosins cooperate from start to completion of the process. Myo7 has been implicated in particle attachment and filopod extension in *Dictyostelium* (Titus, 1999; Tuxworth et al., 2001). Myo2, 9b and 10 are associated with ruffles and might regulate pseudopod extension (Swanson et al., 1999; Cox et al., 2002; Diakonova et al., 2002; Olazabal et al., 2002). Myo1 has been suggested to play a role in the closure of phagosomes and transportation of internalized vesicles might be regulated by Myo5 (Allen and Aderem, 1995; Swanson et al., 1999; Diakonova et al., 2002). The role for myosins in other internalization processes is less well established but Myo1 has been associated with macropinocytosis and clathrin-mediated internalization (Opstap et al., 2003; Jonsdottir and Li, 2004) and Myo6 with clathrin-mediated internalization (Buss et al., 2001; Aschenbrenner et al., 2003). In the internalization process studied here, only Myo1 and Myo6 co-localized with internalizing complexes. The fact that Myo2, 7a, 9b or 10 were not recruited to the site of internalization, implies that the mechanisms underlying pseudopod formation and membrane invagination are very different, even though both processes are based on movements of the plasma membrane. The co-localization stainings with Myo1 suggest that this myosin might be the driving force behind the membrane invagination. Recent findings indeed suggest that Myo1E (formerly known as 1C) might couple polymerizing actin to membranes and thus mediate force production during endocytosis through constraining (and possibly orienting) actin assembly (Sokac et al., 2006). We found that Myo1 was not only up-regulated in infected cells to 2.5 times the amount in uninfected cells, it was also redistributed to the cell periphery (in contrast, staining patterns of the other myosins remained unchanged). Patches of Myo1 could be observed under the viral proteins residing in the plasma membrane. Once internalization started, Myo1 immediately relocated between the antigen-antibody complex and the plasma membrane. As the internalized vesicles moved further inwards, the association with Myo1 remained for at least 10 minutes, which was sufficient to reach the center of the cell. This staining pattern suggests that there might be direct protein-protein interactions between the viral proteins

and Myo1. This implies that Myo1E and/or 1F isoform(s) might be involved in internalization since these are the only two of the eight mammalian Myo1 isoforms that contain a Src Homology 3 (SH3) domain which enables protein-protein interactions (Krendel et al., 2007).

The co-localization stainings also indicated a role for Myo6 in the first steps of the internalization process. In vertebrates, a long and a short isoform of Myo6 are generated through alternative splicing. In non-polarized epithelial cells, the short isoform of Myo6 transports recently uncoated vesicles after clathrin-mediated internalization through the actin barrier (Aschenbrenner et al., 2003, 2004). In the study presented here, we used primary monocytes, which are non-polarized cells containing a cortical actin network. It is highly probable that Myo6 will perform the same task here as in the non-polarized epithelial cells, namely transporting the internalized antigen-antibody complexes through the cortical actin. In this network, actin filaments are oriented in all directions, therefore, association of a vesicle with two motor proteins which move over actin filaments in opposite directions might be very beneficial for the net speed of the vesicle. So, Myo1 (+ end directed) and Myo6 (- end directed) might work together as motor proteins to transport vesicles through the cortical actin network. The fact that two myosins co-localize with the viral antigen-antibody complexes during their passage through the cortical actin, is a strong indication that these myosins might collaborate to move the vesicle through the cortical actin by rearranging the filaments into a corridor and so enabling free passage for the internalizing vesicle through the actin barrier.

Once passed through, the internalized vesicles are further transported over microtubules. This track switch from actin to microtubules might be mediated by Myo6 (Wu et al., 2000). As soon as the vesicles move over the microtubules, association with Myo6 was lost while association with Myo1 was maintained. The relatively long association of vesicles with Myo1 is rather surprising since in phagocytosis, macropinocytosis and clathrin-mediated internalization Myo1 has only been linked to the first steps of internalization (Swanson et al., 1999; Opstap et al., 2003; Krendel et al., 2007). It is unclear why association with Myo1 remained, even during microtubule based transport. It is known that of the microtubule-based motors dynein (inbound traffic) and kinesin (outbound traffic), dynein is less robust and might detach when oppositely moving cargo is passing. At that moment, vesicles might be handed over to actin filaments, a possible role for Myo1, and then back to (another) microtubule filament.

The fact that the actin disrupting agent latrunculin B does not have an effect on internalization might seem contradictory to the finding that myosins are important during internalization. However, if myo1 and 6 are only important to transport vesicles through the cortical actin network, disruption of actin fila-

ments would give free passage to the vesicles and would render the myosins redundant.

Putting the results on actin, microtubules and myosins together, one has to notice the salient finding that vesicles were decorated with an actin tail and Myo1 during their transportation over the microtubules. Nevertheless, the experiments undeniably showed that intracellular transport did not require dynamic or polymerizing actin but microtubules (and thus is driven by dynein or a (-)-end directed kinesin). It could be that Myo1 and actin filaments cooperate with microtubules during intracellular trafficking. Similar observations have been made in mouse hepatoma cells where Myo1 $\alpha$  (an analogue of human Myo1b) contributes to the trafficking of lysosomes along microtubules by controlling the directionality of the long-range movements (Cordonnier et al., 2001). Evidence is accumulating for the existence of motor complexes that combine actin- and microtubule-based transport although efforts are focused on Myo5-mediated outbound trafficking (Wu et al., 2000; Mallik and Gross, 2004). In amoeba and yeast, the role for Myo1 motors is believed not to be transportation as such but rather the regulation and organization of the actin-nucleation polymerization machinery (Soldati, 2003; Kaksonen et al., 2006). The yeast Myo1 isoform contains an acidic domain which interacts with the Arp2/3 complex and enables Myo1 to participate in actin assembly (Evangelista et al., 2000; Lee et al., 2000). Vertebrate Myo1 isoforms however, do not contain such an acidic domain but the isoforms Myo1E and F do contain a Src Homology (SH3) domain which enables protein-protein interactions. It is not yet clarified if mammalian Myo1 isoforms can indirectly participate in actin assembly through interaction with other proteins from the actin nucleation complex. Studies do indicate that Myo1 controls and constrains actin polymerization rather than promoting nucleation, also in mammalian cells (Bose et al., 2002; Diefenbach et al., 2002; Sokac et al., 2006). So, it is possible that the actin tails on the internalizing vesicles are not required for propelling the vesicle but merely to help in orienting its trafficking towards the cell center under the control of Myo1 which constrains the actin polymerization. A hypothetical model combining all results on the internalization process is given in Figure 5.8.

In conclusion, the clathrin- and caveolae-independent internalization pathway through which surface expressed viral proteins are internalized after antibody binding in FIPV infected monocytes did not require actin. Moreover, the cortical actin network formed a barrier that slowed down internalization and that had to be overcome by moving actin filaments. During passage through the cortical actin, antibody-antigen complexes co-localized with Myo1 and Myo6. These myosins might collaborate to reorganize the cortical actin network in order to allow passage of the internalized vesicle. Once passed the cortical actin

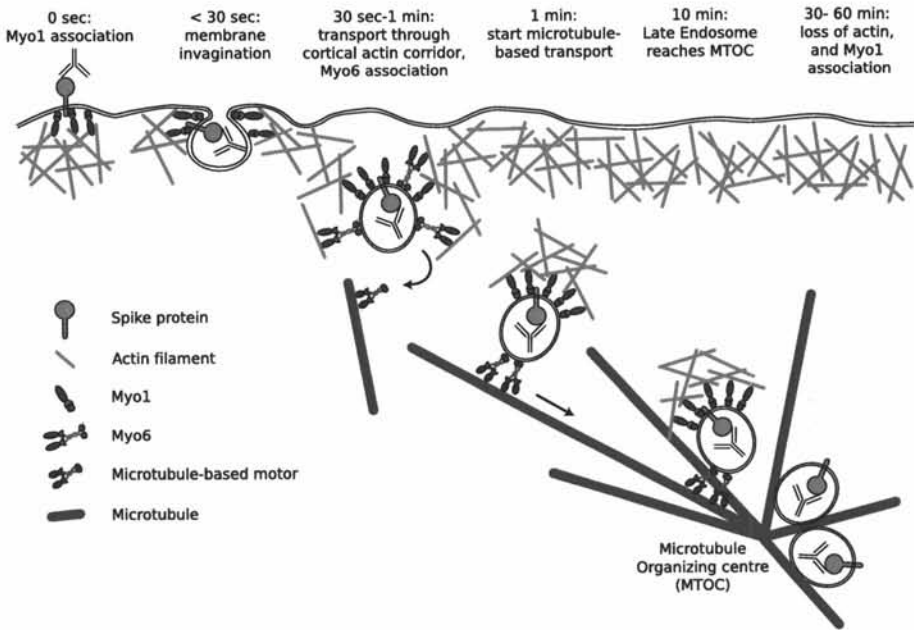


Figure 5.8: Model of the clathrin- and caveolae independent internalization pathway used for antibody-induced internalization of viral antigens in FIPV infected monocytes.

(1 minute), microtubule-based transport started and association with Myo6 was lost. During transport over microtubules, the vesicles were associated with small actin tails and Myo1 indicating that actin and microtubules cooperate during intracellular trafficking, probably mediated by Myo1. After 10 minutes, the internalized vesicles reached the microtubule organizing center where they accumulated and the actin tails and Myo1 association was lost.

## Acknowledgments

We are very grateful to P. Rottier for supplying polyclonal anti-FCoV antibodies and to T. Hohdatsu for monoclonal anti-N protein antibodies. H.L.D. and E.C. were supported by the Institute for the Promotion of Innovation through Science and Technology in Flanders (IWT-Vlaanderen). E.V.H. was supported by the Special Research Fund of Ghent University.

## References

- Aderem, A. and Underhill, D. (1999). Mechanisms of phagocytosis in macrophages. *Annu Rev Immunol*, 17:593–623.
- Allen, L. and Aderem, A. (1995). A role for MARCKS, the alpha isozyme of protein kinase C and myosin I in zymosan phagocytosis by macrophages. *J Exp Med*, 182:829–840.
- Aschenbrenner, L., Lee, T., and Hasson, T. (2003). Myo6 facilitates the translocation of endocytic vesicles from cell peripheries. *Mol Biol Cell*, 14:2728–2743.
- Aschenbrenner, L., Naccache, S., and Hasson, T. (2004). Uncoated endocytic vesicles require the unconventional myosin, myo6, for rapid transport through actin barriers. *Mol Biol Cell*, 15:2253–2263.
- Ayscough, K. (2005). Coupling actin dynamics to the endocytic process in *Saccharomyces cerevisiae*. *Protoplasma*, 226:81–88.
- Benmerah, A. and Lamaze, C. (2007). Clathrin-coated pits: vive la difference? *Traffic*, 8:970–982.
- Bose, A., Guilherme, A., Robida, S., Nicoloso, S., Zhou, Q., Jiang, Z., Pomerleau, D., and Czech, M. (2002). Glucose transporter recycling in response to insulin is facilitated by myosin Myo1c. *Nature*, 420:821–824.
- Brodsky, F., Chen, C.-Y., Knuehl, C., Towler, M., and Wakeham, D. (2001). Biological basket weaving: formation and function of clathrin-coated vesicles. *Annu Rev Cell Dev Biol*, 17:517–568.
- Buss, F., Arden, S., Lindsay, M., Luzio, J., and Kendrick-Jones, J. (2001). Myosin VI isoform localized to clathrin-coated vesicles with a role in clathrin-mediated endocytosis. *EMBO J*, 20:3676–3684.
- Cobbold, C., Coventry, J., Ponnambalam, S., and Monaco, A. (2003). The menkes disease ATPase (ATP7A) is internalized via a Rac1-regulated, clathrin- and caveolae-independent pathway. *Hum Mol Genet*, 12(13):1523–1533.
- Cordonnier, M.-N., Dauzonne, D., Louvard, D., and Coudrier, E. (2001). Actin filaments and myosin I alpha cooperate with microtubules for the movement of lysosomes. *Mol Biol Cell*, 12:4013–4029.

- Cornelissen, E., Dewerchin, H., Van Hamme, E., and Nauwynck, H. (2007). Absence of surface expression of feline infectious peritonitis virus (FIPV) antigens on infected cells isolated from cats with FIP. *Vet Microbiol*, 121:131–137.
- Cox, D., Berg, J., Cammer, M., Chingwundoh, J., Dale, B., Cheney, R., and Greenberg, S. (2002). Myosin X is a downstream effector of PI(3)K during phagocytosis. *Nat Cell Biol*, 4:469–477.
- Dewerchin, H., Cornelissen, E., and Nauwynck, H. (2005). Replication of feline coronaviruses in peripheral blood monocytes. *Arch Virol*, 150(12):2483–2500.
- Dewerchin, H., Cornelissen, E., and Nauwynck, H. (2006). Feline infectious peritonitis virus-infected monocytes internalize viral membrane-bound proteins upon antibody addition. *J Gen Virol*, 87:1685–1690.
- Diakonova, M., Bokoch, G., and Swanson, J. (2002). Dynamics of cytoskeletal proteins during Fc $\gamma$  receptor-mediated phagocytosis in macrophages. *Mol Biol Cell*, 13:402–411.
- Diefenbach, T., Latham, V., Yimlamai, D., Liu, C., Herman, I., and Jay, D. (2002). Myosin 1c and myosin IIB serve opposing roles in lamellipodial dynamics of the neuronal growth cone. *J Cell Biol*, 158:1207–1217.
- Evangelista, M., Klebl, B., Tong, A., Webb, B., Leeuw, T., Leberer, E., White-way, M., Thomas, D., and Boone, C. (2000). A role for Myosin-I in actin assembly through interactions with Vrp1p, Bee1p, and the Arp2/3 complex. *J Cell Biol*, 148:353–362.
- Fujimoto, L., Roth, R., Heuser, J., and Schmid, S. (2000). Actin assembly plays a variable, but not obligatory role in receptor-mediated endocytosis in mammalian cells. *Traffic*, 1:161–171.
- Huckaba, T., Gay, A., Pantalena, L., Yang, H.-C., and Pon, L. (2004). Live cell imaging of the assembly, disassembly, and actin cable-dependent movement of endosomes and actin patches in the budding yeast, *Saccharomyces cerevisiae*. *J Cell Biol*, 167:519–530.
- Insall, R., Muller-Taubenberger, A., Machesky, L., Kohler, J., Simmeth, E., Atkinson, S., Weber, I., and Gerisch, G. (2001). Dynamics of dictyostelium Arp2/3 complex in endocytosis, cytokinesis, and chemotaxis. *Cell Motil Cytoskeleton*, 50:115–128.
- Jonsdottir, G. and Li, R. (2004). Dynamics of yeast myosin I: evidence for a possible role in scission of endocytic vesicles. *Curr Biol*, 14:1604–1609.

- Kaksonen, M., Peng, B., and Rauvala, H. (2000). Association of cortactin with dynamic actin in lamellipodia and on endosomal vesicles. *J Cell Sci*, 113:4421–4426.
- Kaksonen, M., Toret, C., and Drubin, D. (2005). A modular design for the clathrin- and actin-mediated endocytosis machinery. *Cell*, 123:305–320.
- Kaksonen, M., Toret, C., and Drubin, D. (2006). Harnessing actin dynamics for clathrin-mediated endocytosis. *Nature Rev Mol Cell Biol*, 7:404–414.
- Krendel, M., Osterweil, E., and Mooseker, M. (2007). Myosin 1E interacts with synaptojanin-1 and dynamin and is involved in endocytosis. *FEBS letters*, 581:644–650.
- Lamaze, C., Dujancourt, A., Baba, T., Lo, C., Benmerah, A., and Dautry-Varsat, A. (2001). Interleukin 2 receptors and detergent-resistant membrane domains define a clathrin-independent endocytic pathway. *Mol Cell*, 7:661–671.
- Lamaze, C., Fujimoto, L., Yin, L., and Schmid, S. (1997). The actin cytoskeleton is required for receptor-mediated endocytosis in mammalian cells. *J Biol Chem*, 272:20332–20335.
- Lee, W.-L., Bezanilla, M., and Pollard, T. (2000). Fission yeast myosin-I, Myo1p, stimulates actin assembly by Arp2/3 complex and shares functions with WASP. *J Cell Biol*, 151:789–799.
- Mallik, R. and Gross, S. (2004). Molecular motors: strategies to get along. *Curr Biol*, 14:971–982.
- McKeirnan, A., Evermann, J., Hargis, A., and Ott, R. (1981). Isolation of feline coronaviruses from 2 cats with diverse disease manifestations. *Feline Practice*, 11(3):16–20.
- Merrifield, C., Moss, S., Ballestrem, C., Imhof, B., Giese, G., Wunderlich, I., and Almers, W. (1999). Endocytic vesicles move at the tips of actin tails in cultered mast cells. *Nat Cell Biol*, 1:71–74.
- Merrifield, C., Rescher, U., Almers, W., Proust, J., Gerke, V., Sechi, A., and Moss, S. (2001). Annexin 2 has an essential role in actin-based macropinocytic rocketing. *Curr Biol*, 11:1136–1141.
- Mundy, D., Machleidt, T., Ying, Y.-S., Anderson, R., and Bloom, G. (2002). Dual control of caveolar membrane traffic by microtubules and the actin cytoskeleton. *J Cell Sci*, 115:4327–4339.



- Muro, S., Wiewrodt, R., Thomas, A., Koniaris, L., Albelda, S., Muzykantov, V., and Koval, M. (2003). A novel endocytic pathway induced by clustering endothelial ICAM-1 or PECAM-1. *J Cell Sci*, 116:1599–1609.
- Olazabal, I., Caron, E., May, R., Schilling, K., Knecht, D., and Machesky, L. (2002). Rho-kinase and myosin-II control phagocytic cup formation during CR, but not Fc $\gamma$ R, phagocytosis. *Curr Biol*, 12:1413–1418.
- Opstap, E., Maupin, P., Doberstein, S., Baines, I., Korn, E., and Pollard, T. (2003). Dynamic localization of myosin-I to endocytic structures in *Acanthamoeba*. *Cell Motil Cytoskeleton*, 54:29–40.
- Orth, J., Krueger, E., Cao, H., and McNiven, M. (2002). The large GTPase dynamin regulates actin comet formation and movement in living cells. *Proc Natl Acad Sci*, 99:167–172.
- Pedersen, N., Boyle, J., Floyd, K., Fudge, A., and Barker, J. (1981). An enteric coronavirus infection of cats and its relationship to feline infectious peritonitis. *Am J Vet Res*, 42:368–376.
- Pelkmans, L. and Helenius, A. (2002). Endocytosis via caveolae. *Traffic*, 3:311–320.
- Pelkmans, L., Puntener, D., and Helenius, A. (2002). Local actin polymerization and dynamin recruitment in SV40-induced internalization of caveolae. *Science*, 296:535–539.
- Perrais, D. and Merrifield, C. (2005). Dynamics of endocytic vesicle creation. *Dev Cell*, 9:581–592.
- Raposo, G., Cordonnier, M.-N., Tenza, D., Menichi, B., Durbach, A., Louvard, D., and Coudrier, E. (1999). Association of myosin I alpha with endosomes and lysosomes in mammalian cells. *Mol Biol Cell*, 10:1477–1494.
- Razani, B., Woodman, S., and Lisanti, M. (2002). Caveolae: from cell biology to animal physiology. *pharmacol rev*, 54:431–467.
- Sabharanjak, S. and Mayor, S. (2004). Folate receptor endocytosis and trafficking. *Adv Drug Del Rev*, 56:1099–1109.
- Sabharanjak, S., Sharma, P., Parton, R., and Mayor, S. (2002). GPI-anchored proteins are delivered to recycling endosomes via a distinct Cdc42-regulated, clathrin-independent pinocytic pathway. *Dev Cell*, 2:411–423.
- Sokac, A., Schietroma, C., Gundersen, C., and Bement, W. (2006). Myosin-1c couples assembling actin to membranes to drive compensatory endocytosis. *Dev Cell*, 11:629–640.

- Soldati, T. (2003). Unconventional myosins, actin dynamics and endocytosis: a menage a trois? *Traffic*, 4:358–366.
- Soldati, T. and Schliwa, M. (2006). Powering membrane traffic in endocytosis and recycling. *Nature Rev Mol Cell Biol*, 7:897–908.
- Southwick, F., Li, W., Zhang, F., Zeile, W., and Purich, D. (2003). Actin-based endosome and phagosome rocketing in macrophages: activation by the secretagogue antagonists lanthanum and zinc. *Cell Motil Cytoskeleton*, 54:41–55.
- Subtil, A. and Dautry-Varsat, A. (1997). Microtubule depolymerization inhibits clathrin coated-pit internalization in non-adherent cell lines while interleukin 2 endocytosis is not affected. *J cell Sci*, 110:2441–2447.
- Swanson, J., Johnson, M., Beningo, K., Post, P., Mooseker, M., and Araki, N. (1999). A contractile activity that closes phagosomes in macrophages. *J Cell Sci*, 112:307–316.
- Swanson, J. and Watts, C. (1995). Macropinocytosis. *Trends Cell Biol*, 5(11):424–428.
- Taunton, J., Rowling, B., Coughlin, M., Wu, M., Moon, R., Mitchison, T., and Larabell, C. (2000). Actin-dependent propulsion of endosomes and lysosomes by recruitment of N-WASP. *J Cell Biol*, 148:519–530.
- Titus, M. (1999). A class VII unconventional myosin is required for phagocytosis. *Curr Biol*, 9:1297–1303.
- Tuxworth, R., Weber, I., Wessels, D., Addicks, G., Soll, D., Gerisch, G., and Titus, M. (2001). A role for myosin VII in dynamic cell adhesion. *Curr Biol*, 11:318–329.
- Wu, X., Jung, G., and Hammer, J. (2000). Functions of unconventional myosins. *Curr Opin Cell Biol*, 12:42–51.
- Yarar, D., Waterman-Storer, C., and S.L., S. (2005). A dynamic actin cytoskeleton functions at multiple stages of clathrin-mediated endocytosis. *Mol Biol Cell*, 16:964–975.
- Zhang, F., Southwick, F., and Purich, D. (2002). Actin-based phagosome motility. *Cell Motil Cytoskeleton*, 53:81–88.

# 6

## Regulation of a clathrin- and caveolae-independent internalization pathway in FIPV-infected monocytes\*

### Summary

Feline infectious peritonitis virus (FIPV) is a coronavirus that causes a usually fatal pleuritis/peritonitis in cats in spite of a strong humoral immune response. In FIPV-infected monocytes, the *in vivo* target cell, viral proteins are expressed in the plasma membrane which should enable antibody-dependent cell lysis. However, these viral proteins are internalized upon binding of antibodies, explaining why antibodies cannot protect a cat against FIP. The internalization of antigen-antibody complexes occurs through a clathrin- and caveolae-independent pathway. In the present study, we investigated how this internalization pathway is regulated. The experiments showed that the internalization is dependent on serine/threonine kinases and independent of phosphatases and tyrosine kinases. The kinases that were shown to positively regulate the internalization process are MLCK and JNK, a member of the MAPK family. The MAPKs ERK and p38 regulated the internalization in a negative manner and the results suggest that active p38 is required to maintain the viral proteins expressed in the plasma membrane. There were indications that the MAPKs were not only important during the internalization process itself, but also during intracellular trafficking.

---

\*This Chapter is partially based on Dewerchin et al. (2008)-submitted

## 6.1 Introduction

Feline infectious peritonitis virus (FIPV) is one of the two coronaviruses that is described in cats. FIPV has been isolated from cats all over the world and infection with the virus will most likely lead to a chronic and usually fatal pleuritis/peritonitis. Cats with clinical FIP often have very high FIPV-specific antibody titers. These antibodies seem unable to protect the cat against the virus. We have described previously that viral proteins are expressed in the plasma membrane of infected monocytes, the *in vivo* target cell of FIPV, which should enable antibody-dependent cell lysis (Dewerchin et al., 2005). We also presented an immune evasion strategy for FIPV that could clarify why antibodies and antibody-driven immune effectors are unable to efficiently clear the body from infected cells. When mimicking the *in vivo* situation *in vitro* by adding antibodies to the culture medium, we found that infected monocytes internalize their surface expressed viral protein upon binding of FIPV-specific antibodies leaving the cell without visually detectable viral proteins on the plasma membrane (Dewerchin et al., 2006). Also FIPV infected monocytes isolated from naturally infected cats did not express viral proteins in the plasma membrane while expression returned after isolation and *in vitro* cultivation of the monocytes, indicating that this immune evasion strategy might indeed occur *in vivo* (Cornelissen et al., 2007). Investigating the internalization process, we found that the viral antigen-antibody complexes are internalized through a new clathrin- and caveolae-independent pathway which was also independent from rafts, rho-GTPases and actin (Dewerchin et al., 2008b). Myosin 1 and 6 were found to play a role in the internalization process, probably to guide the internalizing vesicles through the actin barrier, and myosin 1 was also found to play a role in the intracellular trafficking of the vesicles over the microtubules (Dewerchin et al., 2008b) and Chapter 5.

The aim of the current study is to elucidate how this new independent pathway is regulated. Regulation in a cell typically occurs through phosphorylation and dephosphorylation by kinases and phosphatases. Based on their substrate, kinases and phosphatases are divided into 2 large groups: the serine/threonine and the tyrosine kinases or phosphatases. These four groups contain numerous kinase or phosphatase families.

Binding of antibodies to the viral proteins must start a signaling cascade leading to the internalization of the antigen-antibody complex. Several kinases have already been identified in the regulation of the different internalization pathways. An overview is given in Figure 6.1. In Fc receptor-mediated phagocytosis, this signaling starts with phosphorylation of tyrosine in the immunoreceptor tyrosine-based activation motif (ITAM) by members of the src family

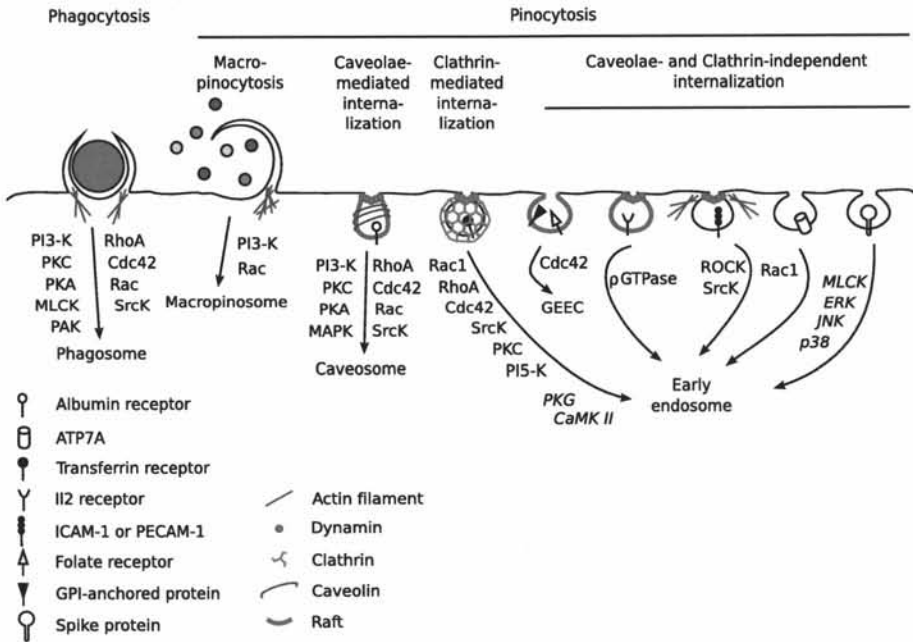


Figure 6.1: Overview of the involvement of kinases and auxiliary Rho GTPase proteins during the different internalization pathways. The kinases in *italic* have been identified in this study. GPI: Glycosyl-phosphatidylinositol, GEEC: GPI-anchored protein-enriched early endosomal compartment.

of tyrosine kinases (Lyn and Hck). This leads to activation of the Syk kinase which will activate several signaling cascades. Further downstream several serine/threonine kinases play a role in phagocytic cup formation and closure: protein kinase C (PKC), protein kinase A (PKA), Phosphatidylinositol 3 kinase (PI-3K), p21-activated kinase-1 (PAK1) and myosin light chain kinase (MLCK). Also the Rho-GTPases Cdc42 and Rac are involved. Various phosphatases have been identified as regulators, among which: Src homology 2 (SH2)-containing tyrosine phosphatase-1, SH2 domain-containing inositol phosphatase 1 and 5'PI phosphatase (reviewed by Aderem and Underhill (1999) and Swanson and Hoppe (2004)). In caveolae-mediated internalization, the src family of tyrosine kinases and a whole list of serine/threonine kinases have been implicated, among which PKA, MAPKs, PI-3K and PKC and the auxiliary rho-GTPases Cdc42 and RhoA proteins (reviewed in Razani et al. (2002)). Also in clathrin-mediated internalization, src kinases were found to play a role, as well as PKC and PI-5K (Perrais and Merrifield, 2005). Here too, the rho-GTPases Cdc42 and Rac play a role. Much less is known about the role of phosphatases in clathrin- or caveolae-mediated internalization. Regulation of the 5 less well studied clathrin- and caveolae-independent internalization pathways (among which the pathway that is studied here) is mainly undiscovered territory. So far, only the Rho-GTPases have been implicated. The pathway that is used by viral surface expressed proteins in FIPV infected monocytes, does not require Rho-GTPases (Dewerchin et al., 2008b).

The experiments presented in this study showed that the internalization pathway is regulated by the serine/threonine kinases MLCK and MAPKs. The extracellular signal regulated kinase (ERK) and the p38 signaling cascades provided negative feedback regulation while the JNK signaling cascade regulated the internalization process in a positive manner.

## 6.2 Material and Methods

**Viruses and antibodies** A third passage of FIPV strain 79-1146 (American Type Culture Collection (ATCC)) on CrFK cells was used (McKeirnan et al., 1981). Polyclonal anti-FCoV antibodies were kindly provided by Dr Rotter (Utrecht University, The Netherlands). The antibodies were purified and biotinylated according to manufacturers instructions (Amersham Bioscience, Buckinghamshire, UK). FITC-labeled polyclonal anti-FIPV antibodies were purchased from Veterinary Medical Research and Development (VMRD, Pullman, Washington, USA). The monoclonal antibodies E22-2 recognizing the N protein, were kindly provided by Dr. Hohdatsu (Kitasato University, Japan). The monocyte marker DH59B, which recognizes CD172a, was purchased from

VMRD. Mouse monoclonals against phosphorylated ERK, p38 and JNK were obtained Santa Cruz Biotechnology (Santa Cruz, California, USA). Secondary antibodies and reagents: goat anti-mouse Texas Red, goat anti-mouse Alexa Fluor 350, streptavidin Texas Red and streptavidin FITC were purchased from Molecular Probes (Molecular Probes-Invitrogen, Eugene, Oregon, USA).

**Isolation and inoculation of blood monocytes** Feline monocytes were isolated as described previously (Dewerchin et al., 2005). Cells were seeded on glass coverslips inserted in a 24-well dish (Nunc A/S, Roskilde, Denmark) in RPMI-1640 medium containing 10% fetal bovine serum (FBS), 0.3 mg/ml glutamine, 100 U/ml penicillin, 0.1 mg/ml streptomycin, 0.1 mg/ml kanamycin, 10 U/ml heparin, 1mM sodium pyruvate, and 1% non-essential amino-acids 100x (GIBCO-Invitrogen, Merelbeke, Belgium). Non-adherent cells were removed by washing the dishes two times with RPMI-1640 at 2 and 24 hours after seeding. The adherent cells consisted for  $86 \pm 7\%$  of monocytes (as assessed by fluorescent staining with the monocyte marker DH59B). At 56 hours post seeding, monocytes were inoculated with FIPV at a multiplicity of infection (m.o.i.) of 5. Between 20 and 60 cells were analyzed per assay.

**Internalization inhibition assays** Twelve hours after inoculation, monocytes seeded on glass coverslips were pre-incubated for 30 minutes at 37°C with 5% CO<sub>2</sub> in the presence of one of the following agents dissolved in RPMI: 300 nM staurosporine (Sigma-Aldrich GmbH), 10mM sodium fluoride (Sigma-Aldrich GmbH), 50 µg/ml genistein (Sigma-Aldrich GmbH), 50 µM dephostatin (Calbiochem), 500 nM Bisindolylmaleimide (Calbiochem), 10 µM ML-7 (Calbiochem), 500 nM H-89 (Calbiochem), 3 µM KN-93 (Calbiochem), 200 µM PKG inhibitor (Calbiochem), 150 nM K-252a (Calbiochem), 0.45M sucrose (Sigma-Aldrich GmbH), 100 µM PD098059 (Sigma-Aldrich GmbH), 500 nM U0126 (Calbiochem), 20µM SB203580 (Calbiochem) or 20µM JNK inhibitor II (Calbiochem).

The working concentration of each reagent was based on literature values and was optimized qualitatively in internalization assays with control ligands (data not shown). Viability of the cells during the inhibition assay was tested for each inhibitor using ethidium bromide monoazide (Molecular Probes-Invitrogen) and was always over 99%. After pre-treatment, the cells were incubated with polyclonal biotinylated anti-FIPV antibodies in presence of one of the given inhibitors for 30 minutes at 37°C. Then, cells were fixed with 1% formaldehyde, permeabilized with 0.1% Triton X-100 (Sigma-Aldrich GmbH) and incubated with streptavidin-Texas Red for 1 hour at 37°C. Next, infected cells were visualized with polyclonal anti-FIPV-FITC. The glass coverslips were mounted

on microscope slides using glycerin-PBS solution (0.9:0.1, vol/vol) with 2.5% 1,4-diazabicyclo(2, 2, 2)octane (DABCO) (Janssen Chimica, Beerse, Belgium) and analyzed with confocal microscopy. Monocytes were scored as cells with fully internalized antigen-antibody complexes when no labeling could be observed at the plasma membrane. Percentages of cells with fully internalized complexes were calculated relative to the total amount of monocytes which showed antibody binding and thus had membrane expression before antibodies were added. Those monocytes constitute about 50% of the total amount of infected cells (Dewerchin et al., 2005). Because of the variability on the amount of cells with membrane expression, visualization of the complexes remaining at the plasma membrane was needed. Therefore, an acid washing step to remove the extracellular antibodies was not performed.

To test the effectiveness of all reagents, a suitable control was used in each experiment. Monocytes seeded on glass coverslips were pre-incubated for 30 minutes at 37°C with 5% CO<sub>2</sub> in the presence of one of the inhibitors. After treatment, the cells were incubated with biotinylated transferrin (Sigma-Aldrich GmbH) or fluorescent 1µm polystyrene microspheres, FluoSpheres (Molecular Probes-Invitrogen), in presence of the inhibitor. Then, cells were fixed with 1% formaldehyde and permeabilized with 0.1% Triton X-100. The biotinylated transferrin was visualized by incubating the cells with streptavidin-FITC for 1 hour at 37°C and cells incubated with fluorescent beads were incubated with phalloidin-Texas Red (Molecular Probes-Invitrogen) for 1 hour at 37°C to visualize the lamellipodia. The glass coverslips were mounted on microscope slides using glycerin-DABCO and analyzed by confocal microscopy. For the controls, the monocytes were scored analogously as FIPV infected cells: ligands were considered “fully internalized” when they were only observed inside the cell. Fluorescent beads were considered internalized when they were found inside the cortical actin labeling.

#### **Co-localization studies with activated MAPKs: p-ERK, p-p38 and p-JNK**

At twelve hours after inoculation, monocytes were incubated with biotinylated anti-FIPV polyclonal antibodies. At different times post antibody addition, cells were fixed with 1% formaldehyde, permeabilized with 0.1% Triton X-100 and the antigen-antibody complexes were visualized with streptavidin-FITC followed by a blocking step with 10% negative goat serum. Next, cells were incubated with mouse anti-p-ERK, anti-p-p38 or anti-p-JNK (in the presence of 10% negative goat serum) followed by goat anti-mouse Texas Red. Finally, infected cells were visualized with anti-N monoclonal antibodies and goat anti-mouse Alexa Fluor 350 (Molecular Probes)(not shown in images). The glass coverslips were mounted on microscope slides using glycerin-DABCO and analyzed by confocal microscopy.



**Inhibitor induced internalization assay** At 12 hours after inoculation, monocytes seeded on glass coverslips were placed on ice, washed twice with ice-cold phosphate buffered saline (PBS) solution and incubated with 2mM of biotinylation reagent EZ-Link sulfo-NHS-LC-Biotin (Pierce). After 30 minutes, the biotin was removed and replaced by cold medium supplemented with 10mM glycine for 10 minutes. Then, the monocytes were washed twice with cold supplemented medium and twice with cold medium without FBS or heparin. Cells were shifted to 37°C and incubated with biotinylated anti-FIPV polyclonal antibodies, ERK-inhibitor PD098059 or JNK inhibitor II for 30 minutes. To visualize internalized biotinylated proteins, cells were fixed with 1% formaldehyde, permeabilized with 0.1% Triton X-100 and incubated with streptavidin-Texas Red for 1 hour at 37°C. Afterward, cells were washed and incubated with FITC-labeled polyclonal anti-FIPV to enable identification of infected cells. The glass coverslips were mounted on microscope slides using glycerin-DABCO and analyzed by confocal microscopy.

**Confocal laser scanning microscopy** The samples were stained as described above and examined with a Leica TCS SP2 laser scanning spectral confocal system (Leica Microsystems GmbH, Wetzlar, Germany) linked to a DM IRB inverted microscope (Leica Microsystems). Argon and Helium/Neon laser lights were used to excite FITC (488 nm line) and Texas-Red (543 nm line) fluorochromes. The images were obtained with Leica confocal software and processed with the GIMP.

**Statistical analysis** Triplicate assays were compared using a Mann-Whitney U test with SPSS 11.0 (SPSS Inc., Chicago, WA). P values <0.05 were considered significantly different. For each assay, between 20 and 60 cells were counted.

## 6.3 Results

### 6.3.1 Internalization of viral antigens is energy-dependent and regulated by a serine/threonine kinase

To obtain a first clue on the regulation of this internalization process, the importance of phosphorylation and/or dephosphorylation was tested with chemical inhibitors. Representative confocal images and quantification of the internalization assays in the presence of inhibitors are shown in Figure 6.2.

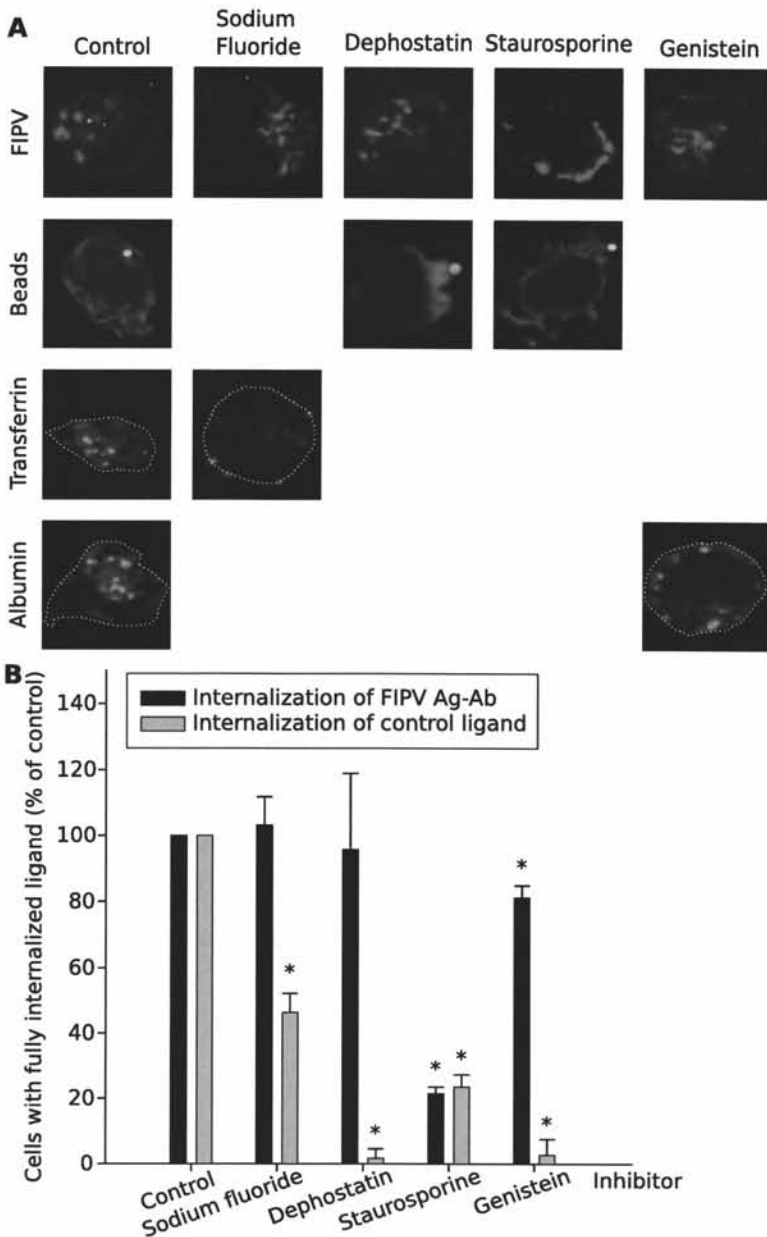


Figure 6.2: Further characterization of the internalization pathway of surface expressed viral antigens in FIPV infected monocytes by inhibiting phosphate transfer during internalization. (A) Confocal images of feline monocytes after the internalization assays (of viral surface expressed proteins or control ligands) performed in presence of different inhibitors for kinases or phosphatases. The activity of each inhibitor was tested with an internalization assay of a suitable control. In row 2, cortical actin was stained (red) to visualize whether or not the lamellipodia were closed around the beads. (B) Results are given relatively to a control of untreated cells. Data are means and standard deviations of triplicate assays. The asterisk marks results that are significantly different from the untreated control ( $p < 0.05$ ).

*Dephosphorylation.* First, the importance of phosphatases for dephosphorylation was tested. Treatment with sodium fluoride (broad range phosphatase inhibitor) gave no reduction of internalization whereas the internalization of the control ligand transferrin amounted to  $46\pm 6\%$  of the untreated control. In addition, treatment of cells with the more specific tyrosine phosphatase inhibitor, dephostatin, gave no reduction of internalized viral proteins either ( $96\pm 23\%$  of untreated control, in contrast to  $2\pm 3\%$  for the control ligand beads). These results indicated that phosphatases do not play a role in antibody-induced internalization.

*Phosphorylation.* Next, it was investigated whether kinases played a role in internalization. Treatment of cells with the broad range serine/threonine kinase inhibitor staurosporine resulted in a reduction in viral protein internalization ( $21\pm 2\%$  of control) to a similar extent as for the control ligand, beads ( $23\pm 4\%$  of control). Using the tyrosine kinase inhibitor genistein, the internalization of viral antigens amounted to  $81\pm 4\%$  of untreated control while the internalization of the control ligand albumin was  $3\pm 5\%$  of the untreated control. The reduction in internalization caused by genistein was significant but small compared to the control ligand albumin. This minor effect could be due to a non-specific action of the drug or it could be that tyrosine kinases play a role in the later stages of the internalization process, like intracellular transportation. Taken together, these data indicate an important role for (a) serine/threonine kinase(s) in the antibody-induced internalization of surface expressed viral proteins in FIPV infected monocytes.

### **6.3.2 Internalization of viral antigens is regulated by myosin light chain kinase**

The serine/threonine kinases are the biggest group of kinases and consist of different classes among which: protein kinase C (PKC), protein kinase A (PKA) or cyclic AMP-dependent protein kinases, protein kinase G (PKG) or cyclic GMP-dependent protein kinases, the family of the calcium/calmodulin-dependent protein kinases (CaM K) and myosin light chain kinases (MLCK). The importance of these classes was tested by performing internalization assays in the presence of pharmacological inhibitors. The internalization of viral antigens remained unaffected in the presence of bisindolylmaleimide I (a PKC-inhibitor), H-89 (a PKA-inhibitor), PKG-inhibitor and KN-93 (a CaM K II-inhibitor) while the internalization of a control ligand was reduced to  $25\pm 13\%$ ,  $33\pm 29\%$ ,  $14\pm 7\%$  and  $23\pm 16\%$  respectively (representative images and results are given in Figure 6.3). In contrast, the specific MLCK inhibitor ML-7, could inhibit the internalization of viral antigens to  $12\pm 21\%$  of the untreated control and the uptake of beads, the control ligand, was equivalently

reduced to  $11 \pm 5\%$  (Figure 6.3). The importance of MLCK was confirmed by another MLCK inhibitor: K252a, which also inhibited the internalization of both the viral antigens as the control ligand (beads) to a similar level (Figure 6.3). These results indicated that MLCK is required to enable the internalization of viral antigens.

### 6.3.3 Internalization of viral antigens is regulated by MAPKs

Mitogen-activated protein kinases or MAPKs are a large subfamily of serine/threonine kinases. They form cascades of kinases through which signal transduction starting from extracellular stimuli to the nucleus occurs. The MAPK network can be divided into 3 main branches which lead to 3 major downstream effector kinases. A first branch, the classical MAPK cascade, is activated by mitogens and growth factors and involves the activation of receptor tyrosine kinases. The cascade results in the activation of 2 closely related MAPKs: the extracellular signal regulated kinase 1 (ERK1) and ERK2. The second branch is the stress-activated protein kinase 1 (SAPK1) or c-Jun N-terminal kinase (JNK) cascade. It is activated by cellular stress resulting from UV radiation or heat shock, inflammatory cytokines and bacterial infection and will lead to the activation of JNK. The third branch is the stress activated protein kinase 2 (SAPK2) or p38 cascade, which is activated by cellular stress resulting from osmotic shock, endotoxins and inflammatory cytokines. This cascade will lead to the activation of p38 kinase or reactivating kinase.

The importance of MAPKs of each of these branches in antibody-induced internalization of surface expressed antigens in FIPV-infected monocytes was tested using pharmacological inhibitors. Representative confocal images of monocytes after 30 minutes of internalization are shown in Figure 6.4. The inhibitors PD098059 and U0126 both inhibit the activation of ERK1/2. The inhibitor PD098059 impedes the activation of MAPK kinase (MAPKK) which is situated just upstream of ERK1/2 in the classical MAPK cascade and U0126 blocks activated MAPKK. Neither inhibitor could block the internalization of antigen-antibody complexes while the internalization of the control ligands, beads, was reduced to  $57 \pm 25\%$  and  $26 \pm 27\%$  of the untreated control for PD098059 and U0126 respectively (Figure 6.4). A small, non-significant, increase in internalization of viral antigens was noted for both inhibitors. Next, the p38 or SAPK2 cascade was checked with the inhibitor SB203580 which blocks p38 kinase. Figure 6.4 shows that the internalization of viral antigens increased to  $130 \pm 8\%$  while the internalization of the control ligand albumin was reduced to 24%. If blocking p38 leads to enhancement of the internalization, than activation of p38 should lead to a reduced rate of internalization. This was checked by activating the p38 cascade with an osmotic shock in-

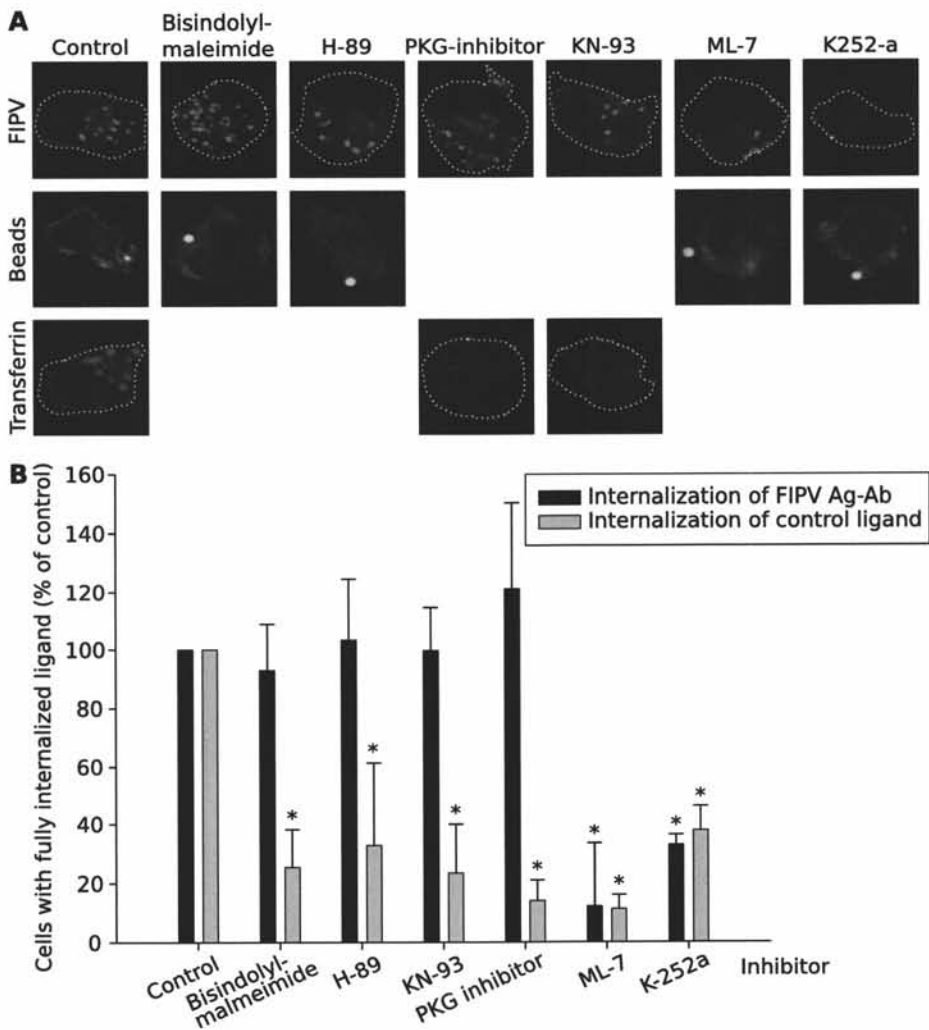


Figure 6.3: Myosin light chain kinase (MLCK) inhibitors can block the internalization of surface expressed viral antigens in FIPV infected monocytes. A range of serine/threonine kinases were tested for their importance during the internalization process by using chemical inhibitors: Bisindolylmaleimide (PKC inhibitor), H-89 (PKA inhibitor), PKG inhibitor, KN-93 (CaM-dependent kinase II inhibitor), ML-7 (MLCK inhibitor) and K252-a (inhibits MLCK, PKA, PKC and PKG). (A) Confocal images of feline monocytes after an internalization assays of 30 minutes using antibodies or control ligands: beads or transferrin. The images show a single optical section through the cell. In row 2, cortical actin was stained (red) to visualize whether or not the lamellipodia were closed around the beads. (B) Quantification of the internalization in presence of inhibitors against serine/threonine kinases. Results are given relatively to a control of untreated cells. Data are means and standard deviations of triplicate assays. The asterisk marks results that are significantly different from the untreated control ( $p < 0.05$ ).

duced by sucrose. Figure 6.4 shows that the internalization of viral antigens was indeed reduced to  $22\pm 22\%$  of the untreated control. These data indicate that the p38 cascade provides a negative regulation of the internalization process. The importance of the JNK cascade was checked with JNK inhibitor II. Treatment of monocytes with this inhibitor lead to a reduction in internalization to  $67\pm 21\%$  which was not significant ( $p=0.053$ ). JNK inhibitor II gave a stronger, significant reduction of the internalization of the control ligand transferrin ( $29\pm 28\%$  of the untreated control).

Taken together, the results showed that the internalization of viral antigens was negatively regulated by the p38 cascade. The results for the ERK1/2 and the JNK cascade were less clear since no significant difference between treated and non-treated monocytes could be observed. However, there was an indication the JNK might (positively) regulate the internalization process.

#### **6.3.4 Co-localization of viral antigen-antibody complexes with p-ERK, p-p38 and p-JNK**

The kinase inhibitors/activators used in the above experiments, can offer indications on the importance of the studied kinase. However, some side-effects can not always be excluded, especially in the case of sucrose treatment, which will activate a range of stress-related proteins. In order to confirm that p38 does indeed regulate the internalization of viral antigens and to verify whether or not ERK and JNK play a role, co-localization stainings were performed. The internalization process was stopped at different time points and phosphorylated (thus activated) p-ERK, p-p38 and p-JNK were detected using phosphospecific antibodies. The confocal images in Figure 6.5 clearly show that viral antigen-antibody complexes co-localized with p-ERK, p-p38 and p-JNK during internalization. p-ERK and p-JNK were recruited to the antigen-antibody complexes right after initiation of internalization. p-ERK remained associated with the complexes for at least 30 minutes, indicating that it might play a role in internalization itself and in intracellular trafficking. In contrast, p-JNK dissociated from the complexes (or was dephosphorylated) between 5 and 10 minutes after the internalization started. No-co-localization could be observed after 30 minutes. The stainings with anti-p-p38 showed that activated p38 is located right underneath the plasma membrane at the sites where viral proteins are embedded even before the internalization started, indicating that p38 might be important to keep the viral proteins in the plasma membrane. This is consistent with the finding that activation of p38 led to inhibition of the internalization while blocking p38 led to spontaneous internalization. During the internalization, antigen-antibody complexes could be observed that did not co-localize with p-p38 (indicated with arrowheads) at 1 and 5 minutes. At

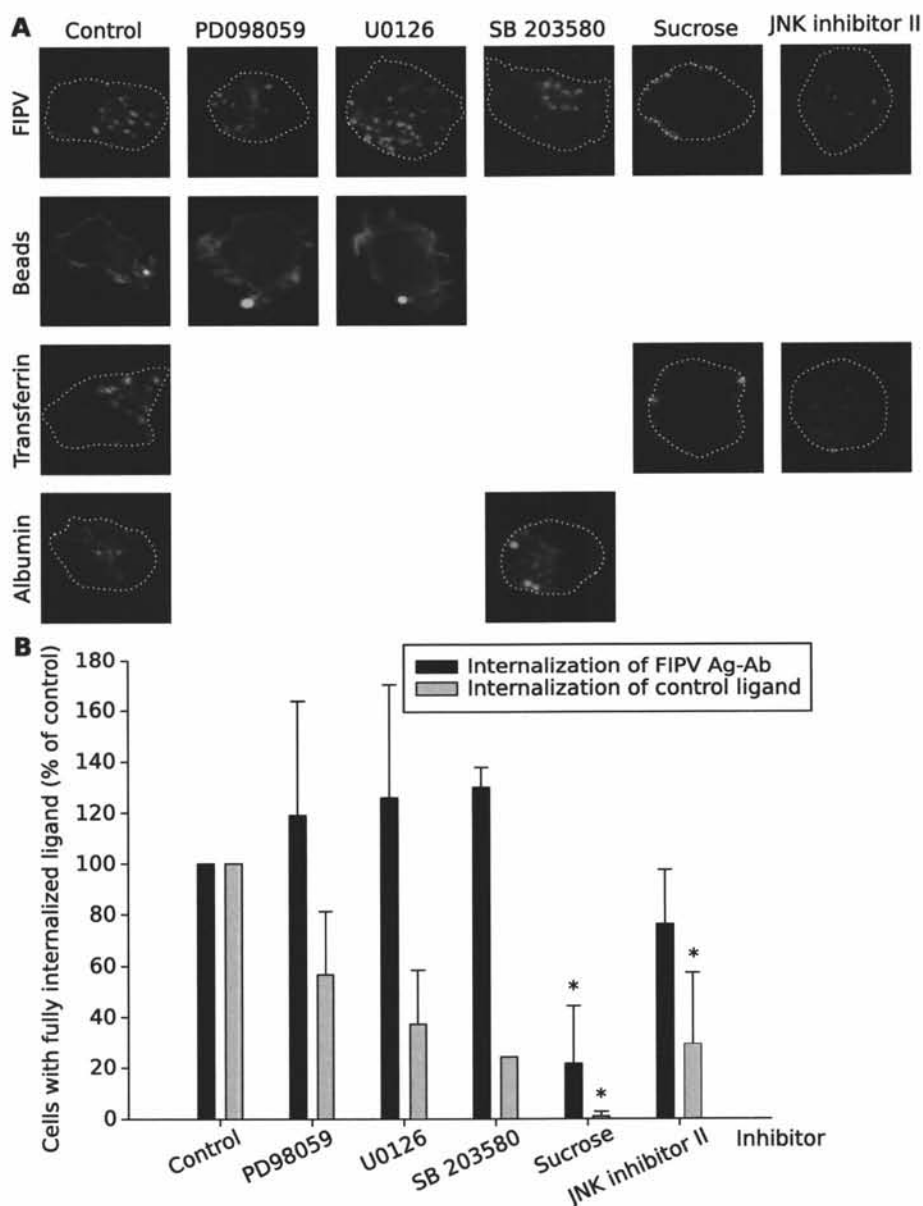


Figure 6.4: The importance of mitogen activated protein kinases (MAPK) in the internalization of surface expressed viral antigens in FIPV infected monocytes. (A) Confocal images of feline monocytes in which the effect was tested of MAPK inhibitors (or activators) on the internalization of surface expressed viral antigens or control ligands: beads, transferrin or albumin. The images show a single optical section through the cell. In row 2, cortical actin was stained (red) to visualize whether or not the lamellipodia were closed around the beads. (B) Quantification of the effect of MAPK inhibitors on internalization. Results are given relatively to a control of untreated cells. Data are means and standard deviations of double or triplicate assays. The asterisk marks results that are significantly different from the untreated control ( $p < 0.05$ ).

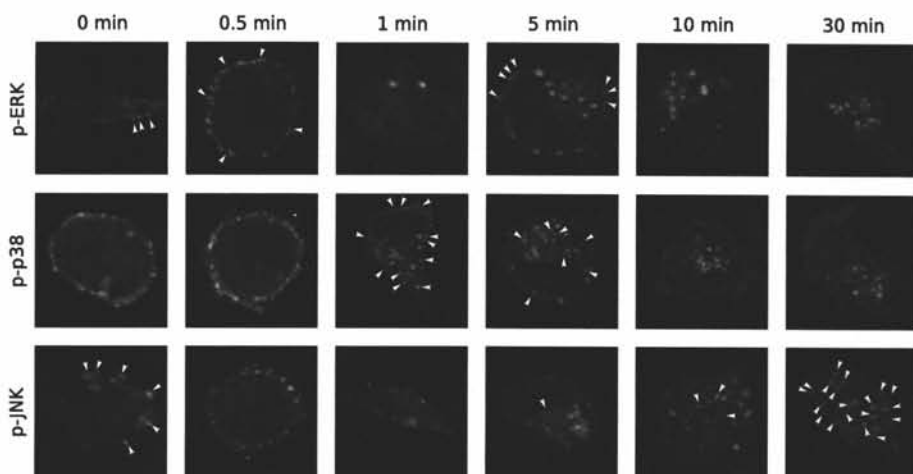


Figure 6.5: Detection of activated MAPKs (phosphorylated ERK, p38 and JNK) during the internalization of surface expressed viral antigens in FIPV infected monocytes. Viral antigen-antibody complexes were visualized with biotin-FITC (green signal) and p-ERK, p-p38 and p-JNK were visualized with goat anti-mouse Texas Red (red signal). The confocal images show a single optical section through a cell. Arrowheads indicate the non-colocalizing antigen-antibody complexes.

later time points, co-localization was fully restored which suggested that p-p38 might be required at different stages of the internalization process.

From these stainings, it can be concluded that ERK, p38 and JNK all play a role at 1 or more stages of the antibody-induced internalization of viral proteins in FIPV infected monocytes.

### 6.3.5 Mode of regulation by MAPKs

The experiments with the inhibitors and the stainings showed that the internalization process was negatively regulated by p38. However, the mode of regulation by ERK and JNK was less clear. The fact that both p-ERK and p-JNK are recruited the antigen-antibody complexes as soon as internalization started, indicated that activated ERK and JNK might regulate the internalization in a positive manner. For JNK, a role in positive regulation was also suggested by the results with the JNK inhibitor II. In contrast, the 2 inhibitors for the ERK1/2 cascade gave a slight increase in internalization, suggesting the ERK might be a negative regulator. During the experiments with the inhibitors, another noteworthy observation was made. Figure 6.6 shows that in the internalization assays with the ERK-inhibitors PD098059 and U0126, the amount of monocytes with surface expressed viral proteins was reduced



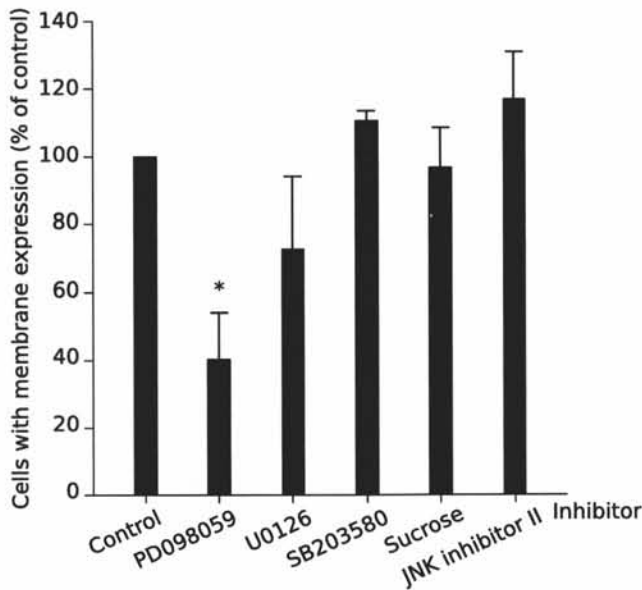


Figure 6.6: Influence of MAPK inhibitors on the amount of FIPV effected monocytes with membrane expression. Results are given relatively to a control of untreated cells. Data are means and standard deviations of double or triplicate assays. The asterisk marks results that are significantly different from the untreated control ( $p < 0.05$ ).

to  $40 \pm 14\%$  and  $73 \pm 21\%$ , respectively. This could only mean that in the 30 minutes of treatment with the inhibitors, before the antibodies were added, the viral proteins had already internalized in more than half of the cells in the case of PD098059. Thus, blocking of the ERK1/2 cascade could trigger spontaneous internalization. Treatment with the other inhibitors did not alter the surface expression of viral proteins. To confirm this “spontaneous” up-take of viral proteins, internalization assays were performed using only inhibitors and no antibodies. To visualize a possible redistribution caused by the inhibitor, surface expressed proteins were biotinylated prior to the internalization assay. Confocal images of the monocytes after the internalization assays are given in Figure 6.7. These images show that treatment with U0126 could indeed induce the internalization of surface expressed proteins in both infected and non-infected cells, confirming that ERK is a negative regulator, not only of the viral proteins but also of some cellular surface expressed proteins. In the monocytes treated with JNK inhibitor II, only the background spontaneous internalization could be observed, indicating that activated JNK does not regulate the internalization in a negative manner.

From these experiments, it can be concluded that ERK regulates the internalization of the viral proteins in a negative way. The experiments also provide

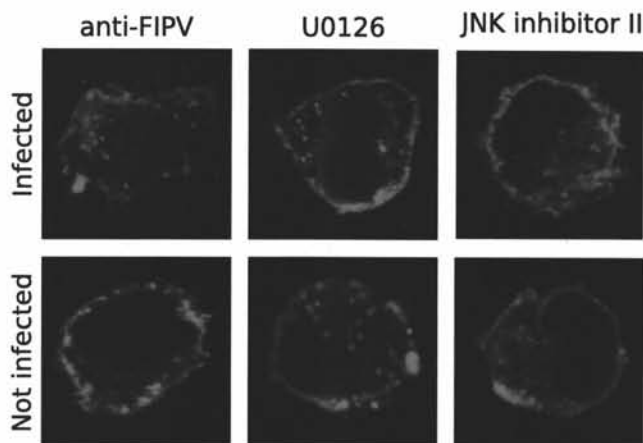


Figure 6.7: Induction of internalization by treatment with ERK-inhibitor U0126 and JNK inhibitor II. All membrane expressed proteins were biotinylated and redistribution of the proteins was visualized (with streptavidin Texas Red) after a 30 minutes of internalization assay in the presence of polyclonal anti-FIPV or an inhibitor. The confocal images show a single optical section through a cell.

another indication that JNK might positively regulate the internalization process.

## 6.4 Discussion

In FIPV infected monocytes, viral proteins are expressed in the plasma membrane in 50% of the cells (Dewerchin et al., 2005). Binding of FIPV-specific antibodies should enable the immune system of an infected cat to eliminate these monocytes. However, high antibody titers do not protect a cat against FIPV suggesting that FIPV possesses an immune evasion mechanism. We have shown previously that antibodies which bind to surface expressed proteins, cause the formed antigen-antibody complexes to internalize through a novel clathrin- and caveolae independent pathway, explaining why antibodies seem unable to mark infected cells for antibody-dependent cell lysis (Dewerchin et al., 2006, 2008b). In the current paper, we wanted to elucidate how this new pathway is regulated.

Regulation of cellular processes generally involves signaling cascades in which proteins are activated or deactivated through phosphorylation and dephosphorylation by kinases and phosphatases, respectively. The amino acid residues at which phosphate groups can be added are tyrosine, threonine or serine. In previous work, we already found the internalization does not require phos-

phatidylinositol 3-kinase (inhibitor: wortmannin) nor Rho-GTPases (inhibitor: Toxin B) (Dewerchin et al., 2008b). The experiments presented here, showed that internalization occurred independent from serine/threonine and tyrosine phosphatases (inhibitors: sodium fluoride, dephostatin) and tyrosine kinases (inhibitor: genistein). However, the pathway was sensitive to the inhibitor staurosporine, indicating dependency on (a) serine/threonine kinase(s).

Serine/threonine kinases are the biggest group of kinases and consist of many different classes. Using chemical inhibitors, a potential role for protein kinase C (PKC), protein kinase A (PKA) or cyclic AMP-dependent protein kinases and for protein kinase G (PKG) or cyclic GMP-dependent protein kinases was investigated. Also two important members of the calcium/calmodulin-dependent protein kinases (CaMK) family were examined: CaMK II and myosin light chain kinase (MLCK). PKC is known to regulate Fc receptor-, complement receptor- and mannose receptor-mediated phagocytosis (Aderem and Underhill, 1999). PKA and MLCK were shown to mediate phagocytosis in neutrophils (Ydrenius et al., 2000). In our experiments, using primary monocytes, we could indeed block the phagocytosis of fluorescent beads in monocytes using the specific PKA, PKC and MLCK inhibitors. A link between PKG or CaMK II and internalization processes could not be found in literature, however, in our experiments, the uptake of transferrin could be blocked using the PKG inhibitor or the CaMK II inhibitor (KN-93). Since the transferrin receptor is internalized through clathrin coated vesicles, these tests indicate a possible role for PKG and CaMK II in clathrin mediated internalization.

Only MLCK was found to play a role in the internalization of surface expressed viral protein in FIPV infected monocytes. It has been described that MLCK co-localizes with cortical actin filaments and, in fibroblast cells, it is MLCK that phosphorylates myosin in the cell periphery while Rho kinase (ROCK) is responsible for phosphorylation of myosin in the cell center (Guerriero et al., 1981; Totsukawa et al., 2000). This complies with a possible role for MLCK in the internalization process. The images in Figure 6.3 show that the antigen-antibody complexes are maintained at or right under the plasma membrane when MLCK is inhibited (only 1 antigen-antibody complex has traveled further into the ML-7 treated monocyte, but chemical inhibitors can rarely block a cellular process by 100%). This is an indication that MLCK plays a role during the first steps of internalization (e.g. membrane remodeling) or during a subsequent step (e.g. trafficking through the cortical actin network). Different MLCKs have been characterized in several species. Sequence comparisons show that vertebrate skeletal muscle and smooth muscle MLCKs belong to two subfamilies derived from different genes (Gallagher et al., 1997). Skeletal muscle MLCKs are exclusively expressed in skeletal muscle, while smooth muscle MLCKs are ubiquitously expressed. Smooth muscle MLCKs are thus

also active in non-muscle cells. In literature it is stated that MLCK has a substrate specificity restricted to the regulatory light chain of myosin-II. However, most research has been done on muscle cells and MLCKs have been shown to function differently in non-muscle cells (Gallagher et al., 1997). So, it is possible that there are members of the MLCK family that are not restricted to myosin 2. The results presented here, show that MLCK is required for the internalization process. Considering the fact that in previous work, we have found that only myosin 1 and 6 are important during the internalization, and not myosin 2a nor 2b (nor myosin 5a, 7a, 9b and 10), this suggests the existence of a MLCK that regulates myosin 1 or 6.

Another important family of serine/threonine kinases that was tested for a role in antibody-induced internalization are the MAPKs. Not much research has been done on the role of MAPKs in internalization processes. Nevertheless, these kinases are promising candidates to be of importance during internalization since the 3 main MAPK signaling cascades can lead to cytoskeleton rearrangements (reviewed in Huang et al. (2004)). ERK can phosphorylate MLCK which will lead to myosin activation and myosins are required for membrane remodeling (Klemke et al., 1997). However, it is unlikely that this is the role for ERK in the internalization process studied here, since the experiments suggest that ERK, or at least MAPK, regulates the internalization negatively while MLCK was clearly a positive regulator. Another possible downstream target for ERK is MAPK-activated protein kinase 2/3 (MAPKAPK 2/3) which is also a substrate for p38. Phosphorylating of MAPKAPK 2/3 leads to the activation of heat shock protein 27 which promotes stress fiber formation (Hedges et al., 1999; Rousseau et al., 1997). Here, the co-localization stainings showed that activated p-ERK was recruited to the antigen-antibody complexes as soon as internalization started and that association remained for at least 30 minutes. In previous work, we reported that actin tails decorated the internalizing vesicles and so ERK could play a role in the regulation of the actin tail (Dewerchin et al., 2008a). However, the actin tails were lost between 10 and 30 minutes after initiation of the internalization process, while ERK association remained. Thus, the precise role (or roles) of ERK remain(s) unclear, and identifying ERKs downstream target(s) during this internalization process could be the first step in clarifying this regulation mechanism. Although p38 can also activate MAPKAPK 2/3, it is unlikely that p38 is involved in the regulation of the actin tails since activated p38 lost its association with the internalizing vesicles between 1 and 5 to 10 minutes, which is when most actin tails are observed. The observation that activated p38 co-localized with surface expressed viral proteins before and only shortly after the internalization started and then again after 10 minutes when the vesicles were fully internalized strongly suggests that p38 plays (at least) 2 distinct roles in the internalization process. The

fact that p38 negatively regulated the internalization and that it was associated with viral proteins before the internalization process started indicates that active p38 is required for maintaining the viral proteins in the plasma membrane. A similar observation was made for the serotonin transporter in neurons which requires constitutively active p38 for its expression in the plasma membrane (Samuvel et al., 2005). The third MAPK cascade that was studied was the JNK cascade. JNK can activate Spir, a member of the Wiscott-Aldrich syndrome protein (WASP) homology domain 2 (WH2) family, which in turn is involved in actin dynamics (Otto et al., 2000). JNK has been reported to suppress actin filament formation and even to disrupt stress fibers (Rennefahrt et al., 2002; Zhang et al., 2003). It could be that JNK performs the same regulatory function here because (i) active JNK is recruited to the antibody-antigen complexes only in the beginning of the internalization process, thus when the vesicles need to cross the cortical actin network and (ii) previous work indicates that this cortical actin forms a barrier for the internalizing vesicles that needs to be disintegrated (or moved aside) to allow the vesicles to pass. Besides JNKs actin regulatory properties, it can also activate some microtubule-associated proteins (MAPs): MAP1B, MAP2 and DCX (Horesh et al., 1999; Chang et al., 2003; Kawauchi et al., 2003). MAPs are proteins that stabilize microtubules, organize them into bundles and mediate their connection with membranes and intermediate filaments. This means that JNK could also be essential for efficient intracellular transport. Previous work showed that internalizing vesicles start to move over microtubules around 1 minute after internalization has started (Dewerchin et al., 2008a). At that time, co-localization with activated JNK can still be observed, so it is possible that JNK also plays a role in the initiation of microtubule-based transport of the vesicles.

Since the internalization was not strongly blocked in the presence of chemicals inhibitors against the MAPKs, it would be interesting to confirm the obtained results with dominant negative mutants.

In summary, it can be concluded that the internalization of surface expressed viral proteins in FIPV infected cells is dependent on serine/threonine kinases but independent of tyrosine kinases and phosphatases. The kinases that were shown to positively regulate the internalization process are MLCK and JNK, a member of the MAPK family. The MAPKs ERK and p38 regulated the internalization in a negative manner and the results suggest that active p38 is even required to maintain the viral proteins expressed in the plasma membrane. There were indications that the MAPKs were not only important during the internalization process itself, but also during intracellular trafficking.

## Acknowledgments

We are very grateful to P. Rottier for supplying polyclonal anti-FCoV antibodies and to T. Hohdatsu for monoclonal anti-N-protein antibodies and to J. Vicca for supplying fluorescent beads. H.L.D. and E.C. were supported by the Institute for the Promotion of Innovation through Science and Technology in Flanders (IWT-Vlaanderen). E.V.H. was supported by the Special Research Fund of Ghent University.

## References

- Aderem, A. and Underhill, D. (1999). Mechanisms of phagocytosis in macrophages. *Annu Rev Immunol*, 17:593–623.
- Chang, L., Jones, Y., Ellisman, M., Goldstein, L., and Karin, M. (2003). JNK1 is required for maintenance of neuronal microtubules and controls phosphorylation of microtubule-associated proteins. *Dev Cell*, 4:521–533.
- Cornelissen, E., Dewerchin, H., Van Hamme, E., and Nauwynck, H. (2007). Absence of surface expression of feline infectious peritonitis virus (FIPV) antigens on infected cells isolated from cats with FIP. *Vet Microbiol*, 121:131–137.
- Dewerchin, H., Cornelissen, E., and Nauwynck, H. (2005). Replication of feline coronaviruses in peripheral blood monocytes. *Arch Virol*, 150(12):2483–2500.
- Dewerchin, H., Cornelissen, E., and Nauwynck, H. (2006). Feline infectious peritonitis virus-infected monocytes internalize viral membrane-bound proteins upon antibody addition. *J Gen Virol*, 87:1685–1690.
- Dewerchin, H., Cornelissen, E., Van Hamme, E., and Nauwynck, H. (2008a). Microtubules, actin and myosins cooperate during internalization and trafficking of antigen-antibody complexes in feline infectious peritonitis virus infected monocytes. *manuscript in preparation*.
- Dewerchin, H., Cornelissen, E., Van Hamme, E., Smits, K., Verhasselt, B., and Nauwynck, H. (2008b). Viral proteins in feline infectious peritonitis virus infected monocytes are internalized through a clathrin- and caveolae-independent pathway. *J Gen Virol*, submitted.
- Gallagher, P., Herring, B., and Stull, J. (1997). Myosin light chain kinases. *J Muscle Res Cell Mot*, 18:1–16.

- Guerriero, V., Rowley, D., and Means, A. (1981). Production and characterization of an antibody to myosin light chain kinase and intracellular localization of the enzyme. *Cell*, 27:449–458.
- Hedges, J., Dechert, M., Yamboliev, I., Martin, J., Hickey, E., L.A., W., and Gerthoffer, W. (1999). A role for p38(MAPK)/HSP27 pathway in smooth muscle cell migration. *J Biol Chem*, 274:24211–24219.
- Horesh, D., Sapir, T., Francis, F., Wolf, S., Caspi, M., Elbaum, M., Chelly, J., and Reiner, O. (1999). Doublecortin, a stabilizer of microtubules. *Hum Molec Genet*, 8:1599–1610.
- Huang, C., Jacobson, K., and Schaller, M. (2004). MAP kinases and cell migration. *J Cell Sci*, 117:4619–4628.
- Kawauchi, T., Chihama, K., Nabeshima, Y., and Hoshino, M. (2003). The in vivo roles of STEF/Tiam1, Rac1 and JNK in cortical neuronal migration. *EMBO J*, 22:4190–4201.
- Klemke, R., Cai, S., Giannini, A., Gallagher, P., deLanerolle, P., and Cheresch, D. (1997). Regulation of cell motility by mitogen-activated protein kinase. *J Cell Biol*, 137:481–492.
- McKeirnan, A., Evermann, J., Hargis, A., and Ott, R. (1981). Isolation of feline coronaviruses from 2 cats with diverse disease manifestations. *Feline Practice*, 11(3):16–20.
- Otto, I., Raabe, T., Rennefahrt, U., Bork, P., Rapp, U., and Kerkhoff, E. (2000). The p150-spir protein provides a link between c-Jun N-terminal kinase function and actin reorganization. *Curr Biol*, 10:345–348.
- Perrais, D. and Merrifield, C. (2005). Dynamics of endocytic vesicle creation. *Dev Cell*, 9:581–592.
- Razani, B., Woodman, S., and Lisanti, M. (2002). Caveolae: from cell biology to animal physiology. *pharmacol rev*, 54:431–467.
- Rennefahrt, U., Illert, B., Kerkhoff, E., Troppmair, J., and Rapp, U. (2002). Constitutive JNK activation in NIH 3T3 fibroblasts induces a partially transformed phenotype. *J Biol Chem*, 277:29510–29518.
- Rousseau, S., Houle, F., Landry, J., and Huot, J. (1997). p38 MAP kinase activation by vascular endothelial growth factor mediates actin reorganization and cell migration in human endothelial cells. *Oncogene*, 15:2169–2177.

- Samuvel, D., Jayanthi, L., Bhat, N., and Ramamoorthy, S. (2005). A role for p38 mitogen-activated protein kinase in the regulation of the serotonin transporter: evidence for distinct cellular mechanisms involved in transporter surface expression. *J Neurosci*, 25:29–41.
- Swanson, J. and Hoppe, A. (2004). The coordination of signaling during fc receptor-mediated phagocytosis. *J Leukoc Biol*, 76:1093–1103.
- Totsukawa, G., Yamakita, Y., Yamashiro, S., Hartshorne, D., Sasaki, Y., and Matsumura, F. (2000). Distinct roles of ROCK (Rho-kinase) and MLCK in spatial regulation of MLC phosphorylation for assembly of stress fibers and focal adhesions in 3T3 fibroblasts. *J Cell Biol*, 150:797–806.
- Ydrenius, L., Majeed, M., Rasmusson, B., Stendahl, O., and Sarndahl, E. (2000). Activation of cAMP-dependent protein kinase is necessary for actin rearrangements in human neutrophils during phagocytosis. *J Leukoc Biol*, 67:520–528.
- Zhang, L., Wang, W., Hayashi, Y., Jester, J., Birk, D., Gao, M., C.Y., L., Kao, W., Karin, M., and Xia, Y. (2003). A role for MEK kinase 1 in TGF-beta/activin-induced epithelium movement and embryonic eyelid closure. *EMBO J*, 22:4443–4454.



# 7

## General Discussion

Feline infectious peritonitis virus (FIPV) and feline enteric coronavirus (FECV) are two coronaviruses described in cats. FIPV and FECV are genetically very much alike; more than 98% of the genome is identical in FIPV and FECV isolates from the same environment (Vennema et al., 1995). Despite this genetic similarity, FIPV and FECV are biologically different. The main target cell of FECV is the enterocyte and although the infection is usually sub-clinical, FECV may cause mild to severe diarrhea, especially in young kittens (Pedersen et al., 1981). In contrast, FIPV has a main tropism for monocytes and causes a chronic and very often fatal pleuritis/peritonitis. It is currently unknown why these viruses manifest so differently.

### **FIPV infection**

In the past, *in vitro* studies on the interactions between FIPV and FECV and their host cells were mainly done in continuous cell lines. In these cells, FIPV and FECV replicate similarly, despite their huge pathological differences. There is no doubt that extrapolating results obtained from cell lines to the *in vivo* situation is not always justified. Therefore, the first part of this thesis consisted in investigating virus-host cell interaction using primary monocytes, the *in vivo* target cell of FIPV.

We found that the infectious power of FIPV was dependent on the origin of the host cells, so on the cat from which the monocytes were isolated (Chapter 2). Three infection patterns were observed. In the monocytes of one group of cats, FIPV infection was progressive; in a second group, monocytes were initially infected but the infection was not sustained and monocytes of a third group were not even susceptible to infection. The maximum infection rate in all cases was around 1%. It is possible that the small percentage of monocytes that can be infected represents a specific sub-population of the cells. A low infection rate was also observed in peritoneal macrophages (Stoddart and Scott, 1989).

In contrast, high percentages of infected cells could be reached in bone-marrow derived macrophages (Rottier et al., 2005). Although these monocytes and macrophages originated from the same progenitor cells, the latter have matured *in vitro* and not in a cat. It is likely that the absence of certain growth factors and/or immune mediators *in vitro* resulted in a different protein expression pattern. The fact that different cell types or the same cells from different cats result in different infection kinetics, indicate that specific cellular properties are needed to establish an infection. Identifying these cellular properties could render great prospects for FIP therapy and also for the selection of cats that are less sensitive for FIPV.

We hypothesize that the fact that 99% of inoculated monocytes remain uninfected, could be attributed to an adequate innate immune response by these cells. While in the cells that demonstrate an abortive infection, the immune response might have been weaker or triggered later. It is known that SARSV and MHV can efficiently evade this innate immune response, maybe FIPV is only successful in 1% of the cells. Investigating the strength and the onset of the interferon response during these different infection kinetics, might shed some light on these observations.

Another interesting observation was the fact that monocytes from some cats could not be infected at all, even though virus could enter those cells. Here too, the innate immune response could be the key factor. Resistance to feline coronavirus (FCoV) infection has also been suggested to occur in natural infections in the field (Addie and Jarret, 2001), and there are several reports of cats that remained seronegative after experimental inoculations with a lethal dose of FIPV (Weiss and Cox, 1989; McArdle et al., 1995; Scott et al., 1995; Poland et al., 1996). It would be most interesting to investigate the correlation between *in vitro* and *in vivo* resistance to FCoV since this opens perspectives for selection of cats insusceptible to FIP.

## **FECV infection**

Interaction of FECV with monocytes was also investigated. Even though the host cell of FECV is the enterocyte, there are reports on FECV making its way into the blood circulation. In several studies, healthy cats from FCoV endemic households were investigated (Herrewegh et al., 1995a, 1997; Gunn-Moore et al., 1998; Meli et al., 2004; Simons et al., 2005). In such households, where the FCoV was most likely FECV, a part of these healthy cats were viremic for FCoV. FCoV was detected both in plasma and in monocytes.

Our experiments showed that FECV could indeed infect monocytes but the infection was never sustained. Therefore, it may be hypothesized that, when

FECV reaches the blood circulation, the lack of sustainability and long-term production of progeny virus (total virus production was up to 100 times lower than in FIPV-infected monocytes) may be the reason for the absence of disease progress. This might form the basis for the pathological difference between FIPV and FECV. For many years now, researchers have been trying to pinpoint this difference to (a) mutation(s) in the genome. There seems to be a correlation between deletions in the 3c and 7b gene and the appearance of FIPV from FECV strains (Vennema et al., 1998). Unfortunately, the precise function of the 3c and 7b protein is not yet elucidated. It is known that the 7b gene is not required for replication in continuous cell lines and is easily lost in *in vitro* passages (Herrewegh et al., 1995b). However, all wild type FIPV strains possess a complete 7b gene which suggests that it provides an *in vivo* selective advantage. In addition, a FIPV mutant strain with a deleted 7ab ORF can no longer cause FIP after inoculation in cats (Haijema et al., 2004). These findings coincide with a role for the 7b protein in efficient monocyte infection, since FECV inoculation resulted in abortive infections in monocytes but not in a continuous cell line. So, it could be that 7b is required for efficient infection of monocytes. At least one additional factor must be involved in the difference between FIPV and FECV since there are some FECV strains (e.g. FECV UCD) that do contain a complete 7b gene (Herrewegh et al., 1995b). This might be a role for the 3c protein. It would be very interesting to investigate if these proteins could be linked to sustainability of infection in monocytes.

### **Evasion of the humoral immune response by FIPV**

Very little is known about the interactions of FIPV with the host immune system. Judging by the devastating development of a FIP infection in cats, the immune system cannot counter this virus during its destructive replication and invasion in spite of very high titers of FIPV-specific antibodies. There are indications that the immune system does even play an adverse role in the development of FIP. It has been reported in experimental infections that cats, which have obtained FIPV-specific antibodies actively or passively, develop FIP faster and more severely than naive cats (Pedersen and Boyle, 1980). This accelerated FIP has been the reason for the failure of most vaccination attempts (Woods and Pedersen, 1979; Pedersen and Black, 1983; Barlough et al., 1984, 1985; Vennema et al., 1990a; McArdle et al., 1992). A mechanism was proposed that could explain this accelerated development of FIP in the presence of antibodies: Antibody-Dependent Enhancement of Infectivity (ADEI) (Hohdatsu et al., 1991; Corapi et al., 1992; Olsen et al., 1992). ADEI suggests that antibodies might help to spread the virus in an infected cat by facilitating the virus uptake through the formation of virus-antibody complexes which are

taken up by uninfected monocytes/macrophages via the Fc-receptor. ADEI may explain why a larger number of cells can be infected in the presence of antibodies than in the absence of antibodies. However, ADEI has never been reported under field conditions but only in *in vitro* experiments with low concentrations of antibodies (Addie et al., 1995). Concentrations as high as the ones found in most FIP cats are neutralizing *in vitro*. Though, it could be that local antibody concentrations, e.g. in granulomas, are low enough to allow ADEI.

ADEI might be the reason why more monocytes are infected in seropositive animals, leading to a faster disease progression. Nevertheless, there is still no explanation why the immune system cannot eliminate the infected cells. In this thesis we propose two putative immune evasion mechanisms: retention and internalization of membrane-bound viral proteins.

**Retention** In Chapter 2, it was shown that about 50% of the infected monocytes express viral proteins on their plasma membrane. This means that in half of the infected monocytes, the proteins are efficiently retained inside the cell. Intracellular retention of viral proteins can be considered as an immune evasion process since it impedes antibody-dependent recognition of infected cells. Retention probably occurs in the ER-to-Golgi intermediate compartment (ER-GIC), the budding site of coronaviruses. Surprisingly, when S or M proteins are expressed separately, they will be transported to the plasma membrane or the Golgi, respectively (Opstelten et al., 1995). Co-expression is needed for proper localization of the proteins to the ERGIC. The SARSV S protein contains an KXHXX ER retrieval signal which seems to mediate these needed S-M interactions (McBride et al., 2007; Lontok et al., 2004). The ER retrieval motif allows recruitment of proteins from the post-ER compartments, such as the Golgi, back to the ER in COPI coated vesicles. However, this retrieval motif is not strong enough to retain the S protein completely and the majority of the S proteins in SARSV infected cells can still be found in the plasma membrane. The S protein of IBV contains the more potent KKXX, or dilysine, motif and is efficiently retained inside the cell (Lontok et al., 2004). The FIPV S and M protein both contain an KXHXX motif. It could be that FIPV infected monocytes show partial membrane expression because these motifs are not strong enough. The M protein actually contains another putative retention signal in its cytoplasmic tail: LVXXXL. This ER retention motif was discovered in the core protein of hepatitis C virus (Okamoto et al., 2004). It would be interesting to investigate which motif is important for retention in the ERGIC and if these KXHXX motifs also mediate S-M interactions in FIPV infected monocytes.

**Internalization** Even if a retention signal is potent, viral proteins might still be found in the plasma membrane when expression levels are so high that the retrieval machinery is saturated (Lontok et al., 2004). The second immune evasion mechanism deals with the monocytes that do express viral proteins on their plasma membrane. To ensure further protection from antibody-dependent cell lysis, these proteins need to be internalized. As with ADEI, FIPV will use the omnipresent antibodies to its own advantage. We found that, when antibodies are present in the culture medium, they will bind to the viral proteins expressed in the plasma membrane of the infected monocytes. This leads to rapid internalization of the formed antibody-antigen complexes (Chapter 3). This immune evasion mechanism leaves the monocytes cleared from visually detectable antigens, possibly providing protection against antibody-mediated cell lysis. A similar immune evasion strategy has been described in pseudorabies virus (PrV) infected pig monocytes (Favoreel et al., 1999). For PrV infected pig monocytes, cells with internalized viral glycoproteins are indeed protected against antibody-dependent complement mediated cell lysis (Van de Walle et al., 2003). Whether this is also true for a FIPV-infected monocyte, is currently under investigation. There are indications that retention and/ or internalization occur *in vivo*, since no surface expression could be observed on FIPV-infected monocytes isolated from naturally infected cats (Cornelissen et al., 2007).

In order to internalize a surface expressed viral protein, an internalization motif must be present in its cytoplasmic tail (or in the tail of an associated protein). Both the S and the M protein of FIPV contain such sequences. In the tail of the S protein a dileucine and an YXX $\Psi$  internalization motif are found. The M protein contains 2 dileucine and 2 YXX $\Psi$  internalization motifs. These sequences are binding site for the adapter protein-2 (AP-2) complex during clathrin-mediated internalization. However, since internalization of the S and M protein occurs independently of clathrin (see below or Chapter 4), it remains to be elucidated how (and even if) these motifs are functional. In clathrin-mediated internalization, some alternative adapter proteins, such as Dab-2, have been identified that lead to AP-2 independent clathrin-mediated internalization (Benmerah and Lamaze, 2007). It is tempting to speculate that the internalization motifs in the S and M protein can also be recognized by other adapter proteins that will mediate this specific independent internalization pathway. There is also the possibility that the YXX $\Psi$  motifs are not internalization motifs. It has been described for a SARSV specific protein, named U274, that a YXX $\Psi$  motif in its tail is required for efficient transportation to the plasma membrane (Tan et al., 2004). Point mutation analysis of these motif in the S and M protein could answer these questions.

In the philosophy that viruses do nothing that is not (at least partially) bene-

ficial to them, one wonders why FIPV allows viral proteins to be expressed at the plasma membrane and has developed an additional mechanism to remove those proteins from the moment they could be harmful. The most logical reason would be to enable cell-to-cell spread. Maybe the S protein can tether other (uninfected) monocytes by binding onto its receptor on the other monocyte, thereby facilitating infection. It could also be that it plays a role in adhesion of infected monocytes on endothelial cells or in the subsequent emigration to target organs. Another hypothesis is that internalization activates a signaling cascade, resulting in an altered cellular status that might be beneficial for the virus (e.g. enhanced protein production and thus more progeny virus assembly).

### **Internalization of surface expressed viral proteins**

The remainder of the thesis was dedicated to elucidating through which pathway the antigen-antibody complexes are internalized, the regulation of the pathway and subsequent intracellular trafficking. The used techniques were mainly based on immunofluorescence and confocal microscopy. Considering the fact that the *in vitro* infection rate of monocytes varies between 0,1 and 1%, of which around 50% have membrane expression, experiments that require a lot of starting material (e.g. flowcytometry or western blots) could not be performed. In addition, we were restricted to monocytes to perform our experiments since internalization could not be induced in CrFK or fcwf cell lines (Dewerchin et al., 2006). On the other hand, the fact that all experiments were performed with monocytes makes the results more relevant for the *in vivo* situation.

We have found that antibody-induced internalization occurred through a new clathrin- and caveolae-independent internalization pathway that was also independent from dynamin, rafts and rho-GTPases (Chapter 4). Internalization was strongly inhibited by staurosporine, a serine/threonine kinase inhibitor. The serine/threonine kinases that were found to play a role in one or more steps of the internalization process were myosin light chain kinase (MLCK) and mitogen-activated protein kinases (MAPKs) while protein kinase A, C and G and Ca/calmodulin dependent protein kinase II were not required (Chapter 6). It cannot be excluded that other serine/threonine kinases are important as well. An interesting candidate is p21-activated kinase (PAK) since it can phosphorylate MLCK, leading to its inactivation (reviewed in Bokoch (2003)). More importantly, PAK can also activate myo1 and myo6, which are both implicated in the internalization process.

The 3 MAPK signaling cascades play a role not only during the internaliza-

tion process itself, but probably also during intracellular trafficking. ERK, p38 and JNK do not interact with the surface expressed viral proteins directly since none of the possible binding motifs were found in the cytoplasmic tails of the S or M proteins. So they must exert their activity during internalization through their downstream targets, which have not yet been identified. Interestingly, many of those targets will lead to actin or microtubule remodeling. Stainings with phospho-specific antibodies showed that activated ERK, p38 and JNK co-localized with antigen-antibody complexes as soon as internalization started, thus when actin remodeling is required to allow passage of the vesicles through the cortical actin network. JNK has been reported to suppress actin filament formation and even to disrupt stress fibers (Rennefahrt et al., 2002; Zhang et al., 2003) and could play a similar role here. The observation that activated p38 co-localized with surface expressed viral proteins before and only shortly after the internalization started and then again after 10 minutes, when the vesicles were fully internalized, strongly suggests that p38 plays (at least) 2 distinct roles in the internalization process. The fact that p38 negatively regulated the internalization and that it was associated with viral proteins before the internalization process started, indicates that active p38 is required for maintaining the viral proteins in the plasma membrane. This implicates that expressing viral proteins in the plasma membrane offers a real advantage to the virus. It remains to be elucidated what the advantage is. ERK can phosphorylate MLCK which was shown to be required in the first steps of other internalization processes as well (Klemke et al., 1997; Mansfield et al., 2000). However, it is unlikely that this is the (only) role for ERK in the internalization process studied here, since the experiments suggested that ERK regulates the internalization negatively while MLCK was clearly a positive regulator. Activated ERK remained associated with internalizing vesicles during intracellular transport and thus might play an (additional) role there. ERK might activate the MAPK-activated protein kinase 2/3 (MAPKAPK 2/3). Phosphorylating of MAPKAPK 2/3 leads to the activation of HSP27 which promotes stress fiber formation (Hedges et al., 1999; Rousseau et al., 1997). Stress fiber formation does indeed occur during intracellular trafficking of the antigen-antibody complexes since stainings revealed that internalizing vesicles were decorated with short actin tails. It would be very interesting to investigate which downstream targets of the MAPKs are activated during internalization and/ or trafficking and when they play a role.

MAPK activation during viral infections in general is well documented but is mainly thought to modulate the host immune responses. However, MAPKs could be important to ensure successful infection since the 3 main MAPK signaling cascades can lead to cytoskeleton rearrangements (reviewed in Huang et al. (2004)). It would be interesting to investigate a possible role for MAPKs

in intracellular transportation of both entering viruses and progeny virus that needs transportation to the plasma membrane. Also virus-induced cytoskeleton changes that are often observed during infection could be regulated by MAPKs. There are many reports of MAPK activation during coronavirus infection and some of them mention cytoskeleton changes. In SARS patients, an increase in p38 levels was reported (Lee et al., 2004). Infection of COS-1 cells by SARSV led to an up-regulation of p38, resulting in activation of heat shock protein 27 (HSP27) and actin reorganization (Surjit et al., 2004). Both the nucleocapsid protein and 7a protein were found to activate p38 (Surjit et al., 2004; Kopecky-Bromberg et al., 2006). p38 was also up-regulated in Vero E6 cells and the downstream targets, MAPKAPK2, HSP27, c-AMP response element-binding protein (CREB) and the translation initiation factor eIF4E were activated (Mizutani et al., 2004). Activation of eIF4E would promote virus-specific protein synthesis and subsequent progeny virus production (Banerjee et al., 2002). Also ERK was found to be involved in viral RNA synthesis of mouse hepatitis virus (Cai et al., 2007).

For future experiments, we are planning to bring the S and M protein into a lentiviral expression system. Transduction of the S and M protein will lead to expression in a much higher percentage of monocytes compared to normal infection. This would enable the use of techniques that require a lot of material like western blots. With these techniques we can demonstrate more robustly the activation of the different signaling molecules (like ERK, p38, JNK...) and investigate which downstream targets are activated.

### **Myosins and internalization of surface expressed viral proteins**

During the internalization of surface expressed antigens in FIPV infected monocytes, myo1 and myo6 are recruited to the internalizing vesicles while myo2a, 2b, 5a, 7a, 9b and 10 are not involved in internalization nor trafficking. All myosins contain a head or motor domain, a light chain binding neck domain for its regulation and a tail domain. In humans, 8 isoforms of Class I myosins have been described, two of which are long-tailed: myo1E and myo1F. The tail domain of myo1 contains a membrane binding tail homology (TH)-1 domain, which binds myo1 to its cargo. Long tailed isoforms contain an additional TH-2, which binds F-actin and Src homology (SH)-3 domain, which enables protein-protein interactions. Yeast myo1 also contains an acidic domain that binds directly to the Arp2/3 complex, through which myo1 can promote actin nucleation (Evangelista et al., 2000). The Arp2/3 complex has indeed been associated with endosome movement in *Xenopus* and it is found in the actin comet tails of some intracellular bacterial pathogens like *Listeria monocytogenes* and *Vaccinia virus* (Taunton et al., 2000; Fehrenbacher et al., 2003). This



is interesting since myo1 and actin tails were observed on internalizing vesicles in the internalization process studied here. However, mammalian myo1 isoforms do not contain such an acidic domain. It has been suggested though, that a mammalian long isoform of myo1 can indirectly link to the Arp2/3 complex through binding of nucleation promoting factors such as Wiscott Aldrich syndrome protein (WASP) with its SH3 domain. Evidence for a similar link has been found in amoeba where myo1 recruits Arp2/3 via the adapter protein CARMIL (Soldati, 2003). Another noteworthy feature of the long tailed myo1 isoform is that they contain 2 actin binding sites. This enables myo1 to slide actin tails relatively to one another while anchored to a membrane. This feature would facilitate enormously actin reorganizations, such as formation of an actin corridor. Taking the special characteristics of long tailed myo1 isoforms together, it is tempting to speculate that (one of) these isoforms are recruited during the internalization process studied here.

Myo1 is known to be important during the first steps of several internalization processes (reviewed in Soldati and Schliwa (2006)). However, there are few reports of a possible role for myo1 during intracellular trafficking. In hepatoma cells, myo1B would play a role in orienting endosomes during their transport over microtubules (Raposo et al., 1999; Cordonnier et al., 2001). However, no actin tails were observed in those experiments and myo1 was suggested to function as a motor protein on actin filaments. It cannot be excluded that in the internalization of FIPV antigen-antibody complexes, myo1 would have a similar function, nevertheless, the presence of actin tails during internalization strongly suggests that intracellular trafficking of the vesicles is regulated differently. It could be that more than one myo1 isoforms cooperate during the different steps in internalization and intracellular trafficking. Isoform specific antibodies or dominant negative mutants could answer this question.

The other myosin that played a role during the internalization process is myo6. Co-localization of myo6 with the internalizing vesicles was only observed briefly, within the first minute of internalization. The most obvious role for myo6 is guiding the vesicles through the cortical actin network, as has been described in non-polarized epithelial cells (Aschenbrenner et al., 2003, 2004). Additionally, myo6 might mediate track switching from actin to microtubules. It has been shown that the *Drosophila* homologue of myo6 binds to the homologue of CLIP-170, a protein that links endocytic vesicles to microtubules (Lantz and Miller, 1998). CLIP-170 is thought to form a complex with dynactin and dynein, which suggests that vesicles can be transferred from CLIP-170 to dynein for further transport along the microtubules (Vaughan et al., 1999). It would be interesting to investigate whether myo6 can mediate this track switch in mammalian cells as well. Myo6 could also perform a third, more hypothetical role in the early steps of internalization. It is known that

myo6 can bind the alternative adapter proteins: Disabled-2 (Dab-2), GAIP-interacting protein-C-terminus (GIPC) (GAIP is a GTPase activating protein) and synapse-associated protein 97 (SAP97) (Hasson, 2003). Dab-2 is of special interest because it has been implicated in the recruitment of myo6 to clathrin coated pits. However, both Dab-2 and myo6 can be found in a different, shorter splicing isoform. These shorter isoforms are not recruited to clathrin coated pits but still associate with each other. It would be very interesting to investigate if this shorter isoform of Dab-2 could lead to targeting of myo6 to clathrin-independent internalization structures before the actual pinching off of the vesicles. This would imply a role in e.g. membrane remodeling or the fission process.

Co-immunoprecipitation experiments can yield a lot of information about the binding partners during internalization. This could quickly lead to a much better characterization of this new internalization pathway. The fact that continuous cell lines do not support this internalization pathway and that FIPV only infects about 1% of inoculated monocytes, has greatly hampered this research. However, expressing S and M proteins in monocytes via a lentiviral based transduction system will open many new avenues leading to better understanding of this enigmatic internalization route.

### **Model of the internalization process**

A schematic representation of the internalization process combining all results is given in Figure 7.1. Before antibodies are added, the viral proteins that are expressed in the plasma membrane are associated with myo1 and activated p38. Myo1 might function as an anchor, connecting the viral proteins to the underlying cortical actin network. p38 might (help to) regulate the cortical actin network. When antibodies bind to the viral proteins, internalization starts immediately. The signaling cascade leading to internalization does not consist of phosphatases, tyrosine kinases, rho-GTPases, protein kinase A, C nor G. It does require myosin light chain kinase (MLCK) and the mitogen activated protein kinases (MAPKs) ERK, p38 and JNK. When internalization starts, myo1 relocates as it appears to be localized between the internalizing structure and the plasma membrane. This suggests that myo1 might be important for membrane remodeling. Activated p38 is still associated with the forming vesicle and activated ERK and JNK are recruited. The precise function of these MAPKs remains to be elucidated but p-p38 and p-JNK might mediate actin breakdown and reorganization, possible together with myo1, to form a corridor through the cortical actin barrier. Between 30 seconds and 1 minute post antibody addition, the internalizing viral proteins co-localize with the early endosome marker, indicating that the vesicles have already pinched

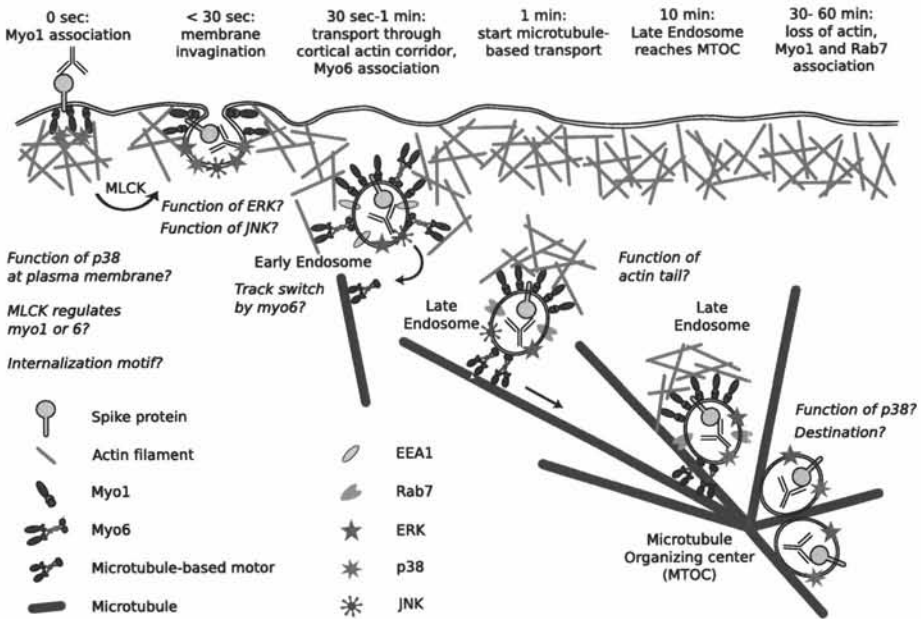


Figure 7.1: Model of the internalization process with remaining questions.

off from the plasma membrane. At this time, myo6 is recruited, probably to guide the vesicle through the cortical actin (in cooperation with myo1) and possibly to subsequently mediate the track switch to microtubules. Association with activated p38 is lost but p-ERK and p-JNK association remains. These might regulate the formation of the actin tail by promoting (ERK) and suppressing (JNK) actin assembly. Also myo1 may play a role in controlling actin filament formation. At 1 minute after antibody addition, the antigen-antibody complexes are already found in late endosomes and start their transportation over the microtubules. Myo6 does no longer co-localize while myo1, ERK and JNK remain associated. The actin tails are now fully formed. At 10 minutes post antibody addition, the antigen-antibody complexes still reside in late endosomes and microtubule organizing center (MTOC) is reached. JNK dissociates from the vesicles while p38 reassociates. Between 30 and 60 minutes after the initiation of the internalization process, the vesicles are still found at the MTOC, though they do not longer co-localize with the late endosome marker. Myo1 and the actin tails disappear. Activated p38 and ERK remain associated with the vesicles until at least 60 minutes, but their possible function is yet unknown. It also remains to be determined whether MLCK regulates myo1 or myo6.

## **FIP pathogenesis, approaches for treatment and open questions**

To conclude, the following hypothetical model may aid in explaining the FIP pathogenesis. In a FIPV infected cat, part of the FIPV-infected monocytes remain immune-masked because no viral antigens are expressed at the plasma membrane while part of the cells do express viral proteins. When antibodies bind to these membrane-bound proteins to mark the infected cells for cell lysis, internalization is triggered. The plasma membrane is cleared from viral proteins and the infected cell remains invisible for the humoral immune system. In this way, the cell is able to continue the production of progeny virus without being eliminated or it may enter a quiescent infection state, as is seen in PrV infected monocytes that were cultured in the presence of specific antibodies (Favoreel et al., 2003). This quiescent infection state would be an excellent cover for a carrier cell and might explain the sometimes long incubation period of a FIP infection. The fact that antibodies have no, or even an adverse, effect on FIPV-infected cells, puts vaccination attempts into a new light. There is no use in building up a humoral immune response if it offers no answer to a FIPV infection. However, there are some alternative paths worth exploring.

- It could be that binding of antibodies to particular regions of the S protein does not lead to internalization if binding does not elicit the needed conformational changes in the S protein that exposes the internalization motif(s). Vaccination of cats with only this region of the S protein could enable antibody-dependent cell lysis. However, once a cat is infected, it is only a matter of time before internalizing antibodies are produced since these will undoubtedly be targeted to the strongest immunogenic sites. The balance between the protecting and the immune evasion eliciting antibodies might be decisive for the vaccine efficacy.
- The fast internalization could be used for administering antibodies that are tagged with toxins which, once internalized, would lead to the death of the infected cell. This system has the advantage of great specificity since only the infected cells are targeted. However, the fact that FIP is normally diagnosed quite late, so when there is already a strong humoral immune response could render this “therapy” useless. It would be unlikely that these toxic antibodies can still find an infected monocyte that has not already internalized its surface expressed viral proteins. This approach could be interesting to use preemptively in catteries where a FIPV outbreak is starting.
- Another possible approach is to treat an infected cat with one or a combination of the chemicals that could block internalization. This will allow

the cats immune system to identify and eliminate infected cells. Unfortunately, since all the active compounds were kinase inhibitors, a lot of side-effects can be expected when these chemical are administered to a cat. More research is needed to find specific inhibitors in order to minimize the side-effects.

- A completely different approach would be to selectively breed with FIPV resistant cats. In order to easily do this, a link between *in vivo* and *in vitro* resistance needs to be established first.

## References

- Addie, D. and Jarret, O. (2001). Use of a reverse-transcriptase polymerase chain reaction for monitoring the shedding of feline coronavirus by healthy cats. *Vet Rec*, 148:649–653.
- Addie, D., Toth, S., Murray, G., and Jarret, O. (1995). Risk of feline infectious peritonitis in cats naturally infected with feline coronavirus. *Am J Vet Res*, 56:429–434.
- Aschenbrenner, L., Lee, T., and Hasson, T. (2003). Myo6 facilitates the translocation of endocytic vesicles from cell peripheries. *Mol Biol Cell*, 14:2728–2743.
- Aschenbrenner, L., Naccache, S., and Hasson, T. (2004). Uncoated endocytic vesicles require the unconventional myosin, myo6, for rapid transport through actin barriers. *Mol Biol Cell*, 15:2253–2263.
- Banerjee, S., Narayanan, K., Mizutani, T., and Makino, S. (2002). Murine coronavirus replication-induced p38 mitogen-activated protein kinase activation promotes interleukin-6 production and virus replication in cultured cells. *J Virol*, 76:5937–5948.
- Barlough, J., Johnson-Lussenburg, C., Stoddart, C., Jacobson, R., and Scott, F. (1985). Experimental inoculation of cats with human coronavirus 229E and subsequent challenge with feline infectious peritonitis virus. *Can J Comp Med*, 49:303–307.
- Barlough, J., Stoddart, C., Sorresso, G., Jacobson, R., and Scott, F. (1984). Experimental inoculation of cats with canine coronavirus and subsequent challenge with feline infectious peritonitis virus. *Lab Anim Sci*, 34:592–597.

- Benmerah, A. and Lamaze, C. (2007). Clathrin-coated pits: vive la difference? *Traffic*, 8:970–982.
- Bokoch, G. (2003). Biology of the p21-activated kinases. *Annu Rev Biochem*, 72:734–781.
- Cai, Y., Liu, Y., and Zhang, X. (2007). Suppression of coronavirus replication by inhibition of the mek signaling pathway. *J Virol*, 81:446–456.
- Corapi, W., Olsen, C., and Scott, F. (1992). Monoclonal antibody analysis of neutralization and antibody-dependent enhancement of feline infectious peritonitis virus. *J Virol*, 11:6695–6705.
- Cordonnier, M.-N., Dauzonne, D., Louvard, D., and Coudrier, E. (2001). Actin filaments and myosin I alpha cooperate with microtubules for the movement of lysosomes. *Mol Biol Cell*, 12:4013–4029.
- Cornelissen, E., Dewerchin, H., Van Hamme, E., and Nauwynck, H. (2007). Absence of surface expression of feline infectious peritonitis virus (FIPV) antigens on infected cells isolated from cats with FIP. *Vet Microbiol*, 121:131–137.
- Dewerchin, H., Cornelissen, E., and Nauwynck, H. (2006). Feline infectious peritonitis virus-infected monocytes internalize viral membrane-bound proteins upon antibody addition. *J Gen Virol*, 87:1685–1690.
- Evangelista, M., Klebl, B., Tong, A., Webb, B., Leeuw, T., Leberer, E., White-way, M., Thomas, D., and Boone, C. (2000). A role for Myosin-I in actin assembly through interactions with Vrp1p, Bee1p, and the Arp2/3 complex. *J Cell Biol*, 148:353–362.
- Favoreel, H., Nauwynck, H., Halewyck, H., Van Oostveldt, P., Mettenleiter, T., and Pensaert, M. (1999). Antibody-induced endocytosis of viral glycoproteins and major histocompatibility complex class I on pseudorabies virus-infected monocytes. *J Gen Virol*, 80(5):1283–1291.
- Favoreel, H., Van de Walle, G., Nauwynck, H., Mettenleiter, T., and Pensaert, M. (2003). Pseudorabies virus (PRV)-specific antibodies suppress intracellular viral protein levels in PRV-infected monocytes. *J Gen Virol*, 84(11):2969–2973.
- Fehrenbacher, K., Boldogh, I., and Pon, L. (2003). Taking the a-train: actin-based force generators and organelle targeting. *Trends Cell Biol*, 13:472–477.

- Gunn-Moore, D., Gruffydd-Jones, T., and Harbour, D. (1998). Detection of feline coronaviruses by culture and reverse transcriptase-polymerase chain reaction of blood samples from healthy cats and cats with clinical feline infectious peritonitis. *Vet Microbiol*, 62:193–205.
- Haijema, B., Volders, H., and Rottier, P. (2004). Live, attenuated coronavirus vaccines through the directed deletion of group-specific genes provide protection against feline infectious peritonitis. *J Virol*, 78:3863–3871.
- Hasson, T. (2003). Myosin VI: two distinct roles in endocytosis. *J Cell Sci*, 116:3453–3461.
- Hedges, J., Dechert, M., Yamboliev, I., Martin, J., Hickey, E., L.A., W., and Gerthoffer, W. (1999). A role for p38(MAPK)/HSP27 pathway in smooth muscle cell migration. *J Biol Chem*, 274:24211–24219.
- Herrewegh, A., de Groot, R., Cepica, A., Egberink, H., Horzinek, M., and Rottier, P. (1995a). Detection of feline coronavirus RNA in feces, tissues, and body fluids of naturally infected cats by reverse transcriptase PCR. *Clin Microbiol*, 33:684–689.
- Herrewegh, A., Mahler, M., Hedrich, H., Haagmans, B., Egberink, H., Horzinek, M., Rottier, P., and de Groot, R. (1997). Persistence and evolution of feline coronavirus in a closed cat-breeding colony. *Virology*, 234:349–363.
- Herrewegh, A., Vennema, H., Horzinek, M., Rottier, P., and de Groot, R. (1995b). The molecular genetics of feline coronaviruses: comparative sequence analysis of the ORF7a/7b transcription unit of different biotypes. *Virology*, 212:622–631.
- Hohdatsu, T., Nakamura, M., Ishizuka, Y., Yamada, H., and Koyama, H. (1991). A study on the mechanism of antibody-dependent enhancement of feline infectious peritonitis virus infection in feline macrophages by monoclonal antibodies. *Arch Virol*, 120:207–217.
- Huang, C., Jacobson, K., and Schaller, M. (2004). MAP kinases and cell migration. *J Cell Sci*, 117:4619–4628.
- Klemke, R., Cai, S., Giannini, A., Gallagher, P., deLanerolle, P., and Cheresch, D. (1997). Regulation of cell motility by mitogen-activated protein kinase. *J Cell Biol*, 137:481–492.
- Kopecky-Bromberg, S., Martinez-Sobrido, L., and Palese, P. (2006). 7a protein of severe acute respiratory syndrome coronavirus inhibits cellular pro-

- tein synthesis and activates p38 mitogen-activated protein kinase. *J Virol*, 80:785–793.
- Lantz, V. and Miller, K. (1998). A class VI unconventional myosin is associated with a homologue of a microtubule-binding protein, cytoplasmic linker protein-170, in neurons and at the posterior pole of *Drosophila* embryos. *J Cell Biol*, 140:897–910.
- Lee, C.-H., Chen, R.-F., Liu, J.-W., Yeh, W.-T., Chang, J.-C., Liu, P.-M., Eng, H.-L., Lin, M.-C., and Yang, K. (2004). Altered p38 mitogen-activated protein kinase expression in different leukocytes with increment of immunosuppressive mediators in patients with severe acute respiratory syndrome. *J Immunol*, 172:7841–7847.
- Lontok, E., Corse, E., and Machamer, C. (2004). Intracellular targeting signals contribute to localization of coronavirus spike proteins near the virus assembly site. *J Virol*, 78:5913–5922.
- Mansfield, P., Shayman, J., and Boxer, L. (2000). Regulation of polymorphonuclear leukocyte phagocytosis by myosin light chain kinase after activation of mitogen-activated protein kinase. *Blood*, 95:2407–2412.
- McArdle, F., Bennet, M., Gaskell, R., Tennant, B., Kelly, D., and Gaskell, C. (1992). Induction and enhancement of feline infectious peritonitis by canine coronavirus. *Am J Vet Res*, 53:1500–1506.
- McArdle, F., Tennant, B., Bennett, M., Kelly, D., Gaskell, C., and Gaskell, R. (1995). Independent evaluation of a modified live FIPV vaccine under experimental conditions (University of Liverpool experience). *Feline Pract*, 23 (3):67–71.
- McBride, C., Li, J., and Machamer, C. (2007). The cytoplasmic tail of the severe acute respiratory syndrome coronavirus spike protein contains a novel endoplasmic reticulum retrieval signal that binds COPI and promotes interaction with membrane protein. *J Virol*, 81:2418–2428.
- Meli, M., Kipar, A., Muller, C., Jenal, K., Gonczi, E., Borel, N., Gunn-Moore, D., Chalmers, S., Lin, F., Reinacher, M., and Lutz, H. (2004). High viral loads despite absence of clinical and pathological findings in cats experimentally infected with feline coronavirus (FCoV) type I and in naturally FCoV-infected cats. *J Feline Med Surg*, 6:69–81.
- Mizutani, T., Fukushi, S., Saijo, M., Kurane, I., and Morikawa, S. (2004). Phosphorylation of p38 mapk and its downstream targets in sars coronavirus-infected cells. *Biochem Biophys Res Commun*, 319:1228–1234.



- Okamoto, K., Moriishi, K., Miyamura, T., and Matsuura, Y. (2004). Intramembrane proteolysis and endoplasmic reticulum retention of hepatitis C virus core protein. *J Virol*, 78:6370–6380.
- Olsen, C., Corapi, W., Ngichabe, C., Baines, J., and Scott, F. (1992). Monoclonal antibodies to the spike protein of feline infectious peritonitis virus mediate antibody-dependent enhancement of infection of feline macrophages. *J Virol*, 66:956–965.
- Opstelten, D.-J., Raamsman, M., Wolfs, K., Horzinek, M., and Rottier, P. (1995). Envelope glycoprotein interactions in coronavirus assembly. *J Cell Biol*, 131:339–349.
- Pedersen, N. and Black, J. (1983). Attempted immunization of cats against feline infectious peritonitis using either avirulent virus or sublethal amounts of virulent virus. *Am J Vet Res*, 44:229–234.
- Pedersen, N. and Boyle, J. (1980). Immunologic phenomena in the effusive form of feline infectious peritonitis. *Am J Vet Res*, 41:868–876.
- Pedersen, N., Boyle, J., Floyd, K., Fudge, A., and Barker, J. (1981). An enteric coronavirus infection of cats and its relationship to feline infectious peritonitis. *Am J Vet Res*, 42:368–376.
- Poland, A., Vennema, H., Foley, J., and Pedersen, N. (1996). Two related strains of feline infectious peritonitis virus isolated from immunocompromised cats infected with a feline enteric coronavirus. *J clin microbiol*, 34:3180–3184.
- Raposo, G., Cordonnier, M.-N., Tenza, D., Menichi, B., Durbach, A., Louvard, D., and Coudrier, E. (1999). Association of myosin I alpha with endosomes and lysosomes in mammalian cells. *Mol Biol Cell*, 10:1477–1494.
- Rennefahrt, U., Illert, B., Kerkhoff, E., Troppmair, J., and Rapp, U. (2002). Constitutive JNK activation in NIH 3T3 fibroblasts induces a partially transformed phenotype. *J Biol Chem*, 277:29510–29518.
- Rottier, P., Nakamura, K., Schellen, P., Volders, H., and Haijema, B. (2005). Acquisition of macrophage tropism during pathogenesis of feline infectious peritonitis is determined by mutations in the feline coronavirus spike protein. *J Virol*, 79:14122–14130.
- Rousseau, S., Houle, F., Landry, J., and Huot, J. (1997). p38 MAP kinase activation by vascular endothelial growth factor mediates actin reorganization and cell migration in human endothelial cells. *Oncogene*, 15:2169–2177.

- Scott, F., Wayne, V., and Olsen, C. (1995). Independent evaluation of a modified live FIPV vaccine under experimental conditions (Cornell experience). *Feline Pract*, 23 (3):74–76.
- Simons, F., Vennema, H., Rofina, J., Pol, J., Horzinek, M., Rottier, P., and Egberink, H. (2005). A mRNA PCR for the diagnosis of feline infectious peritonitis. *J Virol Methods*, 124:111–116.
- Soldati, T. (2003). Unconventional myosins, actin dynamics and endocytosis: a menage a trois? *Traffic*, 4:358–366.
- Soldati, T. and Schliwa, M. (2006). Powering membrane traffic in endocytosis and recycling. *Nature Rev Mol Cell Biol*, 7:897–908.
- Stoddart, M. and Scott, F. (1989). Intrinsic resistance of feline infectious peritoneal macrophages to coronavirus infection correlates with in vivo virulence. *J Virol*, 63:436–440.
- Surjit, M., Liu, B., Jameel, S., Chow, V., and Lal, S. (2004). The SARS coronavirus nucleocapsid protein induces actin reorganization and apoptosis in cos-1 cells in the absence of growth factors. *Biochem J*, 383:13–18.
- Tan, Y.-J., Teng, E., Shen, S., Tan, T., Goh, P.-Y., Fielding, B., Ooi, E.-E., Tan, H., Lim, S., and Hong, W. (2004). A novel severe acute respiratory syndrome coronavirus protein, U274, is transported to the cell surface and undergoes endocytosis. *J Virol*, 78:6723–6734.
- Taunton, J., Rowling, B., Coughlin, M., Wu, M., Moon, R., Mitchison, T., and Larabell, C. (2000). Actin-dependent propulsion of endosomes and lysosomes by recruitment of N-WASP. *J Cell Biol*, 148:519–530.
- Van de Walle, G., Favoreel, H., Nauwynck, H., and Pensaert, M. (2003). Antibody-induced internalization of viral glycoproteins and gE-gI Fc receptor activity protect pseudorabies virus-infected monocytes from efficient complement-mediated lysis. *J Gen Virol*, 84(4):939–947.
- Vaughan, K., Tynan, S., Faulkner, N., Echeverri, C., and Vallee, R. (1999). Colocalization of cytoplasmic dynein with dynactin and CLIP-170 at microtubule distal ends. *J Cell Sci*, 112:1437–1447.
- Vennema, H., de Groot, R., Harbour, D., Dalderup, M., Gruffydd-Jones, T., Horzinek, M., and Spaan, W. (1990a). Early death after feline infectious peritonitis challenge due to recombinant vaccinia virus immunization. *J Virol*, 64:1407–1409.

- Vennema, H., Poland, A., Floyd Hawkins, K., and Pedersen, N. (1995). A comparison of the genomes of FECVs and FIPVs: what they tell us about the relationships between feline coronaviruses and their evolution. *Feline Pract*, 23:40–44.
- Vennema, H., Poland, A., Foley, J., and Pedersen, N. (1998). Feline infectious peritonitis viruses arise by mutation from endemic feline enteric coronaviruses. *Virology*, 243:150–157.
- Weiss, R. and Cox, N. (1989). Evaluation of immunity to feline infectious peritonitis in cats with cutaneous viral-induced delayed hypersensitivity. *Vet Immunol Immunopathol*, 21:293–309.
- Woods, R. and Pedersen, N. (1979). Cross-protection studies between feline infectious peritonitis and porcine transmissible gastroenteritis viruses. *Vet Microbiol*, 4:11–16.
- Zhang, L., Wang, W., Hayashi, Y., Jester, J., Birk, D., Gao, M., C.Y., L., Kao, W., Karin, M., and Xia, Y. (2003). A role for MEK kinase 1 in TGF-beta/activin-induced epithelium movement and embryonic eyelid closure. *EMBO J*, 22:4443–4454.



## Summary

Two closely related coronaviruses are described in cats: feline enteric coronavirus, or FECV and feline infectious peritonitis virus, or FIPV. FECV is endemic in cat populations. Most infections pass by unnoticed but occasionally FECV mutates to its highly virulent counterpart: FIPV. Infection with FIPV causes chronic, mostly fatal peritonitis/vasculitis. After decades of research, it is still unknown how FIPV causes such a fulminating disease and why the cats immune system can rarely overcome an infection. Although the interaction of FIPV with the host immune system is poorly understood, it is clear that FIPV must have one or more immune evasion mechanisms at its disposal.

Therefore, the aims of this doctoral research were (1) to examine the virus-host cell interactions of FIPV (and FECV) with the *in vivo* target and carrier cell of FIPV, the feline blood monocyte and (2) to find and (3) characterize (a) putative immune evasion mechanism(s).

In Chapter 1, an introduction is given on the feline coronaviruses, their relation, structure, replication cycle and pathogenesis. Additionally, an overview of immune evasion mechanisms used by coronaviruses is given.

In Chapter 2, infection kinetics of FIPV (strain 79-1146) in peripheral blood monocytes were determined. It was the first time that FIPV replication was studied in its *in vivo* target and carrier cell, the monocyte. Both titers and antigen expression were examined. Surprisingly, the infection kinetics differed depending on the cat from which the monocytes were isolated. Three infection patterns were observed. In the monocytes of one group of cats, FIPV infection was progressive; in a second group, monocytes were initially infected but the infection was not sustained and monocytes of a third group were not susceptible to infection. The maximum infection rate was around 1%. The infection kinetics of FECV (strain 79-1683) were also studied. An FECV infection in monocytes was never sustained and viral production was up to 100 times lower than in FIPV-infected monocytes. The lack of sustainability and long-term production of progeny virus may be the reason for the absence of

disease progress in an *in vivo* FECV infection. This might form the basis for the pathological difference between FIPV and FECV. The infection kinetics in monocytes were also compared to those in Crandell feline kidney (CrFK) cells, a feline continuous cell line that is often used in FIPV and FECV research. In CrFK cells, FIPV and FECV replicated identically (but differently than in monocytes). It is clear that CrFK cells are not suited for studying virus-host cell interaction of FIPV or FECV. Therefore only monocytes were used in the remainder of the thesis. Another important observation was that about 50% of the FIPV- (and FECV-)infected monocytes expressed viral proteins in their plasma membrane. This means that the other half of the infected monocyte efficiently retained the proteins inside the cell. Intracellular retention may be an immune evasion process as it can impede antibody-dependent recognition of infected cells.

In Chapter 3, it was investigated what happens to the 50% of infected monocytes that do express viral proteins in their plasma membrane. In order to study the effect of the humoral immune response on infected monocytes, the *in vivo* situation was mimicked by cultivating infected monocytes in the presence of antibodies. As expected, these antibodies did bind to the surface expressed viral antigens. However, the formed antigen-antibody complexes were internalized into the monocyte through a highly efficient and fast process, leaving the plasma membrane cleared from visually detectable antigens. Already at 3 minutes post antibody addition,  $89 \pm 9\%$  of the infected monocytes were internalizing their membrane expressed viral proteins. This antibody-induced internalization process might explain why the humoral immune response is not effective against a FIPV infection and is thus a putative immune evasion process. Further investigation revealed that internalization was also induced by monoclonal antibodies against the S and the M protein, though to a somewhat lesser extent, suggesting that both proteins play a role in the internalization process. Internalization did not occur spontaneously, as it was not observed in cells that were incubated with medium or with non-specific antibodies. Interestingly, also FECV infected monocytes efficiently internalized the membrane expressed proteins. This implicates that the potential to evade antibody-mediated cell lysis through internalization is not what separates FIPV from FECV strains. Additionally, the internalization process could not be reproduced in feline cell lines indicating its cell type specificity.

In Chapter 4, the internalization pathway and subsequent trafficking of the antigen-antibody complexes was characterized using biochemical, cell biological and genetic approaches. Internalization into cells can occur via several pathways. There are 4 "classical" pathways: phagocytosis, macropinocytosis, clathrin-mediated internalization and caveolae-mediated internalization and 4 less well defined "non-classical" pathways. These pathways are distinguished

form one another by their dependence on rafts, dynamin and/or Rho-GTPases. Using chemical inhibitors, it was found that the pathway presented in this thesis was independent from actin, phosphatidylinositol 3-kinase, clathrin, rafts, dynamin, and Rho-GTPases. This implies that antigen-antibody complexes are not internalized through one of the known internalization pathways. To confirm those results, internalization assays were performed in monocytes expressing dominant negative (DN) mutants of major structural proteins driving the known internalization pathways: DN eps15 (blocks formation of clathrin coated pits), DN caveolin (impedes formation of caveolae) and DN dynamin (inhibits pinching off of clathrin coated vesicles, caveolae and vesicles formed during two clathrin- and caveolae-independent pathways). In order to express these DN mutants in monocytes, a lentiviral delivery and expression system was used. None of these mutants could block the internalization of the viral antigen-antibody complexes confirming that internalization occurred through a new pathway. With co-localization stainings it was found that, after internalization, the viral antigen-antibody complexes passed through the early endosomes. The complexes resided only briefly in the early endosomes and quickly traveled further into the cell, where they accumulated in the late endosomes. Between 30 and 60 minutes post antibody addition, the complexes left the late endosomes but were not trafficked to the lysosomes.

In the next two Chapters, the new internalization process was further characterized. First, the involvement of microtubules, actin and myosins, during internalization and intracellular transport was examined in Chapter 5. The experiments showed that internalization and trafficking was dependent on microtubules. When microtubules were disrupted with chemical inhibitors, a reduction in internalization was observed. Using co-localization stainings, trafficking of the internalizing antigen-antibody complexes over the microtubules could be visualized. The experiments also indicated that actin polymerization is not required. In fact, the cortical actin network formed a barrier that slowed down internalization and that had to be overcome by moving or disintegrating actin filaments. With co-localization stainings, it was found that myosin 2a, 2b, 5a, 7a, 9b and 10 were not involved in the internalization or subsequent trafficking of the antigen-antibody complexes. However, myosin 1 and 6 co-localized with the internalizing complexes during passage through the cortical actin and might thus be involved in the required actin reorganization. One minute after internalization started, vesicles had passed the cortical actin, co-localized with microtubules and association with myosin 6 was lost. The vesicles were further transported over the microtubules and accumulated at the microtubule organizing center after 10 to 30 minutes. Interestingly, the vesicles were associated with myosin 1 and small actin tails during transport over microtubules, indicating that actin, myosin 1 and microtubules cooperated

during intracellular trafficking.

In Chapter 6 we investigated how this internalization pathway is regulated. Experiments with chemical inhibitors showed that the internalization is dependent on serine/threonine kinases and independent of tyrosine kinases and phosphatases. Serine/threonine kinases are the biggest group of kinases and consist of many different classes. To further specify within the family of the serine/threonine kinases, a potential role for protein kinase C, protein kinase A, protein kinase G and mitogen activated protein kinases (MAPKs) was investigated. Also two important members of the calcium/calmodulin-dependent protein kinases (CaMK) sub-family were examined: CaMK II and myosin light chain kinase (MLCK). Only MLCK and the MAPKs were found to play a role. Not much research has been done on the role of MAPKs in internalization processes. Nevertheless, these kinases are promising candidates to be of importance during internalization since the 3 main MAPK signaling cascades can lead to cytoskeleton rearrangements. The first cascade comprises the extracellular signal regulated kinase (ERK). The second branch is the c-Jun N-terminal kinase (JNK) cascade and the third branch is the p38 cascade. The kinases that were shown to positively regulate the internalization process of the viral antigen-antibody complexes are MLCK and JNK. The MAPKs ERK and p38 regulated the internalization in a negative manner and the results suggest that active p38 is even required to maintain the viral proteins expressed in the plasma membrane. There were indications that the MAPKs were not only important during the internalization process itself, but also during intracellular trafficking.

In Chapter 7 all the results were combined into a model for the internalization process. This model is shown in Figure 1. On this figure it is shown that, before antibodies are added, the viral surface expressed proteins are associated with myosin I and activated p38. Myosin I might function as an anchor, connecting the viral proteins to the underlying cortical actin network. p38 might (help to) regulate the cortical actin network. When antibodies bind to the viral proteins, internalization starts immediately. The signaling cascade leading to internalization did not consist of phosphatases, tyrosine kinases, rho-GTPases, protein kinase A, C nor G. It did require MLCK and the MAPKs ERK, p38 and JNK. When internalization starts, myosin I relocates and is found between the internalizing structure and the plasma membrane. This suggests that myosin I might be important for membrane remodeling. Activated p38 is still associated with the forming vesicle and activated ERK and JNK are recruited. The precise function of these MAPKs remains to be elucidated but p-p38 and p-JNK might mediate actin breakdown and reorganization, possibly together with myosin I, to form a corridor through the cortical actin barrier. Between 30 seconds and 1 minute post antibody addition, the internalizing viral pro-



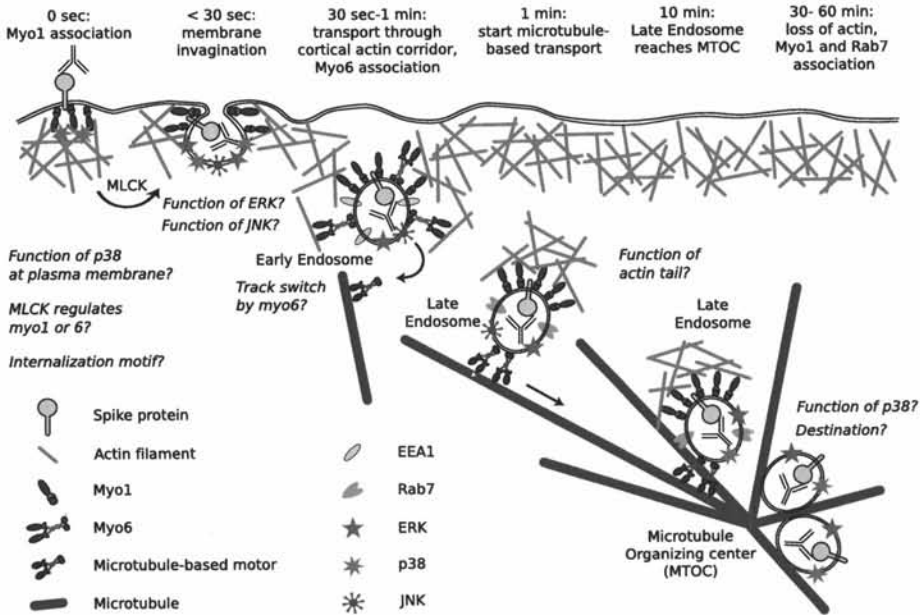


Figure 1: Model of the internalization process with remaining questions.

teins co-localize with the early endosome marker, indicating that the vesicles have already pinched off from the plasma membrane. At this time, myosin 6 is recruited, probably to guide the vesicle through the cortical actin (in cooperation with myosin 1) and possibly to subsequently mediated the track switch to microtubules. Association with activated p38 is lost but p-ERK and p-JNK association remains. These might regulate the formation of the actin tail by promoting (ERK) and suppressing (JNK) actin assembly. Also myosin 1 may play a role in controlling actin filament formation. At 1 minute after antibody addition, the antigen-antibody complexes are already found in late endosomes and start their transportation over the microtubules. Myosin 6 does no longer co-localize while myosin 1, ERK and JNK remain associated. The actin tails are now fully formed. At 10 minutes post antibody addition, the antigen-antibody complexes still reside in late endosomes and the microtubule organizing center (MTOC) is reached. JNK dissociates from the vesicles while p38 reassociates. Between 30 and 60 minutes after the initiation of the internalization process, the vesicles are still found at the MTOC, though they do no longer co-localize with the late endosome marker. Myosin 1 and the actin tails disappear. Activated p38 and ERK remain associated with the vesicles until at least 60 minutes, but there possible function is yet unknown. It also remains to be determined whether MLCK regulates myosin 1 or 6.

The combined results were discussed and compared to literature and remain-

ning questions and possible future research topics were pointed out. Several conclusions can be drawn for this thesis:

- The outcome of a FIPV-infection in monocytes is determined by the origin of the cells, being the cat from which the monocytes were isolated.
- FECV can infect monocytes but infection is always abortive. This lack of long-term, productive infection could constitute the difference in FIPV and FECV pathogenesis.
- Half of the FIPV infected monocytes do not express viral proteins on their plasma membranes. This is a first putative immune evasion process.
- FIPV-infected monocytes that do express viral proteins will internalize these upon binding of antibodies: the second putative immune evasion process.
- The internalization of viral antigen-antibody complexes occurs through a novel clathrin-and caveolae-independent internalization pathway.
- Actin, myosin 1 and 6 and microtubules cooperate during internalization and trafficking.
- This pathway is regulated by MLCK and the MAPKs: ERK, JNK and p38.

## Samenvatting

Twee nauw verwante coronavirussen worden beschreven in katten: het felien enterisch coronavirus, of FECV, en het felien infectieuze peritonitis virus, of FIPV. FECV komt endemisch voor in katten populaties. Meestal gaat een FECV infectie onopgemerkt voorbij maar soms muteert FECV naar zijn hoog virulente tegenhanger: FIPV. Een infectie met FIPV veroorzaakt een chronische, meestal fatale peritonitis/vasculitis. Na decennia van onderzoek is het nog steeds niet geweten hoe FIPV een zo hevige ziekte kan opwekken en waarom het immuunsysteem van een kat een infectie niet kan overwinnen. Alhoewel de interacties tussen FIPV en het immuunsysteem van de gastheer nog slecht gekend zijn, is het duidelijk dat FIPV over een of meer immuno-evasie mechanismen moet beschikken.

Daarom was het doel van deze thesis om (1) de virus-gastheer cel interacties van FIPV (en FECV) met de *in vivo* doelwitcel van FIPV, de feliene monocyt, te onderzoeken en (2) om mogelijke immuno-evasie mechanisme(n) te identificeren en (3) te karakteriseren.

In Hoofdstuk 1 wordt een inleiding gegeven over de feliene coronavirussen, hun onderlinge relatie, de virion structuur, de replicatie cyclus en de pathogenese. Daarnaast wordt een overzicht gegeven van de immuno-evasie mechanismen die gebruikt worden door coronavirussen.

In Hoofdstuk 2 werden de infectiekinetieken van FIPV (stam 79-1146) bepaald in perifere bloed monocyten. Het was de eerste maal dat de vermeerdering van FIPV werd bestudeerd in de *in vivo* doelwitcel, de monocyt. Zowel virustiters als antigeenexpressie werden onderzocht. De infectiekinetieken bleken, verrassend genoeg, afhankelijk te zijn van de kat waaruit de monocyten waren geïsoleerd. Drie infectiepatronen werden waargenomen. In de monocyten van de eerste groep verliep een FIPV infectie progressief; in de tweede groep werden de monocyten wel geïnfected maar de infectie was van korte duur; de monocyten van de derde groep waren niet vatbaar voor infectie. De maximale

infectiegraad bedroeg ongeveer 1%. De infectiekinetieken van FECV (stam 79-1683) werden ook bestudeerd. Een FECV infectie was altijd abortief en de productie van nieuw virus was tot 100 maal lager dan in FIPV geïnfecteerde monocytten. Het gebrek aan lange termijn infectie en virusproductie kan de reden zijn waarom een FECV infectie *in vivo* niet leidt tot een progressief ziektebeeld. Dit gebrek kan de basis vormen van het verschil tussen de pathogenese van FIPV en FECV. De infectiekinetieken in monocytten werden ook vergeleken met deze in Crandell feline kidney (CrFK) cellen, een felienne continue cellijn die vaak gebruikt wordt in het onderzoek op FIPV en FECV. In CrFK cellen vermeerderden FIPV en FECV gelijkaardig (maar verschillend dan in monocytten). Het is duidelijk dat CrFK cellen niet geschikt zijn voor de studie van virus-gastheercel interacties van FIPV en FECV. Daarom werden in de rest van de thesis enkel monocytten gebruikt. Een andere belangrijke observatie was dat ongeveer 50% van de FIPV (en FECV) geïnfecteerde monocytten virale proteïnen tot expressie brachten op hun plasmamembraan. Dit houdt in dat de andere helft van de geïnfecteerde monocytten de virale proteïnen efficiënt weerhield binnenin de cel. Deze intracellulaire retentie kan een immuno-evasie mechanisme zijn aangezien het antistof-afhankelijke herkenning van geïnfecteerde cellen kan verhinderen.

In Hoofdstuk 3 werd bestudeerd wat er gebeurt met de 50% geïnfecteerde cellen die wel virale proteïnen tot expressie brengen op hun plasmamembraan. Om het effect van de humorale immuunrespons op geïnfecteerde monocytten te bestuderen, werd de *in vivo* situatie nagebootst door geïnfecteerde monocytten te cultiveren in de aanwezigheid van antistoffen. Zoals verwacht bonden de antistoffen wel degelijk op de virale proteïnen in de plasmamembraan. Maar de gevormde antigeen-antistof complexen werden in de monocyt geïnternaliseerd via een heel efficiënt en snel proces waardoor er niet langer visueel detecteerbare antigenen aanwezig waren op de plasmamembraan. Al op 3 minuten na toediening van de antistoffen waren  $89 \pm 9\%$  van de geïnfecteerde monocytten hun virale proteïnen aan het internaliseren. Deze antistof geïnduceerde internalisatie kan verklaren waarom de humorale immuunrespons niet werkzaam is tegen een FIPV infectie en is dus een mogelijk immuno-evasie mechanisme. Verder onderzoek toonde aan dat internalisatie ook geïnduceerd kon worden door monoklonale antistoffen tegen het S en M proteïne, zij het dan tot op een lager niveau. Dit suggereert dat beide proteïnen een rol spelen in het internalisatie proces. Spontane internalisatie kwam niet voor aangezien het niet geobserveerd werd in cellen die in medium of met aspecifieke antistoffen geïncubeerd werden. Een ander interessant resultaat was dat monocytten geïnfecteerd met FECV ook in staat waren om de virale proteïnen in de plasmamembraan efficiënt te internaliseren. Dit houdt in dat het ontwijken van antistof-gemedieerde cellyse met behulp van internalisatie niet is wat FIPV

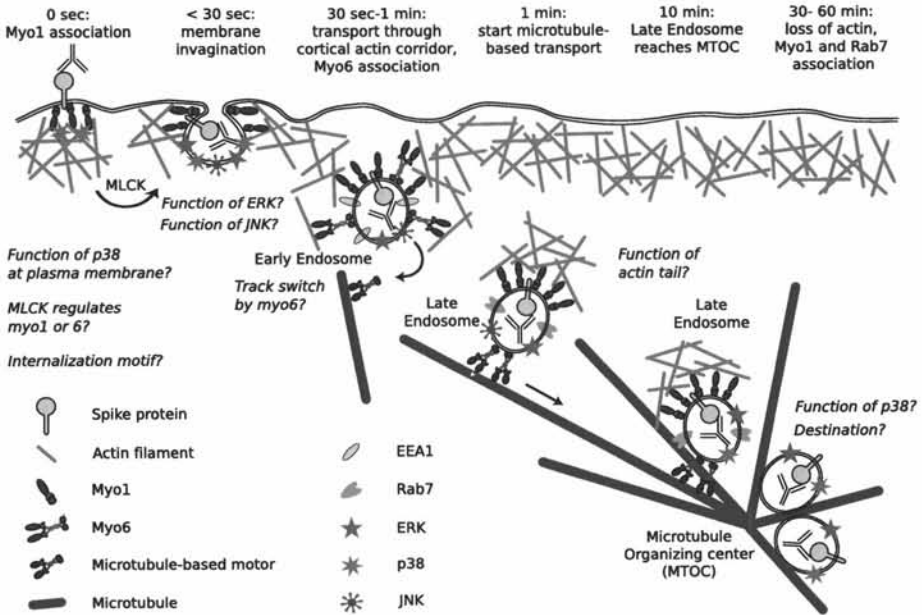
en FECV stammen van elkaar onderscheidt. Daarnaast kon internalisatie niet gereproduceerd worden in feliene continue cellijnen, wat inhoudt dat het internalisatie proces celtype specifiek is.

In Hoofdstuk 4 werd de internalisatie weg en het erop volgende transport van de antigeen-antistof complexen gekarakteriseerd met behulp van biochemische, celbiologische en genetische methoden. Internalisatie in een cel kan op verscheidene manieren gebeuren. Er zijn 4 "klassieke" internalisatie wegen: fagocytose, macropinocytose, clathrine gemedieerde internalisatie en caveolae gemedieerde internalisatie en 4 minder goed gedefiniëerde "niet-klassieke" internalisatie wegen. Deze laatste worden van elkaar onderscheiden door hun afhankelijkheid van rafts, dynamine en/of rho-GTPasen. Met behulp van chemische inhibitoren werd aangetoond dat de hier bestudeerde internalisatie weg onafhankelijk was van actine, fosfatidylinositol 3-kinase, clathrine, rafts, dynamine en rho-GTPasen. Dit houdt in dat de antigeen-antistof complexen niet via één van de gekende internalisatie wegen geïnternaliseerd wordt. Om deze resultaten te bevestigen, werden er internalisatie testen uitgevoerd met monocytten waarin dominant negatieve (DN) mutanten van structurele proteïnen die cruciaal zijn tijdens de gekende internalisatie wegen, tot expressie werden gebracht. De volgende DN mutanten werden gebruikt: DN eps15 (blokkeert de vorming van vesikels met een clathrine mantel), DN caveoline (verhindert de vorming van caveolae) en DN dynamine (inhibeert het loskomen van vesikels met een clathrine mantel, van caveolae en van vesikels die gevormd worden na twee clathrine en caveolae onafhankelijke internalisatie wegen). Om deze DN mutanten tot expressie te kunnen brengen in monocytten, werd een lentiviraal overdracht- en expressiesysteem gebruikt. Geen enkele van de geteste mutanten was in staat om de internalisatie van de virale antigeen-antistof complexen te verhinderen. Internalisatie moet dus via een nieuwe weg gebeuren. Aan de hand van colocalisatiekleuringen werd er verder aangetoond dat de antigeen-antistof complexen na internalisatie naar de vroege endosomen getransporteerd werden. De complexen verbleven slechts gedurende een korte tijd in de vroege endosomen en ze werden snel verder getransporteerd naar het centrum van de cel. Daar accumuleerden de complexen in de late endosomen. Tussen 30 en 60 minuten na antistof toediening verlieten de complexen de late endosomen maar ze werden niet naar de lysosomen getransporteerd.

In de volgende twee Hoofdstukken werd dit nieuwe internalisatie proces verder gekarakteriseerd. Eerst werd het belang van microtubuli, actine en myosines tijdens de internalisatie en het daarop volgende transport onderzocht in Hoofdstuk 5. De experimenten toonden aan dat internalisatie en intracellulair transport afhankelijk waren van microtubuli. Destructie van de microtubuli door chemische inhibitoren leidde immers tot een reductie in internalisatie. Met colocalisatiekleuringen kon transport van de antigeen-antistof complexen over

de microtubuli gevisualiseerd worden. Verder toonden de experimenten ook aan dat polymerisatie van actine filamenten niet vereist is. Integendeel, het corticale actine netwerk vormde een barrière die internalisatie vertraagde en die enkel kon gepasseerd worden door actine filamenten te verplaatsen of af te breken. Met colocalisatiekleuringen werd ook aan getoond dat myosine 2a, 2b, 5a, 7a, 9b en 10 niet betrokken zijn in de internalisatie noch in het daarop volgende transport van de complexen. Myosine 1 en 6 daarentegen, colocaliseerden met de internaliserende complexen tijdens hun passage door de corticale actine en kunnen bijgevolg betrokken zijn in de vereiste actine reorganisatie. Een minuut na de start van de internalisatie waren de vesikels al door de corticale actine gepasseerd en colocaliseerden ze met de microtubuli. Daarbij ging de associatie met myosine 6 verloren. De vesikels werden verder getransporteerd over de microtubuli en accumuleerden in het microtubuli organiserend centrum na 10 tot 30 minuten. Een interessante observatie was dat vesikels, tijdens hun transport over de microtubuli, geassocieerd waren met myosine 1 en beschikten over een kleine actine staart. Dit suggereert dat actine, myosine 1 en microtubuli samenwerken tijdens het intracellulair transport.

In Hoofdstuk 6 werd onderzocht hoe deze internalisatie weg is gereguleerd. Experimenten met chemische inhibitoren toonden aan de internalisatie afhankelijk is van serine/threonine kinasen en onafhankelijk van tyrosine kinasen en fosfatasen verloopt. Serine/threonine kinasen vormen de grootste groep kinasen en worden onderverdeeld in vele verschillende klassen. Een verdere specificatie binnen de familie van de serine/threonine kinasen werd uitgevoerd. Hiervoor werd een mogelijke rol onderzocht voor proteïne kinase C, proteïne kinase A, proteïne kinase G en mitogeen geactiveerde proteïne kinasen (MAPKs). Ook werden twee belangrijke kinasen van de calcium/calmoduline-afhankelijke proteïne kinasen (CaMK) sub-familie onderzocht: CaMK II en myosine lichte arm kinase (myosin light chain kinase: MLCK). Enkel MLCK en de MAPKs bleken een rol te spelen. Er is nog niet veel onderzoek gedaan naar het belang van MAPKs tijdens internalisatie processen. Nochtans zijn deze kinasen veelbelovende kandidaten om een rol te spelen tijdens internalisatie aangezien de 3 belangrijkste MAPK signalisatie cascades kunnen leiden tot cytoskelet reorganisaties. De eerste MAPK signalisatie cascade is die rond de extracellulair signaal gereguleerde kinase (ERK), de tweede cascade is de c-Jun N-terminale kinase (JNK) cascade en de derde is de p38 cascade. De kinasen die zorgden voor een positieve regulatie van het internalisatie proces van de virale antigeen-antistof complexen zijn MLCK en JNK. De MAPKs ERK en p38 zorgden voor negatieve regulatie. De resultaten suggereerden ook dat actieve p38 zelf noodzakelijk was om de virale proteïnen in de plasmamembraan vast te houden en dat MAPKs niet enkel een rol speelden tijdens de internalisatie, maar ook tijdens het intracellulair transport.



Figuur 1: Model van het internalisatie proces met open vragen.

In Hoofdstuk 7 werden alle resultaten verenigd en werd een model van het internalisatie proces opgesteld. Dit model wordt weergegeven in Figuur 1. Daarop is te zien dat de virale proteïnen in de plasmamembraan geassocieerd zijn met myosine 1 en geactiveerde p38, ook vooraleer de antistoffen worden toegevoegd. Myosine 1 kan dienst doen als een anker die de virale proteïnen vasthecht aan het ondergelegen corticale actine netwerk. p38 kan de regulatie van dit actine netwerk (helpen) reguleren. Wanneer de antistoffen op de virale proteïnen binden, start de internalisatie onmiddellijk. De signalisatie cascade die leidt tot deze internalisatie bevat geen fosfatasen, tyrosine kinasen, rho-GTPasen noch proteïne kinase A, C of G. Het proces was wel afhankelijk van MLCK en de MAPKS ERK, p38 en JNK. Bij de start van de internalisatie, verplaatst myosine 1 zich tussen het internaliserende vesikel en de plasmamembraan. Dit suggereert dat myosine 1 een rol speelt in de vervorming van de membraan. Ook geactiveerde p38 blijft geassocieerd met het vormend vesikel en ERK en JNK worden gerecrueteerd. De precieze functie van deze MAPKS is nog niet opgehelderd maar p-p38 en p-JNK zouden kunnen de afbraak en reorganisatie van actine bewerkstelligen om zo, mogelijk samen met myosine 1, een tunnel te vormen door de barrière van de corticale actine. Tussen 30 seconden en 1 minuut na de toediening van antistoffen, colocaliseren de virale proteïnen met een vroege endosoom merker. Dit is een indicatie dat de vesikels reeds gesloten en losgekomen zijn van de plasmamembraan. Op dat

moment wordt myosine 6 gerecruteerd, waarschijnlijk om het vesikel door de corticale actine te gidsen (in samenwerking met myosine 1). Myosine 6 zou ook kunnen van belang zijn voor de daarop volgende omschakeling van actine-naar microtubuli-gemedieerd transport. Associatie met geactiveerde p38 gaat nu ook verloren, terwijl de binding met p-ERK en p-JNK behouden blijft. p-ERK en p-JNK zouden kunnen instaan voor de regulatie van de vorming van de actine staart door stimulatie (ERK) en onderdrukking (JNK) van actine polymerisatie. Ook myosine 1 speelt mogelijks een rol in de vorming van de actine staarten. Op 1 minuut na antistof toediening, bevinden de antigeen-antistof complexen zich reeds in de late endosomen en wordt transport over de microtubuli gestart. Myosine 6 colocaliseert niet langer met de vesikels, tegenstelling tot myosine 1, ERK en JNK. De actine staarten zijn nu volledig gevormd. Op 10 minuten na antistof toediening bevinden de antigeen-antistof complexen zich nog steeds in de late endosomen, die ondertussen het microtubuli organiserend centrum (MTOC) hebben bereikt. Daar dissocieert JNK van de vesikels terwijl p38 opnieuw gerecruteerd wordt. Tussen 30 en 60 minuten na de start van de internalisatie bevinden de vesikels zich nog steeds in het MTOC maar ze colocaliseren niet langer met de merker voor de late endosomen. Nu verdwijnen ook de actine staarten en myosine 1. Geactiveerde p38 en ERK blijven echter geassocieerd met de vesikels tot minstens 60 minuten na de start van de internalisatie. Het is nog niet gekend wat hun functie dan is. Ook moet nog bepaald worden of MLCK instaat voor de regulatie van myosine 1 of van myosine 6.

Deze resultaten werden bediscussieerd en vergeleken met bevindingen in de literatuur. Ook werden de open vragen vermeld en mogelijke toekomstige onderzoeksonderwerpen voorgesteld. Verscheidene conclusies kunnen uit dit werk getrokken worden:

- Het verloop van een FIPV infectie in monocytten wordt bepaald door de oorsprong van de cellen, dus door de kat waaruit de monocytten geïsoleerd werden.
- FECV is in staat monocytten te infecteren maar een infectie wordt altijd afgebroken. Dit gebrek aan productieve infectie op lange termijn kan het verschil tussen de pathogenese van FIPV en FECV bepalen.
- De helft van de FIPV geïnfecteerde monocytten brengt geen virale proteïnen tot expressie op hun plasmamembraan. Dit is mogelijks een eerste immuno-evasie proces.
- De FIPV geïnfecteerde monocytten die wel virale proteïnen tot expressie brengen, zullen deze internaliseren op het moment dat er antistoffen op binden. Dit is mogelijks een tweede immuno-evasie proces.



- De internalisatie van de virale antigeen-antistof complexen gebeurt via een nieuwe clathrine- en caveolae-onafhankelijke internalisatie weg.
- Actine, myosine 1 en 6 en microtubuli werken samen om de internalisatie en het intracellulair transport te bewerkstelligen.
- De internalisatie wordt gereguleerd door MLCK en de MAPKs: ERK, JNK en p38.



# Curriculum Vitae

## Personalialia

Hannah Dewerchin werd op 9 februari 1979 geboren te Kortrijk. In 1997 beëindigde zij haar humaniora opleiding aan het Koninklijk Atheneum te Kortrijk richting Latijn-Wiskunde. In 2003 behaalde zij het diploma van bio-ingenieur in de cel-en genbiotechnologie met onderscheiding. Vanaf januari 2004 tot op heden beschikte zij over een specialisatie beurs van het Instituut voor Aanmoediging van Innovatie door Wetenschap en Technologie in Vlaanderen (IWT). Het onderzoek werd verricht in het Laboratorium voor Virologie, Vakgroep Virologie, Parasitologie en Immunologie, aan de Faculteit Diergeneeskunde van de Universiteit Gent en handelde over de interacties van het feliene infectieuze peritonitis virus (FIPV) en het feliene enterische coronavirus met hun gastheercel, de bloed monocyt. Verder werd een mechanisme beschreven hoe FIPV-geïnfecteerde monocytten kunnen ontsnappen aan de antistof-gemedieerde immuniteit. In dit immuno-evasie proces worden de virale proteïnen die zich in de plasmamembraan bevinden, geïnternaliseerd. Tenslotte werd het internalisatie proces tot op cel-biologisch niveau gekarakteriseerd en bleek het te gaan om een voordien nog nooit beschreven endocytoseweg.

## Publicaties

H. Dewerchin, E. Cornelissen, and H.J. Nauwynck. Replication of feline coronaviruses in peripheral blood monocytes. *Archives of Virology*, 150:2483–2500, 2005. doi: 10.1007/s00705-005-0598-6.

H. Dewerchin, E. Cornelissen and H.J. Nauwynck. Feline infectious peritonitis virus-infected monocytes internalize viral membrane-bound proteins upon

antibody addition. *Journal of General Virology*, 87:1685–1690, 2006. doi: 10.1099/vir.0.81692-0.

E. Cornelissen, H. Dewerchin, E. Van Hamme and H.J. Nauwynck. Absence of surface expression of feline infectious peritonitis virus (FIPV) antigens on c cells isolated from cats with FIP. *Veterinary Microbiology*, 121:131–137, 2007. doi: 10.1016/J.VETMIC.2006.11.026.

E. Van Hamme, H. Dewerchin, E. Cornelissen and H.J. Nauwynck. Attachment and internalization of feline infectious peritonitis virus in feline blood monocytes and Crandell feline kidney cells. *Journal of General Virology*, 88: 2527–2532, 2007. doi: 10.1099/vir.0.82991-0.

E. Van Hamme, H. Dewerchin, E. Cornelissen, B. Verhasselt and H.J. Nauwynck. Clathrin- and caveolae-independent entry of feline infectious peritonitis virus in monocytes depends on dynamin. *Journal of General Virology*, in press, 2008.

H. Dewerchin, E. Cornelissen, E. Van Hamme, K. Smits, B. Verhasselt and H.J. Nauwynck. Viral proteins in feline infectious peritonitis virus infected monocytes are internalized through a clathrin- and caveolae-independent pathway. *Journal of General Virology*, accepted.

## Abstracts

H. Dewerchin, E. Cornelissen, and H.J. Nauwynck. Internalization of plasma membrane-bound viral proteins upon antibody addition in feline infectious peritonitis virus infected monocytes occurs through a novel internalization pathway, a putative immune-evasion process. In *10th International Nidovirus symposium: Toward control of SARS and other nidovirus diseases*, Colorado Springs, Colorado, USA, 2005.

E. Cornelissen, H. Dewerchin, E. Van Hamme, and H.J. Nauwynck. Replication of feline coronaviruses in feline peripheral blood monocytes. In *International Congress of Veterinary Virology: Comparative and emerging virus infections of dogs and cats*, Liverpool, England, 2005.

H. Dewerchin, E. Cornelissen, E. Van Hamme, and H.J. Nauwynck. Possible immune evasion strategies of feline infectious peritonitis virus. In *Annual meeting of the Belgian Society for Microbiology*, Brussels, 2006.

E. Cornelissen, H. Dewerchin, E. Van Hamme, and H.J. Nauwynck. Absence

of surface expression of feline infectious peritonitis virus (FIPV) antigens on infected cells isolated from cats with FIP. In *7th International Congress of Veterinary Virology*, Lisbon, Portugal, 2006.

H. Dewerchin, E. Cornelissen, E. Van Hamme, and H.J. Nauwynck. A new internalization pathway revealed by an immune evasion strategy used by feline infectious peritonitis virus. In *11th International Nidovirus symposium*, Oxford, UK, 2008.

E. Cornelissen, H.L. Dewerchin, E. Van Hamme, L. Bosseler, H.J. Nauwynck. Absence of antibody-dependent complement-mediated lysis of feline infectious peritonitis virus (FIPV)-infected cells. In *11th International Nidovirus symposium*, Oxford, UK, 2008.

E. Van Hamme, H. Dewerchin, E. Cornelissen, B. Verhasselt and H.J. Nauwynck. Clathrin- and caveolae-independent entry of feline infectious peritonitis virus in monocytes depends on dynamin. In *11th International Nidovirus symposium*, Oxford, UK, 2008.



## Dankwoord

In de eerste plaats wil ik mijn promotor Prof. Hans Nauwynck bedanken voor de kans om in zijn labo een nieuwe onderzoekslijn te helpen opstarten. Er moesten nog heel wat kinderziekten overwonnen worden, maar dat maakte het des te leerzamer. Bedankt voor de vele uren die je vrijgemaakt hebt om samen resultaten te bespreken en nieuwe strategieën te bedenken. Misschien waren er soms meningsverschillen maar dat leidde altijd tot interessante discussies. Bedankt ook om mij uiteindelijk de vrijheid te geven om mijn eigen weg in het onderzoek uit te stippelen.

Ik wil ook de andere leden van de 'FIP groep', Els Cornelissen en Evelien Van Hamme, bedanken. Els, je was erbij vanaf het moeilijke begin. Ik herinner me nog de gevechten met de katten van de diervoeding voor enkele milliliters bloed, de lange besprekingen over hoe we een bepaald experiment zouden opzetten, de uren aan de microscoop waarin we probeerden op te maken wat we nu precies zagen en het bedenken van hypothesen over de eigenlijke betekenis van onze resultaten. Ook later, toen we elk onze eigen (onderzoeks)weg opgingen, wist ik dat ik steeds op je kon rekenen en niet alleen om te helpen met de praktische zaken. Evelien, jij kwam ons pas 2 jaar later vergezellen maar je bent al lang niet meer weg te denken uit de groep. En dat is niet alleen omdat je een meester bent in het vertellen van sappige verhalen over wat je nu weer is overkomen.

Ook mijn medepromotor, Prof. Herman Favoreel, wens ik te bedanken. Herman, je hebt mij op weg geholpen met het moleculaire werk, en dat ging toch niet van een leien dakje. Bedankt voor de vele suggesties om de soms illustere problemen op te lossen en voor het kritisch lezen van mijn schrijfsels.

Daarnaast was ook de inbreng van medepromotor Prof. Bruno Verhasselt van onschatbare waarde voor deze thesis. Bedankt dat ik heb mogen gebruik maken van jullie lentiviraal expressiesysteem en L3 labo en voor de tijd die je hebt vrijgemaakt voor het lezen van de verschillende versies van de publicatie.

Ook Kaatje Smits en Evelien Naessens wil ik bedanken voor hun uitleg en hulp bij het praktische werk.

De leden van de begeleidingscommissie wens ik te bedanken voor het kritisch lezen van dit proefschrift en voor hun raadgevingen.

Verder wil ik nog de vele toffe collega's vermelden die het (soms late) werk in het labo heel aangenaam gemaakt hebben. En daarbij gaat er toch speciale dank uit naar de 'eerste bureau', soms ook wel 'het kiekenkot' genoemd. Ik wil er de andere mensen in het labo toch maar eens op wijzen dat wij wel eens durven kakelen maar dat we niet echt beschikken over pluimen (alhoewel we er eigenlijk verdienen) en we ook geen eieren leggen (dat ei in Sarah's labojas werd er wel degelijk door iemand anders gelegd). Els, Evelien, Sarah C, Sarah G en An, het was heel plezant om met jullie een bureau te delen en onze uitstapjes zijn altijd supergezellig! Hopelijk volgen er nog heel wat. In alle geval wens ik jullie het allerbeste voor de komende (of laatste!) onderzoeksjaren. Maar ook Peter, An, Nick, Filip, David, Annick, Annebel en Matthias C. wil ik graag bedanken voor de al dan niet wetenschappelijke babbels. Matthias D, Celine, Wander, Iris, Hanne, Merijn en Annelies, jullie zijn misschien nog niet zo lang op het labo maar toch hebben we al leuke tijden beleefd. Ik vind dat we van de sportnamiddag en daaropvolgende barbeque een traditie zouden moeten maken. Gerald, Constaninos, Kalina and Meezanur, thanks for bringing something extra to the lab.

Chantal, van jou hebben Els en ik heel veel geleerd in de eerste maanden op het labo. Ook wisten we dat onze (vele) titraties in goeie handen waren. Ik kan je niet genoeg bedanken voor al het werk dat je voor ons verzet hebt! Chris, ik wil jou ook bedanken voor de vele hulp tijdens onze eerste kleuringen en voor de begeleidende gesprekken. Lieve, Carine en Nele, wij hebben niet veel kunnen samenwerken, maar toch heeft elk van jullie mij wat kunnen bijleren. Bedankt dat ik jullie altijd mocht storen met een of andere vraag.

Fernand en Geert, zelfs al moeten jullie niet al te veel weten van die katten, toch mocht ik altijd alles vragen. Bedankt.

Ook Mieke, Gert en Dirk wil ik bedanken. Jullie waren altijd onmiddellijk bereid om mij te helpen met kleine of grote problemen, zelfs al waren jullie al bedolven onder het werk.

Dit onderzoek zou ook nooit kunnen uitgevoerd worden zonder Streepje, Maya, Belle en Godzilla, onze katten. Toen Streepje bij ons kwam was het meer een grote bol zachte bont dan een kat. Na enkele jaren is het al heel wat beter, maar ze blijft een dikke knuffelkat. Maya was ook flink uit de kluiten gewassen, maar schijn bedriegt. Ze zou geen vlieg kwaad doen en is bij wijze van spreken bang van haar eigen schaduw. Die vlieg zou trouwens snel gevangen



en verorberd worden door één van de twee jongste katten, Belle of Godzilla. De spraakzame Belle zou alles doen voor wat aandacht. Godzilla deed haar naam alle eer aan en was compleet onhandelbaar in het eerste half jaar dat ze bij ons was. Maar ze is toch ontdooid en hopelijk wordt haar temperament nog wat milder over de komende jaren.

Een bijzondere dank gaat ook uit naar mijn familie, zonder hen zou ik nooit staan waar ik nu sta. Pa en ma, bedankt voor de kansen en de vrijheid die jullie mij al die jaren gegeven hebben om mijn weg in leven en werk te vinden en voor de nooit aflatende steun. Sarah, Maite en Loïc bedankt voor het luisteren naar mijn enthousiaste verhalen of mijn geklaag, naargelang de voortgang van de experimenten.

Ten slotte wil ik nog Sam bedanken. Voor de interesse in mijn onderzoek, voor het gezelschap tijdens nachtelijk labowerk, of tijdens de lange uren aan de confocale in het weekend, voor het oplossen van computerproblemen, voor het mij aansmeren van linux, voor de hulp in deze laatste drukke maanden, voor de vele verhelderende gesprekken, maar vooral voor je ijzersterke geloof in mij en voor je nooit verminderende steun en liefde. En sinds kort ben je nu ook nog een superpapa voor ons dochttertje Mina. Samen vullen jullie mijn leven met kleur en liefde. Ik kan mij geen gelukkigere thuis voorstellen en ik hoop dan ook dat er nog vele prachtige jaren volgen!

Hannah.

Dit werk kwam tot stand met steun van het Instituut voor Aanmoediging van Innovatie door Wetenschap en Technologie in Vlaanderen (IWT).

This work was supported by het Instituut voor Aanmoediging van Innovatie door Wetenschap en Technologie in Vlaanderen (IWT).